Supporting Information

Colour Tuneability of Heteroleptic Iridium Complexes Through Second-Sphere Coordination

Barbora Balónová, T. Harri Jones, Allison E. True, Sydney M. Hetherington and Barry A. Blight*

University of New Brunswick, Department of Chemistry,
Fredericton, New Brunswick, Canada, E3B 5A3

Table of Contents

S0. Materials and Techniques

Materials. All starting materials were purchased from commercial sources (Sigma Aldrich, Fisher Scientific and TCI) and used without further purification. Analytical thin layer chromatography (TLC) was carried out on precoated TLC plates Alugram Sil G/ UV254. Column chromatography purifications were done with silica gel (ultrapure, 60-200 μm (60 Å)). Experiments were performed as follows:

(i) A conventional hotplate (IKA™ RCT Basic magnetic hot plate stirrer (Stirring range: 50 to 1500 rpm; Size: 5.3 in. dia; Supplier: IKA™ 3810001) - fumehood), under a dry N_2 atmosphere using standard Schlenk Line techniques when specified.

(ii) Microwave reactor – Anton Paar-Monowave 400 (max. temp. 300°C, power 850 W and pressure of 30 bar) with 10- and 30-mL borosilicate glass vials with a cap material of PEEK. The seal material is made from Teflon-coated silicone. Supplier: Anton Paar.

Nuclear Magnetic Resonance (NMR). ^{1}H (400 MHz) and ^{13}C (101 MHz) NMR spectra were recorded on an Agilent 400 MR spectrometer in deuterated solvents, namely chloroform-*d* ($CDCl_3$) and dimethyl sulfoxide-d_6 (DMSO-d_6), which were purchased from Fisher Scientific. All chemical shifts are reported in δ (ppm) referenced to tetramethylsilane ($Si(CH_3)_4$) and the peak multiplicities are referred to as singlet (s), doublet (d), triplet(t), quartet (q), multiplet (m). Spin-spin coupling effect is quantify with the coupling constants, which is abbreviated with the capital letter J.

Mass Spectrometry. High-resolution mass spectral data measurements were performed by Xiao Feng at the Mass Spectrometry Laboratoy (Dalhousie University, Halifax, Canada). High-resolution mass spectra were recorded on Bruker Daltonics MicrOTOF instrument. The ionization method used for low/high-resolution analysis was positive electrospray ionization (ESI+). The sample was introduced by a syringe pump at a flow rate of 2 μL/min and the spray voltage applied to the ESI needle was 4.5 kV. The dry gas flow rate was 4 L/min with a pressure of 1 Bar and a temperature of 180°C. For the analysis, samples sizes were between 1-2.5 mg and the experiment was replicated 2-3 times to ensure the viability of the results (sample sizes of 5-7 mg were sent).

Elemental Analysis. Elemental analysis was performed by Patricia Granados at the Centre for Environmental Analysis and Remediation (Saint Mary's University, Halifax, Canada). Carbon, hydrogen, and nitrogen analyses were conducted on a PerKin Elmer 2400 Series II CHN Analyser. CHN results were processed as a percentage by weight of each element and were measured as a function of thermal conductivity. For the analysis, samples sizes were between 2.5-3.5 mg and the experiment was replicated 2-3 times to ensure the viability of the results (sample sizes of 15-20 mg were sent).

UV-Vis Spectroscopy. UV-Vis spectra for the cyclometalated Ir(III) complexes **1**-**4** were recorded with a Cary Series UV-Vis Spectrophotometer (Agilent Technologies). Chloroform – HPLC grade (C606-1, LOT 214513) was used as the blank solution and the solvent to prepare the solutions of the several Ir(III) complexes **1**-**4**. Two standard Q macro cuvettes with an optical path length of 10 millimetres which are made of fused quartz glass were used to measure the absorbance of these compounds. UV-Vis spectra

were collected with a concentration of the cyclometalated Ir(III) complexes **1-4** of 1.10^{-4} M.

Photoluminescence Emission Spectroscopy. Emission and excitation spectra, PLQY, and decay lifetime measurements were recorded with a FS5 Spectrofluorometer (Edinburgh Instruments).

- Excitation and emission spectra for the cyclometalated Ir(III) complexes **1-4** were recorded with a FS5 Spectrofluorometer (Edinburgh Instruments) and a SC-05 (Standard Cuvette Holder) at 298 K. A Hellma Fluorescence Cuvette (Suprasil 6 Quartz, spectral range 200-2,500 nm, pathlength 10x4 mm and chamber volume 3,500 µL) was used to measure the excitation and emission spectra of **1-4**. The sample solutions were prepared in chloroform – HPLC grade (C606-1, LOT 214513), which was used as a blank solution and the solvent to prepare the solutions of **1-4** (concentration of $1.1 \cdot 10^{-5}$ – $2.8 \cdot 10^{-6}$ M (**Table S1**)). All solutions were degassed in the cuvette for one minute (Argon) before each measurement.

- Photoluminescence quantum yields were calculated using the relative method. A solution of quinine sulphate in 0.1 M sulfuric acid (PLQY 54.6 %) was used as a reference sample for emission wavelengths between 400-480 nm. For wavelengths between 480-560 nm rhodamine 6G in ethanol (PLQY 95 %) was used as a reference and for wavelengths greater than 560 nm rhodamine B in ethanol (PLQY 56 %) was used. Ir(III) compounds **1-4** were measured at a concentration depicted in **Table S2**. Absorbance

spectra were recorded in triplicate for both the reference and Ir(III) complexes **1-4** at a fixed absorbance value below 0.1, ranging from 0.075 to 0.085. All solutions were degassed in the cuvette for 20 minutes (Ar) before each measurement.

(absorbance value recommended by Edinburgh Instruments). An average of these absorbances was used as the standard value for both the reference and the Ir(III) complexes **1-4**. Emission spectra were then recorded in triplicate for both the reference and Ir(III) complexes **1-4** with all samples being excited at 350 nm. The area under the curve of the emission scan was then calculated. An average of these integration values was used as the standard value for both the reference and the Ir(III) complexes **1-4**. Photoluminescence quantum yields for each Ir(III) complex **1-4** were then calculated using **eq. 1**, and the values reported in **Table S5**.

Equation 1:

$$\boldsymbol{QY}\ of\ Ir(III)\ complexes = \boldsymbol{QY}_{ref} \times \frac{I_{sample}}{I_{ref}} \times \frac{A_{ref}}{A_{sample}} \times \frac{\eta^2_{sample}}{\eta^2_{ref}}$$

I = Integrated area under the emission curve

A = Absorbance at the wavelength of excitation maxima

$\boldsymbol{\eta}$ = Refractive index

Citation: Brouwer, A. M. (2011). Pure and Applied Chemistry, 83(12), 2213–2228 [1]

Table S1. Quinine sulphate, rhodamine 6G, rhodamine B and Ir(III) complexes' concentrations.

Compound	Concentration (M^{-1})

1	$9.5 \cdot 10^{-6}$
2	$1.1 \cdot 10^{-5}$
3	$2.8 \cdot 10^{-6}$
4	$9.3 \cdot 10^{-6}$
RB	$9.0 \cdot 10^{-6}$
RG	$7.2 \cdot 10^{-6}$
QS	$1.25 \cdot 10^{-5}$

- Decay lifetime measurements were recorded with a FS5 Spectrofluorometer (Edinburgh Instruments) and a SC-05 (Standard Cuvette Holder). All solutions of **1-4** were prepared to a concentration of ~$1 \cdot 10^{-6}$ M using chloroform – HPLC grade (C606-1, LOT 214513) that was degassed in a cuvette for 20 minutes (Ar) before each measurement at 298 K. A QF2001 – 10 mm Lightpath Spectrophotometer Screw Cap Cuvette (Threaded – Quartz 3.5 mL) was used to measure the excitation spectra of each Ir(III) complexes (**1-4**). The excited state lifetimes were measured by the time correlated single photon counting spectra (TCSPC) technique using an EPLED-365 (Edinburgh Instruments) laser with emission detection at 520 nm for all complexes. Each lifetime measurement was calculated through an Exponential Fit Time Scan that follows the formula:

Fit: $B_1 e^{(-t/\tau_1)} + B_2 e^{(-t/\tau_2)} + B_3 e^{(-t/\tau_3)} + B_4 e^{(-t/\tau_4)}$

A chi-squared (χ^2) of values between 1-1.3 were found suitable. These complexes showed either monoexponential decay or biexponential decay.

PMMA solid state PLQY and lifetime measurements. PMMA films were prepared through an electrospinning technique using a 'VWR International KINETIC ENERGY 26 JOULES GALAXY MINI CENTREFUGE'

100 mg of 35kDA PMMA in 1 mL of dry degassed (with argon) chloroform along with 2mM of the Iridium complex **1-4**. For co-system **1-4•5** an equimolar 1:1 equivalent amount of compound **5** based upon 2mM of complex **1-4** was added to the mixture.

The mixtures were thoroughly stirred under argon until full dissolution of PMMA, and emitters. Upon full dissolution of the solids, the films were formed through dropwise electrospinning, each 1 mL solution was added 1 drop at a time between spins of the device allowing for an even coating of emitter polymer thin film mixture.

Measurements of the quantum yield in the solid state were carried out with use of an FS5 SC-30 integrating sphere module and a Xenon lamp at 25 °C. Excitation wavelengths will be specified with figures as compounds have significant variation in excitation.

$$PLQY = \frac{\#\ emitted\ photons}{\#\ absorbed\ photons}$$

Number of absorbed photons was inferred by comparing the difference in the excitation light scattering of the blank and the sample (Ex_{blank} and Ex_{sample}) – whereas the number of emitted photons can be inferred by comparing the difference between the sample and the blank (Em_{sample} and Em_{blank})

$$PLQY = \frac{Em_{sample} - Em_{blank}}{Ex_{blank} - Ex_{sample}}$$

Cyclic Voltammetry. CV was carried out in an argon filled glovebox using a potentiostat/galvanostat (BioLogic SP-150) with a cell consisting of a working electrode (platinum disk, 0.07 cm^2), counter electrode (platinum wire, 5 cm) and Ag/Ag^+ reference electrode (0.01M $AgNO_3$ in 0.1 M NBu_4PF_6 in anhydrous chloroform). All E_{ox} and E_{red} values were referenced to a ferrocene standard. The electrode was washed thoroughly with the electrolyte solution before each sample run. Each sample concentration was measured to be 2mM, when compound **5** was used with each of the complexes **1-4**, it was used in a 1:1 equimolar ratio to determine its effect on the oxidation and reduction potentials of the Iridium complexes.

DFT methodology. DFT calculations were performed using the Gaussian16 revision c.01 [2] software package provided by the University of Waterloo (University of Waterloo) through the Digital Research Alliance of Canada (alliancecan.ca). The ground state geometries were optimised at the B3LYP [3] level using LANL2DZ [4] basis set for iridium and the 6-31G** basis set for all other atoms. [4] The energy minima were confirmed using frequency analysis and the absence of any imaginary frequencies. The butyl chains on the 'guanidine' ligand were truncated to methyl groups to reduce disorder and computational costs. Time-dependant DFT (TD-DFT) was also undertaken to calculate the singlet and triplet excited energetic states. All relevant orbital and geometries are given in section S8.

All initial input structures were created using and optimised Avogadro2 1.91.0 [5]

Orbital plots were generated using Avogadro2 1.91.0 [5]

UV-vis plots were generated using GaussSum 3.0.2 [6]

S1. Synthetic Routes of Ir(III) complexes 1-5

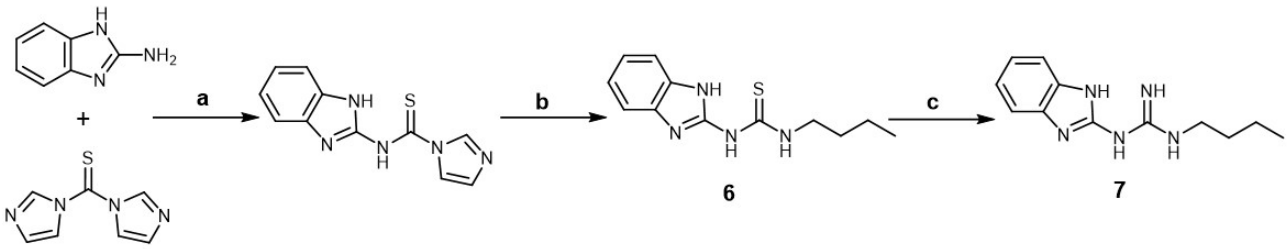

Scheme S1. The two-step synthetic route for the preparation of 1-(1H-benzo[d]imidazole-2-yl)-3-butylguanidine ligand. Reagents and conditions: a) acetonitrile, 50 °C, 20 h, 80 %; b) *n*-butyl amine, catalytic DMAP, DMF, 100°C, 18 h, 70 %; c) mercuric oxide, ammonia in methanol (NH_3/MeOH (2M)), $CHCl_3$, 3 h, r.t., 50 %.

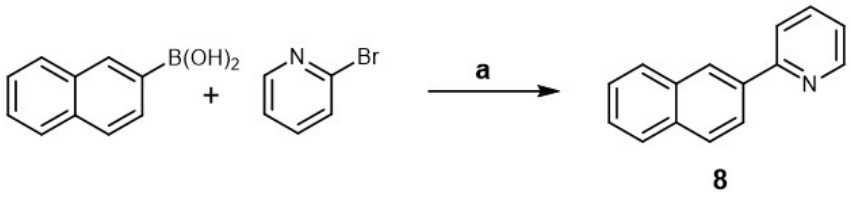

Scheme S2. Synthesis of ligand **8**. Reagents and conditions: a) 0.5 mol % $Pd(PPh_3)_4$, Na_2CO_3, EtOH:H_2O, (1.3 mL : 0.8 mL), M.W. irradiation, 150°C, 15 min, 67%.

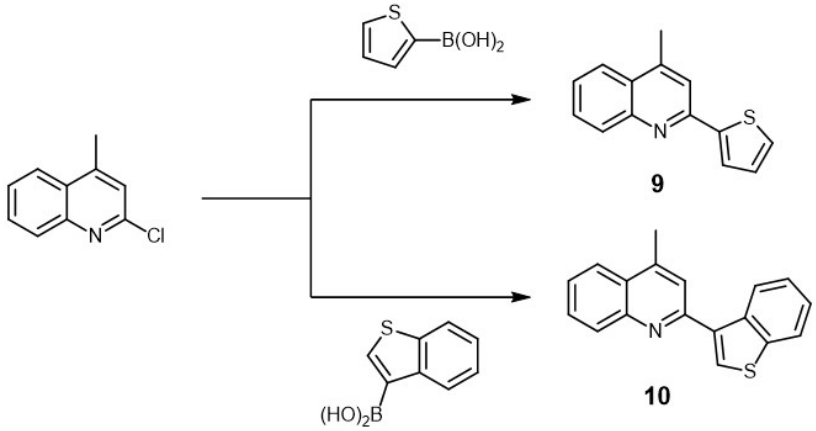

Scheme S3. Synthesis of ligand **9** and **10**. Reagents and conditions: 3 mol % $Pd(Ph_3)_4$, 5% solution of Na_2CO_3, dry THF, reflux, 24 h, N_2 (g).

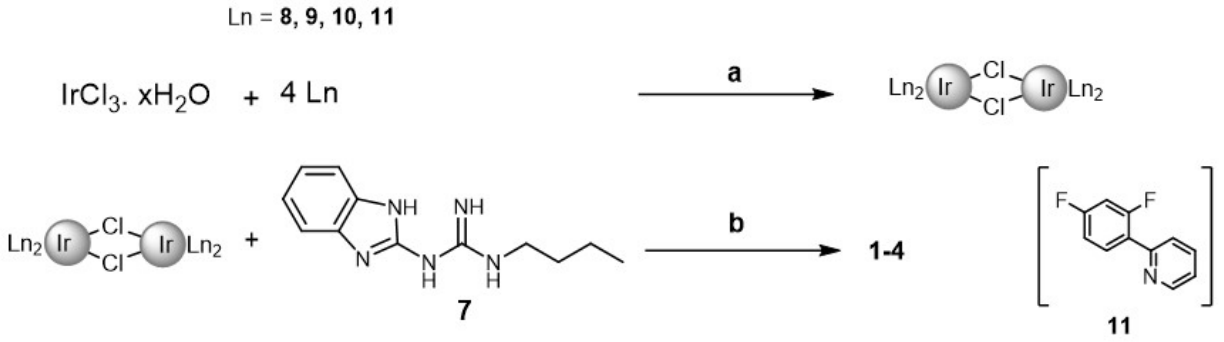

Scheme S4. The general synthetic route of all iridium complexes herein. Reagents and conditions: a) 2- ethoxyethanol: water (3:1), reflux, 19 h; b) 1-(1H-benzo[d]imidazole-2-yl)-3- butylguanidine **17**, K_2CO_3, toluene, N_2 (g).

Iridium dimers

All iridium μ-chloro bridged dimers were synthesised following Nonoyama's procedure.[1] Iridium chloride hydrate **14** (1 equivalent) and 2 equivalents of appropriate ligand were added into a mixture of 2-ethoxyethanol: water (3:1) and refluxed for 19-24 h under nitrogen atmosphere. After cooling to room temperature, a precipitate was formed and filtered off. The solid was washed with water (5 mL), ethanol (5 mL) and acetone (5 mL) and dried on Schlenk line for 48 h.

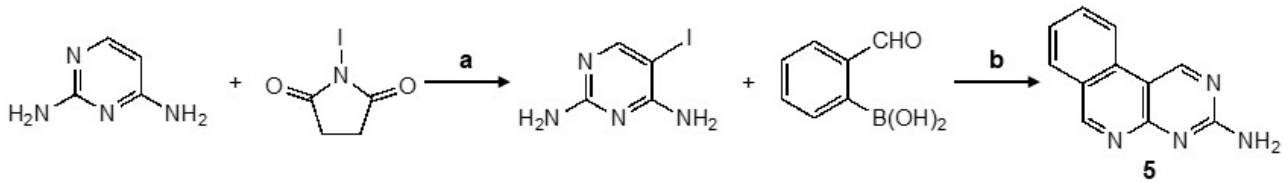

Scheme S5. The synthetic route of compound **5**. Reagents and conditions: a) DMF, 0°C to rt., 3 h, 88%; b) MW, K_2CO_3, $Pd(PPh_3)_4$, dioxane:water (3:1), 150°C, 3h N_2 (g).

S2. Synthetic Procedures

Iridium complex 1

Ir(dFppy) chloro-briged dimer (64 mg, 0.052 mmol, 1.0 eq) was combined with 2.1 equivalents of (1-(1H-benzo[d]imidazole-2-yl)-3-butylguanidine) ligand **7** (25 mg, 0.11 mmol) and 10 equivalents of potassium carbonate (72 mg, 0.52 mmol) were added to 9 mL of dry toluene and refluxed under nitrogen atmosphere for 18 hours. After the reaction was completed, it was cooled to room temperature and solvent was removed under reduced pressure. The solid was re-dissolved in dichloromethane and extracted with water, organic phases were combined, and solvent removed under reduced pressure. A check of the organic layer under UV light (365 nm) resulted in active solution of green-blue (turquoise) colour. The sample was dried and subjected to purification via column chromatography (neutral alumina as stationary phase, DCM: MeOH 10:0.5 as mobile phase). Fractions were collected (Rf = 0.08, DCM: MeOH, 10: 0.5), combined and solvent was removed under reduced pressure. The final product **1** was obtained in (31.7 mg ,76%) yield.

^{1}H NMR (400 MHz, $CDCl_3$, 298 K) δ: 8.63 (dd, *J* = 5.8, 0.9 Hz, 1H), 8.28 (d, *J* = 8.9 Hz, 1H), 8.18 (d, *J* = 14.0 Hz, 1H), 8.09 (dd, *J* = 5.8, 0.9 Hz, 1H), 7.82 – 7.75 (m, 1H), 7.71 (dt, *J* = 11.6, 5.6 Hz, 1H), 7.19 (d, *J* = 7.8 Hz, 1H), 7.12 – 7.05 (m, 1H), 7.05 – 6.92 (m, 2H), 6.79 – 6.71 (m, 1H), 6.65 (s, 1H), 6.54 – 6.39 (m, 2H), 6.23 – 6.12 (m, 1H), 5.90 - 5.83 (m, 1H), 5.60 (dd, *J* = 8.4, 2.4 Hz, 1H), 5.22 (s, 2H), 4.43 (s, 1H), 3.07 – 2.91 (m, 2H), 1.51 – 1.36 (m, 2H), 1.23 (dt, *J* = 14.9, 7.5 Hz, 2H), 0.81 (dt, *J* = 22.3, 7.2 Hz, 3H).

^{13}C NMR (101 MHz, $CDCl_3$, 298 K) δ: 157.14, 157.08, 156.66, 154.67, 154.61, 151.44, 149.91, 148.79, 146.10, 140.36, 138.07, 137.98, 132.52, 128.63, 128.18, 123.23, 123.03,

122.59, 122.28, 122.20, 119.36, 116.50, 114.88, 114.71, 114.16, 113.97, 111.16, 98.43, 98.16, 97.77, 41.08, 30.70, 20.08, 13.75. HMRS [ESI+] ion $[C_{34}H_{29}F_4IrN_7]^+$ m/z calculated: 804.2044 Found: 804.2034 [M+].

Iridium complex 2

Iridium chloro-briged dimer made from ligand **8** (100 mg, 0.079 mmol) was combined with 2.1 equivalents of (1-(1H-benzo[d]imidazole-2-yl)-3-butylguanidine) ligand **7** (40 mg, 0.17 mmol) and 10 equivalents of potassium carbonate (106 mg, 0.79 mmol) were added to 12 mL of dry toluene and refluxed under nitrogen atmosphere for 18 hours. After the reaction was completed, it was cooled to room temperature and solvent was removed under reduced pressure. The solid was re-dissolved in dichloromethane and extracted with water, the organic phases were combined, and solvent removed under reduced pressure. The sample was dried and subjected to purification via column chromatography (neutral alumina as stationary phase, DCM: MeOH 10:0.5 as mobile phase). Fractions were collected (Rf = 0.43, DCM: MeOH, 10:0.5), and solvent was removed under reduced pressure. The product was dried in vacuo (Schlenk line) for 48 h. The final product **2** was obtained as a dark yellow powder in (36.1 mg, 55%) yield.

^{1}H NMR (400 MHz, $CDCl_3$, 298 K) δ: 8.78 (d, *J* = 6.4 Hz, 1H), 8.26 (d, *J* = 5.8 Hz, 1H), 8.15 (t, *J* = 3.9 Hz, 2H), 8.11 (s, 1H), 8.08 (d, *J* = 8.1 Hz, 1H), 7.91 – 7.85 (m, 1H), 7.83 – 7.78 (m, 1H), 7.73 – 7.68 (m, 2H), 7.21 (dt, *J* = 6.6, 3.7 Hz, 5H), 7.13 (t, *J* = 6.6 Hz, 2H), 6.93 (t, *J* = 7.7 Hz, 1H), 6.73 (s, 1H), 6.53 (s, 1H), 6.47 (t, *J* = 7.9 Hz, 1H), 6.15 (d, *J* = 8.3 Hz, 1H), 6.09 (s, 1H), 4.69 (s, 1H), 2.89 (ddd, *J* = 24.7, 15.2, 9.0 Hz, 3H), 1.41 (dd, *J* = 16.0, 6.9 Hz, 3H), 1.18 (dd, *J* = 15.1, 7.5 Hz, 2H), 0.76 (t, *J* = 7.3 Hz, 3H). ^{13}C NMR (101 MHz, $CDCl_3$, 298 K) δ: 168.30, 167.32, 150.54, 150.20, 149.06, 145.43, 145.25, 145.07,

144.57, 143.72, 140.39, 137.15, 136.99, 135.36, 135.25, 131.32, 130.20, 129.92, 129.76, 129.01, 128.93, 128.78, 126.74, 126.66, 125.96, 125.92, 124.15, 123.69, 123.62, 123.54, 123.14, 123.00, 122.70, 122.38, 119.83, 117.40, 110.61, 41.06, 30.73, 19.99, 13.77. HRMS m/z calculated: 832.2732. Found: 832.2734 [M+].

Iridium complex 3

Iridium chloro-bridged dimer made from ligand **10** (47 mg, 0.03 mmol), (1-(1H-benzo[d]imidazole-2-yl)-3-butylguanidine) ligand **7** (20 mg, 0.088 mmol), and potassium carbonate (48 mg, 0.35 mmol) were added to 5 mL of dry toluene and refluxed under nitrogen atmosphere for 18 hours. After the reaction was completed, it was cooled to room temperature and solvent was removed under reduced pressure. The solid was re-dissolved in dichloromethane and extracted with water, organic phases were combined, and dried over magnesium sulphate and solvent was removed under reduced pressure. The sample was dried and subjected to purification via column chromatography (neutral alumina as stationary phase, DCM: MeOH 10:0.5 as mobile phase). Fractions were collected (Rf = 0.18, DCM: MeOH, 10:0.5), and solvent was removed under reduced pressure. The product was dried in vacuo (Schlenk line) for 48 h. The final product **3** was obtained in (17.5 mg, 60%) yield as a dark red powder.

^{1}H NMR (400 MHz, $CDCl_3$, 298 K) δ 8.64 (d, *J* = 8.9 Hz, 1H), 8.28 (dd, *J* = 11.1, 7.3 Hz, 2H), 8.22 (d, *J* = 8.3 Hz, 1H), 8.01 (t, *J* = 8.5 Hz, 1H), 7.84 – 7.79 (m, 1H), 7.52 (d, *J* = 7.8 Hz, 1H), 7.45 – 7.35 (m, 2H), 7.34 – 7.28 (m, 1H), 7.21 (dd, *J* = 11.5, 7.6 Hz, 1H), 7.02 (ddd, *J* = 23.2, 14.7, 7.8 Hz, 3H), 6.88 – 6.79 (m, 1H), 6.44 – 6.37 (m, 1H), 5.71 (d, *J* = 8.3 Hz, 1H), 3.95 (br s, 1H), 2.97 (d, *J* = 9.6 Hz, 6H), 1.25 (s, 2H), 1.25 – 1.19 (m,

2H), 1.09 (dd, *J* = 15.2, 7.6 Hz, 2H), 0.71 (t, *J* = 7.3 Hz, 3H). ^{13}C NMR (400 MHz, $CDCl_3$, 298 K) δ: HRMS m/z calculated: 972.2488. Found: 972.2498 [M+].

Iridium complex 4

Iridium chloro-bridged dimer made from ligand **9** (118 mg, 0.088 mmol) was combined with 2.5 equivalents of (1-(1H-benzo[d]imidazole-2-yl)-3-butylguanidine) ligand **7** (51 mg, 0.22 mmol) and 10 equivalents of potassium carbonate (120 mg, 0.88 mmol) were added to 20 mL of dry toluene and refluxed under nitrogen atmosphere for 20 hours. After the reaction was completed, it was cooled to room temperature and solvent was removed under reduced pressure. The solid was re-dissolved in dichloromethane and extracted with water, organic phases were combined, and solvent was removed under reduced pressure (Figure 6). The sample was dried and subjected to purification via column chromatography (neutral alumina as stationary phase, DCM: MeOH 10:0.5 as mobile phase). Fractions were collected (Rf = 0.28, DCM: MeOH, 10:0.5), and solvent was removed under reduced pressure. The product was dried in vacuo (Schlenk line) for 48 h. The final product **4** was obtained in (41.4 mg, 54%) yield as a red powder.

^{1}H NMR (400 MHz, $CDCl_3$, 298 K) δ: 8.38 (d, *J* = 8.5 Hz, 1H), 7.97 (d, *J* = 8.2 Hz, 1H), 7.90 (d, *J* = 8.6 Hz, 1H), 7.78 (dd, *J* = 8.2, 1.2 Hz, 1H), 7.64 (s, 1H), 7.55 (s, 1H), 7.47 (d, *J* = 4.7 Hz, 1H), 7.40 (t, *J* = 7.6 Hz, 1H), 7.22 (dd, *J* = 9.6, 4.4 Hz, 2H), 7.08 (d, *J* = 4.8 Hz, 1H), 7.02 (d, *J* = 4.7 Hz, 1H), 7.00 (s, 1H), 6.95 (dd, *J* = 15.0, 7.2 Hz, 1H), 6.82 – 6.75 (m, 1H), 6.49(t, *J* = 7.8, Hz 1H), 6.36 (s, 1H), 6.07 (d, *J* = 4.8 Hz, 1H), 5.81 (d, *J* = 8.3 Hz, 1H), 4.21 (br s, 2H), 2.87 (s, 3H), 2.82 (s, 3H), 1.25 (br s, 1H), 1.23 – 1.16 (m, 2H), 1.07-1.02 (m, *J* = 14.9, 7.4 Hz, 2H), 0.72 (t, *J* = 7.3 Hz, 3H). ^{13}C NMR (101 MHz, $CDCl_3$, 298 K) δ: 165.97, 160.42, 155.06, 153.11, 149.93, 149.59, 147.78, 147.12, 146.90, 144.62,

140.39, 140.18, 139.11, 134.71, 132.07, 131.58, 131.04, 130.38, 130.09, 128.66, 127.39, 126.74, 126.51, 125.64, 125.44, 125.09, 124.70, 124.37, 122.56, 122.26, 118.88, 118.02, 115.58, 111.00, 40.85, 30.55, 19.96, 19.25, 19.02, 13.63. HRMS m/z calculated: 872.2176. Found: 872.2202 [M+].

Pyrimido[4,5-c]isoquinolin-3-amine – Compound 5

5-iodopyrimidine-2,4-diamine (197 mg, 0.834 mmol), 2-formylphenylboronic acid (182 mg, 1.2 mmol), potassium carbonate (461 mg, 3.3 mmol) and tetrakis(triphenylphosphine)palladium(0) (1.40 mg, 0.5 mol%) were added to a mixture of dioxane and water (3:1, 9 mL of dioxane, 3 mL of water). The reaction mixture was heated under reflux for 3 h, then cooled to room temperature and placed in a cold bath. The precipitate was filtered and washed with water (2 x 30 mL), three times suspended and sonicated in water and filtered, then finally dried in a vacuum oven (24 h, 40 °C).

Product **5** (82 mg) was obtained as a fine bright yellow powder in (81.8 mg, 50%) yield. ^{1}H NMR (400 MHz, 298K, DMSO-d_6): δ 9.88 (s, 1H), 9.50 (s, 1H), 8.72 (d, 1H, J = 8.1 Hz), 8.17 (d, 1H, J = 7.5 Hz), 7.92 (ddd, 1H, J = 8.4, 7.3, 1.3 Hz), 7.70 – 7.63 (m, 1H), 7.18 (s, 2H).^{13}C NMR (100 MHz, 298 K, DMSO-d_6): δ 163.68, 161.43, 158.80, 158.50, 132.58, 132.22, 129.33, 126.43, 124.43, 124.41, 120.35, 107.00. EI-MS m/z calcd.: 196.07 found: 197.08 [M+]. M.p. > 280°C. Anal. calcd. for $C_{11}H_8N_4$: C, 67.34; H, 4.11; N, 28.55. Found: C, 67.19; H, 4.25; N, 28.35.

1-(1H-Benzo[d]imidazole-2-yl)-3-butylthiourea – Compound 6

A previously reported procedure was employed for the synthesis of **6**.[2] N- (benzoimidazol-2-yl)imidazole-1-carbothioamide (0.50 g, 2.1 mmol) and catalytic DMAP (25 mg, 0.2

mmol, 0.1 eq) were dissolved in 2 mL of DMF. Next, n-butyl amine (0.22 mL, 2.2 mmol) was slowly added dropwise while stirring. The reaction mixture was stirred at 100°C under N_2 for 18 hours. After cooling down to room temperature, the reaction mixture was poured over ice and stirred for 1 hour. A white-milky color precipitate was filtered and was washed with water (2 x 15 mL) and further purified by column chromatography (EtOAc / hexane, 3:2, Rf = 0.2). Fractions were collected and the solvent removed by rotary evaporation. The product **6** was dried in a vacuum oven at 40 °C overnight. Pale yellow title compound **6** was obtained in (364.7 mg, 70%) yield.

^{1}H NMR (400 MHz, 298 K, DMSO-d_6): δ 11.26 (br s, 1H), 11.15 (br s, 1H), 10.97 (br s, 1H), 7.44 (s, 2H), 7.19 – 7.04 (m, 2H), 3.64 (d, 2H, J = 5.8 Hz), 1.69 – 1.53 (m, 2H), 1.46 – 1.32 (m, 2H), 0.94 (t, 3H, J = 7.3 Hz). ^{13}C NMR (100 MHz, 298 K, DMSO-d_6): δ 177.82, 148.19, 140.39, 131.32, 121.78, 116.91, 111.45, 44.36, 39.52, 30.59, 19.94, 13.92. M.p. 147-150°C. EI-MS m/z calcd.: 247.10 found: 248.11 [M+]. Anal. calcd. for $C_{12}H_{16}N_4S$: C, 58.04; H, 6.49; N, 22.56. Found: C, 57.93; H, 6.54; N, 22.40.

1-(1H-benzo[d]imidazole-2-yl)-3-butylguanidine – Compound 7

From a modified procedure,[2] compound **6** (0.27 g, 1.08 mmol) was suspended in 15 mL of $CHCl_3$ and to this were added HgO (0.32 g, 1.51 mmol) and 2 M methanolic NH_3 (6 mL). The reaction mixture was stirred at room temperature for 3 h and a color change from wine red to brown was observed. The reaction was then filtered through celite and concentrated under reduced pressure. The resulting solid was dissolved in 2 M acetic acid (~ 8 mL) and stirred for 1 h, then filtered through celite. The pH was adjusted to 8.0 by addition of a 10 M solution of NaOH. The formed precipitate was filtered, washed with water and dried. The product was dissolved in chloroform and extracted 3 x with saturated

solution of $NaHCO_3$. The organic phase was separated and dried over $MgSO_4$ and the solvent removed under reduced pressure. The final product was dried overnight in a vacuum oven at 40°C. Compound **7** was obtained as white powder in (31.2 mg, 50%) yield.

^{1}H NMR (400 MHz, 298 K, DMSO-d_6): δ 11.00 (s, 1H), 7.20 (d, 1H, *J* = 7.3 Hz), 7.07 (d, 1H, *J* = 7.1 Hz), 6.98 – 6.78 (m, 2H), 3.21 (dd, 2H, *J* = 12.7, 6.9 Hz), 1.48 (dd, 2H, *J* = 14.8, 7.3 Hz), 1.36 (dt, 2H, *J* = 14.7, 7.2 Hz), 0.92 (t, 3H, *J* = 7.3 Hz). ^{13}C NMR (100 MHz, 298K, DMSO-d_6): δ 159.05, 157.66, 142.59, 132.21, 119.65, 118.99, 114.94, 108.48, 40.07, 39.52, 31.49, 19.66, 13.80. M.p. 190-208°C. EI-MS m/z calculated: 231.15 found: 232.16 [M+]. Anal. calcd. for $C_{12}H_{17}N_5$: C, 62.31; H, 7.41; N, 30.28. Found: C, 62.12; H, 7.55; N, 30.06.

2-Napthalen-2-yl pyridine – Compound 8

Napthalen-2-yl-boronic acid (163 mg, 0.95 mmol), tetrakis(triphenylphosphine) palladium (0.5 mol%, 5.4 mg) and sodium carbonate (201 mg, 2 eq) were added together to mixture of ethanol and deionized water (1.3: 0.8 mL). 2-bromopyridine (0.1 mL, 0.95 mmol) was added dropwise (syringe) into the reaction tube (Vial Type G10). The tube was sealed and placed into a microwave reactor, and the reaction was monitored through the built-in camera. Reaction conditions were set for 150°C, 15 min and the cooling process was set to reach 55°C. After completion of the microwave process, the tube was placed in an ice-cold bath and stirred for 1 h to support the formation of precipitate (Figure 12). The precipitate was collected and washed multiple times with water and air dried (Figure 12). The product was further purified through flash column chromatography (silica, DCM, Rf =

0.44). Fractions were combined and solvent removed under reduced pressure. Final product **8** was obtained as off-white powder in (130.6 mg, 67%) yield.

^{1}H NMR (400 MHz, $CDCl_3$, 298 K) δ: 8.76 (d, *J* = 4.7 Hz, 1H), 8.50 (s, 1H), 8.15 (dd, *J* = 8.6, 1.7 Hz, 1H), 7.96 (d, *J* = 8.4 Hz, 2H), 7.87 (d, *J* = 8.0 Hz, 2H), 7.78 (td, *J* = 7.8, 1.7 Hz, 1H), 7.52 (dd, *J* = 6.1, 3.4 Hz, 2H), 7.26 (t, *J* = 6.1 Hz, 1H). ^{13}C NMR (101 MHz, $CDCl_3$, 298 K) δ: 157.43, 149.88, 136.92, 136.78, 133.76, 133.63, 128.83, 128.56, 127.78, 126.63, 126.44, 126.41, 124.67, 122.26, 120.93, 77.16.

4-methyl-2-thiophen-2-yl-quinoline – Compound 9

Thiophen-2-yl-boronic acid (0.73 g, 5.3 mmol), 2-chloro-4-methylquinoline (0.85 g, 4.7 mmol) and $Pd(PPh_3)_4$ (3 mol%) was added to 20 mL of THF and 2M aqueous Na_2CO_3 solution (9 mL). Nitrogen was bubbled through the reaction mixture before the reflux started. After 24h, the reaction mixture was cooled to room temperature (the colour of the solution was very dark- almost black). The mixture was filtered through celite before extraction with water/EtOAc. The organic phases were combined and dried over magnesium sulfate and solvent was removed under reduced pressure. TLC control of the crude mixture revealed only one spot but from the ^{1}H NMR minor impurities were present. The crude mixture was subjected to column chromatography (silica, DCM) and fractions were collected. Fractions containing the desired product (Rf = 0.78, DCM) were combined and solvent was removed under reduced pressure. The final product **9** was obtained in (741.3 mg, 70%) yield as a clear oil with a little hint of yellow. Characterization data matched those reported in literature.

^{1}H NMR (400 MHz, $CDCl_3$, 298 K) δ: 8.09 (d, *J* = 9.0 Hz, 1H), 7.95 (dd, *J* = 8.3, 1.0 Hz, 1H), 7.73 (dd, *J* = 3.7, 1.1 Hz, 1H), 7.68 (ddd, *J* = 8.4, 6.9, 1.4 Hz, 1H), 7.65 (d, *J* = 0.8

Hz, 1H), 7.50 (ddd, *J* = 8.2, 6.9, 1.3 Hz, 1H), 7.45 (dd, *J* = 5.0, 1.1 Hz, 1H), 7.16 (dd, *J* = 5.0, 3.7 Hz, 1H), 2.74 (s, 3H). ^{13}C NMR (101 MHz, $CDCl_3$, 298 K) δ: 152.16, 148.11, 144.83, 129.98, 129.61, 128.47, 128.15, 127.48, 126.00, 125.78, 123.76, 118.44, 19.08.

Benzo-thiophen-2-yl-4-methylquinoline – Compound 10

To one equivalent of 2-chloro-4-methylquinoline (1.28 g, 7.25 mmol) with 1.2 equivalents of benzo[b]thiophene-2-boronic acid in 30 mL of dry THF, 6 mol% of $Pd(PPh_3)_4$ was added. A 5% solution of Na_2CO_3 (~ 10 mL) was added to the mixture and nitrogen was bubbled through (15 min) prior to the reaction start. The reaction was refluxed for one day (25 h), under nitrogen atmosphere. After being cooled down, the mixture was poured into water and the organic part was extracted with ethyl acetate. The organic layers were combined, dried over magnesium sulphate, and solvent was removed under reduced pressure. The crude mixture was dark red/brown with an oily texture. The product was further purified with column chromatography (Rf = 0.6, EtOAc: hexane, 2:8) and solvent removed under reduced pressure. The product was then recrystallised from diethyl ether. The final product **10** was obtained in (1.5 g, 74%) yield as off-white crystals.

^{1}H NMR (400 MHz, $CDCl_3$, 298 K) δ: 8.80 (d, *J* = 8.1 Hz, 1H), 8.23 (d, *J* = 8.4 Hz, 1H), 8.02 (d, *J* = 8.7 Hz, 1H), 7.93 (d, *J* = 5.9 Hz, 2H), 7.75 (t, *J* = 7.6 Hz, 1H), 7.67 (s, 1H), 7.58 (t, *J* = 7.6 Hz, 1H), 7.50 (t, *J* = 7.6 Hz, 1H), 7.43 (t, *J* = 7.5 Hz, 1H), 2.78 (s, 3H). ^{13}C NMR (101 MHz, $CDCl_3$, 298 K) δ: 154.38, 148.10, 144.79, 141.03, 137.70, 136.94, 130.30, 129.53, 127.39, 127.27, 126.27, 125.04, 124.90, 124.84, 123.78, 122.73, 121.64, 77.48, 77.16, 77.16, 76.84, 19.06. HRMS m/z calculated: 276.0841. Found: 276.0840 [M+]. Anal.Calcd for $C_{18}H_{13}NS$: C, 78.51; H, 4.76; N, 5.09. Found: C, 78.28; H, 4.63; N, 5.08.

S3. ^{1}H and ^{13}C NMR Spectra, Mass Spectra, Elemental Analysis and Crystallographic Data

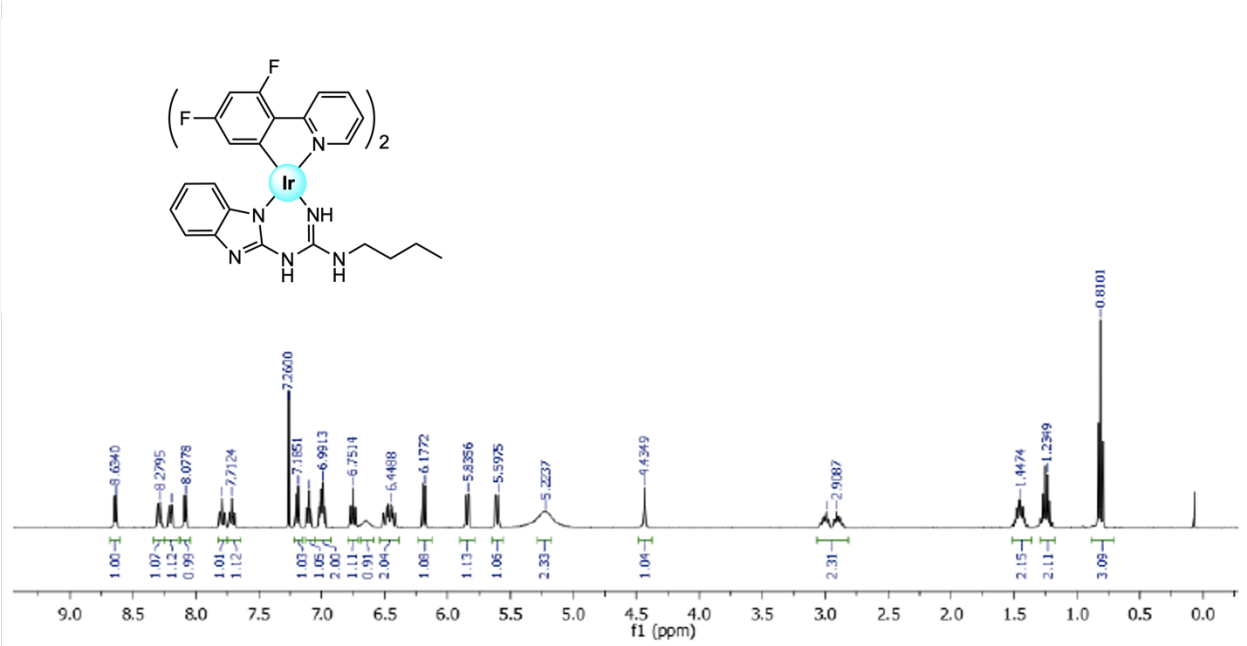

Figure S1. ^{1}H NMR spectrum of blue iridium complex **1**, $CDCl_3$, 400 MHz, 298 K.

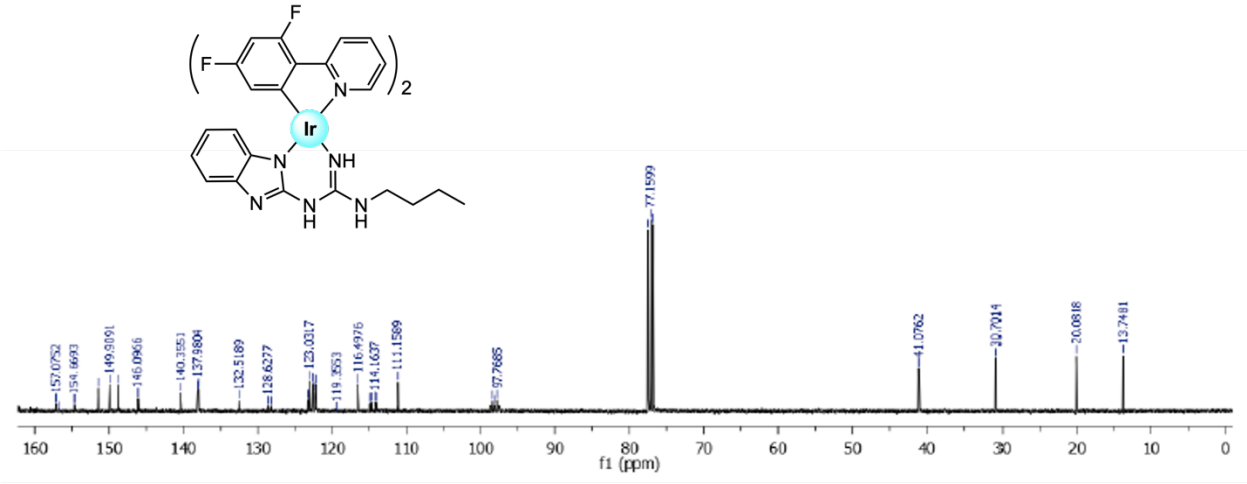

Figure S2. ^{13}C NMR spectrum of blue iridium complex **1,** $CDCl_3$, 101 MHz, 298 K.

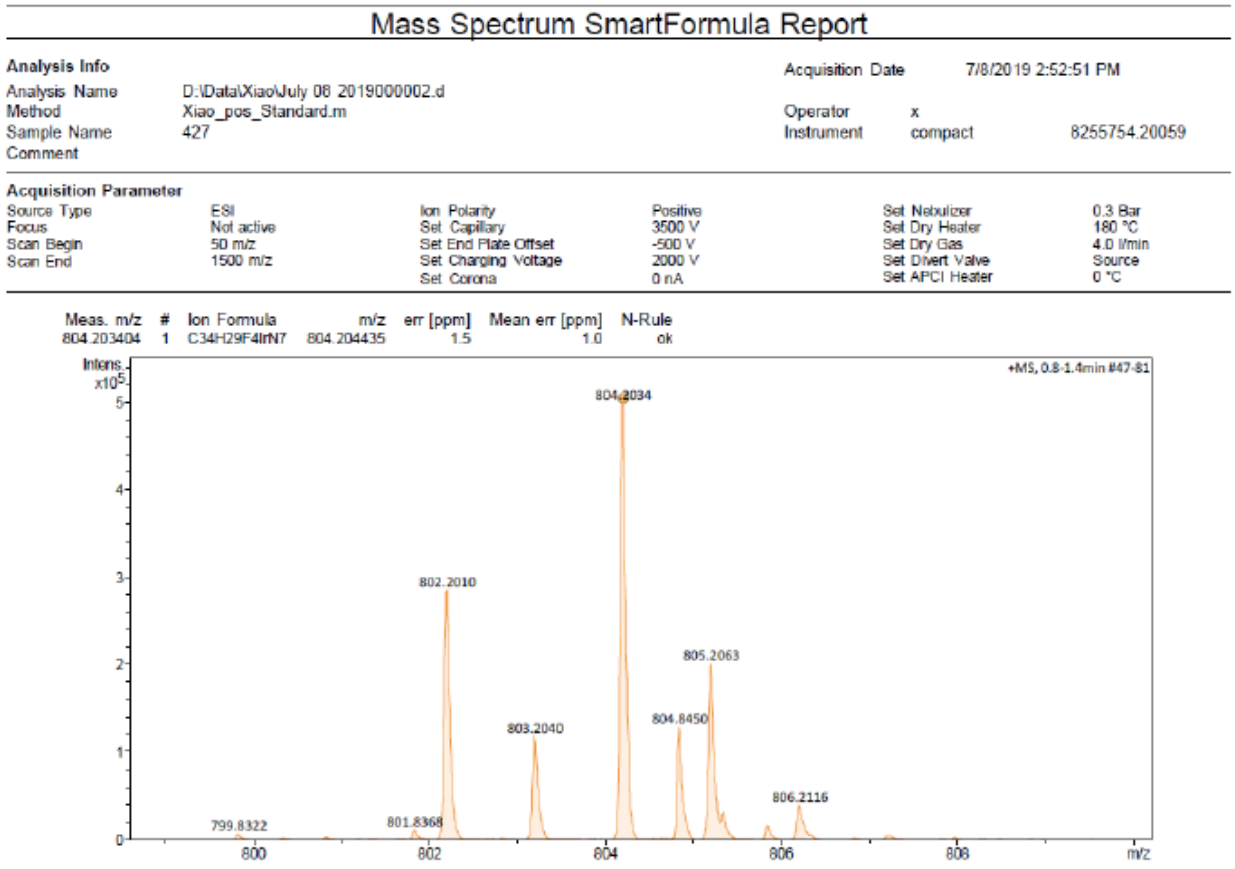

Figure S3. Mass spectrum of iridium complex **1**. HMRS [ESI+] ion $[C_{34}H_{29}F_4IrN_7]^+$ m/z calculated: 804.2044 Found: 804.2034 [M+].

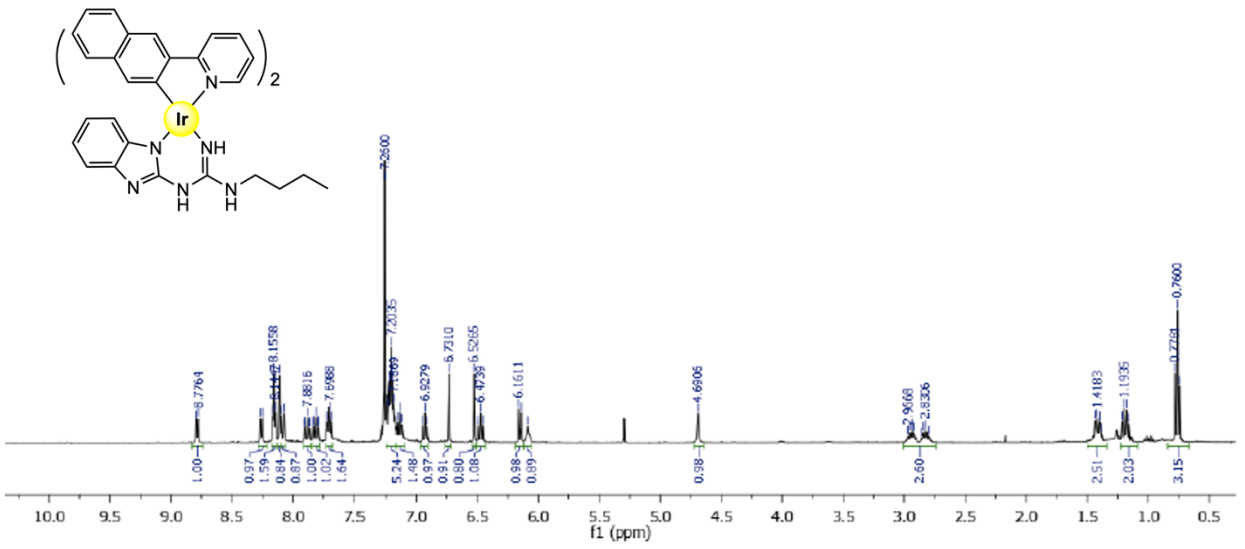

Figure S4. ^{1}H NMR spectrum of yellow iridium complex **2**, $CDCl_3$, 400 MHz, 298 K.

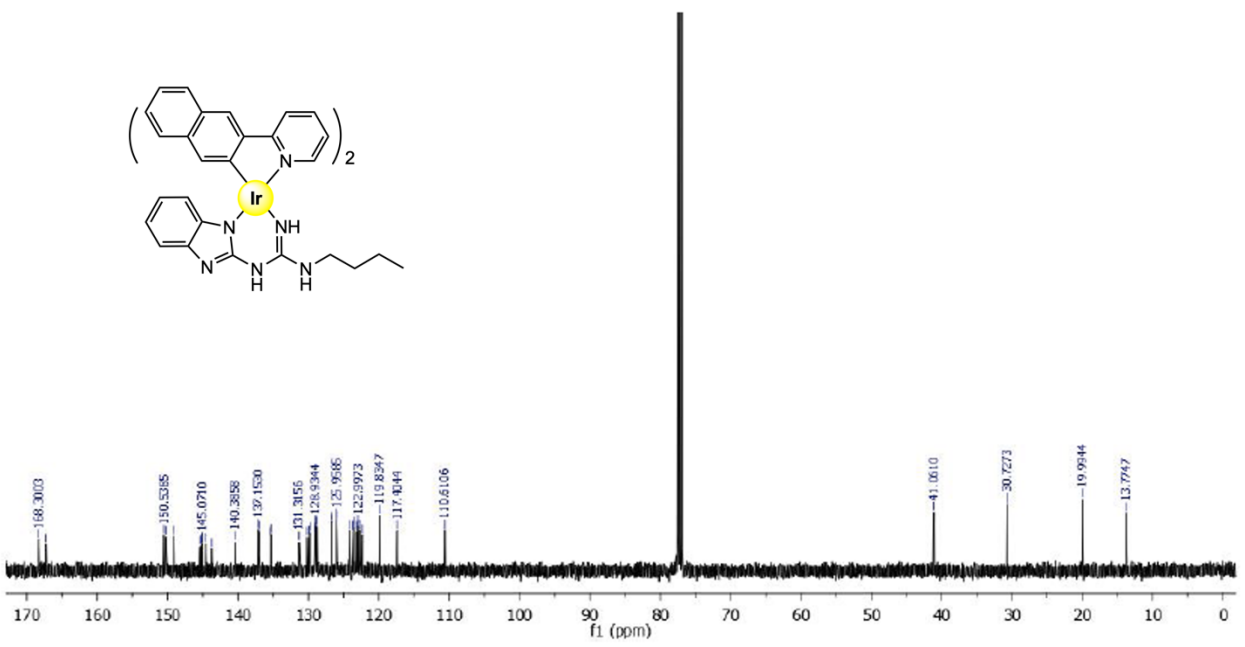

Figure S5. ^{13}C NMR spectrum of yellow iridium complex **2**, $CDCl_3$, 101 MHz, 298 K.

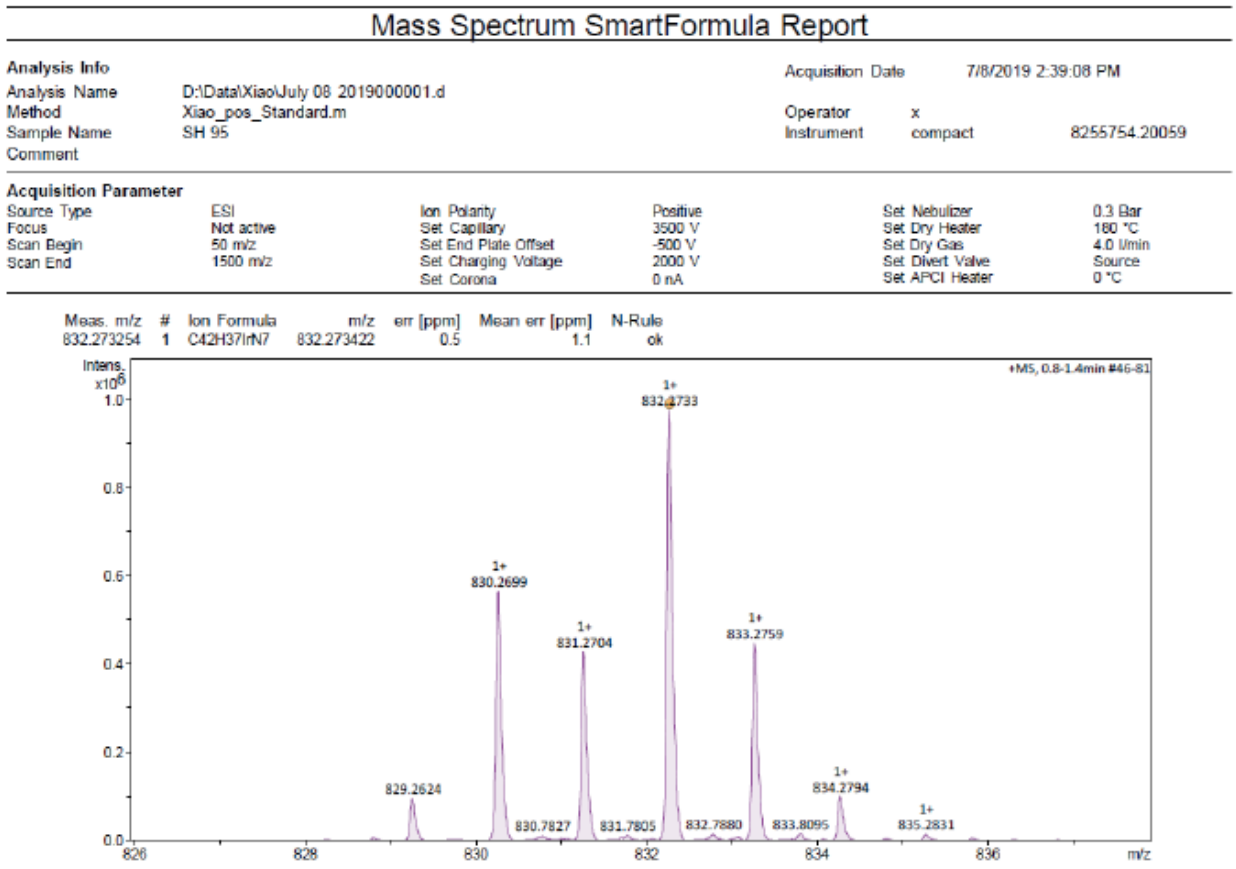

Figure S6. Mass spectrum of iridium complex **2**. HMRS [ESI+] ion $[C_{42}H_{37}IrN_7]^+$ m/z calculated: 804.2732 Found: 832.1733 [M+].

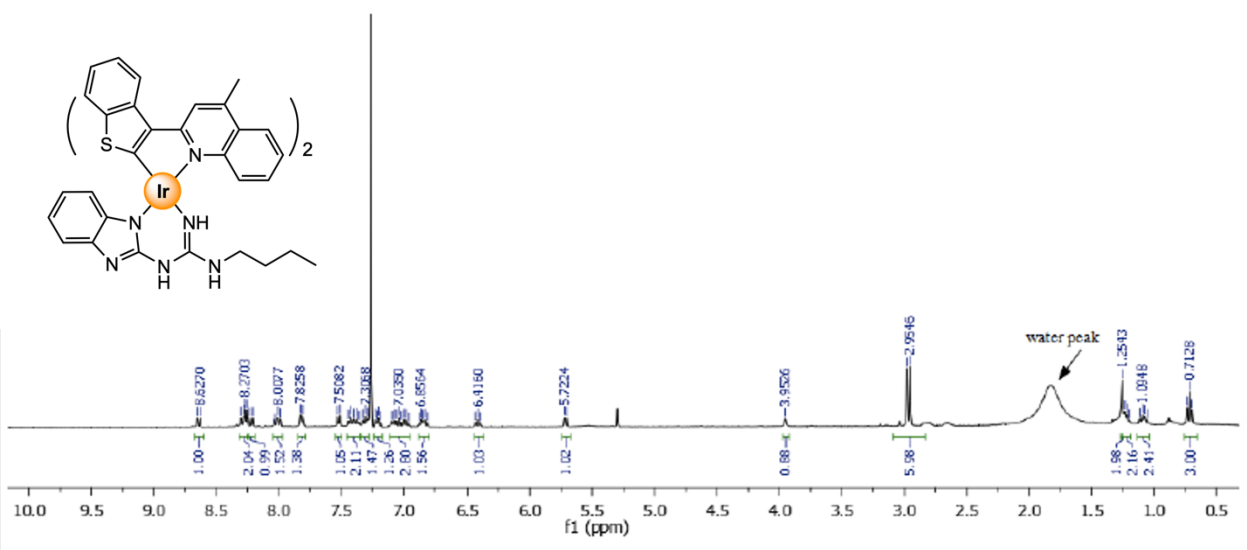

Figure S7. ^{1}H NMR spectrum of orange iridium complex **3**, $CDCl_3$, 400 MHz, 298 K.

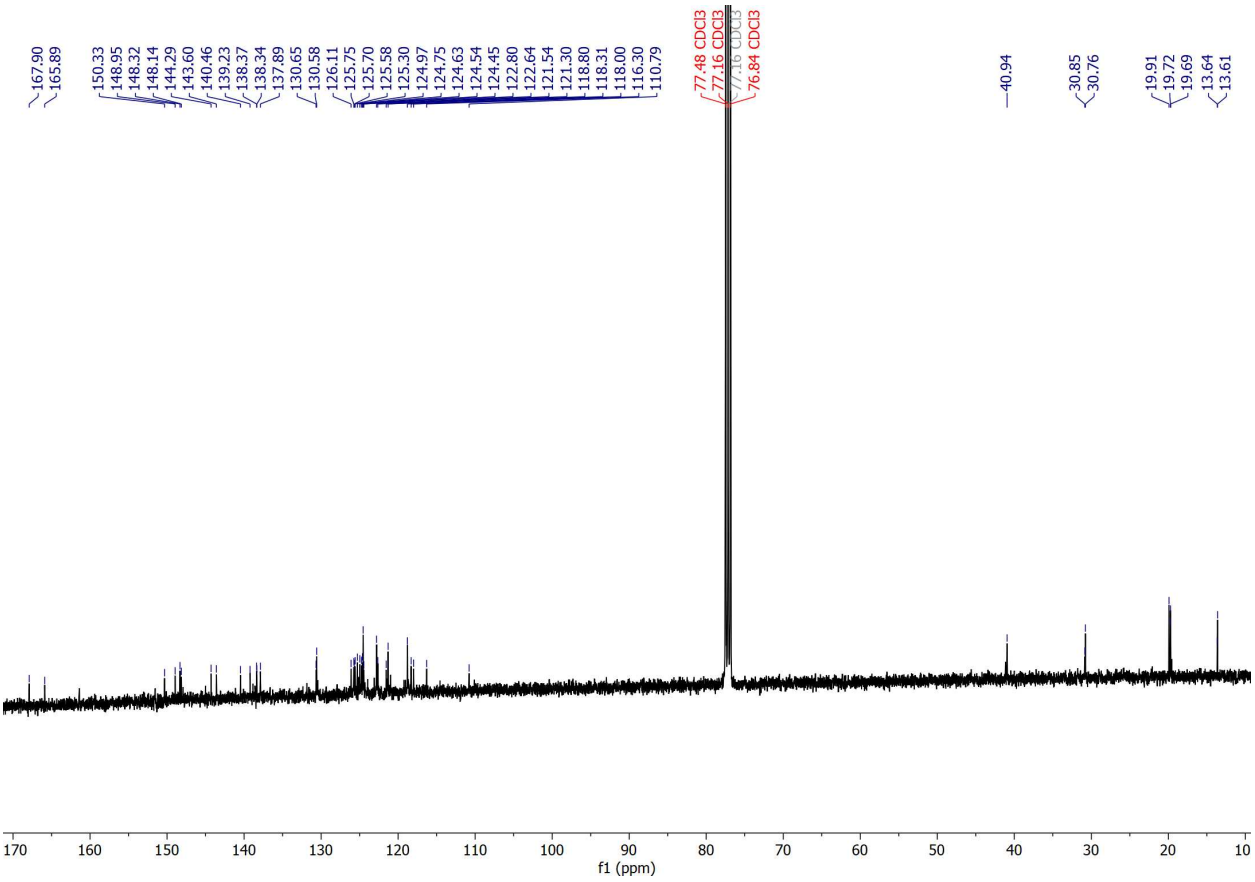

Figure S8. ^{13}C NMR spectrum of orange iridium complex **3**, $CDCl_3$, 101 MHz, 298 K.

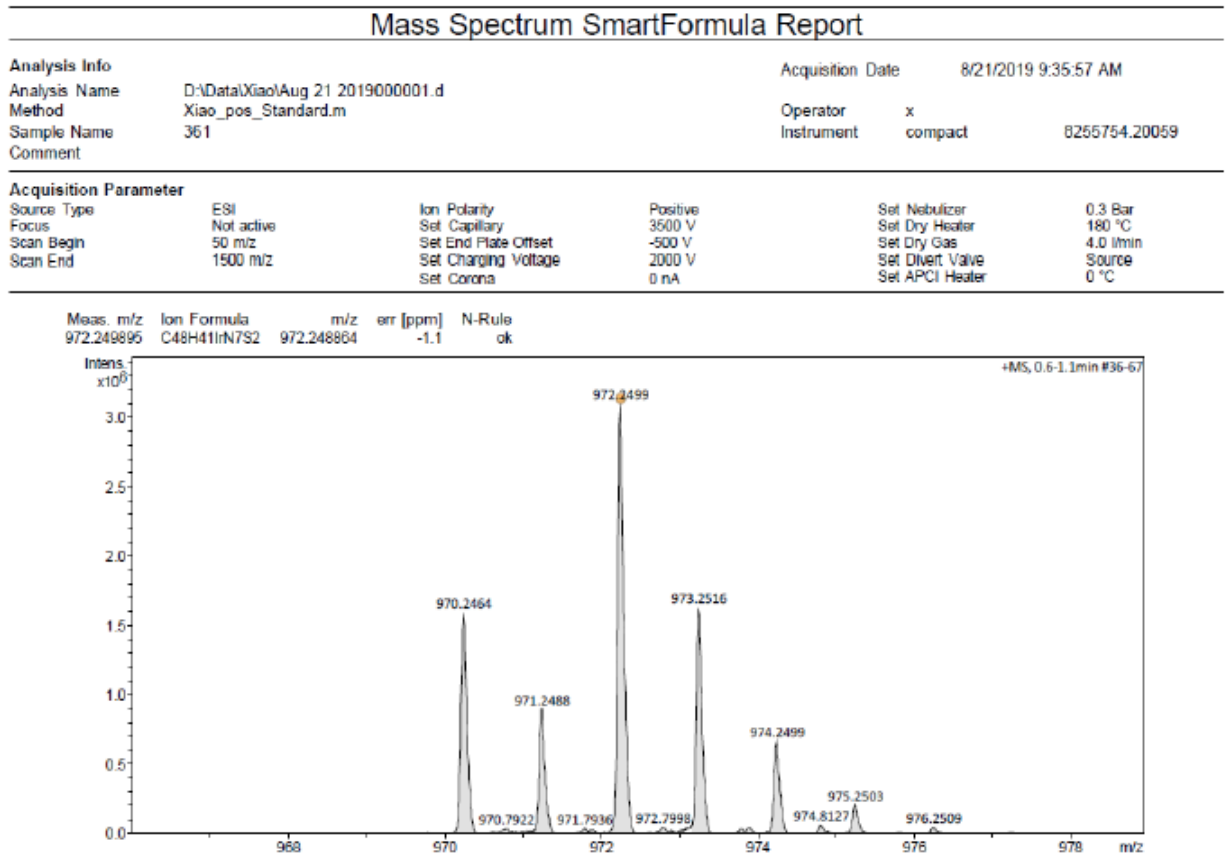

Figure S9. Mass spectrum of iridium complex **3**. HMRS [ESI+] ion $[C_{48}H_{41}IrN_7S_2]^+$ m/z calculated: 972.2488. Found: 972.2498 [M+].

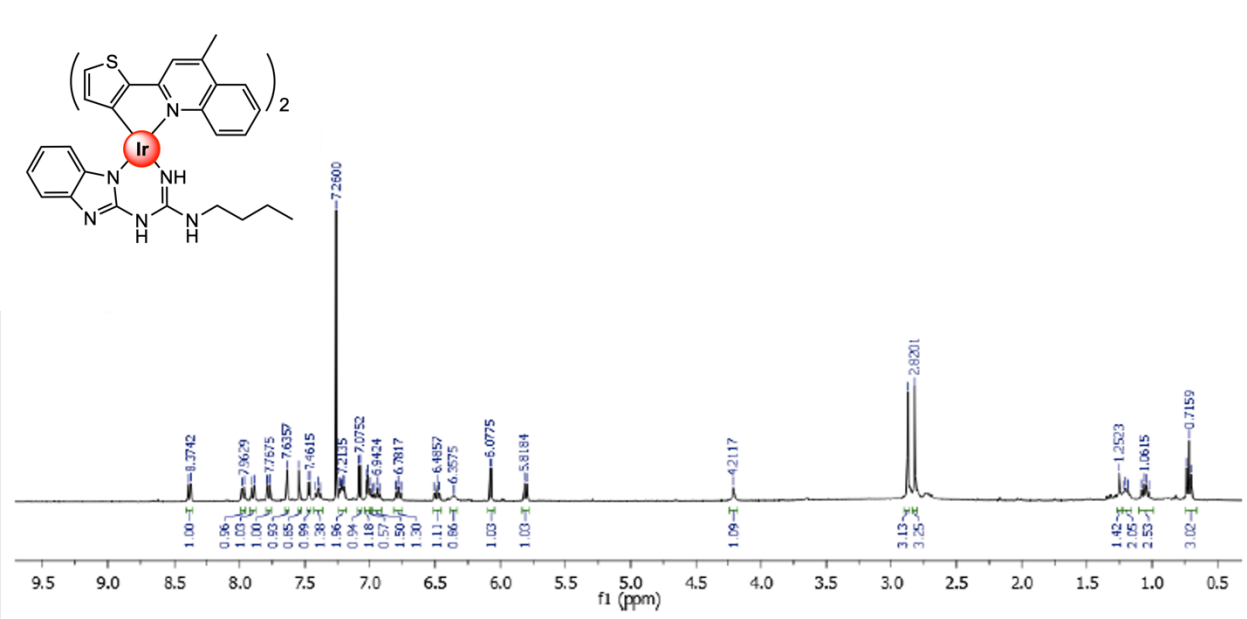

Figure S10. ^{1}H NMR spectrum of red iridium complex **4**, $CDCl_3$, 400 MHz, 298 K.

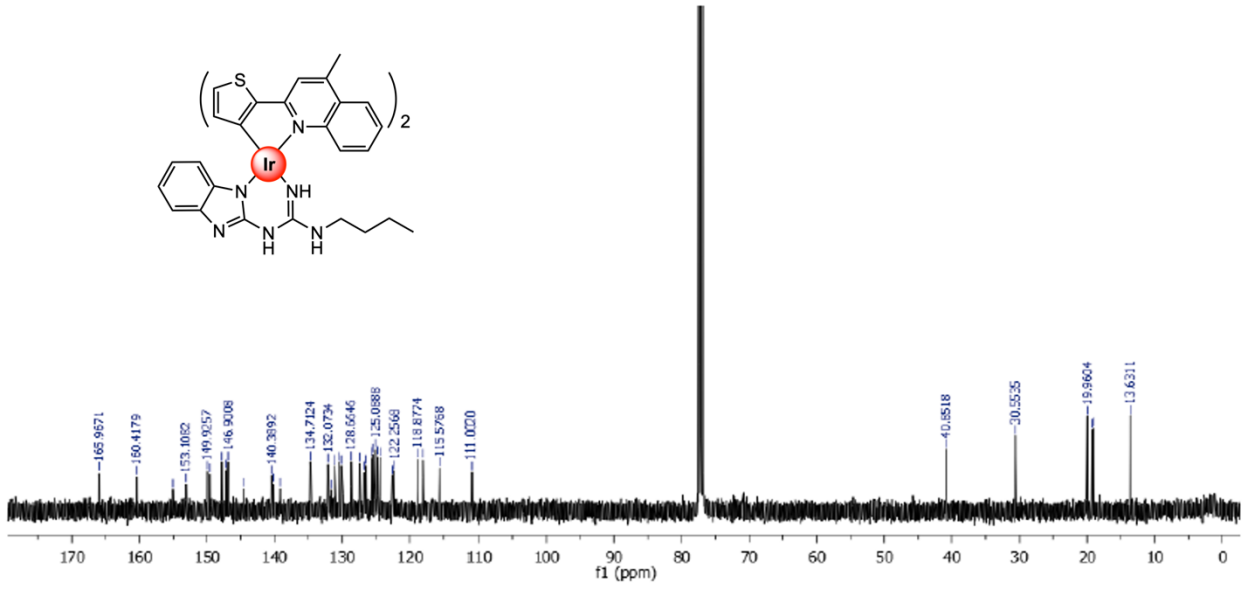

Figure S11. ^{13}C NMR spectrum of red iridium complex **6**, $CDCl_3$, 101 MHz, 298 K.

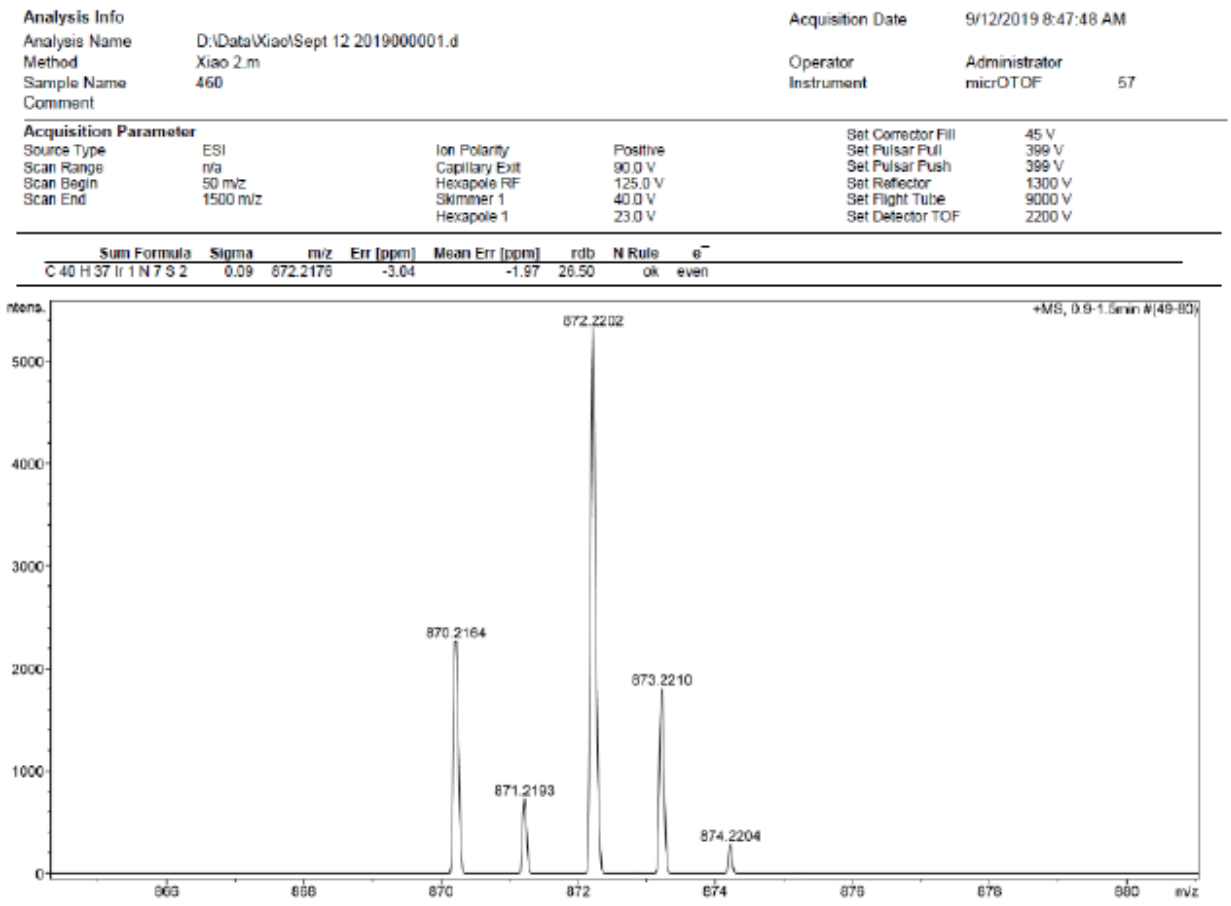

Figure S12. Mass spectrum of iridium complex **4**. HMRS [ESI+] ion $[C_{48}H_{41}IrN_7S_2]^+$ m/z calculated: 872.2176. Found: 872.2202 [M+].

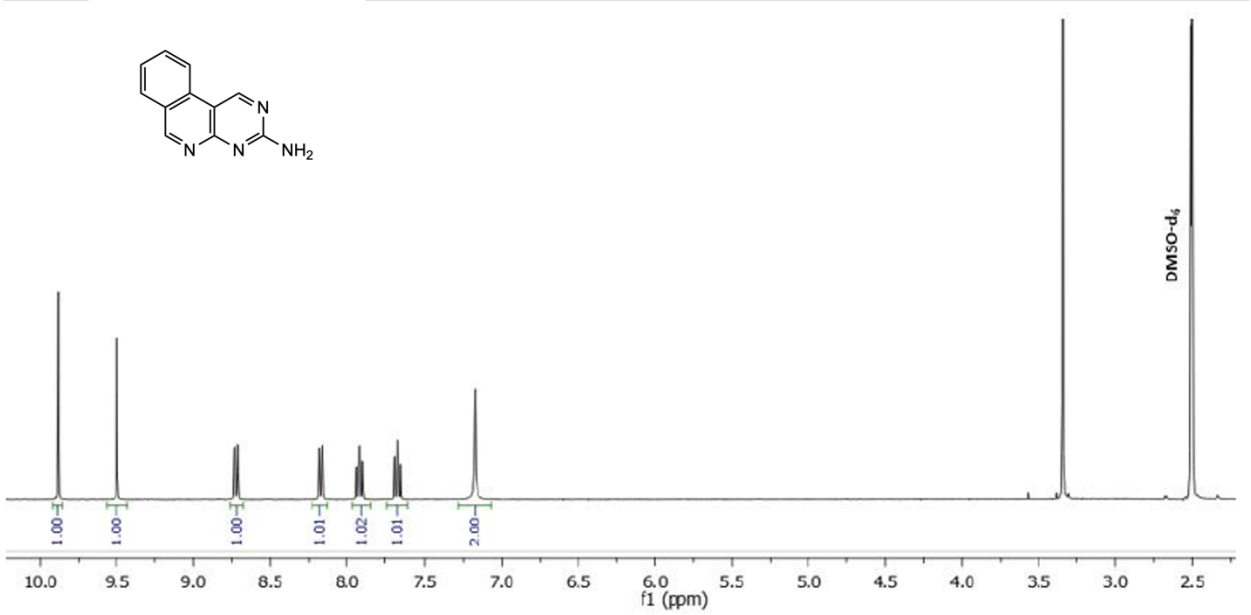

Figure S13. ^{1}H NMR spectrum of compound **5,** DMSO-d_6, 400 MHz, 298 K.

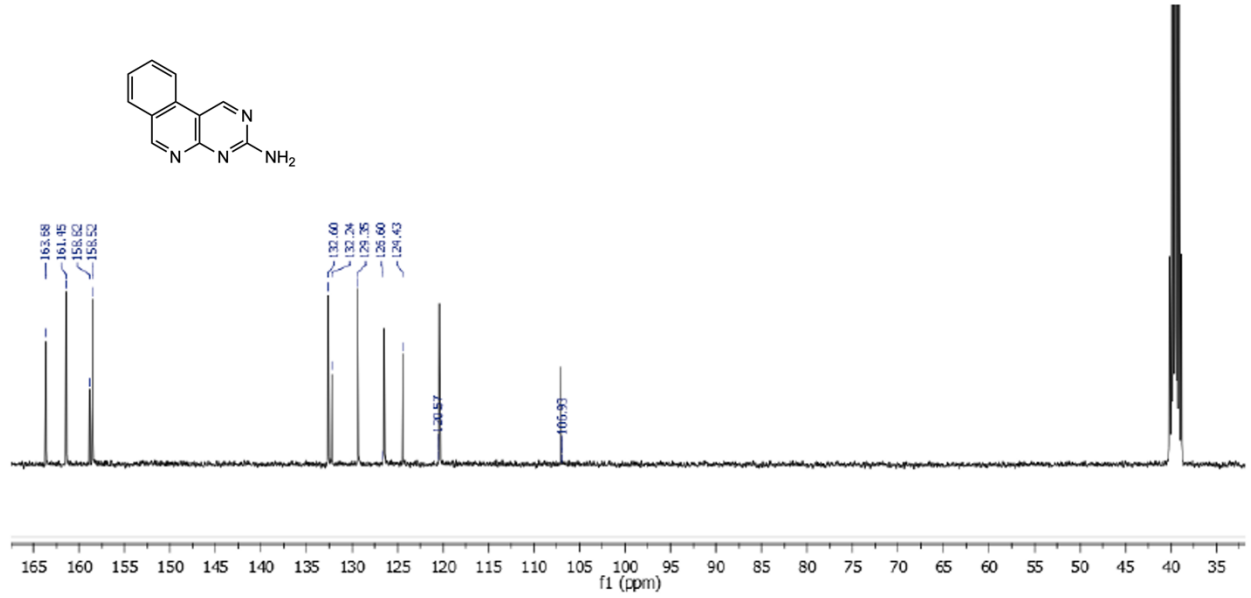

Figure S14. ^{13}C NMR spectrum of compound **5**, DMSO-d_6, 101 MHz, 298 K.

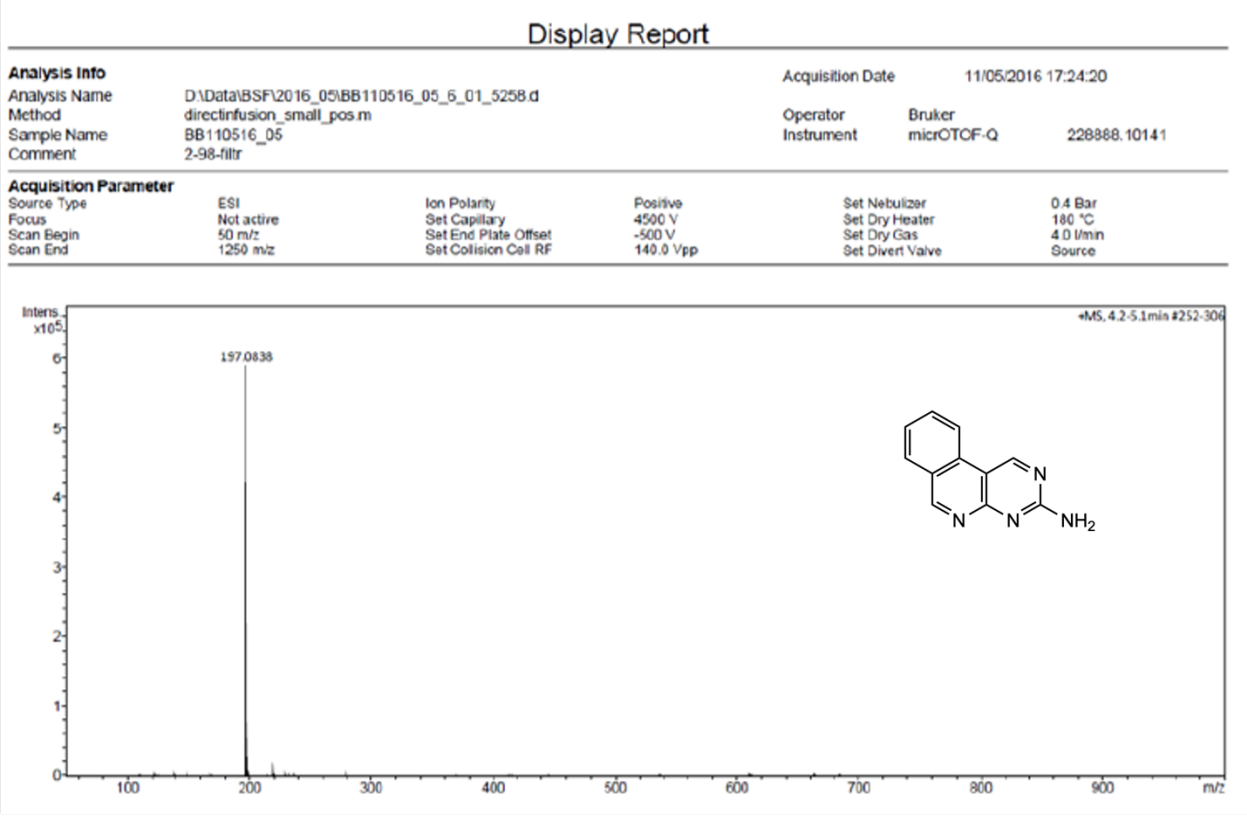

Figure S15. Mass spectrum for compound **5**. LMRS [ESI+] ion $[C_{11}H_8N_4]^+$

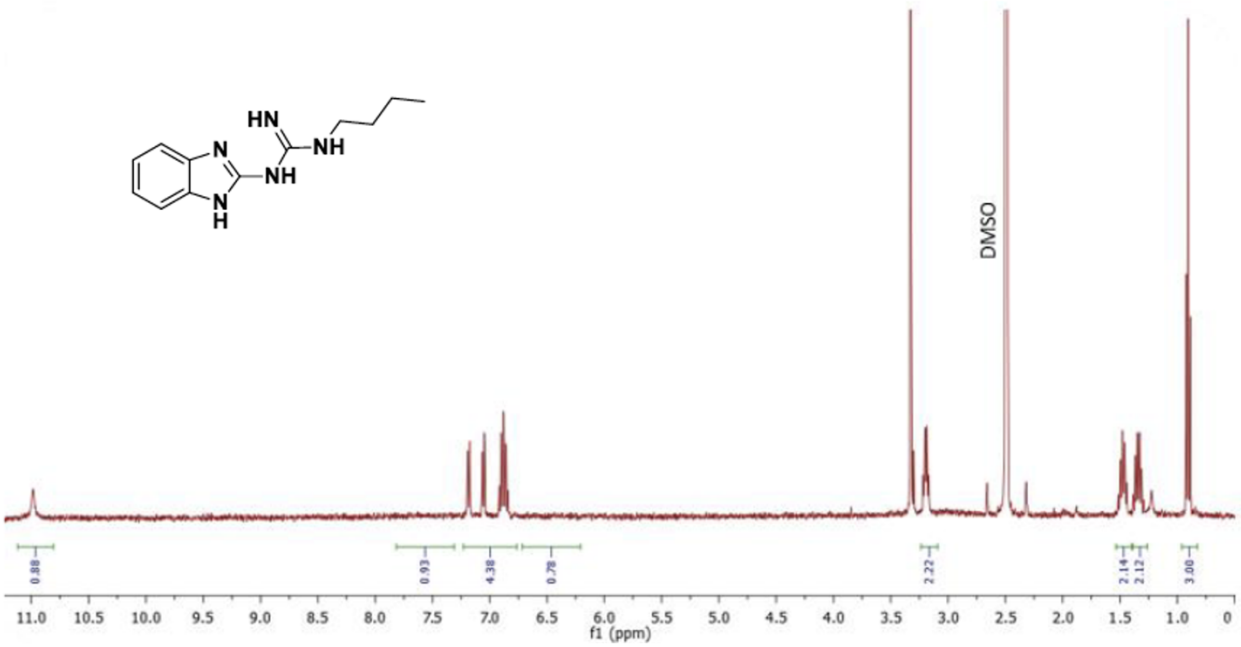

Figure S16. ^{1}H NMR spectrum of compound **7** DMSO-d_6, 400 MHz, 298 K**.**

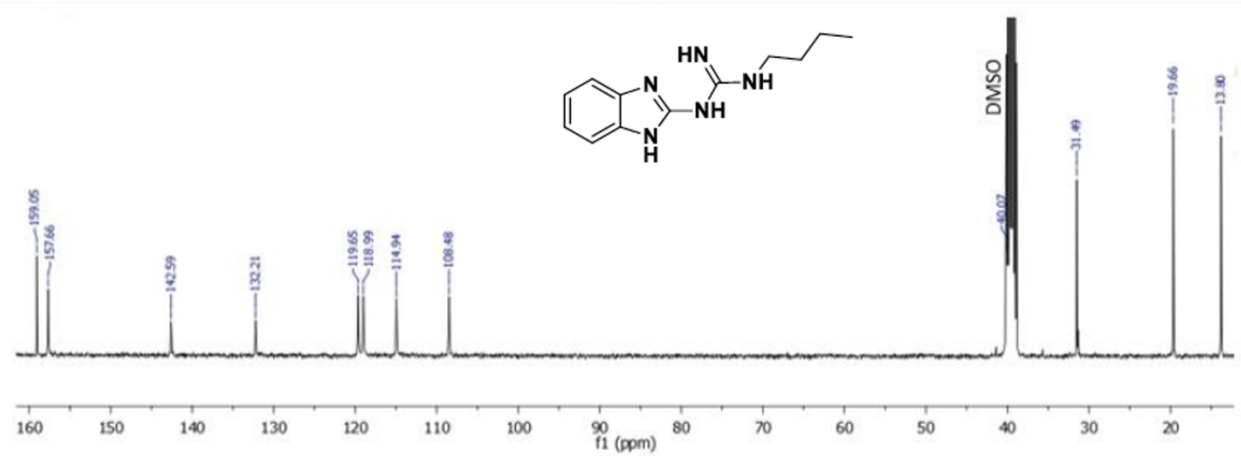

Figure S17. ^{13}C NMR spectrum of compound **7** DMSO-d_6, 101 MHz, 298 K**.**

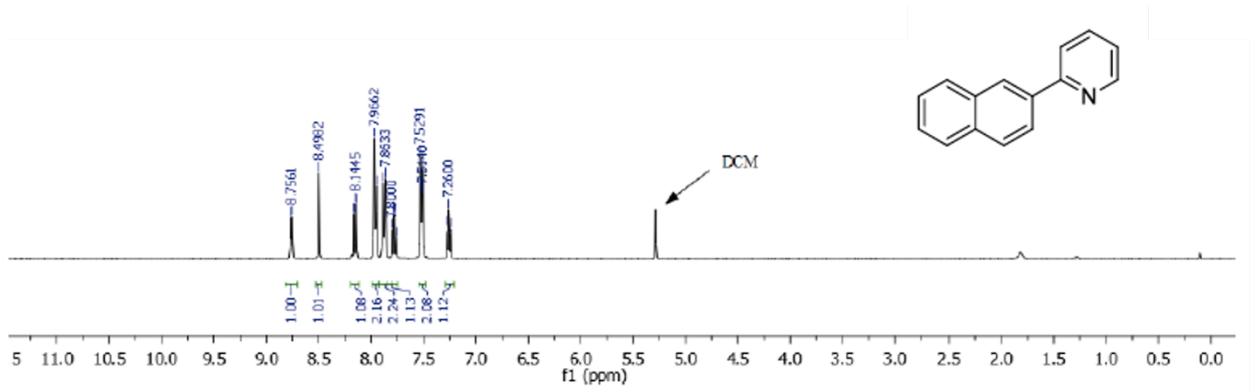

Figure S18. ^{1}H NMR spectrum of compound **8,** $CDCl_3$, 400 MHz, 298 K.

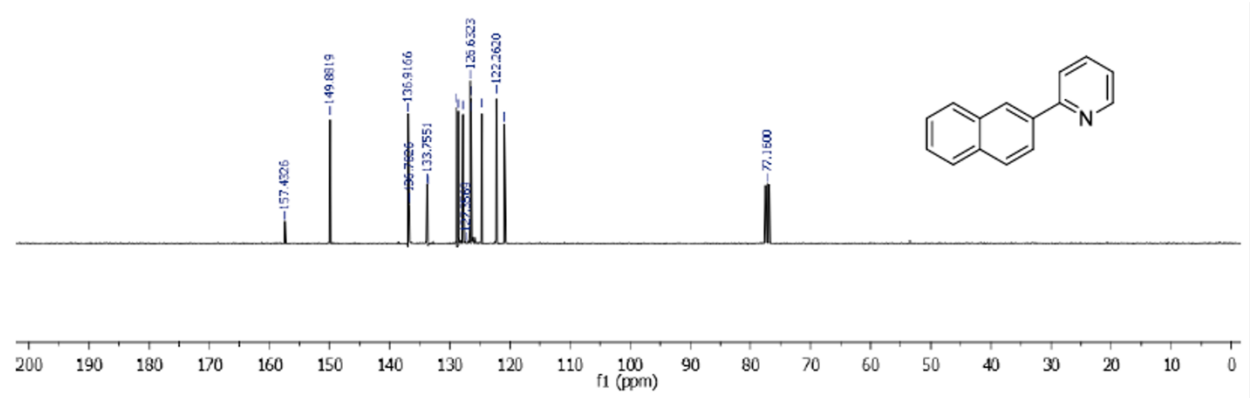

Figure S19. ^{13}C NMR spectrum of compound **8,** $CDCl_3$, 101 MHz, 298 K.

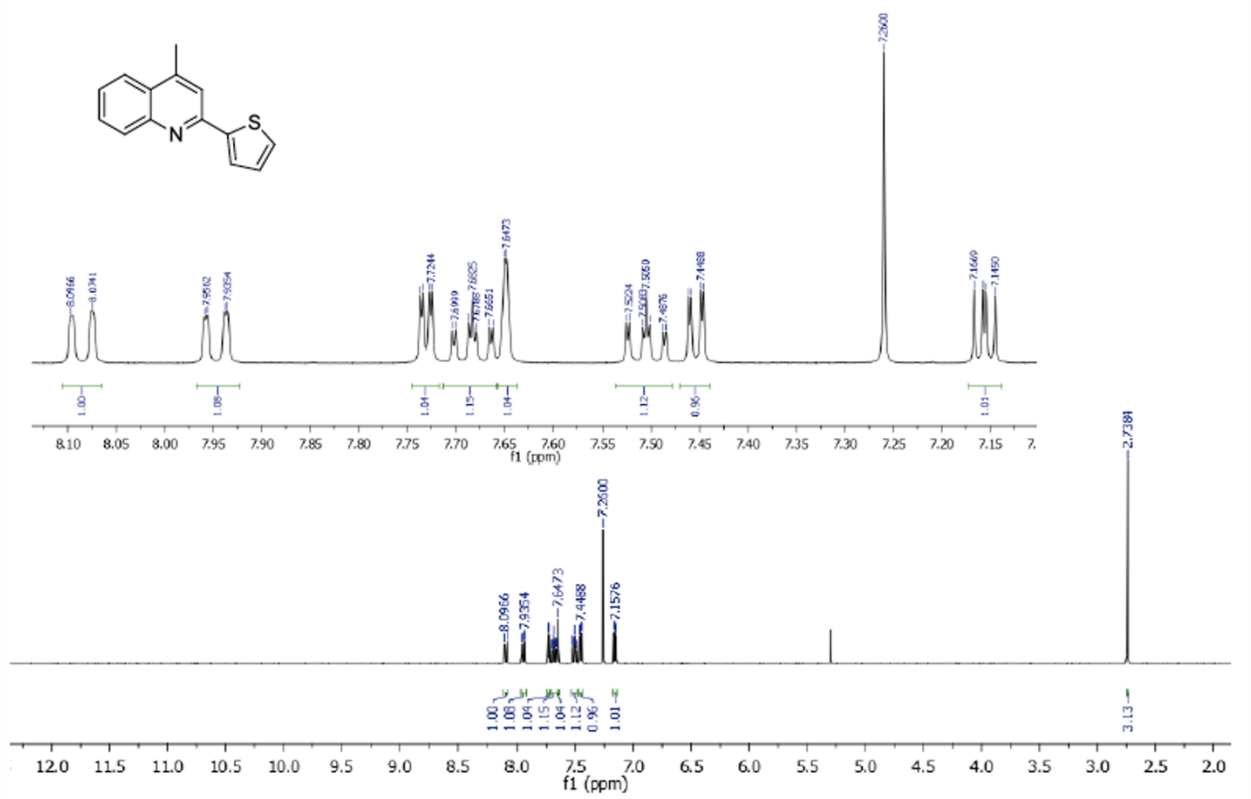

Figure S20. ^{1}H NMR spectrum of compound **9** with inset ^{1}H NMR spectrum expanded into aromatic region, $CDCl_3$, 400 MHz, 298 K.

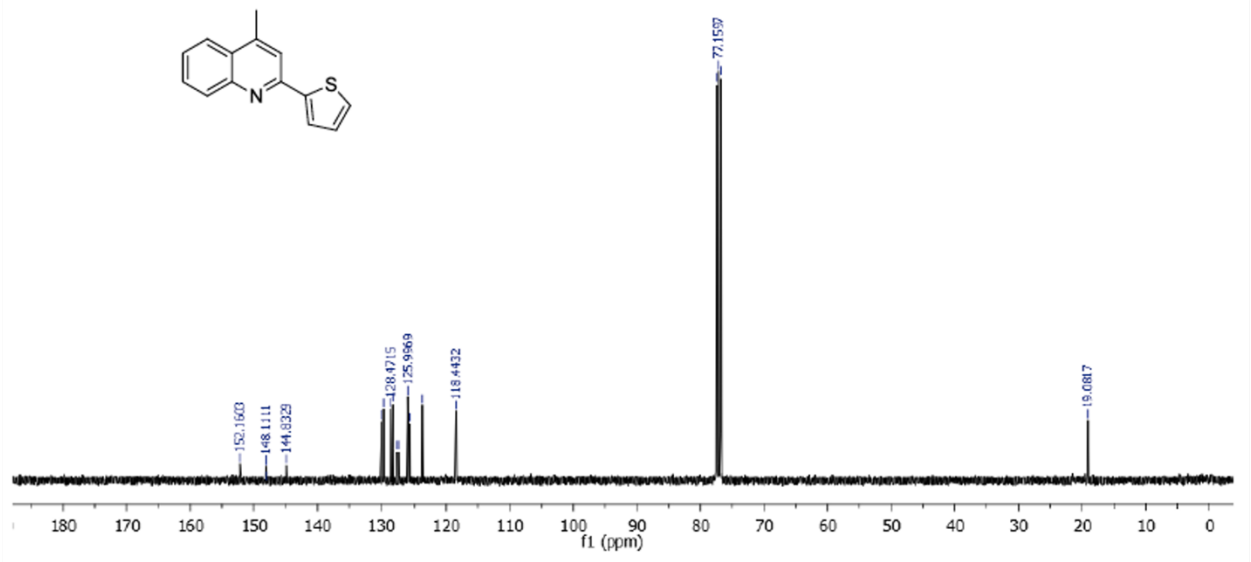

Figure S21. ^{13}C NMR spectrum of compound **9**, $CDCl_3$, 101 MHz, 298 K.

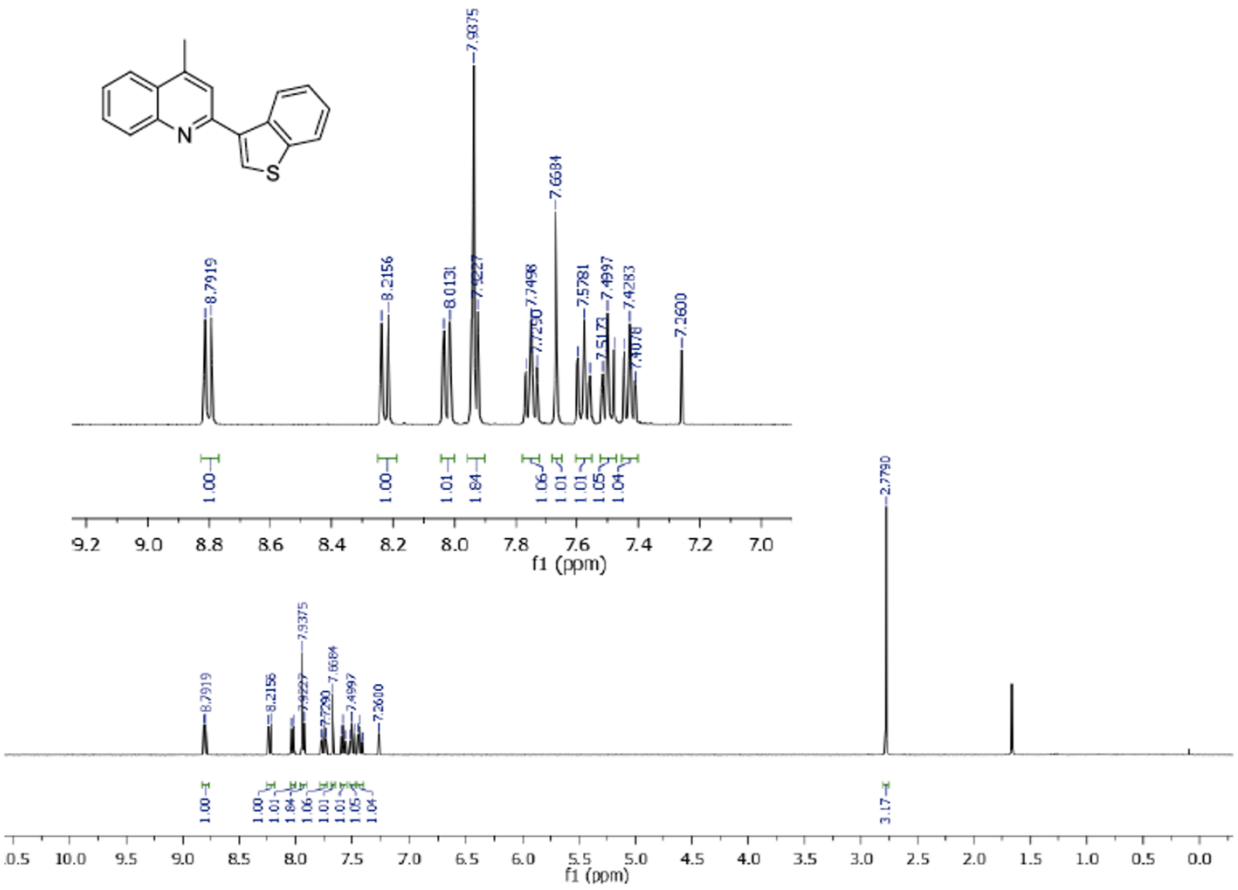

Figure S22. ^{1}H NMR spectrum of compound **10** with inset ^{1}H NMR spectrum expanded into aromatic region, $CDCl_3$, 400 MHz, 298 K.

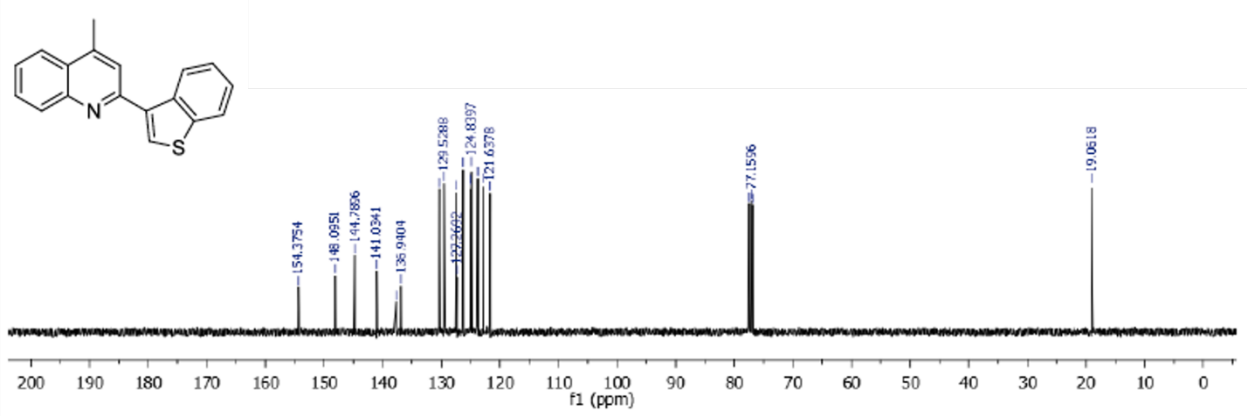

Figure S23. ^{13}C NMR spectrum of compound **10**, $CDCl_3$, 101 MHz, 298 K.

SAINT MARY'S UNIVERSITY SINCE 1802 | FACULTY OF SCIENCE
One University. One World. Yours.

CENTRE FOR ENVIRONMENTAL ANALYSIS AND REMEDIATION
Saint Marys University, Halifax NS B3H 3C3. Science Building Room 501
Phone (902)420-5135 Email: Patricia.Granados@smu.ca

CHN Analyzer, Perkin Elmer 2400 Series II

User's Name	Barbora Balonova
Analyzed by:	Patricia Granados
Date:	05-Dec-18
Standard Calibration	Acetanilide
Supplier	Perkin Elmer

Expected Values		Carbon %	Hydrogen %	Nitrogen %
QC:Cyclohexanone-2,4-dinitro-phenylhydrazone		51.79	5.07	20.14
BB387		78.51	4.76	5.09
BB393		46.46	3.55	9.29

Quality Control Standard Results

Sample Name	Weight mg	Carbon %	Hydrogen %	Nitrogen %
QC	3.363	52.09	5.08	20.16
	3.368	51.62	4.97	20.06

Sample Results

Sample Name	Weight mg	Carbon %	Hydrogen %	Nitrogen %
BB387	3.169	78.26	4.67	5.08
BB387b	2.700	78.29	4.58	5.08
BB393	2.787	46.16	3.66	9.49
BB393b	2.553	45.90	3.59	9.49

Figure S24. Copy of elemental analysis for compound **10** (code used for analysis: BB 387). Expected values highlighted in red, measured in blue.

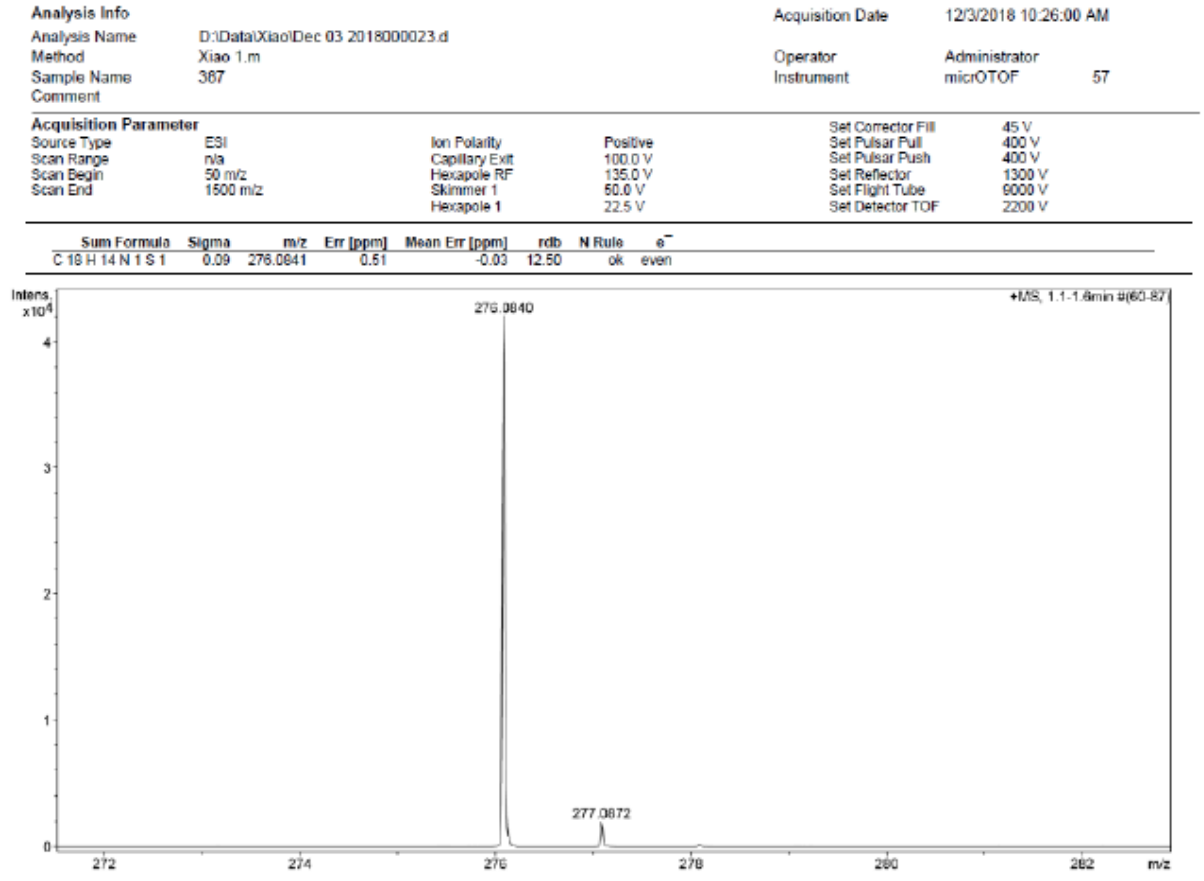

Figure S25. Mass spectrum of compound **10**. HRMS [ESI+] ion $[C_{19}H_{14}NS]^+$ m/z calculated: 276.0841. Found: 276.0840 [M+]. Anal.Calcd for $C_{18}H_{13}NS$

S4. UV-Vis, Excitation and Emission data

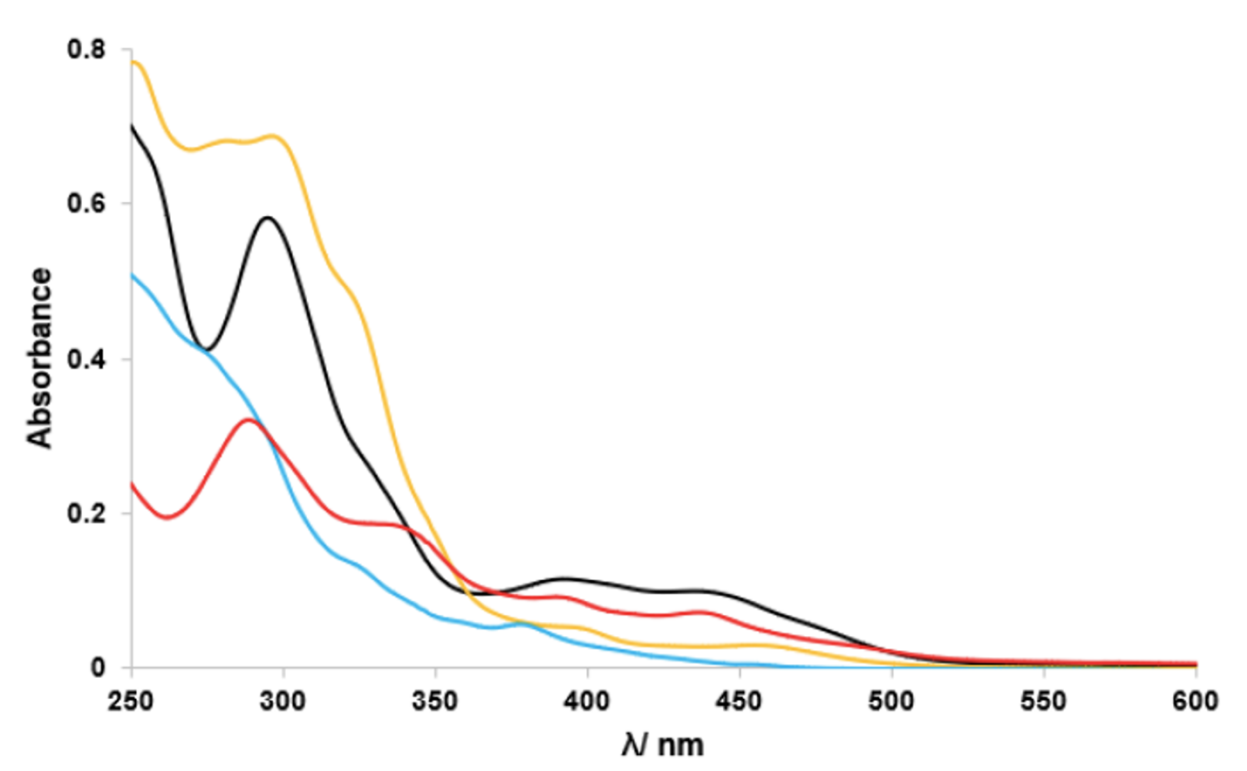

Figure S26. UV-vis absorption spectra of complexes **1** (blue line), **2** (yellow line), **3** (black line) and **4** (red line) in $CHCl_3$, c = 1×10^{-5} M.

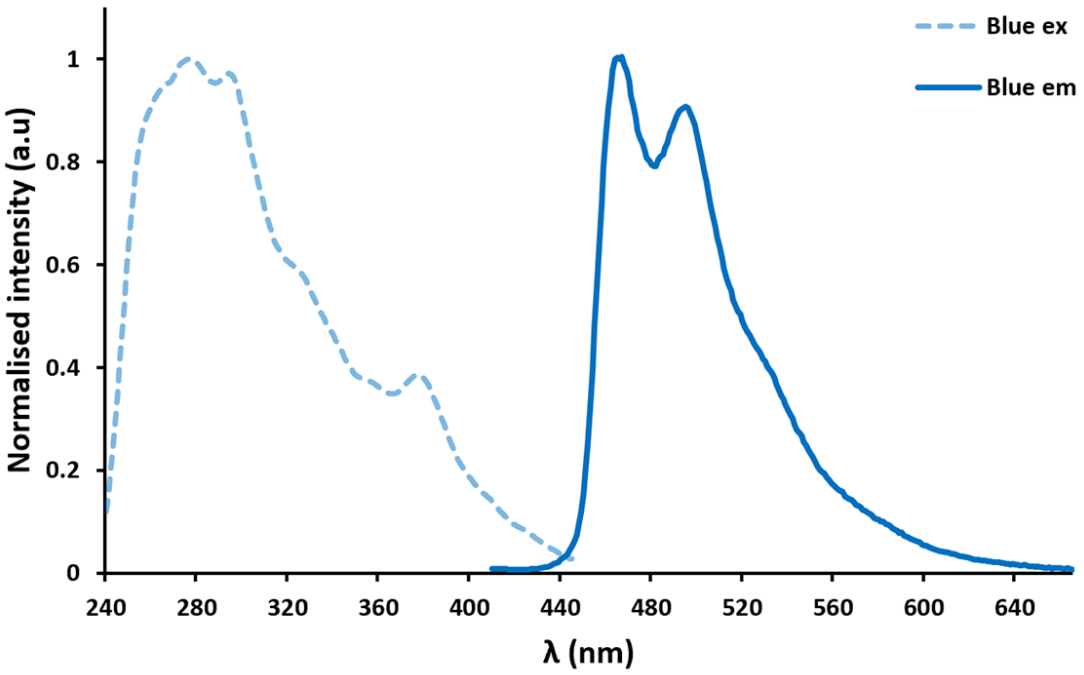

Figure S27. Normalised emission and excitation spectra of iridium complex **1** (c = 1×10^{-5} M) measured in $CHCl_3$ solution.

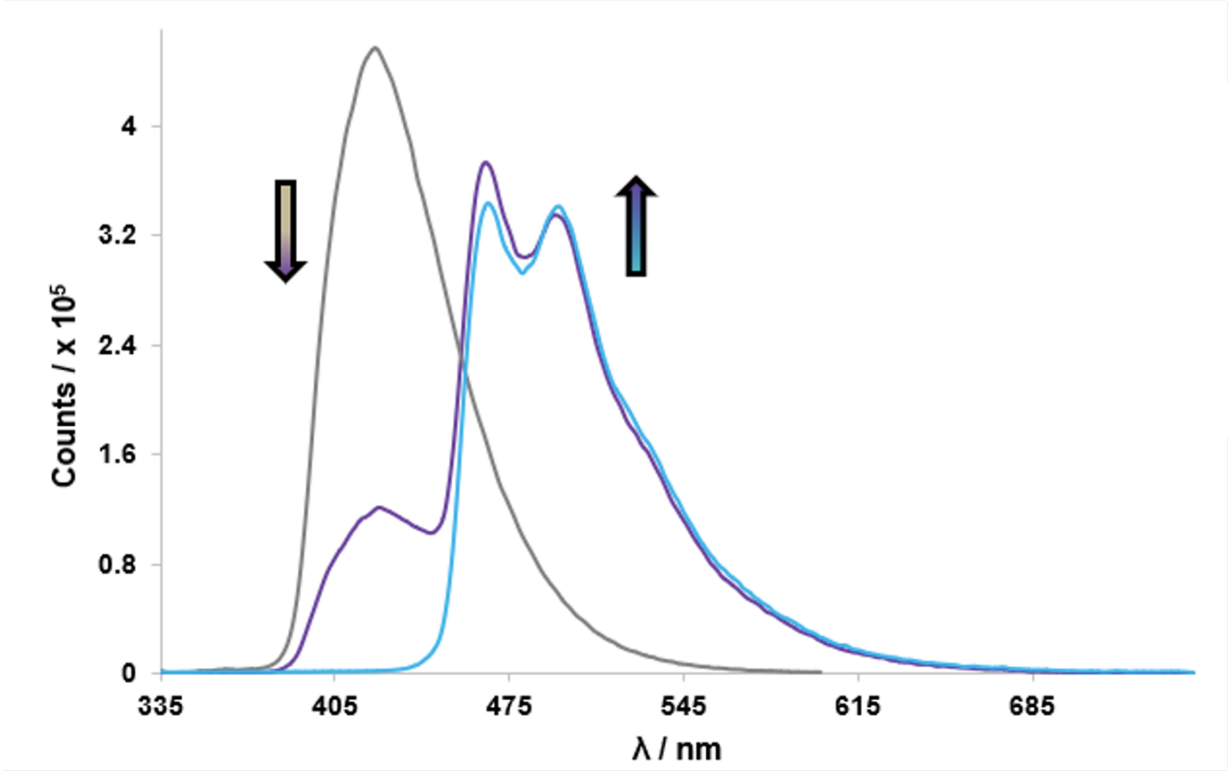

Figure S28. Overlaid emission spectra of complex **1** (blue), compound **5** (grey) and co-system **1•5** (purple) from FRET studies in $CHCl_3$ solution. All samples excited at λ_{ex} = 350 nm.

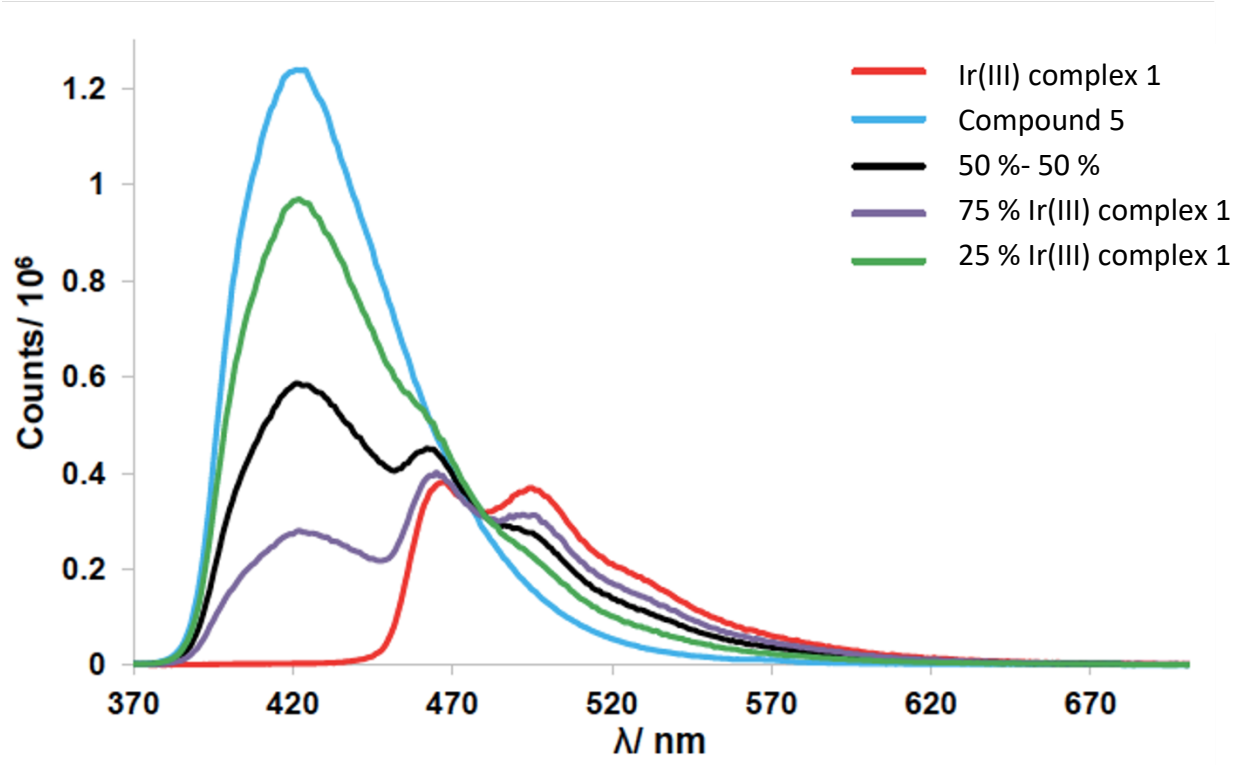

Figure S29. Emission spectra from studies of complex **1** with additions of compound **5** measured in $CHCl_3$ solution. All samples excited at 350 nm.

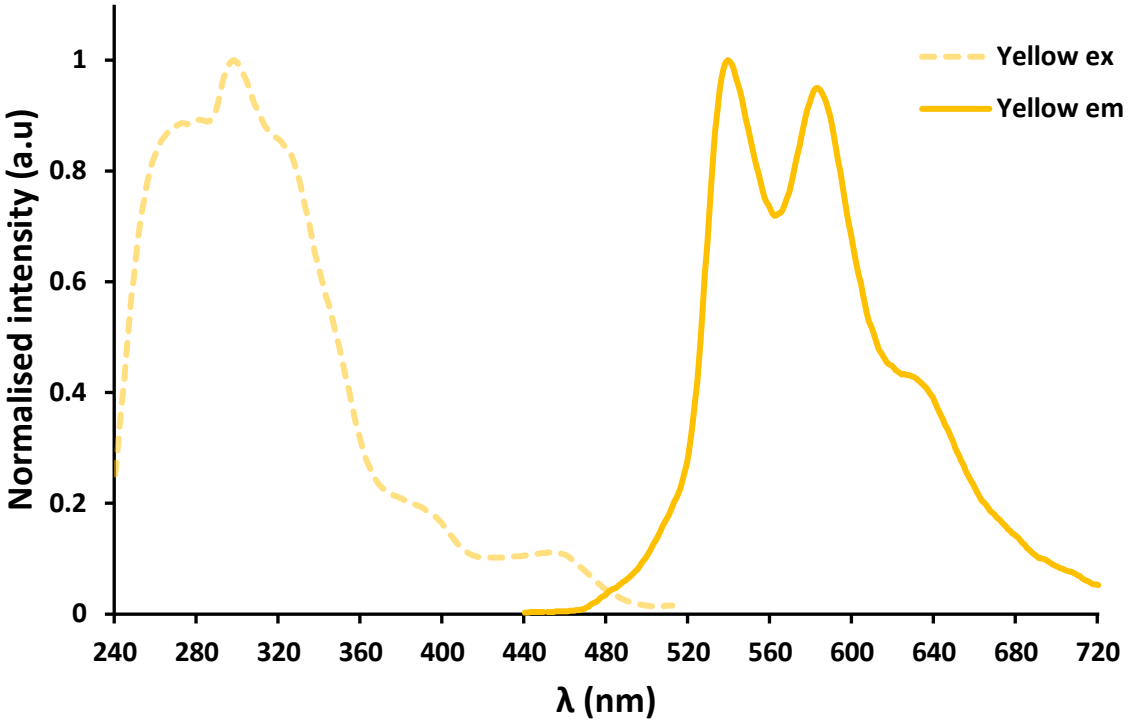

Figure S30. Normalised emission and excitation spectra of iridium complex **2**(c = 1×10^{-5} M) measured in $CHCl_3$ solution.

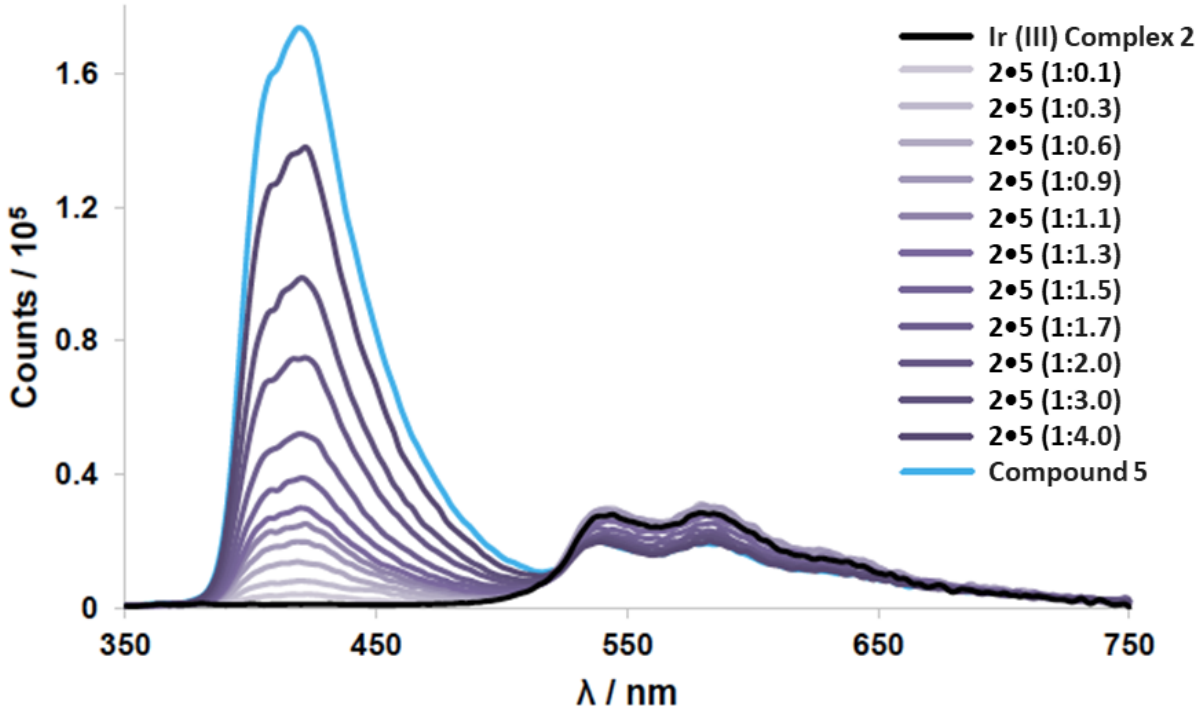

Figure S31. Emission spectra from titration studies of complex **2** with additions of compound **5** measured in $CHCl_3$ solution. Black line represents emission of iridium complex **2** without any additions.

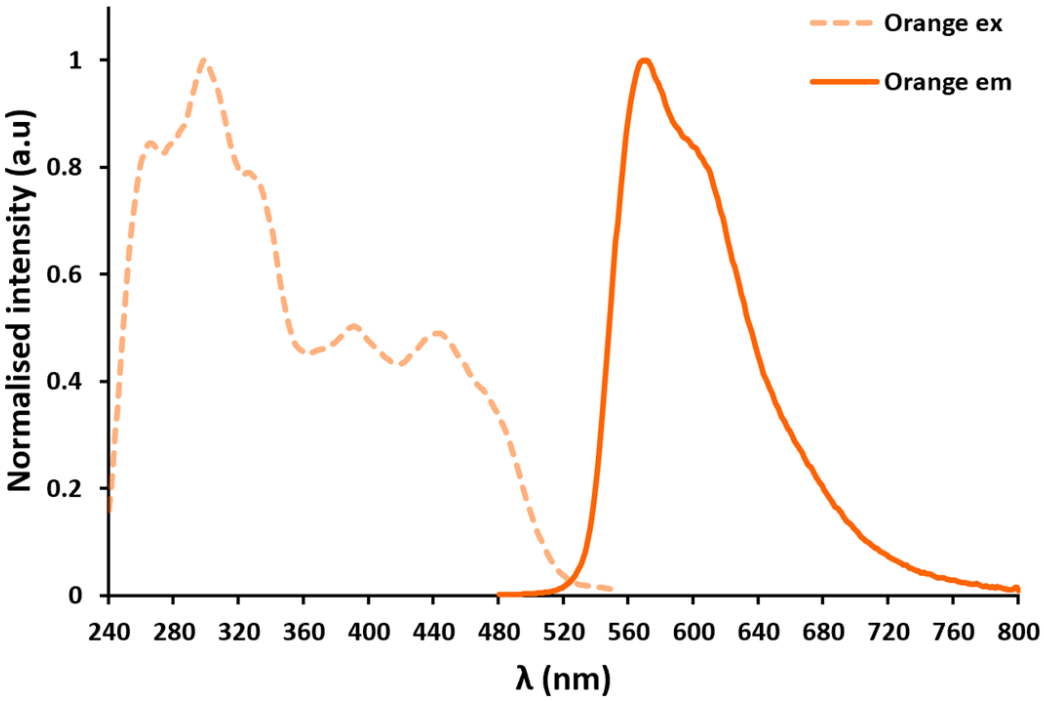

Figure S32. Normalised emission and excitation spectra of iridium complex **3** (c = 1×10^{-5} M) measured in $CHCl_3$ solution.

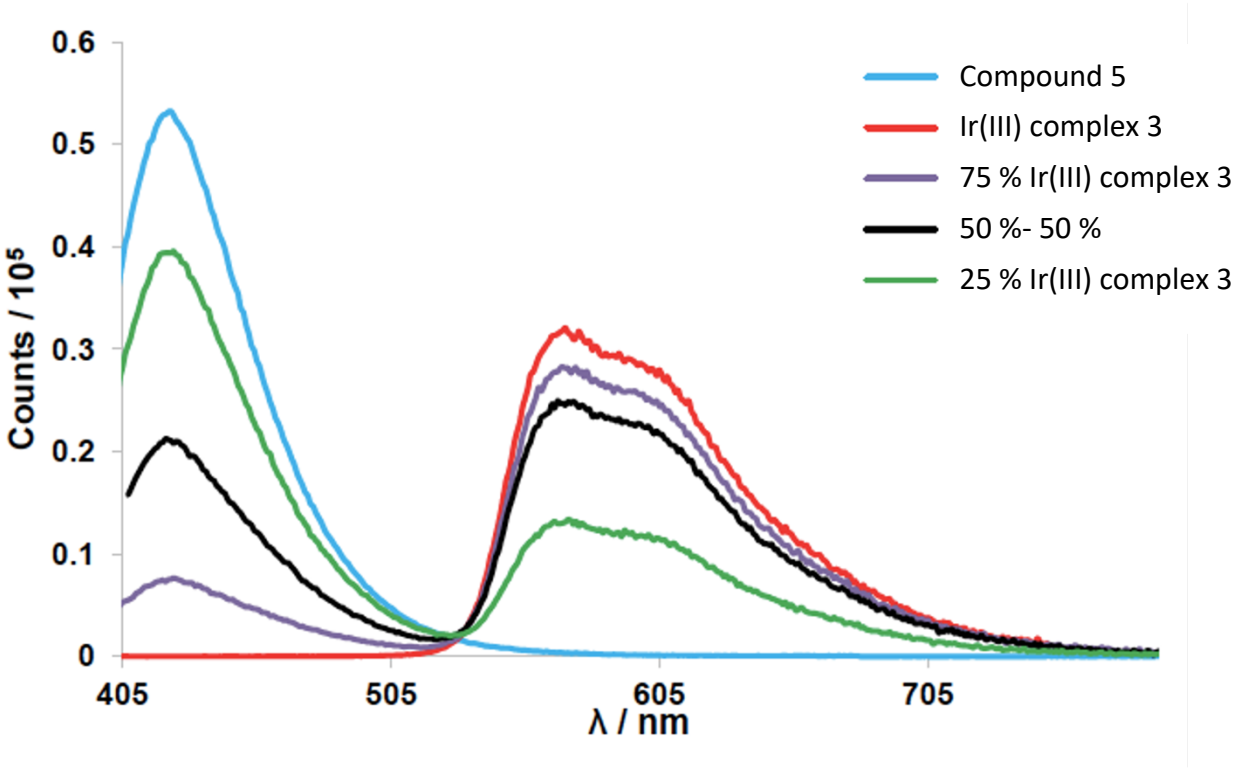

Figure S33. Emission spectra from studies of complex **3** with additions of compound **5** measured in $CHCl_3$ solution. All samples excited at 350 nm.

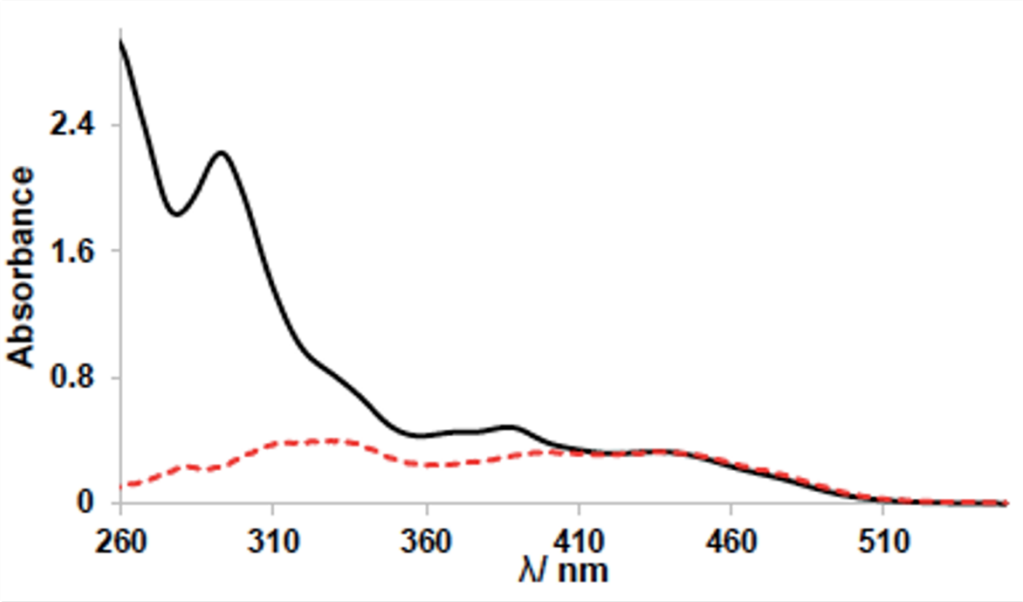

Figure S34. Absorption (solid black line) and corrected PL excitation (red dashed line measured at 570 nm) for co-system **3•5** (1:1 ratio). Spectra normalised to absorbance at 440 nm.

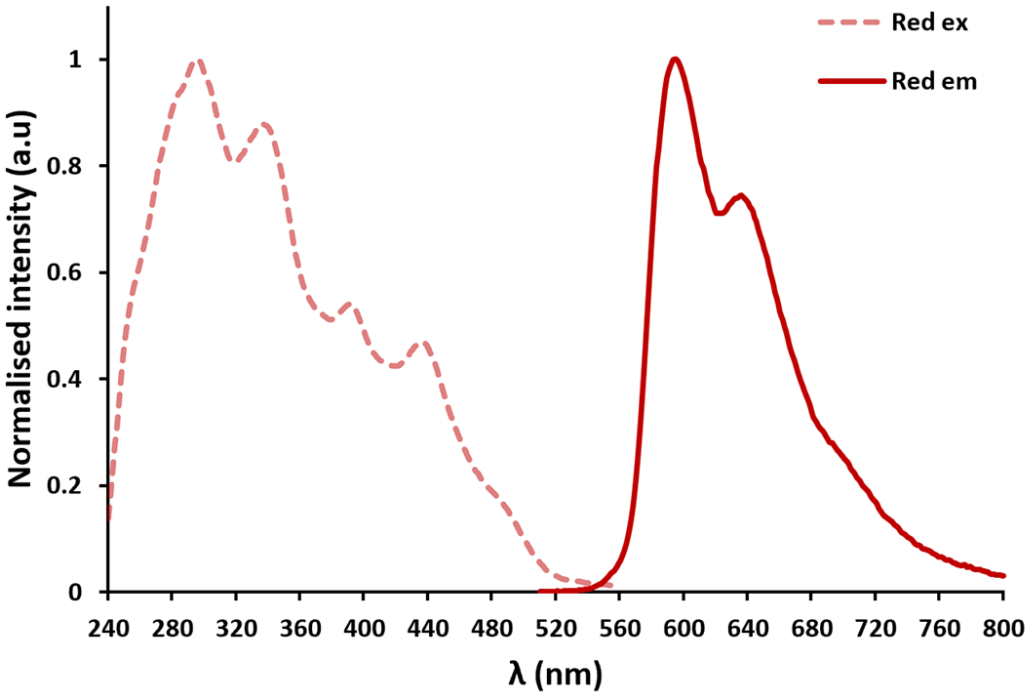

Figure S35. Normalised emission and excitation spectra of iridium complex **4** (c = 1×10^{-5} M) measured in $CHCl_3$ solution.

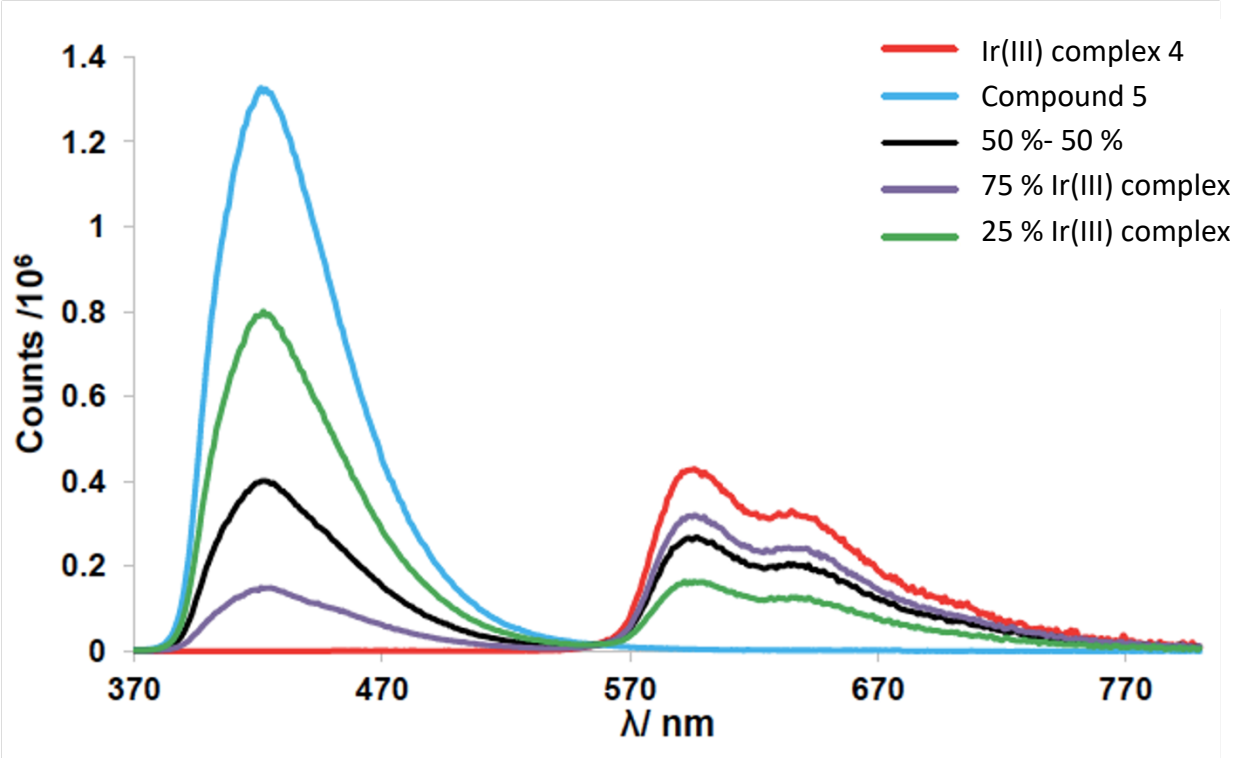

Figure S36. Emission spectra from studies of complex **4** with additions of compound **5** measured in $CHCl_3$ solution. All samples excited at 360 nm.

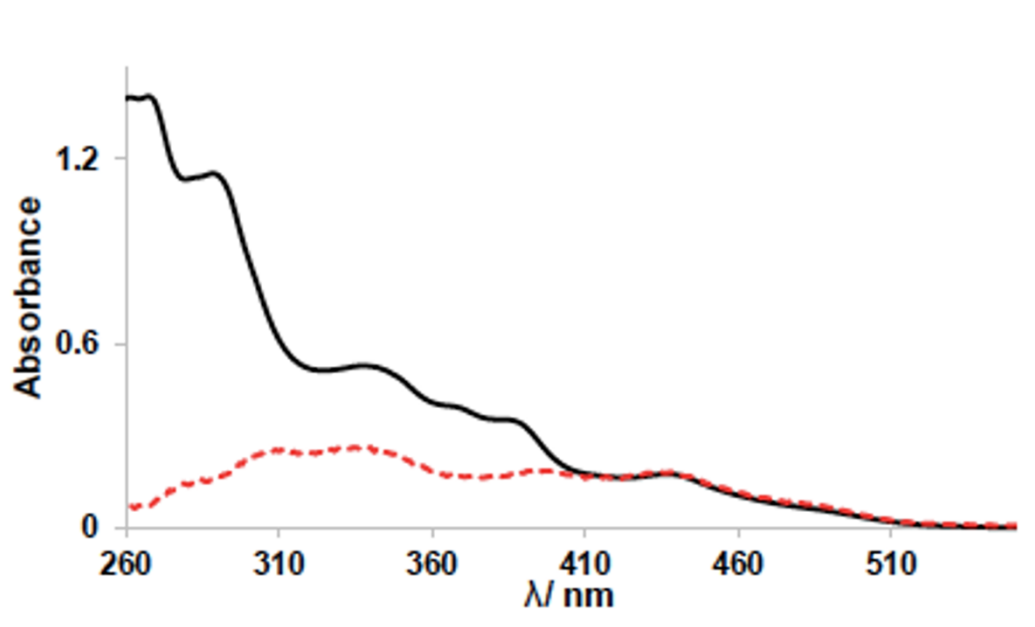

Figure S37. Absorption (solid black line) and corrected PL excitation (red dashed line measured at 640 nm) for co-system **4•5** (1:1 ratio). Spectra normalised to absorbance at 440 nm.

S5. K_a Binding studies

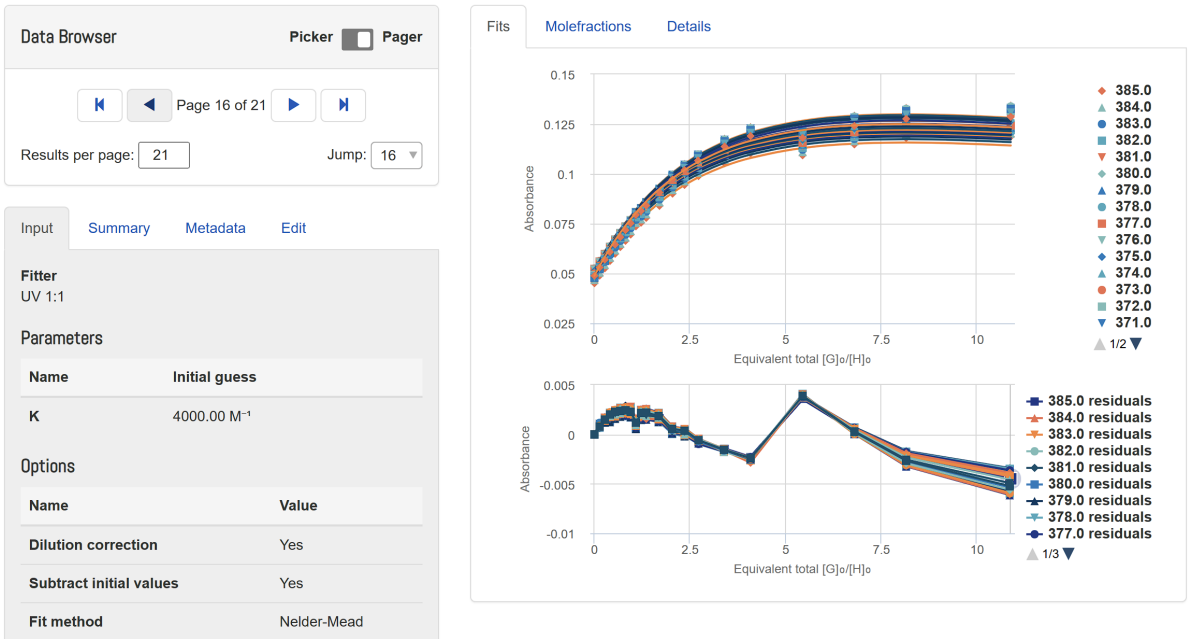

Figure S38. Screengrab of linear regression bindfit calculation data of co-system **1•5**.

Links to open-source calculations of titration runs presented below.[3]

1: http://app.supramolecular.org/bindfit/view/6ff69500-3339-4738-9efd-23f07acd5d88

2: http://app.supramolecular.org/bindfit/view/89e37f52-eea5-43b1-8af7-c9bf5eba4444

3: http://app.supramolecular.org/bindfit/view/c55ba47e-2dc6-4f59-9c9b-fab6a62341fd

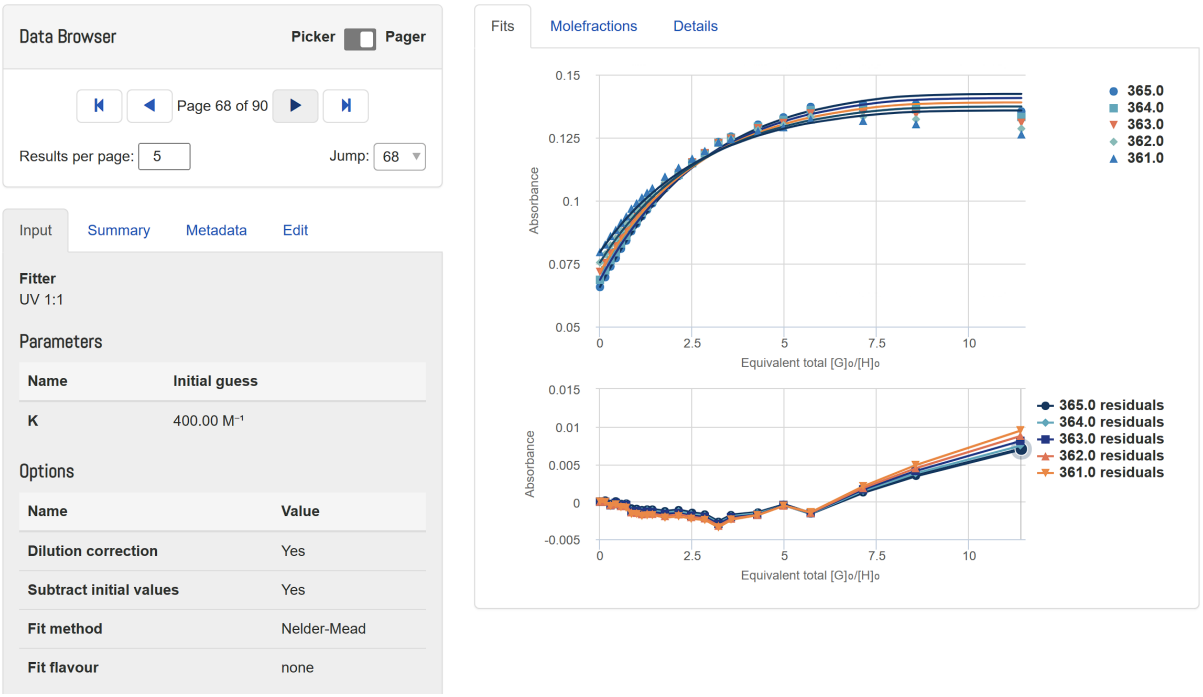

Figure S39. Screengrab of linear regression bindfit calculation data of co-system **2•5**.

Links to open-source calculations of titration runs presented below.[3]

1: http://app.supramolecular.org/bindfit/view/392ca8d9-acb3-474b-af2c-86083be9da51

2: http://app.supramolecular.org/bindfit/view/6b743661-c2e6-404b-a8b9-cf56a2b4afde

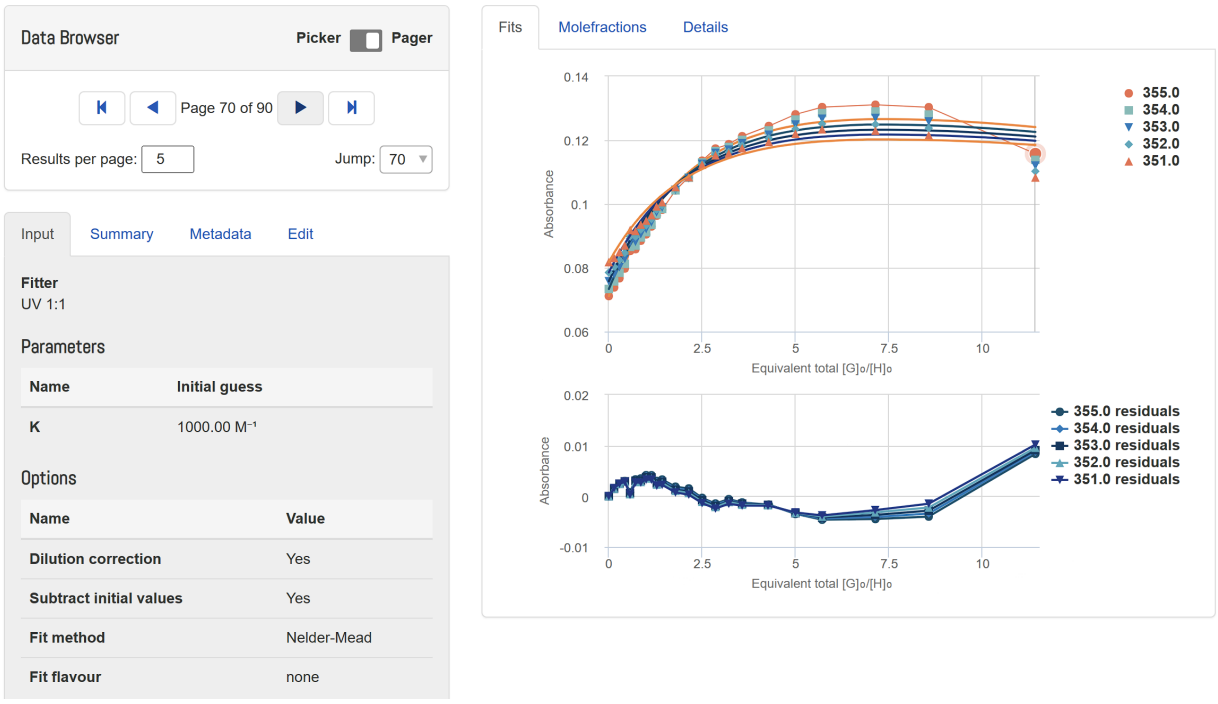

Figure S40. Screengrab of linear regression bindfit calculation data of co-system **3•5**.

Links to open-source calculations of titration runs presented below.[3]

1: http://app.supramolecular.org/bindfit/view/ee837607-e4fb-4ad8-b225-3b3304dbbf66

2: http://app.supramolecular.org/bindfit/view/8c71c12c-8169-433c-b70f-168e0cdb444f

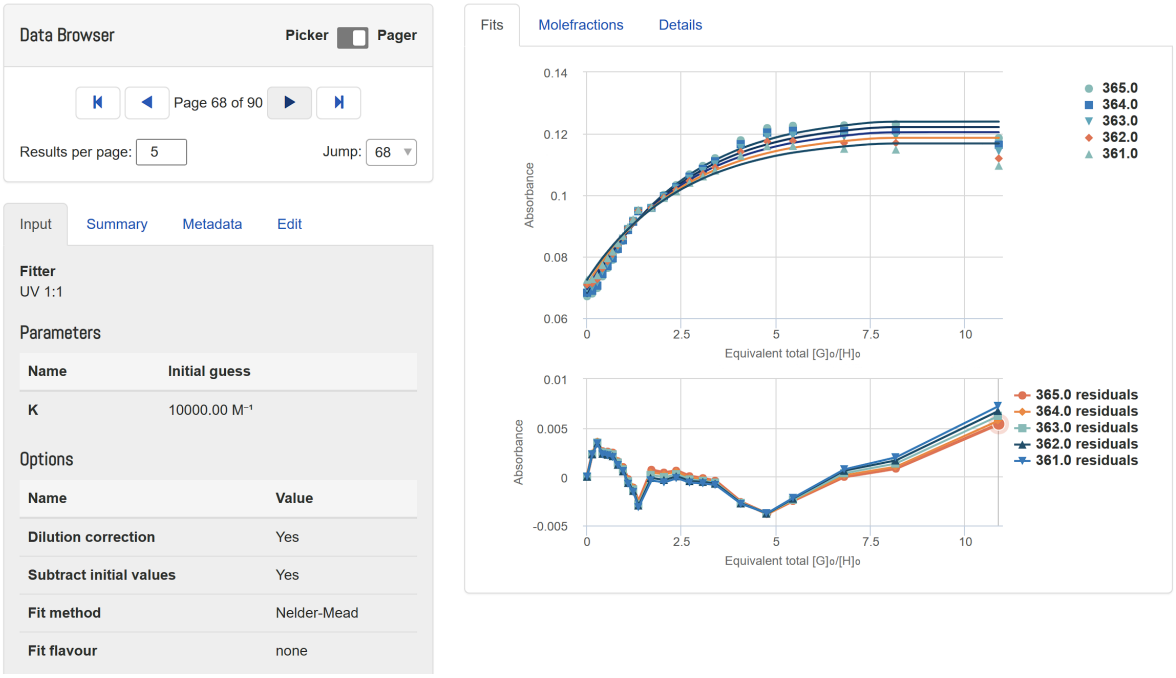

Figure S41. Screengrab of linear regression bindfit calculation data of co-system **4•5**.

Links to open-source calculations of titration runs presented below.[3]

1: http://app.supramolecular.org/bindfit/view/f065cb38-22f6-49af-9fdf-05343806e3b9

2: http://app.supramolecular.org/bindfit/view/39e932ce-5180-4a64-b925-cb0ea5f36c70

3: http://app.supramolecular.org/bindfit/view/715e6a14-22b3-4f98-8c13-8129e238e812

S6. PLQYs and decay lifetimes

Table S2. a) Significant excitation and emission peaks for Ir(III) complexes **1**-**4**; in $CHCl_3$ degassed for 1 min (Argon) at 298 K. **b)** PLQYs for Ir(III) complexes **1**-**4**; in $CHCl_3$ degassed for 20 mins (Ar) at 298 K determined using the relative method with quinine sulfate in 0.1 M H_2SO_4 as a reference (ϕ_{PL}=54.6%) for wavelengths between 400-480 nm. The other references were rhodamine 6G in ethanol (PLQY 95 %) for wavelengths 480-560 nm and rhodamine B in ethanol (PLQY 56 %) for wavelengths above 560 nm. **c)** decay lifetimes using TCSPC excited at 365 nm and their corresponding chi-squared values for Ir(III) complexes **1**-**4**; in $CHCl_3$ degassed for 20 mins (Ar) at 298 K. Complexes **1**, **2**, **3**, and **4** decay biexponentially. **d)** the radiative (k_r) and nonradiative (k_{nr}) rate constants were calculated as $k_r = \phi_{PL}/\tau_{PL}$ and $k_{nr} = (1-\phi_{PL})/\tau_{PL}$.

Ir(III) Complex	Excitation (nm)[a]	Emission (nm)[a]	PLQY (%)[b]	Lifetime (ns) (τ_{PL}, χ^2)[c]	k_r (× 10^5 s^{-1})[d]	k_{nr} (× 10^5 s^{-1})[d]
1	264, 378	467, 493	86.7	(2260.07, 1.057) (79%)	3.84	0.59
2	296, 320	548, 583	8.7	(1.94, 1.029)	448.45	4706.19
3	298, 332	570	23.4	(1703.39, 0.991) (65%)	1.38	4.50
4	296, 338	594, 640	36.1	(3623.93, 0.976)	1.00	1.76
1•5 (1:1)	280, 378	425, 462	82.2	(2088.43, 0.922) (97%)	0.39	0.85
2•5 (1:1)	298, 325	538 ,584	15.6	(3.62, 1.186)	430.94	2331.49
3•5 (1:1)	297, 340	570	43.3	(4298.43, 0.972) (90%)	1.01	1.32
4•5 (1:1)	308, 391	596, 638	41.4	(3586.05, 0.994) (99%)	1.15	1.63
2•5 (1:1.3)	298, 326	538 ,584	33.2	(3.37, 1.372)	985.16	1982.20

Table S3. PLQY of Ir(III) complex **1**; in $CHCl_3$ degassed for 20 mins (Ar) at 298 K, excited at 350 nm.

Table 1: Data Concerning the Standard			
Stock solution reference	Quinine Sulfate		
Solvent	0.1 M Sulfuric Acid		
Refractive Index	1.33		
Wavelength used (nm)	350		
Run	1	2	3
Volume of Mother solution (mL)	3	3	3
Theoritical Abs (optical)	0.065	0.065	0.065
Theoritical Abs (average)	0.065		
Emission Integral	4.67E+07	4.49E+07	4.38E+07
Emission Integral (average)	4.51E+07		
Standard Quantum Yield (%)	54.6		

Table 2: Data Concerning the Sample			
Sample Structure	IrBG		
Solvent	CHCl3		
Refractive Index	1.445		
Wavelength used (nm)	350		
Run	1	2	3
Volume of Mother solution (mL)	3.05	3.05	3.05
Total Volume (mL)	3	3	3
Theoritical Abs (optical)	0.065	0.065	0.065
Theoritical Abs (average)	0.065		
Emission Integral	6.26E+07	6.11E+07	6.03E+07
Emission Integral (average)	6.13E+07		
Calculated QY (%)	87.66		

Table S4. PLQY of Ir(III) complex **2**; in $CHCl_3$ degassed for 20 mins (Ar) at 298 K, excited at 350 nm.

Table 1: Data Concerning the Standard			
Stock solution reference	Rhodamine 6G		
Solvent	Ethanol		
Refractive Index	1.36		
Wavelength used (nm)	350		
Run	1	2	3
Volume of Mother solution (mL)	3	3	3
Theoritical Abs (optical)	0.084	0.085	0.085
Theoritical Abs (average)	0.084666667		
Emission Integral	4.43E+07	4.49E+07	4.38E+07
Emission Integral (average)	4.43E+07		
Standard Quantum Yield (%)	95		

Table 2: Data Concerning the Sample			
Sample Structure	IrYG		
Solvent	CHCl3		
Refractive Index	1.445		
Wavelength used (nm)	350		
Run	1	2	3
Volume of Mother solution (mL)	3.05	3.05	3.05
Total Volume (mL)	3	3	3
Theoritical Abs (optical)	0.084	0.082	0.081
Theoritical Abs (average)	0.082333333		
Emission Integral	3.49E+06	3.49E+06	3.48E+06
Emission Integral (average)	3.48E+06		
Calculated QY (%)	8.66		

Table S5. PLQY of Ir(III) complex **3**; in $CHCl_3$ degassed for 20 mins (Ar) at 298 K, excited at 350 nm.

Table 1: Data Concerning the Standard			
Stock solution reference	Rhodamine RG		
Solvent	ethanol		
Refractive Index	1.36		
Wavelength used (nm)	350		
Run	1	2	3
Volume of Mother solution (mL)	3	3	3
Theoritical Abs (optical)	0.084	0.083	0.081
Theoritical Abs (average)	0.082666667		
Emission Integral	4.43E+07	4.49E+07	4.38E+07
Emission Integral (average)	4.43E+07		
Standard Quantum Yield (%)	95		

Table 2: Data Concerning the Sample			
Sample Structure	IrOG		
Solvent	CHCl3		
Refractive Index	1.445		
Wavelength used (nm)	350		
Run	1	2	3
Volume of Mother solution (mL)	3.05	3.05	3.05
Total Volume (mL)	3	3	3
Theoritical Abs (optical)	0.072	0.07	0.069
Theoritical Abs (average)	0.070333333		
Emission Integral	8.31E+06	8.23E+06	8.13E+06
Emission Integral (average)	8.22E+06		
Calculated QY (%)	23.38		

Table S6. PLQY of Ir(III) complex **4**; in $CHCl_3$ degassed for 20 mins (Ar) at 298 K, excited at 350 nm.

Table 1: Data Concerning the Standard			
Stock solution reference	Rhodamine B		
Solvent	Ethanol		
Refractive Index	1.36		
Wavelength used (nm)	350		
Run	1	2	3
Volume of Mother solution (mL)	3	3	3
Theoritical Abs (optical)	0.08	0.079	0.081
Theoritical Abs (average)	0.08		
Emission Integral	9.52E+07	4.49E+07	4.38E+07
Emission Integral (average)	6.13E+07		
Standard Quantum Yield (%)	56		

Table 2: Data Concerning the Sample			
Sample Structure	IrRG		
Solvent	CHCl3		
Refractive Index	1.445		
Wavelength used (nm)	350		
Run	1	2	3
Volume of Mother solution (mL)	3.05	3.05	3.05
Total Volume (mL)	3	3	3
Theoritical Abs (optical)	0.08	0.076	0.074
Theoritical Abs (average)	0.076666667		
Emission Integral	3.38E+07	3.35E+07	3.33E+07
Emission Integral (average)	3.35E+07		
Calculated QY (%)	36.08		

Table S7. PLQY of Ir(III) complex with DAA **1•5** (1:1); in $CHCl_3$ degassed for 20 mins (Ar) at 298 K, excited at 350 nm.

Table 1: Data Concerning the Standard			
Stock solution reference	Quinine Sulfate		
Solvent	0.1 M Sulfuric Acid		
Refractive Index	1.33		
Wavelength used (nm)	350		
Run	1	2	3
Volume of Mother solution (mL)	3	3	3
Theoritical Abs (optical)	0.065	0.065	0.065
Theoritical Abs (average)	0.065		
Emission Integral	4.67E+07	4.49E+07	4.38E+07
Emission Integral (average)	4.51E+07		
Standard Quantum Yield (%)	54.6		

Table 2: Data Concerning the Sample			
Sample Structure	IrBG:DAA		
Solvent	CHCl3		
Refractive Index	1.445		
Wavelength used (nm)	350		
Run	1	2	3
Volume of Mother solution (mL)	3.05	3.05	3.05
Total Volume (mL)	3	3	3
Theoritical Abs (optical)	0.065	0.065	0.065
Theoritical Abs (average)	0.065		
Emission Integral	5.91E+07	5.75E+07	5.59E+07
Emission Integral (average)	5.75E+07		
Calculated QY (%)	82.17		

Table S8. PLQY of Ir(III) complex with DAA **2•5** (1:1); in $CHCl_3$ degassed for 20 mins (Ar) at 298 K, excited at 350 nm.

Table 1: Data Concerning the Standard			
Stock solution reference	Rhodamine 6G		
Solvent	Ethanol		
Refractive Index	1.36		
Wavelength used (nm)	350		
Run	1	2	3
Volume of Mother solution (mL)	3	3	3
Theoritical Abs (optical)	0.081	0.08	0.079
Theoritical Abs (average)	0.08		
Emission Integral	4.43E+07	4.49E+07	4.38E+07
Emission Integral (average)	4.43E+07		
Standard Quantum Yield (%)	95		

Table 2: Data Concerning the Sample			
Sample Structure	IrYG:DAA		
Solvent	CHCl3		
Refractive Index	1.445		
Wavelength used (nm)	350		
Run	1	2	3
Volume of Mother solution (mL)	3.05	3.05	3.05
Total Volume (mL)	3	3	3
Theoritical Abs (optical)	0.085	0.081	0.079
Theoritical Abs (average)	0.081666667		
Emission Integral	6.64E+06	6.56E+06	6.57E+06
Emission Integral (average)	6.59E+06		
Calculated QY (%)	15.61		

Table S9. PLQY of Ir(III) complex with DAA **3•5** (1:1); in $CHCl_3$ degassed for 20 mins (Ar) at 298 K, excited at 350 nm.

Table 1: Data Concerning the Standard			
Stock solution reference	Rhodamine RG		
Solvent	ethanol		
Refractive Index	1.36		
Wavelength used (nm)	350		
Run	1	2	3
Volume of Mother solution (mL)	3	3	3
Theoritical Abs (optical)	0.084	0.083	0.081
Theoritical Abs (average)	0.082666667		
Emission Integral	4.43E+07	4.49E+07	4.38E+07
Emission Integral (average)	4.43E+07		
Standard Quantum Yield (%)	95		

Table 2: Data Concerning the Sample			
Sample Structure	IrOG:DAA		
Solvent	CHCl3		
Refractive Index	1.445		
Wavelength used (nm)	350		
Run	1	2	3
Volume of Mother solution (mL)	3.05	3.05	3.05
Total Volume (mL)	3	3	3
Theoritical Abs (optical)	0.08	0.074	0.078
Theoritical Abs (average)	0.077333333		
Emission Integral	1.66E+07	1.67E+07	1.68E+07
Emission Integral (average)	1.67E+07		
Calculated QY (%)	43.25		

Table S10. PLQY of Ir(III) complex with DAA **4•5** (1:1); in $CHCl_3$ degassed for 20 mins (Ar) at 298 K, excited at 350 nm.

Table 1: Data Concerning the Standard			
Stock solution reference	Rhodamine B		
Solvent	Ethanol		
Refractive Index	1.36		
Wavelength used (nm)	350		
Run	1	2	3
Volume of Mother solution (mL)	3	3	3
Theoritical Abs (optical)	0.08	0.079	0.081
Theoritical Abs (average)	0.08		
Emission Integral	9.52E+07	4.49E+07	4.38E+07
Emission Integral (average)	6.13E+07		
Standard Quantum Yield (%)	56		

Table 2: Data Concerning the Sample			
Sample Structure	IrRG:DAA		
Solvent	CHCl3		
Refractive Index	1.445		
Wavelength used (nm)	350		
Run	1	2	3
Volume of Mother solution (mL)	3.05	3.05	3.05
Total Volume (mL)	3	3	3
Theoritical Abs (optical)	0.085	0.084	0.085
Theoritical Abs (average)	0.084666667		
Emission Integral	4.26E+07	4.24E+07	4.24E+07
Emission Integral (average)	4.24E+07		
Calculated QY (%)	41.38		

Table S11. PLQY of Ir(III) complex with DAA **2•5** tuned for white light emission (1:1.3); in $CHCl_3$ degassed for 20 mins (Ar) at 298 K, excited at 350 nm.

Table 1: Data Concerning the Standard			
Stock solution reference	Rhodamine 6G		
Solvent	Ethanol		
Refractive Index	1.36		
Wavelength used (nm)	350		
Run	1	2	3
Volume of Mother solution (mL)	3	3	3
Theoritical Abs (optical)	0.081	0.08	0.08
Theoritical Abs (average)	0.080333333		
Emission Integral	4.43E+07	4.49E+07	4.38E+07
Emission Integral (average)	4.43E+07		
Standard Quantum Yield (%)	95		

Table 2: Data Concerning the Sample			
Sample Structure	IrYG:DAA (white light)		
Solvent	CHCl3		
Refractive Index	1.445		
Wavelength used (nm)	350		
Run	1	2	3
Volume of Mother solution (mL)	3.05	3.05	3.05
Total Volume (mL)	3	3	3
Theoritical Abs (optical)	0.084	0.082	0.081
Theoritical Abs (average)	0.082333333		
Emission Integral	1.43E+07	1.40E+07	1.39E+07
Emission Integral (average)	1.41E+07		
Calculated QY (%)	33.22		

Decay Lifetime Measurement of Ir(III) complex 1

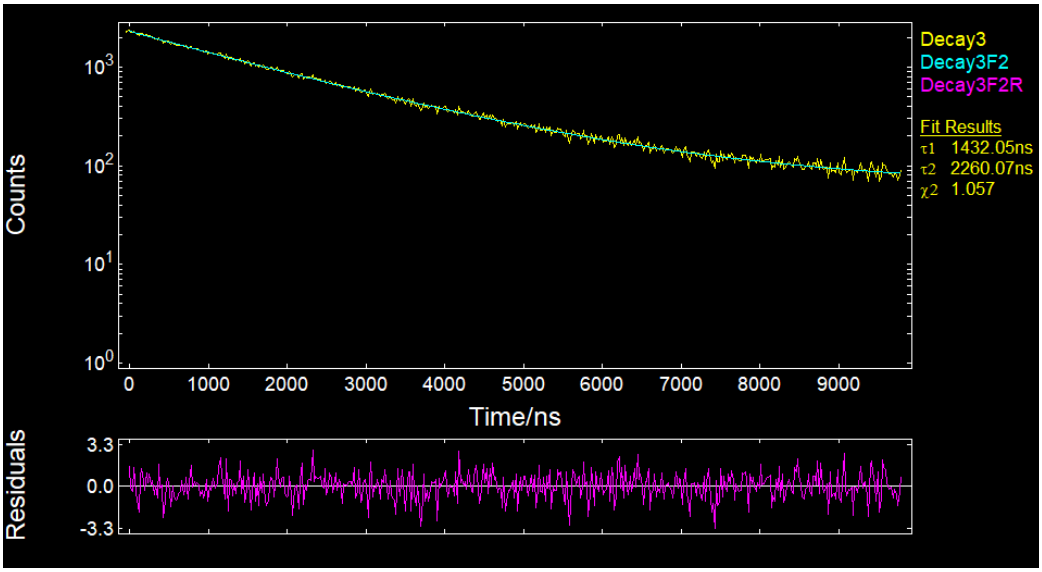

Figure S42. Biexponential lifetime decay of Ir(III) complex **1**, ~1·10^{-5} M (Absorbance of 0.065 from UV-Vis) in $CHCl_3$ degassed for 20 mins (Ar) at 298 K after excitation at 365 nm. Data collected at λ_{max} = 470 nm.

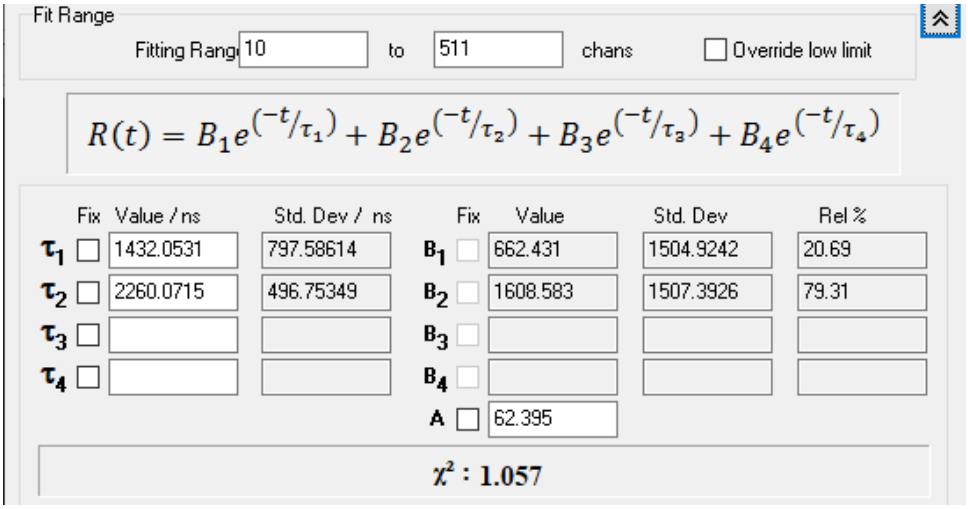

Figure S43. Fit result of Ir(III) complex **1**, ~1·10^{-5} M (Absorbance of 0.065 from UV-Vis) in $CHCl_3$ degassed for 20 mins (Ar) at 298 K after excitation at 365 nm. Data collected at λ_{max} = 470 nm.

Decay Lifetime Measurement of Ir(III) complex 2

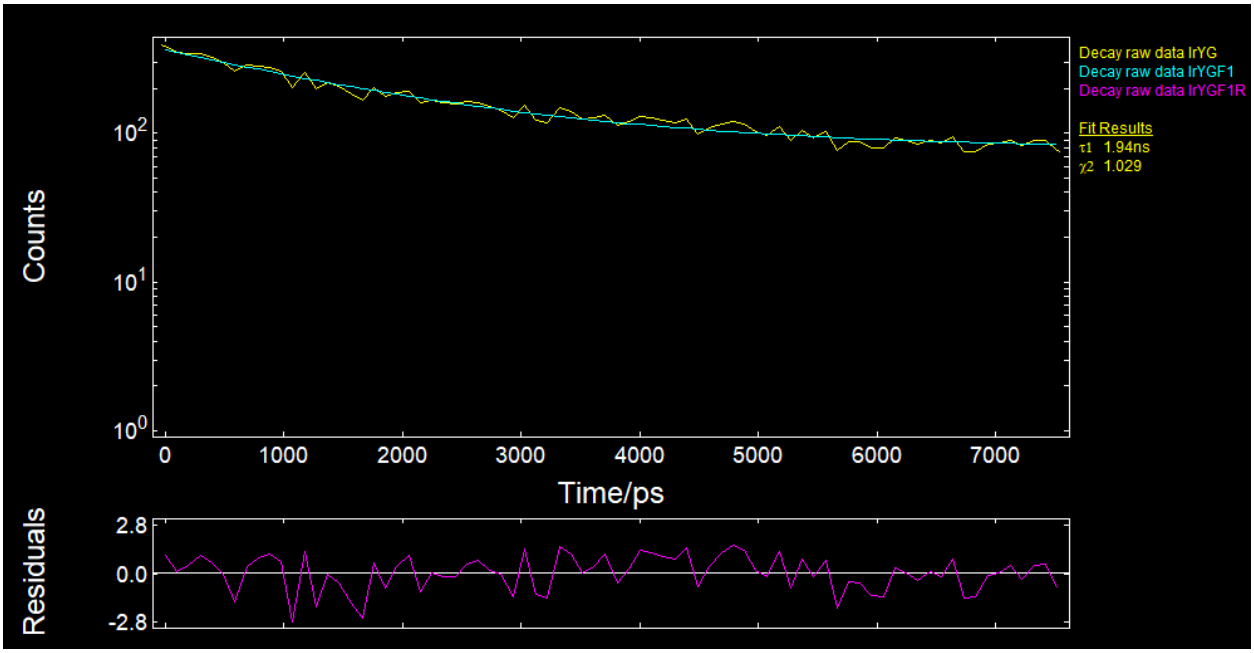

Figure S44. Monoexponential lifetime decay of Ir(III) complex **2**, ~1·10^{-5} M (Absorbance of 0.081 from UV-Vis) in $CHCl_3$ degassed for 20 mins (Ar) at 298 K after excitation at 365 nm. Data collected at λ_{max} = 540 nm.

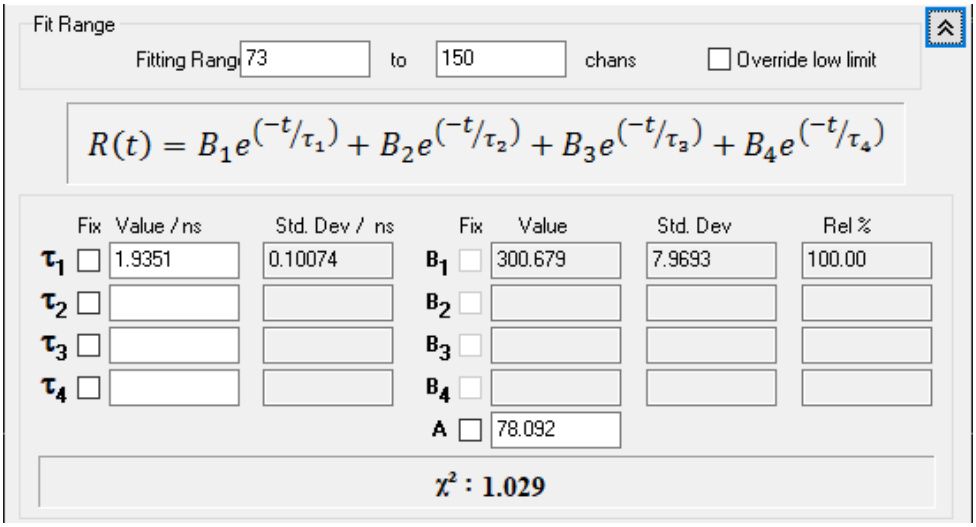

Figure S45. Fit result of Ir(III) complex **2**, ~1·10^{-5} M (Absorbance of 0.081 from UV-Vis) in $CHCl_3$ degassed for 20 mins (Ar) at 298 K after excitation at 365 nm. Data collected at λ_{max} = 540 nm.

Decay Lifetime Measurement of Ir(III) complex 3

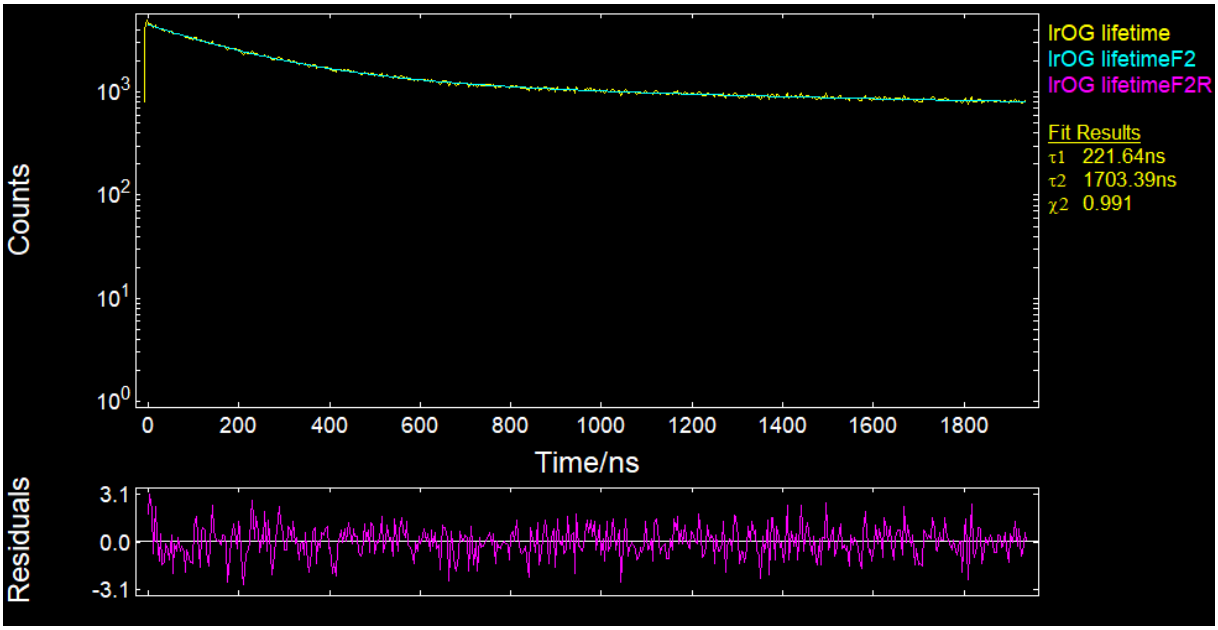

Figure S46. Biexponential lifetime decay of Ir(III) complex **3,** ~$1 \cdot 10^{-6}$ M (Absorbance of 0.079 from UV-Vis) in $CHCl_3$ degassed for 20 mins (Ar) at 298 K after excitation at 365 nm. Data collected at λ_{max} = 570 nm.

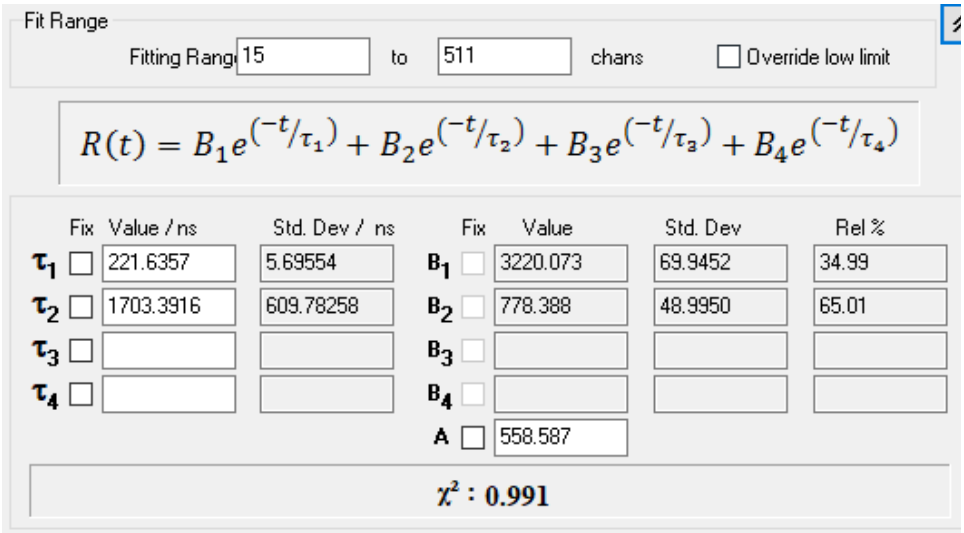

Figure S47. Fit result of Ir(III) complex **3**, ~$1 \cdot 10^{-6}$ M (Absorbance of 0.079 from UV-Vis) in $CHCl_3$ degassed for 20 mins (Ar) at 298 K after excitation at 365 nm. Data collected at λ_{max} = 570 nm.

Decay Lifetime Measurement of Ir(III) complex 4

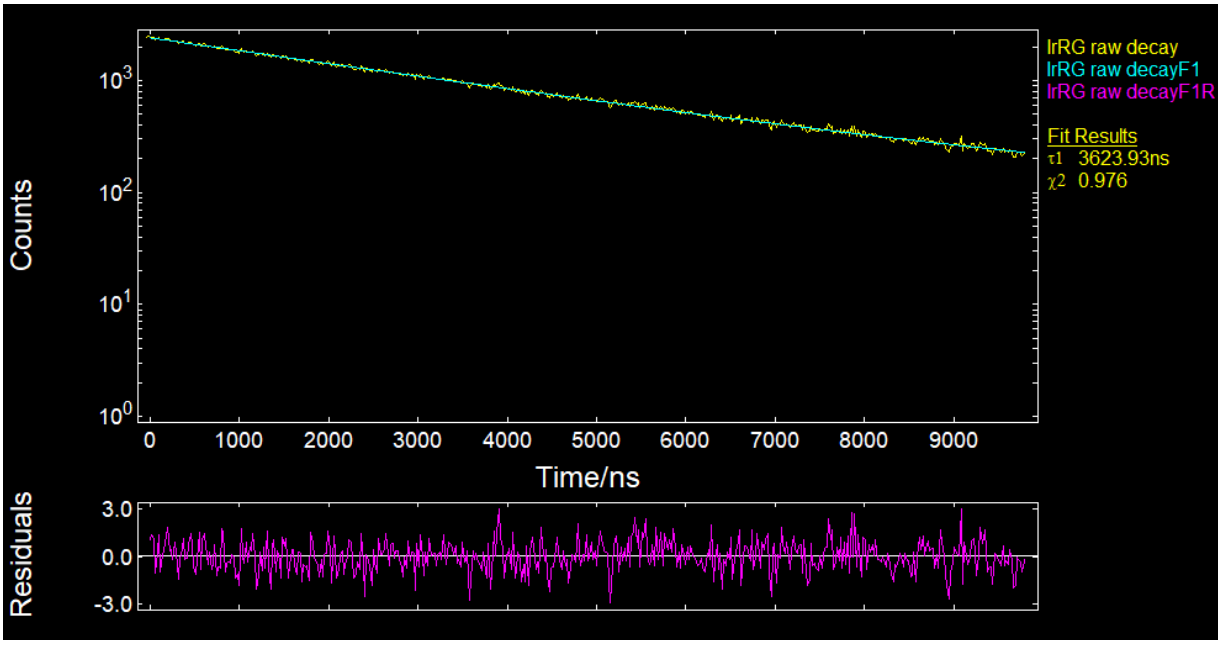

Figure S48. Monoexponential lifetime decay of Ir(III) complex **4,** ~$1 \cdot 10^{-6}$ M (Absorbance of 0.076 from UV-Vis) in $CHCl_3$ degassed for 20 mins (Ar) at 298 K after excitation at 365 nm. Data collected at λ_{max} = 590 nm.

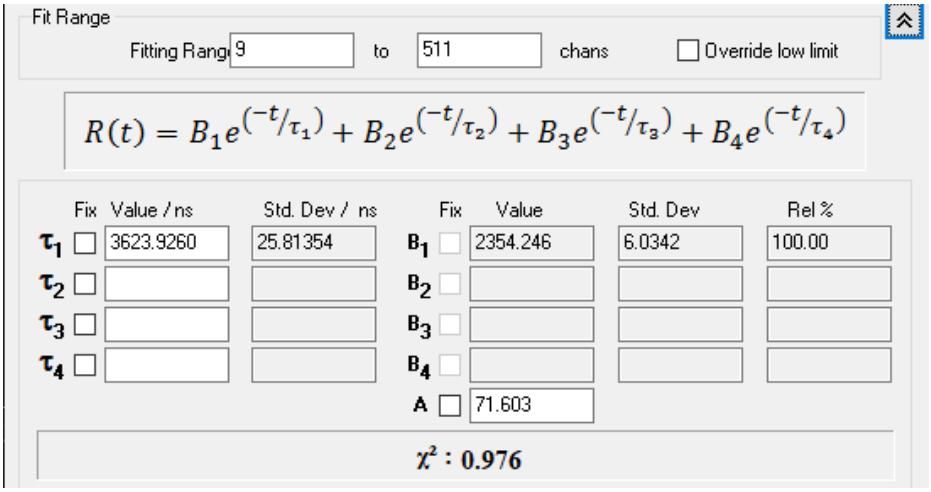

Figure S49. Fit result of Ir(III) complex **4**, ~$1 \cdot 10^{-6}$ M (Absorbance of 0.076 from UV-Vis) in $CHCl_3$ degassed for 20 mins (Ar) at 298 K after excitation at 365 nm. Data collected at λ_{max} = 590 nm.

Decay Lifetime Measurement of Ir(III) complex 1•5

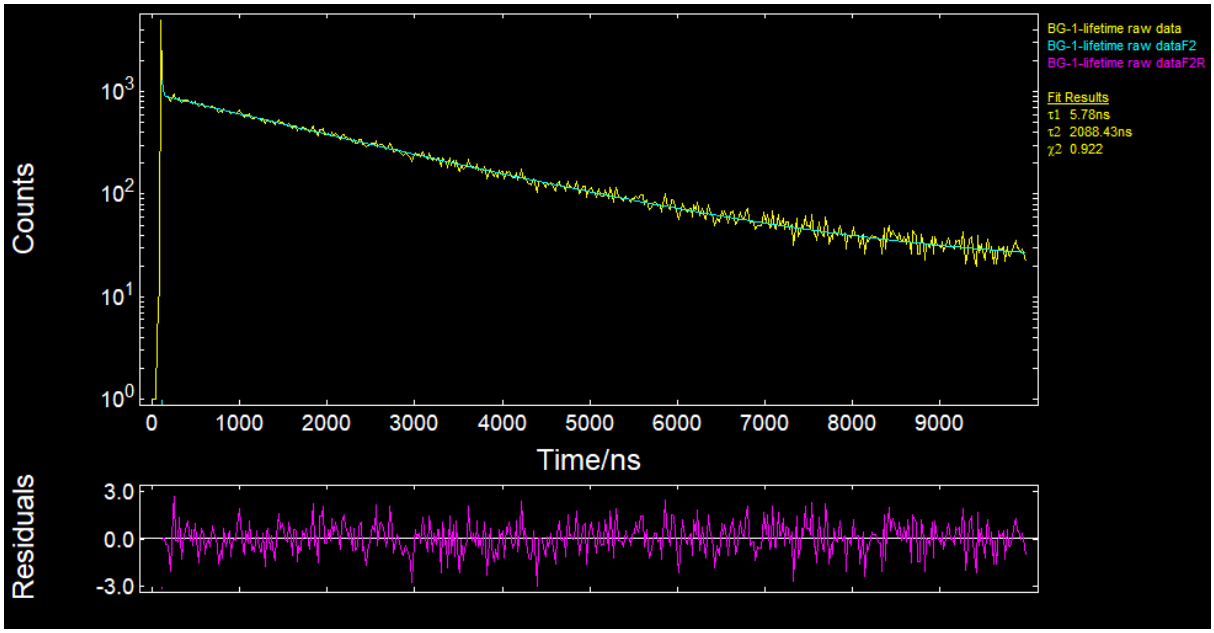

Figure S50. Biexponential lifetime decay of Ir(III) complex **1•5,** (1:1) ~1·10^{-5} M (Absorbance of 0.071 from UV-Vis) in $CHCl_3$ degassed for 20 mins (Ar) at 298 K after excitation at 365 nm. Data collected at λ_{max} = 470 nm.

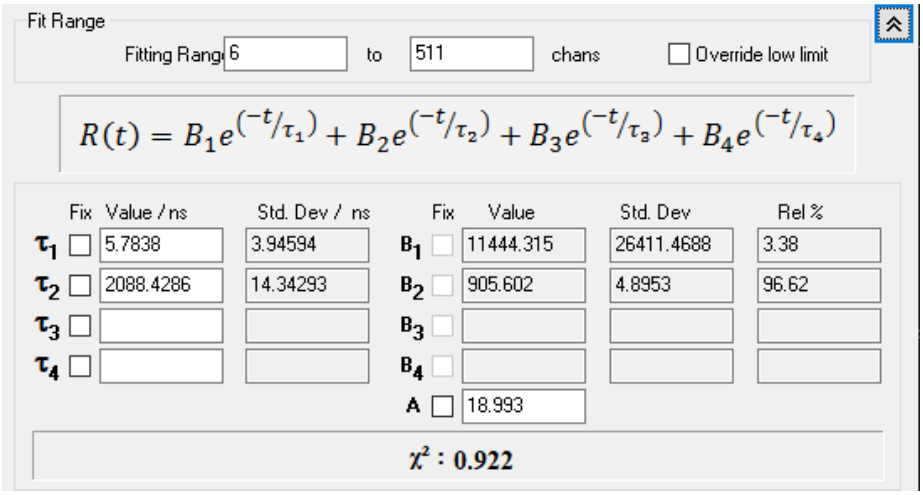

Figure S51. Fit result of Ir(III) complex **1•5,** (1:1) ~1·10^{-5} M (Absorbance of 0.071 from UV-Vis) in $CHCl_3$ degassed for 20 mins (Ar) at 298 K after excitation at 365 nm. Data collected at λ_{max} = 470 nm.

Decay Lifetime Measurement of Ir(III) complex 2•5

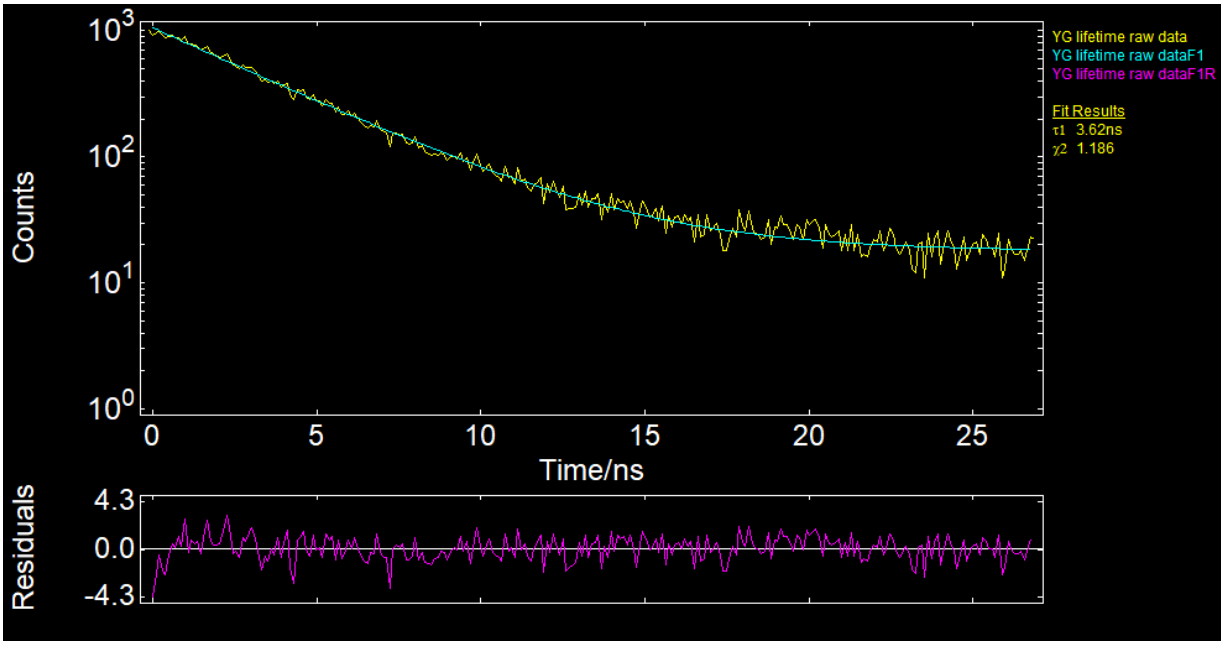

Figure S52. Monoexponential lifetime decay of Ir(III) complex **2•5,** (1:1) ~$1 \cdot 10^{-5}$ M (Absorbance of 0.085 from UV-Vis) in $CHCl_3$ degassed for 20 mins (Ar) at 298 K after excitation at 365 nm. Data collected at λ_{max} = 540 nm.

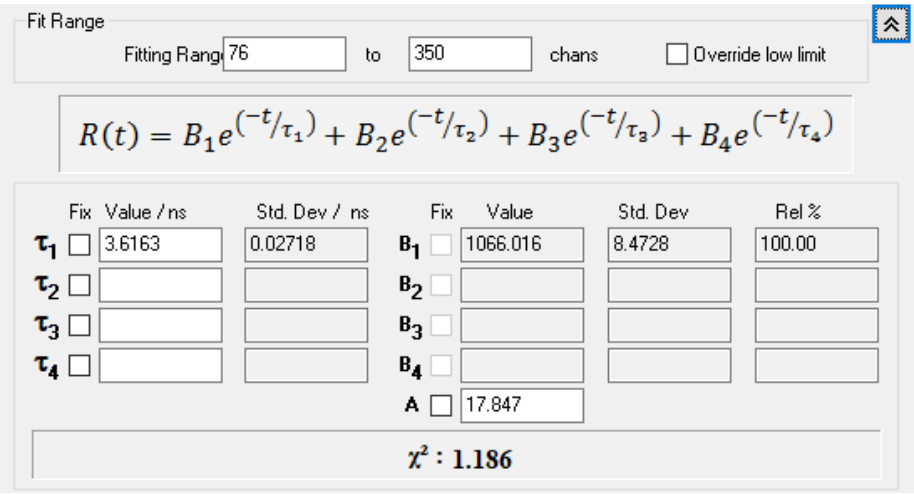

Figure S53. Fit result of Ir(III) complex **2•5,** (1:1) ~$1 \cdot 10^{-5}$ M (Absorbance of 0.085 from UV-Vis) in $CHCl_3$ degassed for 20 mins (Ar) at 298 K after excitation at 365 nm. Data collected at λ_{max} = 540 nm.

Decay Lifetime Measurement of Ir(III) complex 3•5

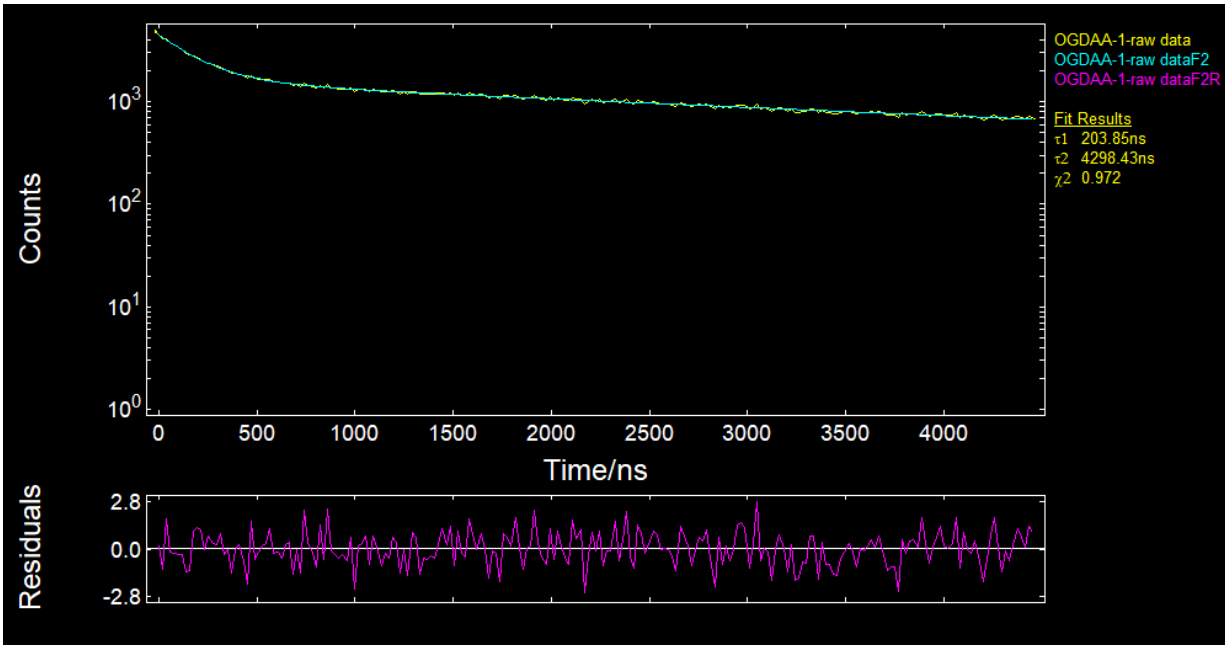

Figure S54. Biexponential lifetime decay of Ir(III) complex **3•5,** (1:1) ~1·10^{-6} M (Absorbance of 0.080 from UV-Vis) in $CHCl_3$ degassed for 20 mins (Ar) at 298 K after excitation at 365 nm. Data collected at λ_{max} = 570 nm.

Fit Range

Fitting Rang 7 to 235 chans Override low limit

$$R(t) = B_1 e^{(-t/\tau_1)} + B_2 e^{(-t/\tau_2)} + B_3 e^{(-t/\tau_3)} + B_4 e^{(-t/\tau_4)}$$

	Fix	Value / ns	Std. Dev / ns		Fix	Value	Std. Dev	Rel %
τ_1	☐	203.8530	4.66155	B_1	☐	3216.909	41.7443	9.59
τ_2	☐	4298.4310	482.08524	B_2	☐	1438.720	67.3146	90.41
τ_3	☐			B_3	☐			
τ_4	☐			B_4	☐			
				A	☐	168.481		

χ^2 : 0.972

Figure S55. Fit result of Ir(III) complex **3•5,** (1:1) ~1·10^{-6} M (Absorbance of 0.080 from UV-Vis) in $CHCl_3$ degassed for 20 mins (Ar) at 298 K after excitation at 365 nm. Data collected at λ_{max} = 570 nm.

Decay Lifetime Measurement of Ir(III) complex 4•5

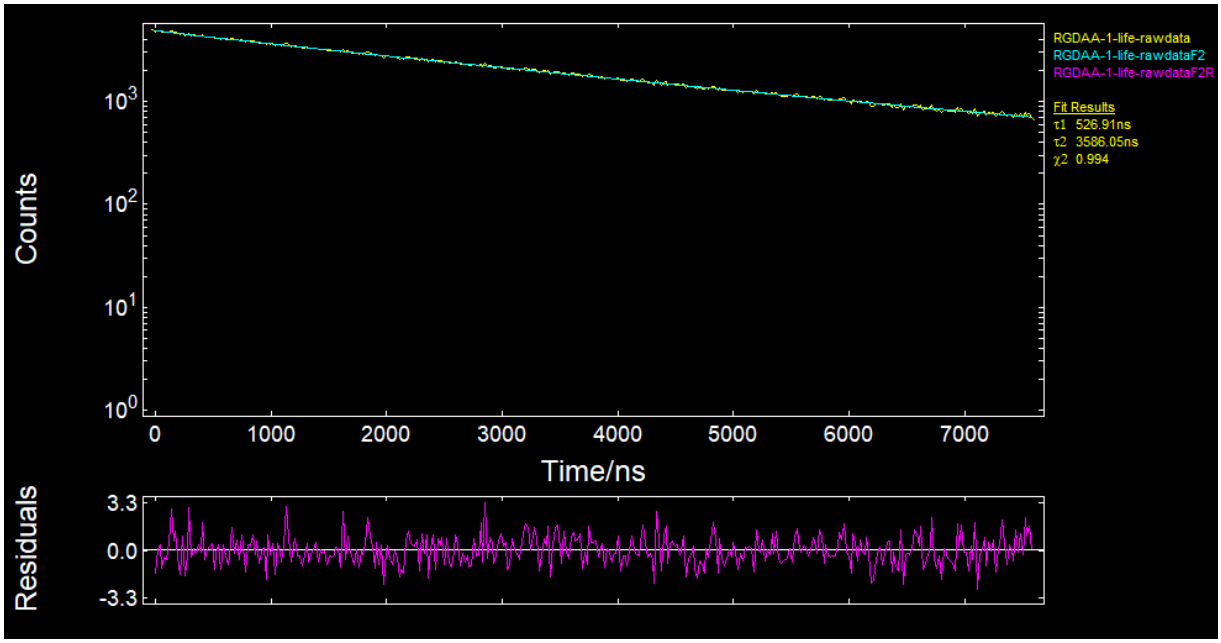

Figure S56. Biexponential lifetime decay of Ir(III) complex **4•5,** (1:1) ~1·10^{-6} M (Absorbance of 0.085 from UV-Vis) in $CHCl_3$ degassed for 20 mins (Ar) at 298 K after excitation at 365 nm. Data collected at λ_{max} = 590 nm.

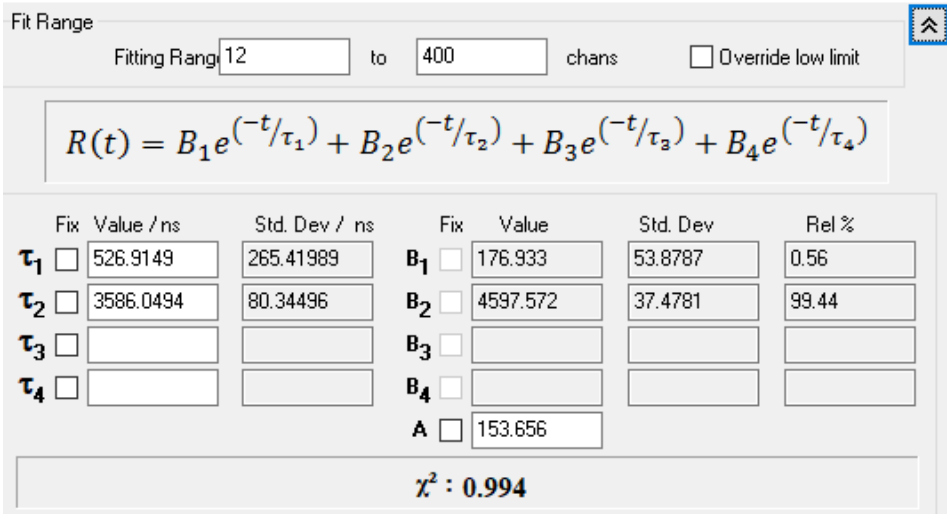

Figure S57. Fit result of Ir(III) complex **4•5,** (1:1) ~1·10^{-6} M (Absorbance of 0.085 from UV-Vis) in $CHCl_3$ degassed for 20 mins (Ar) at 298 K after excitation at 365 nm. Data collected at λ_{max} = 590 nm.

Decay Lifetime Measurement of Ir(III) complex 2•5 (white light)

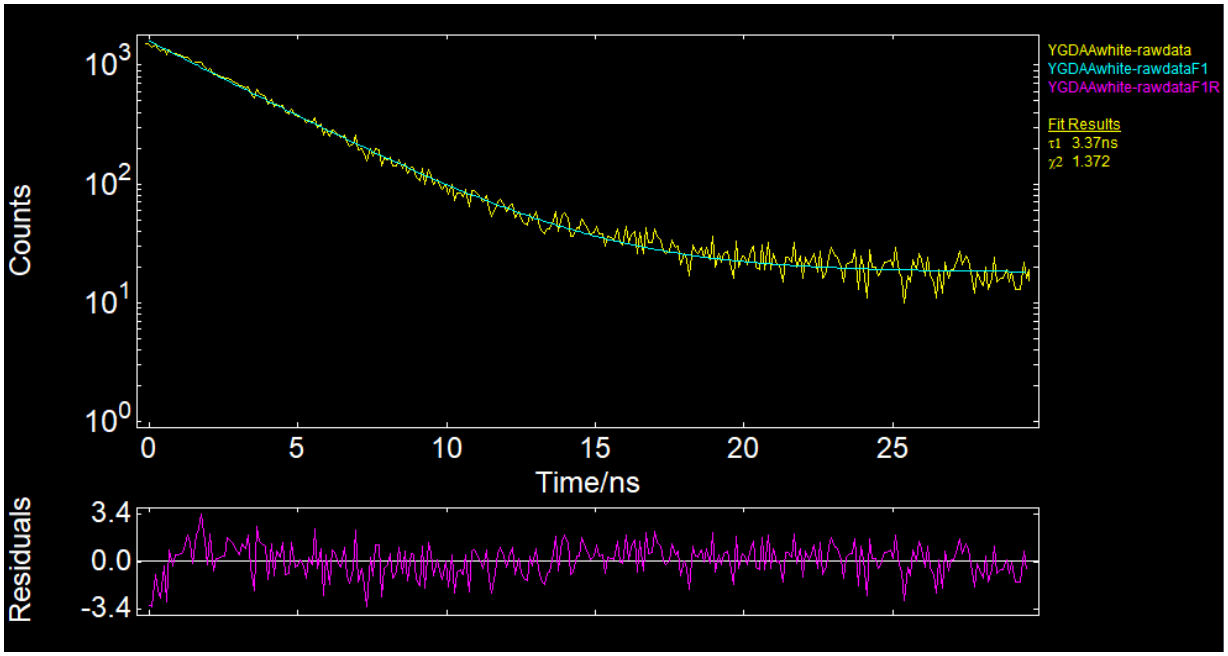

Figure S58. Monoexponential lifetime decay of Ir(III) complex **2•5,** (1:1.3) ~1·10^{-5} M (Absorbance of 0.082 from UV-Vis) in $CHCl_3$ degassed for 20 mins (Ar) at 298 K after excitation at 365 nm. Data collected at λ_{max} = 540 nm.

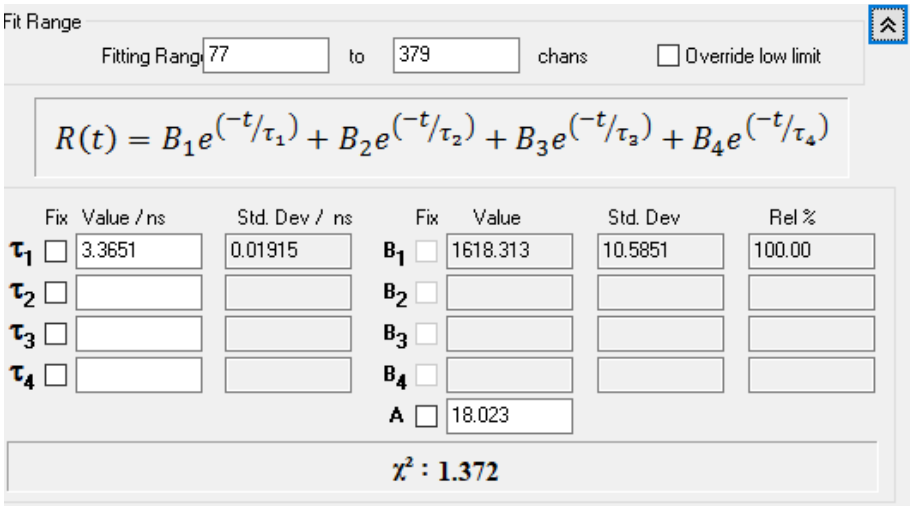

Figure S59. Fit result of Ir(III) complex **2•5,** (1:1) ~1·10^{-5} M (Absorbance of 0.082 from UV-Vis) in $CHCl_3$ degassed for 20 mins (Ar) at 298 K after excitation at 365 nm. Data collected at λ_{max} = 540 nm.

S7. PMMA solid state PLQYs and decay lifetimes

Table S12. a) Significant excitation and emission peaks for Ir(III) complexes **1**-**4** in PMMA films at 298 K. **b)** PLQYs for Ir(III) complexes **1**-**4**; in PMMA film at 298 K determined using an SC-30 integrating sphere module. **c)** decay lifetimes using TCSPC excited at 365 nm and their corresponding chi-squared values for Ir(III) complexes **1**-**4**; in PMMA films at 298 K. Complexes **1**, **2**, **3**, and **4** decay biexponentially. **d)** the radiative (k_r) and nonradiative (k_{nr}) rate constants were calculated as $k_r = \phi_{PL}/\tau_{PL}$ and $k_{nr} = (1-\phi_{PL})/\tau_{PL}$.

Ir(III) Complex	Excitation (nm)[a]	Emission (nm)[a]	PLQY (%)[b]	Lifetime (ns) (τ_{PL}, χ^2)[c]	k_r ($\times 10^5$ s^{-1})[d]	k_{nr} ($\times 10^5$ s^{-1})[d]
1	250, 295	473, 495	91.3	(1932.14, 0.959) 92%	4.73	0.45
2	302, 328	540, 581	15.1	(0.5778, 1.199) 71.5%	2613.36	14693.67
3	298, 390	565, 597	70.1	(1155.79, 1.092) 95%	6.07	2.59
4	342, 440	595, 634	74.0	(3830.21, 0.979) 95%	1.93	0.68
1•5 (1:1)	261, 329	473, 497	83.4	(2079.96, 1.113) 86%	4.01	0.80
2•5 (1:1)	326, 456	537, 581	15.7	(3.2596, 1.114) 51%	481.65	2586.21
3•5 (1:1)	299, 388	561, 599	65.1	(4042.90, 1.079) 90%	1.61	0.86
4•5 (1:1)	340, 440	595, 693	71.3	(4177.25, 0.989) 80%	1.71	0.69

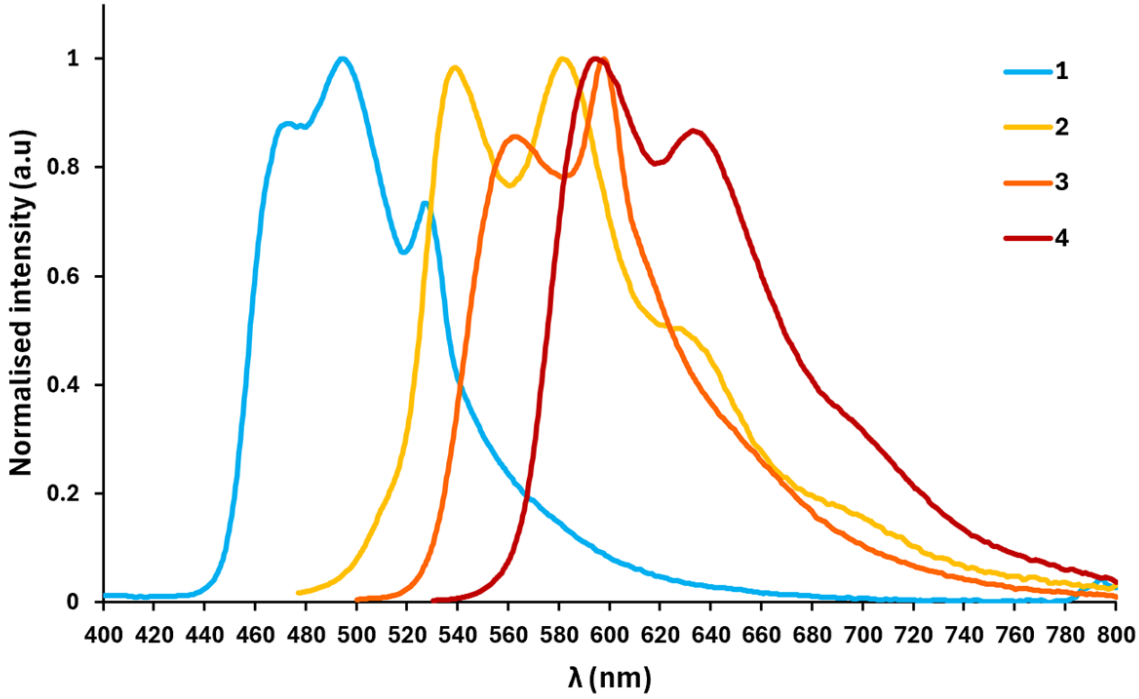

Figure S60. Combined normalised emission spectra of complex **1**-**4** obtained through solid state excitation of PMMA thin films.

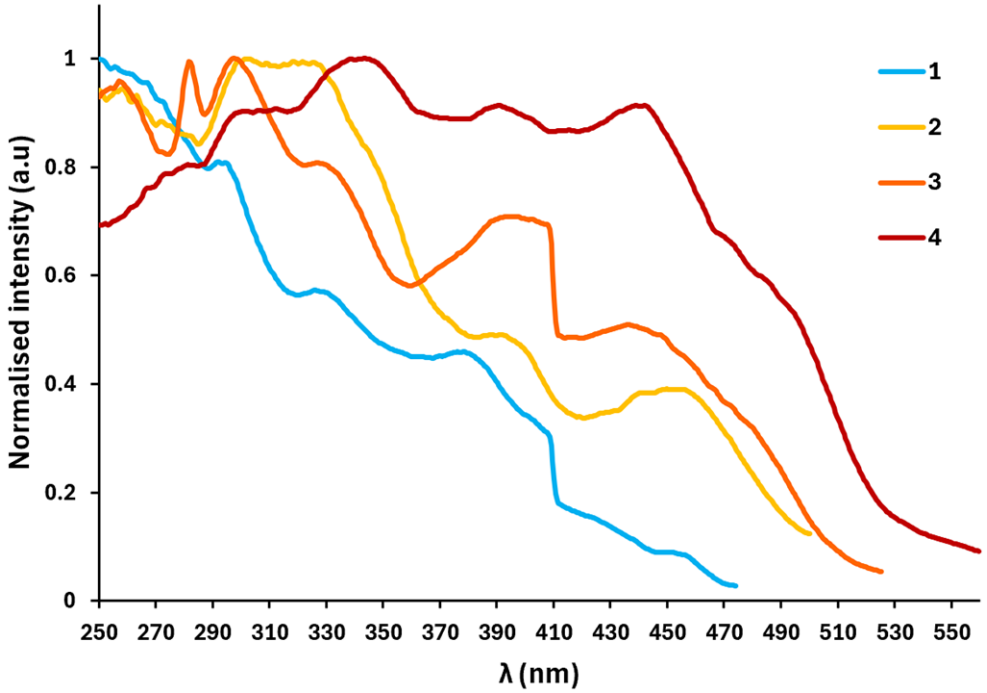

Figure S61. Combined normalised absorption spectra of complex **1**-**4** obtained through solid state analysis of PMMA thin films.

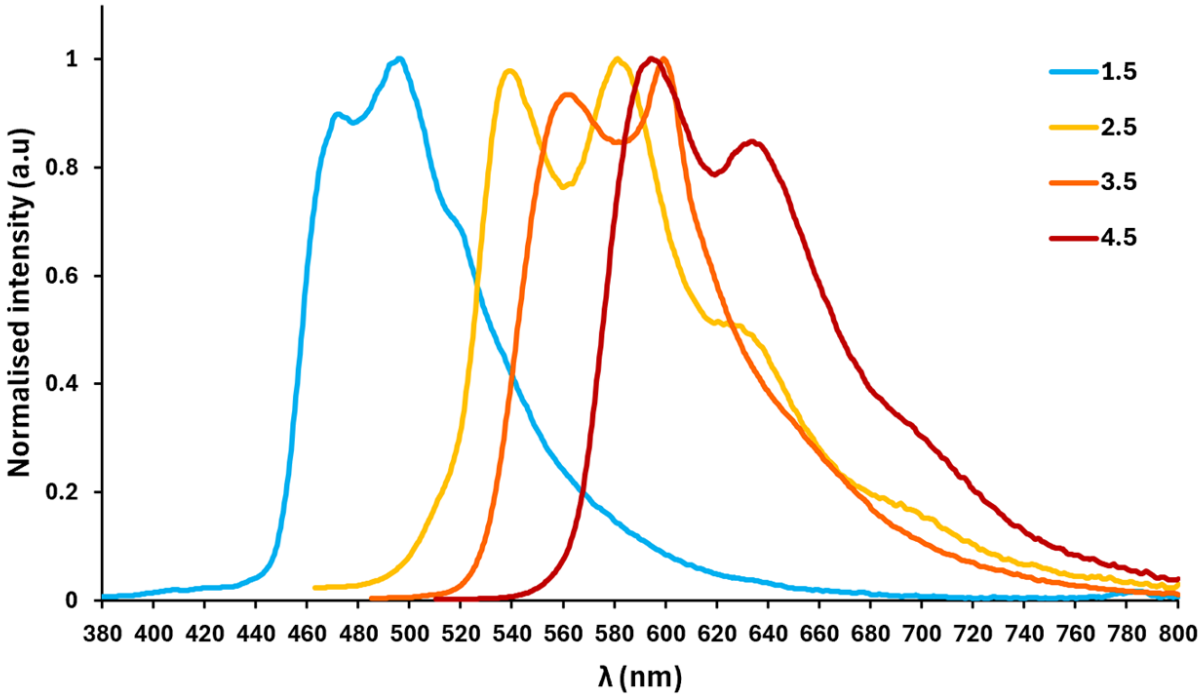

Figure S62. Combined normalised emission spectra of co-complex **1-4•5** obtained through solid state excitation of PMMA thin films.

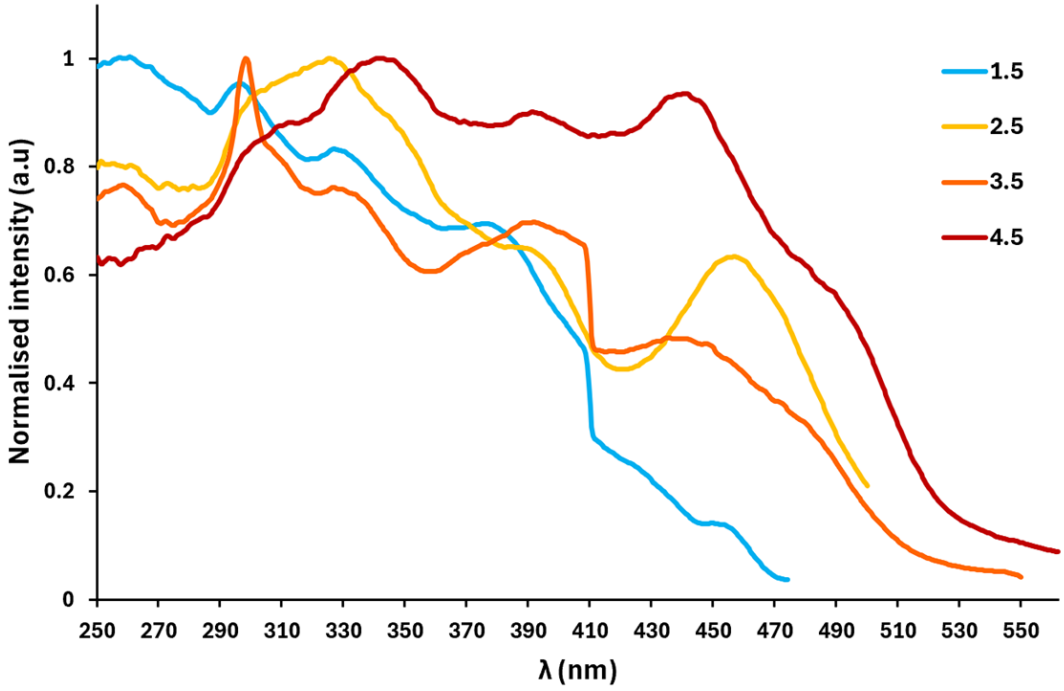

Figure S63. Combined normalised absorption spectra of co-complex **1-4•5** obtained through solid state analysis of PMMA thin films.

Solid State Decay Lifetime Measurement of Ir(III) complex 1

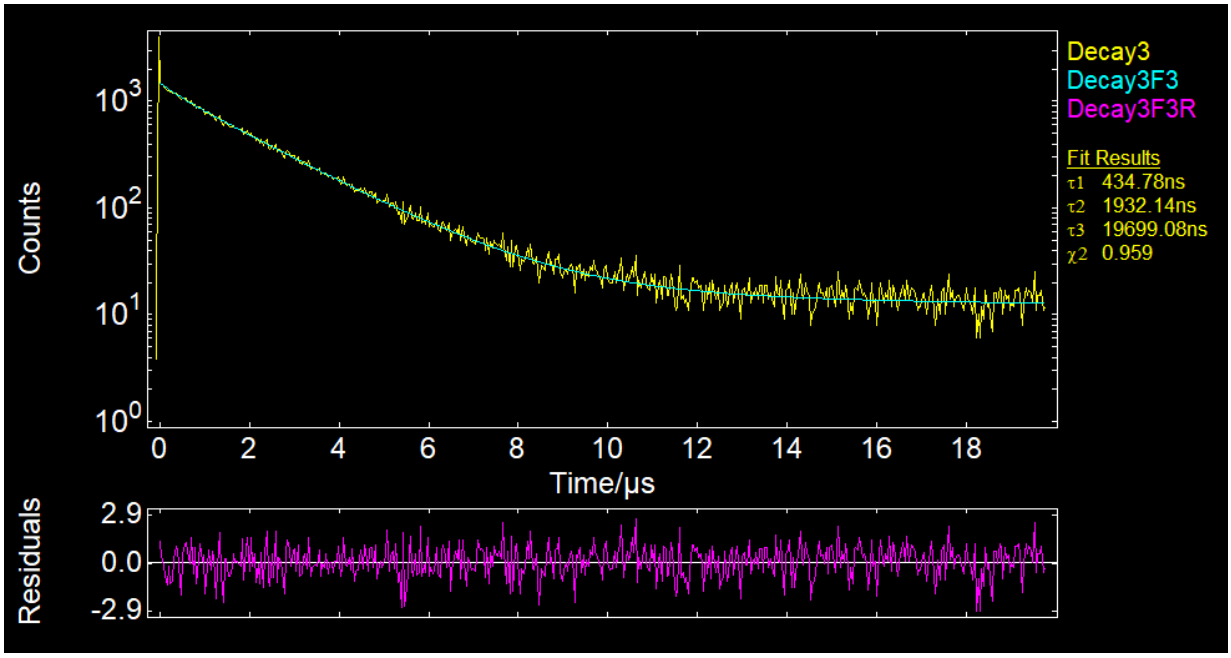

Figure S64. Biexponential lifetime decay of Ir(III) complex **1** in PMMA film at 298 K, excited at 365 nm. Data collected at λ_{max} = 495 nm.

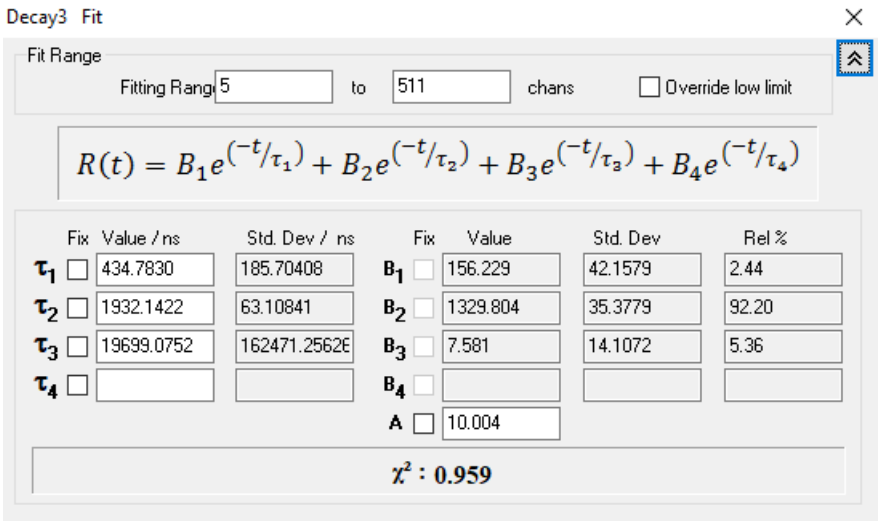

Figure S65. Fit result of Ir(III) complex **1** in PMMA film at 298 K, excited at 365 nm. Data collected at λ_{max} = 495 nm.

Solid State Decay Lifetime Measurement of Ir(III) complex 2

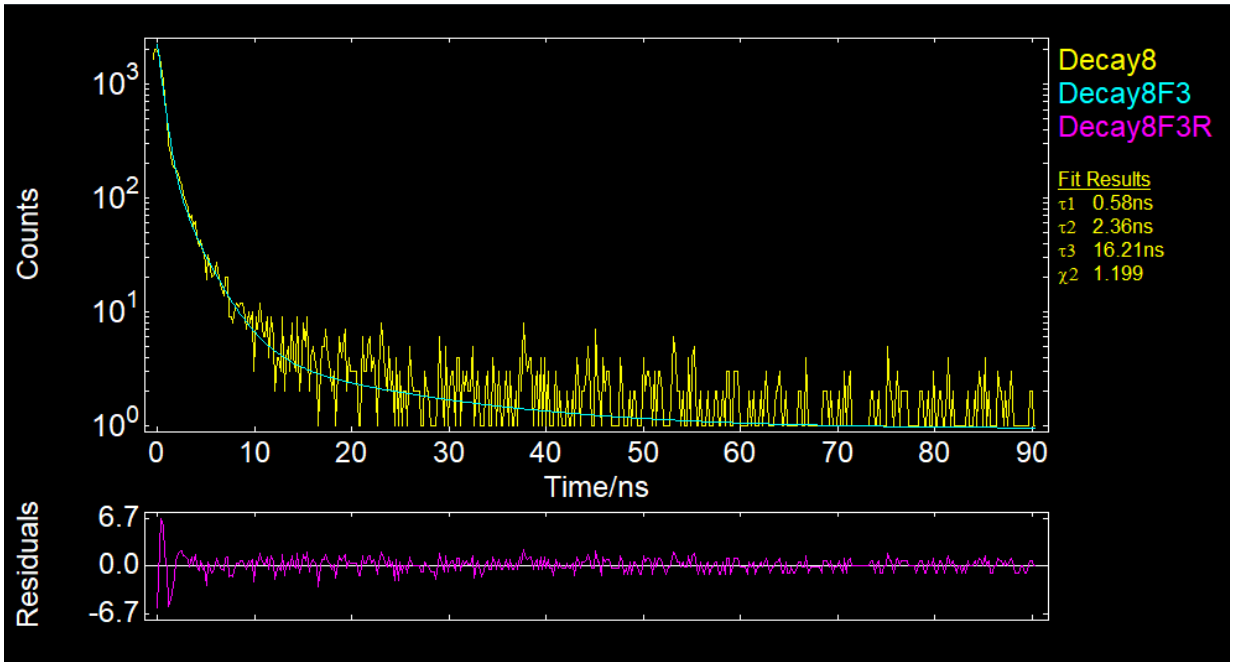

Figure S66. Biexponential lifetime decay of Ir(III) complex **2** in PMMA film at 298 K, excited at 365 nm. Data collected at λ_{max} = 580 nm.

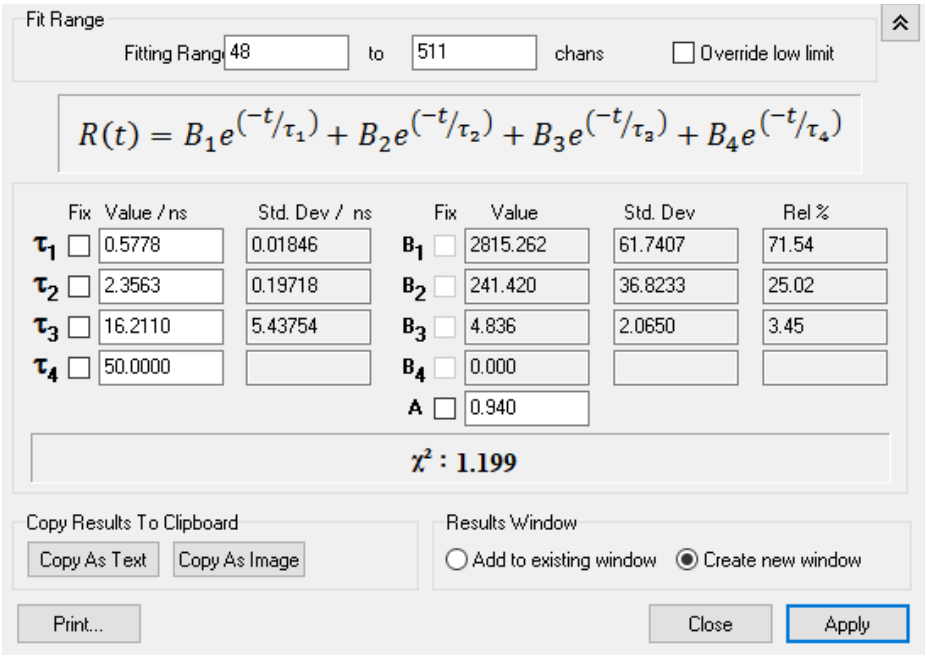

Figure S67. Fit result of Ir(III) co-system **2** in PMMA film at 298 K, excited at 365 nm. Data collected at λ_{max} = 580 nm.

Solid State Decay Lifetime Measurement of Ir(III) complex 3

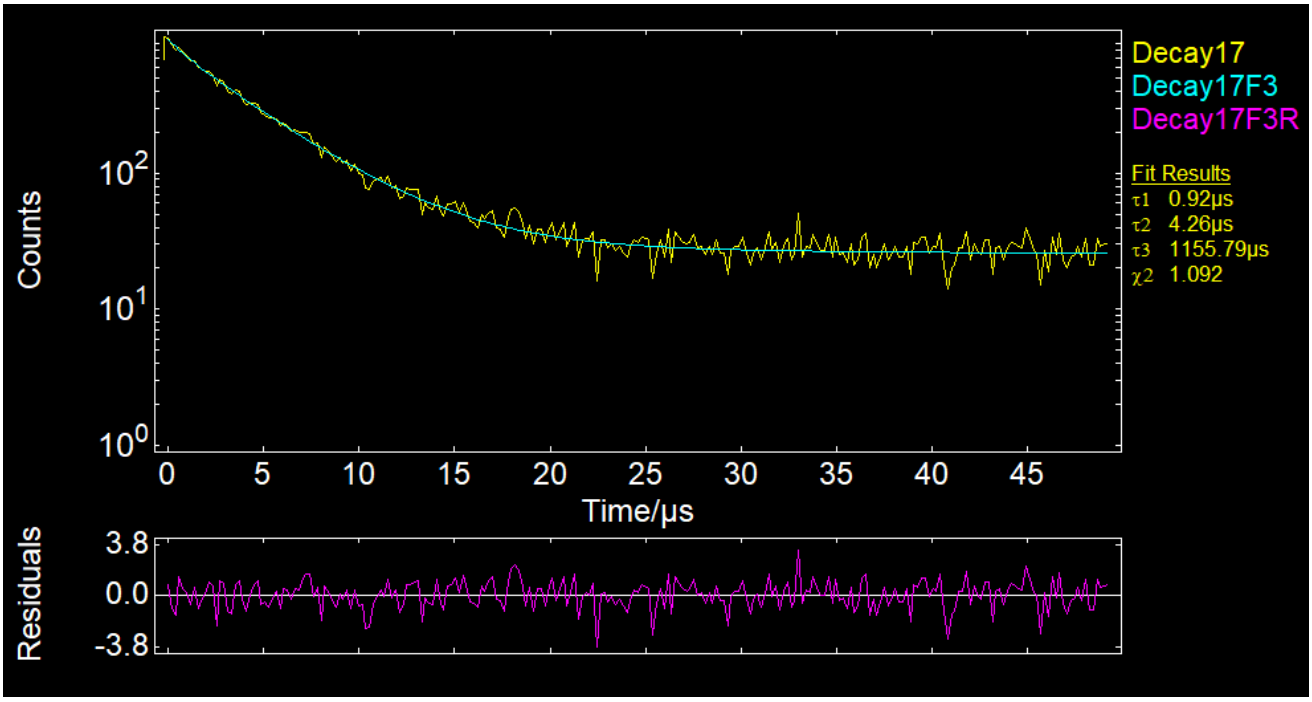

Figure S68. Biexponential lifetime decay of Ir(III) complex **3** in PMMA film at 298 K, excited at 365 nm. Data collected at λ_{max} = 598 nm.

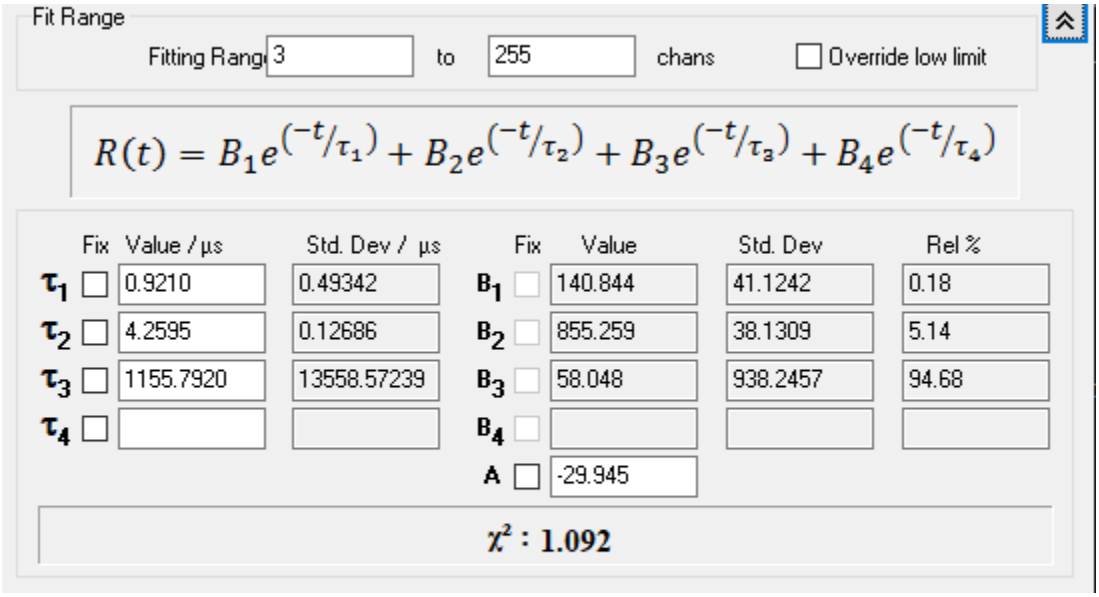

Figure S69. Fit result of Ir(III) co-system **3** in PMMA film at 298 K, excited at 365 nm. Data collected at λ_{max} = 598 nm.

Solid State Decay Lifetime Measurement of Ir(III) complex 4

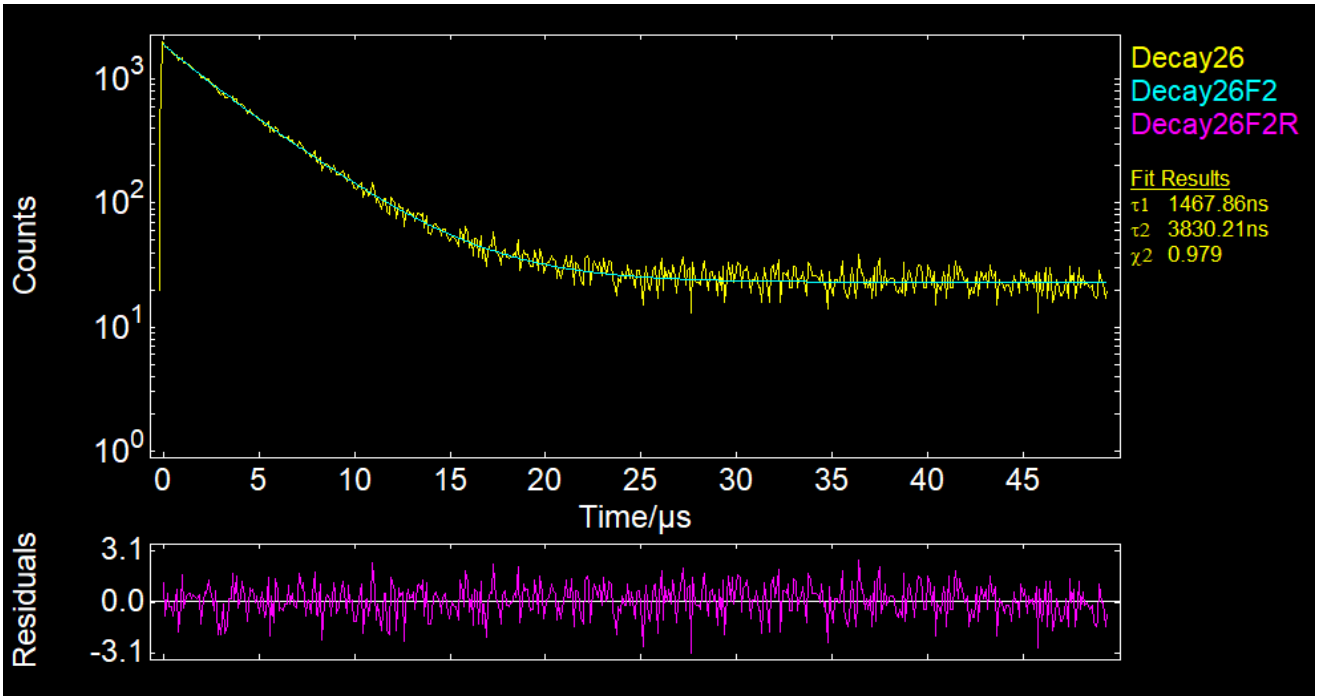

Figure S70. Biexponential lifetime decay of Ir(III) complex **4** in PMMA film at 298 K, excited at 365 nm. Data collected at λ_{max} = 595 nm.

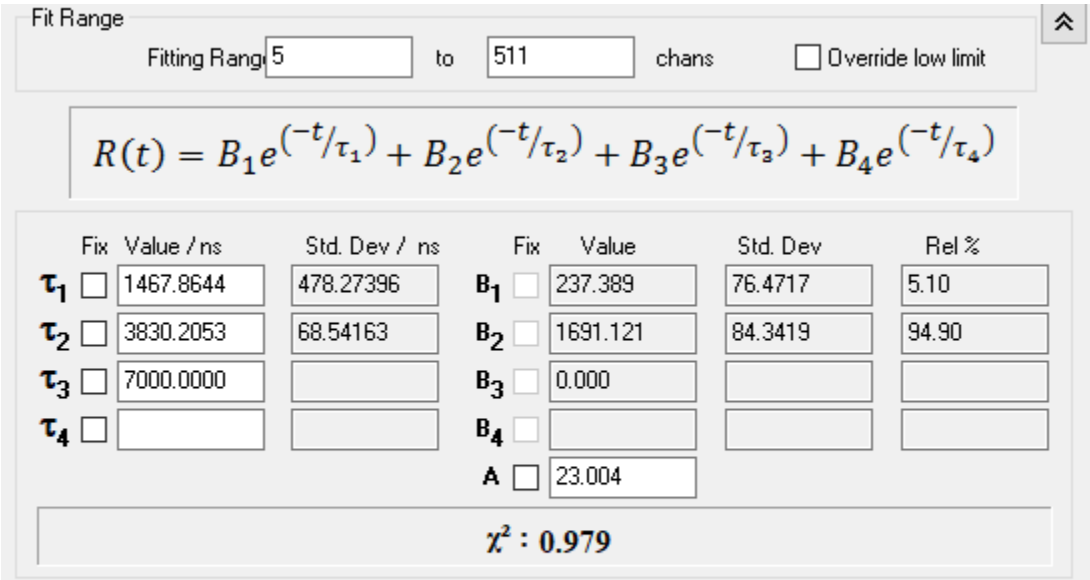

Figure S71. Fit result of Ir(III) co-system **4** in PMMA film at 298 K, excited at 365 nm. Data collected at λ_{max} = 595 nm.

Solid State Decay Lifetime Measurement of Ir(III) complex 1•5

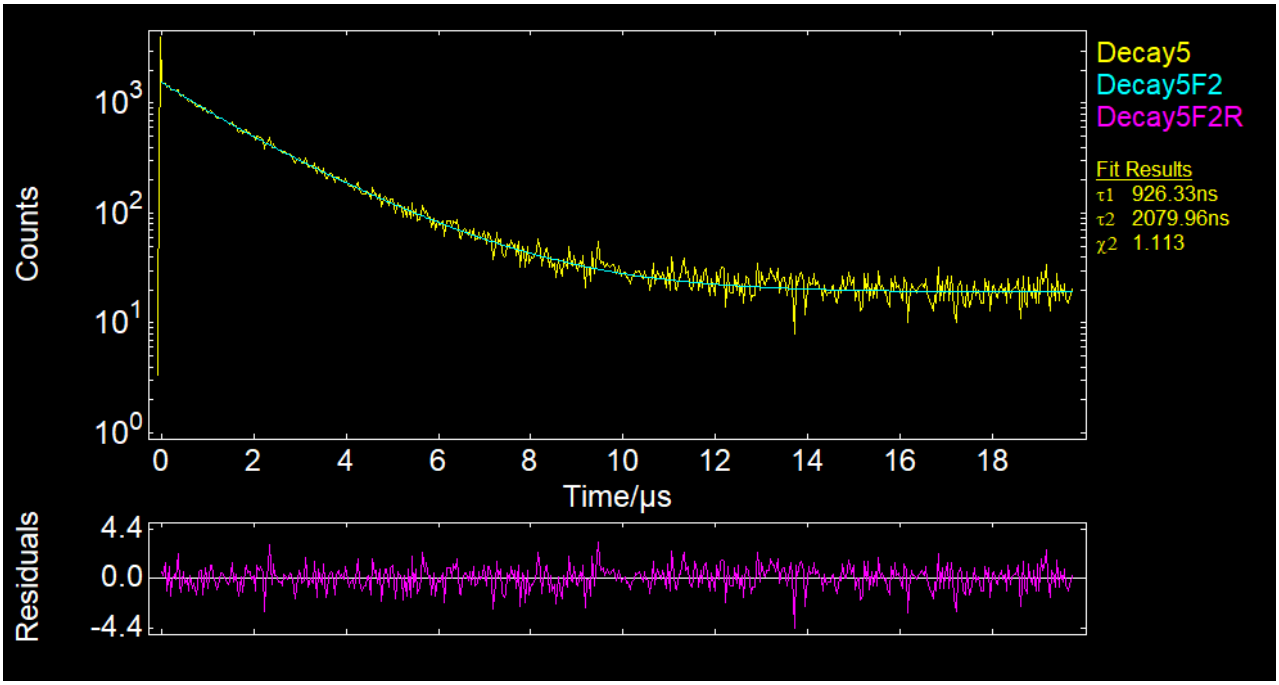

Figure S72. Biexponential lifetime decay of Ir(III) co-system **1•5** in PMMA film at 298 K, excited at 365 nm. Data collected at λ_{max} = 496 nm.

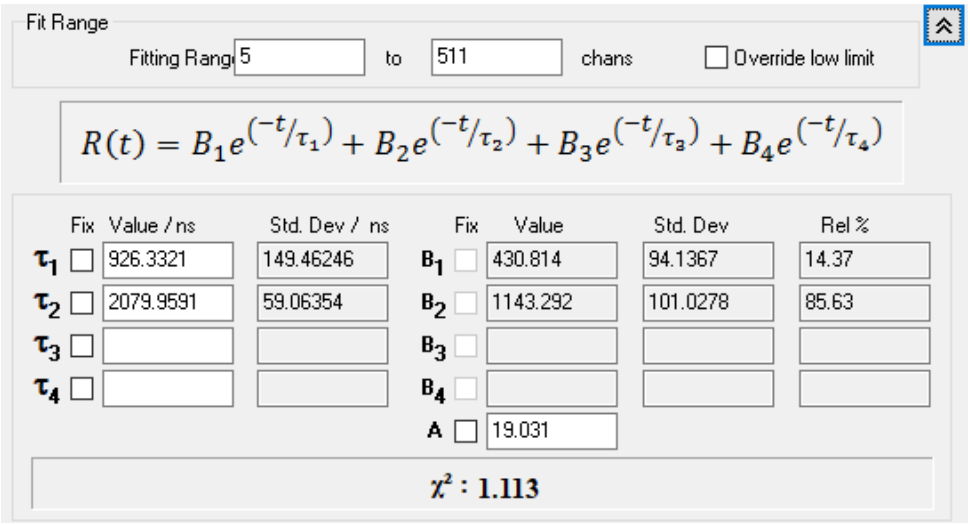

Figure S73. Fit result of Ir(III) co-system **1•5** in PMMA film at 298 K, excited at 365 nm. Data collected at λ_{max} = 496 nm.

Solid State Decay Lifetime Measurement of Ir(III) complex 2•5

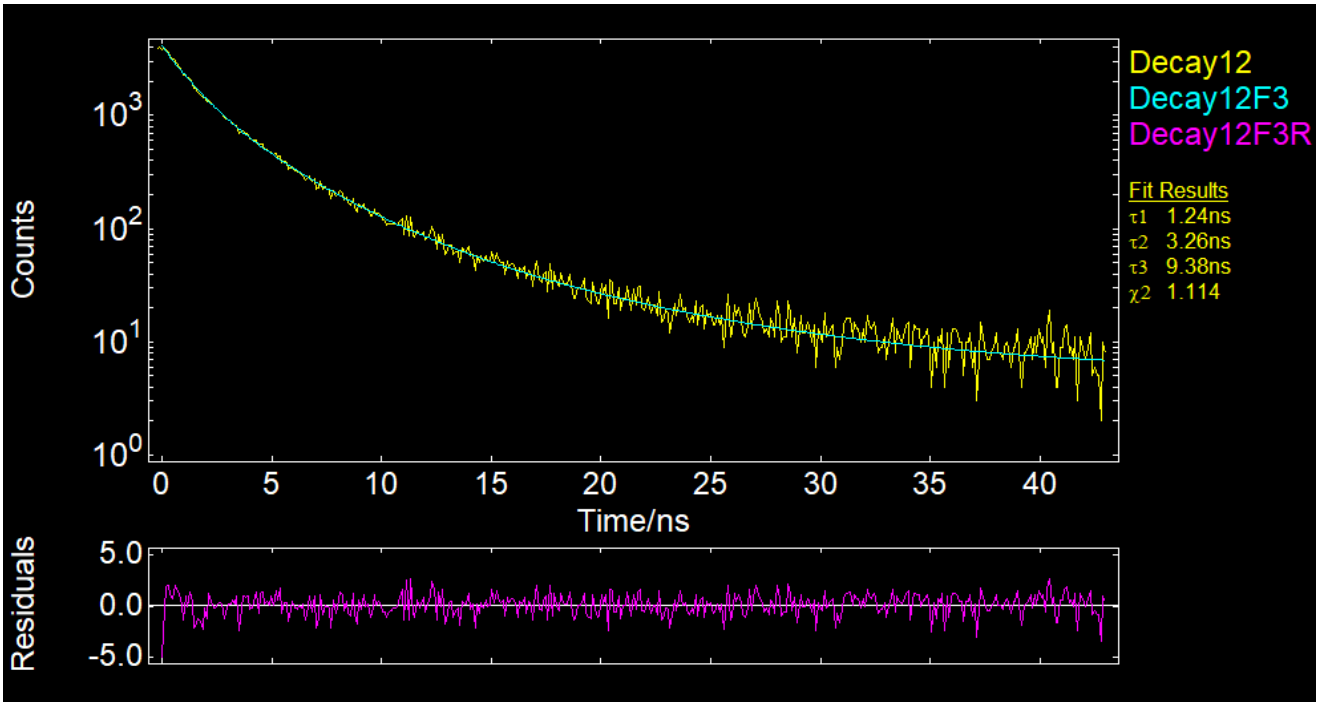

Figure S74. Biexponential lifetime decay of Ir(III) complex **2•5** in PMMA film at 298 K, excited at 365 nm. Data collected at λ_{max} = 581 nm.

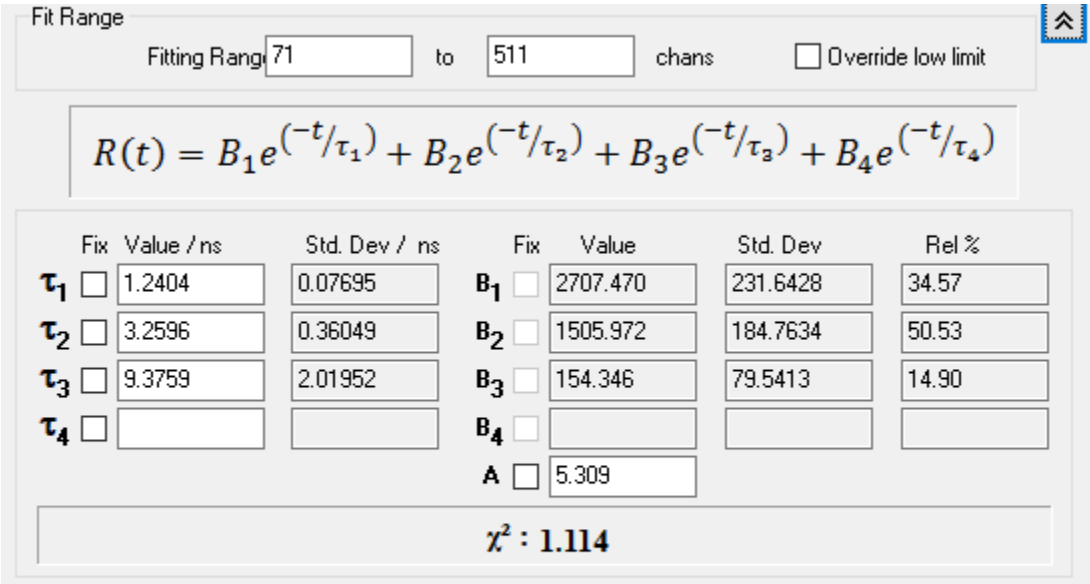

Figure S75. Fit result of Ir(III) co-system **2•5** in PMMA film at 298 K, excited at 365 nm. Data collected at λ_{max} = 581 nm.

Solid State Decay Lifetime Measurement of Ir(III) complex 3•5

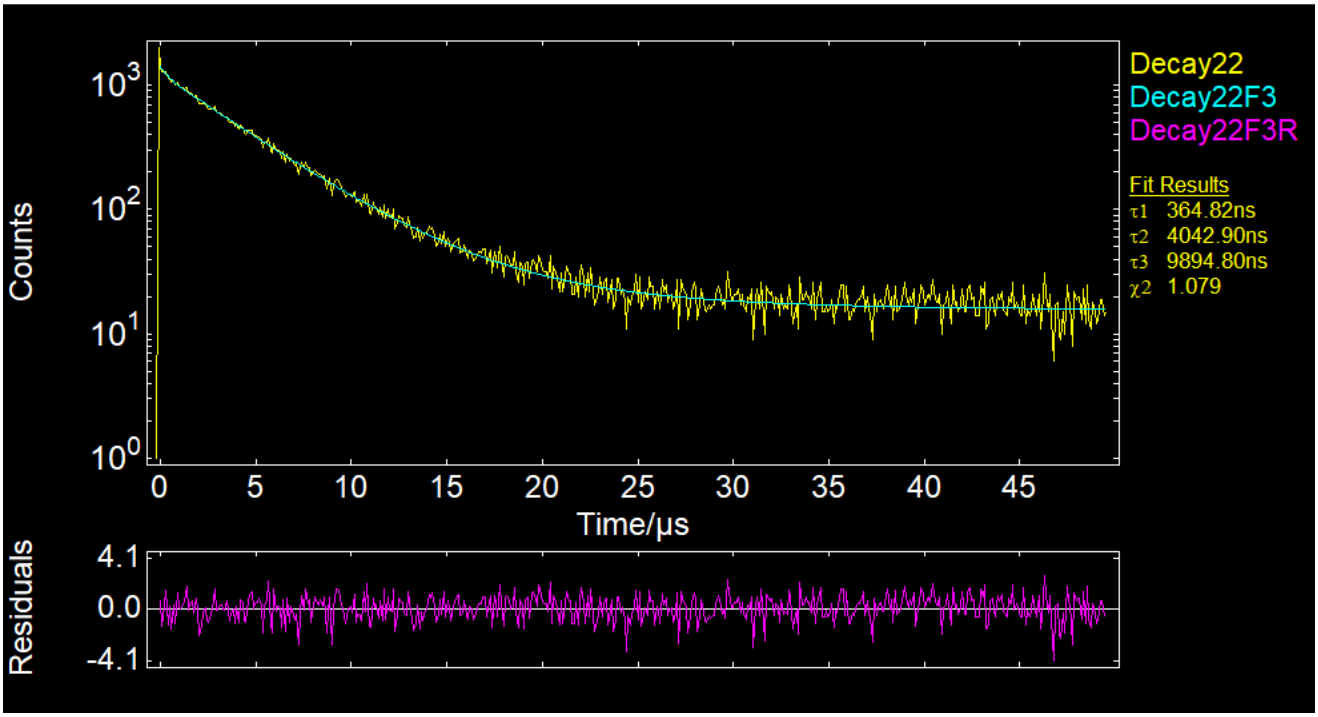

Figure S76. Biexponential lifetime decay of Ir(III) complex **3•5** in PMMA film at 298 K, excited at 365 nm. Data collected at λ_{max} = 599 nm.

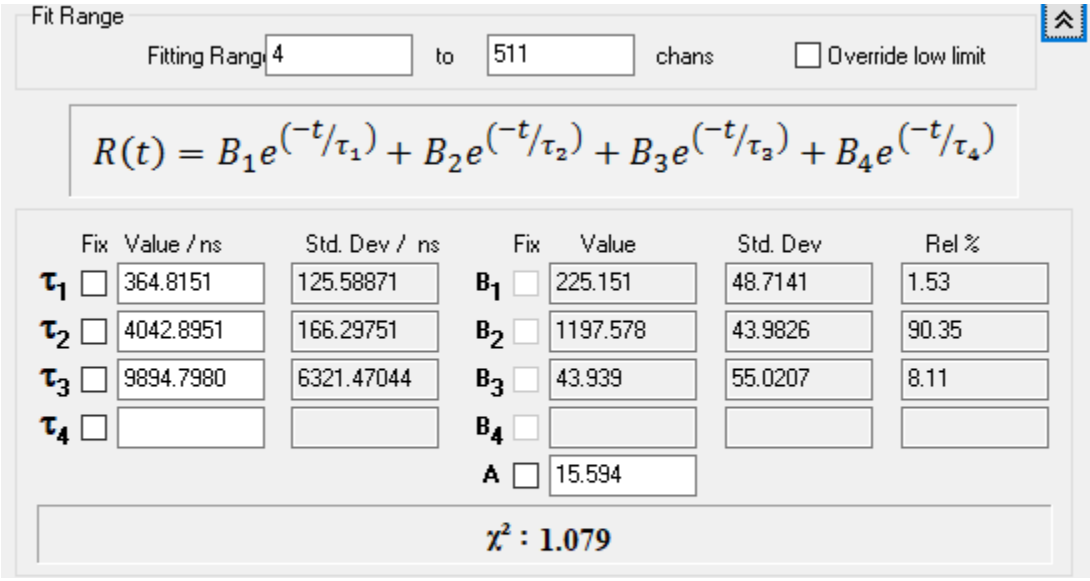

Figure S77. Fit result of Ir(III) co-system **3•5** in PMMA film at 298 K, excited at 365 nm. Data collected at λ_{max} = 599 nm.

Solid State Decay Lifetime Measurement of Ir(III) complex 4•5

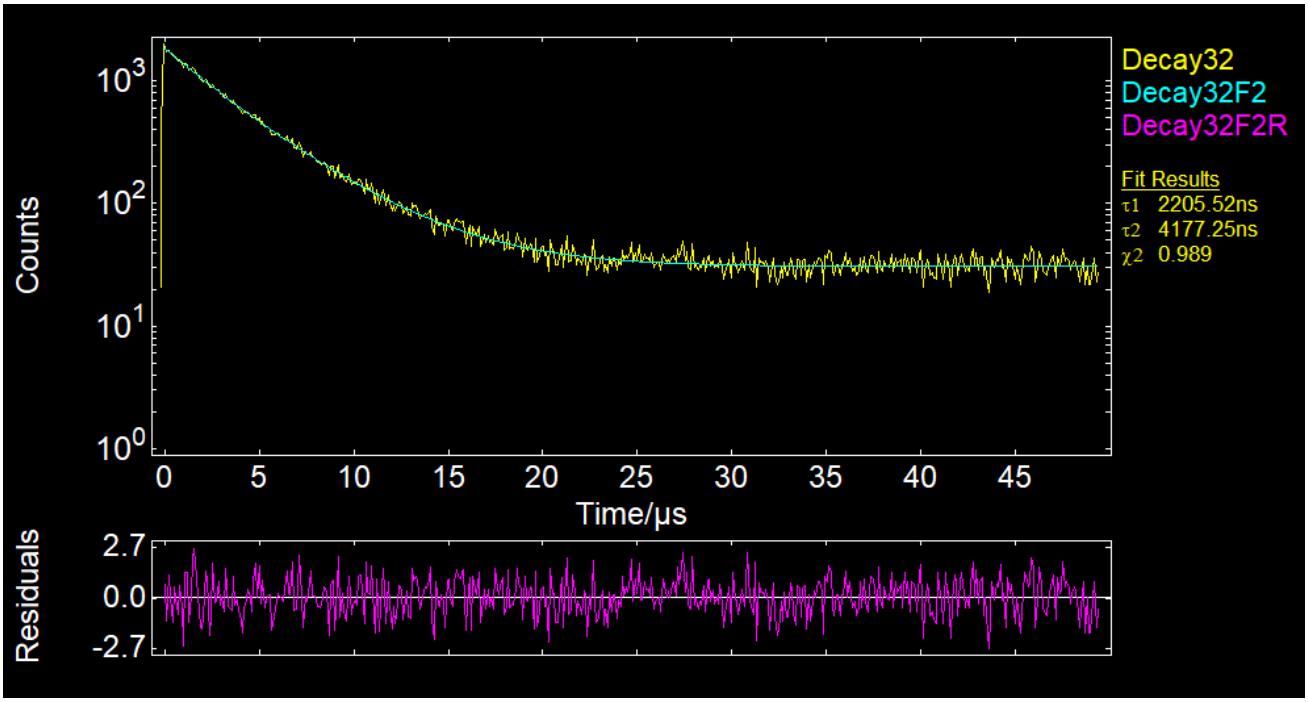

Figure S78. Biexponential lifetime decay of Ir(III) complex **4•5** in PMMA film at 298 K, excited at 365 nm. Data collected at λ_{max} = 595 nm.

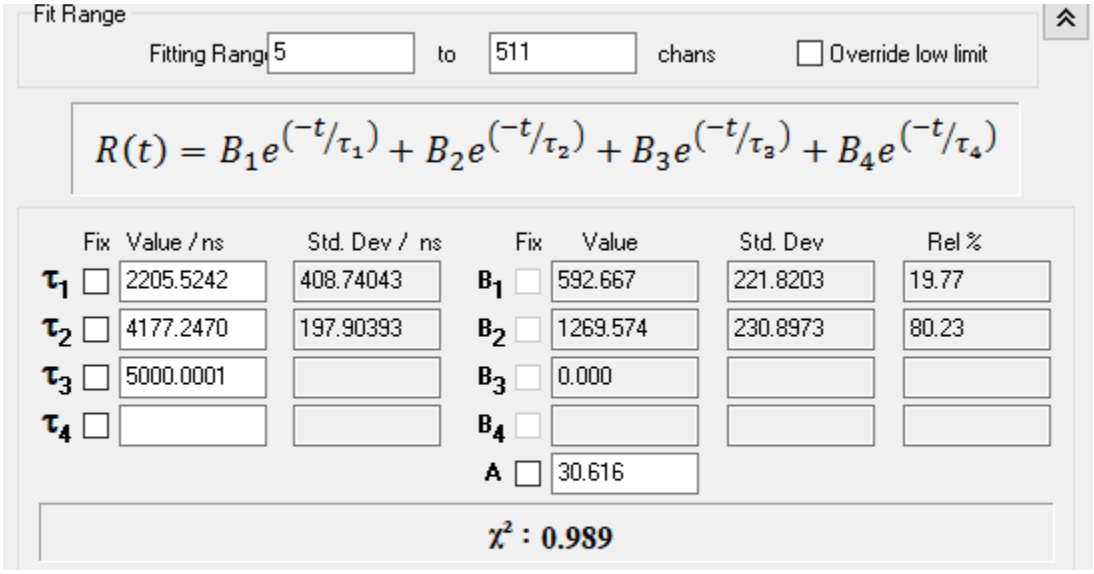

Figure S79. Fit result of Ir(III) co-system **4•5** in PMMA film at 298 K, excited at 365 nm. Data collected at λ_{max} = 595 nm.

S8. Cyclic voltammetry

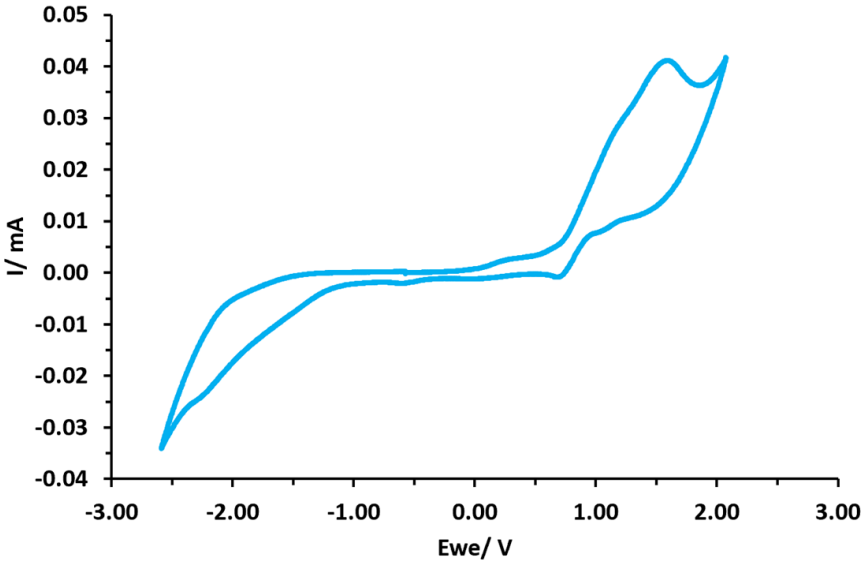

Figure S80. Cyclic voltammetry of complex **1** 2mM in dry degassed $CHCl_3$ normalised to a ferrocene standard.

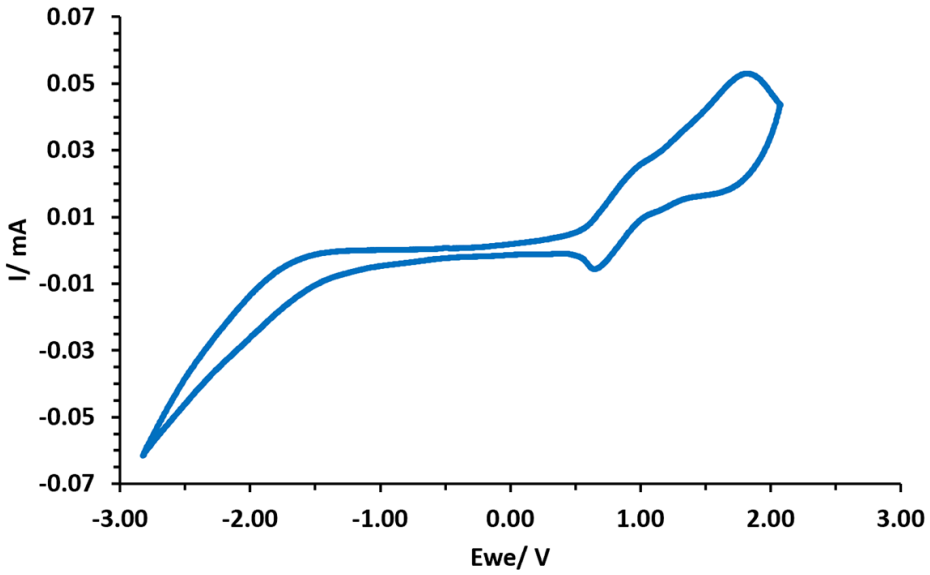

Figure S81. Cyclic voltammetry of co-system **1•5** 2mM 1:1 ratio between complex and binder in dry degassed $CHCl_3$ normalised to a ferrocene standard.

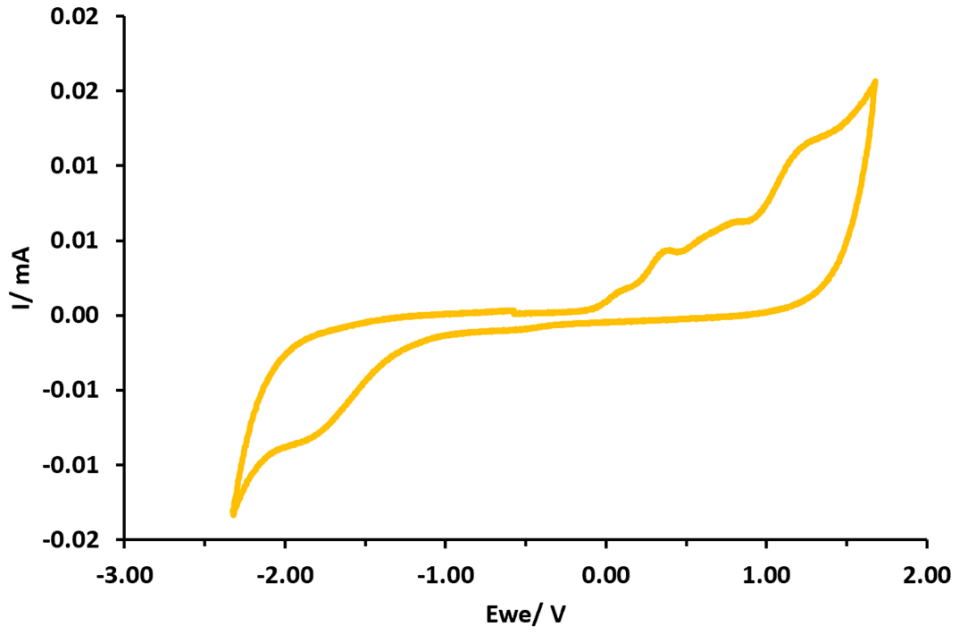

Figure S82. Cyclic voltammetry of complex **2** 2mM in dry degassed $CHCl_3$ normalised to a ferrocene standard.

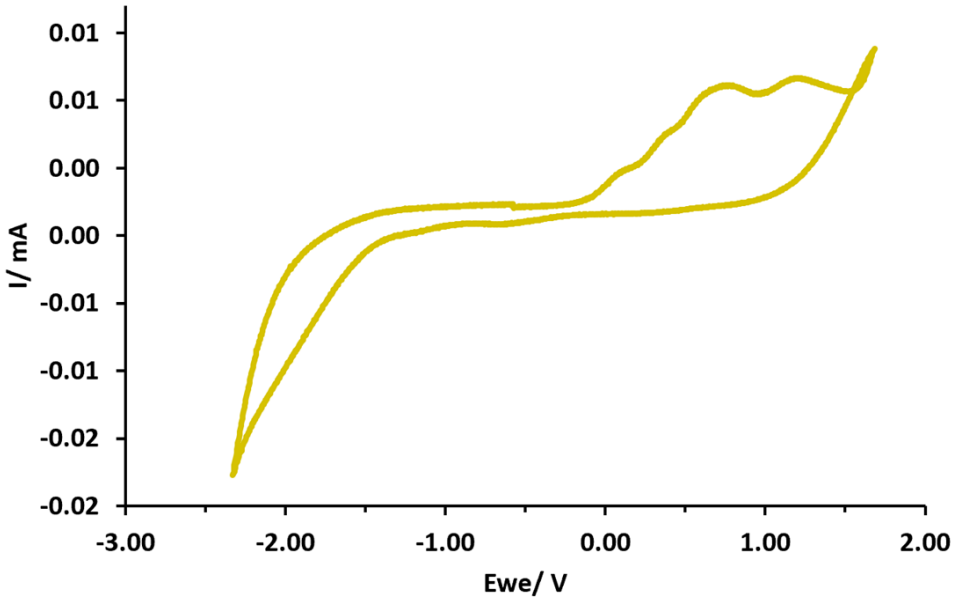

Figure S83. Cyclic voltammetry of co-system **2•5** 2mM 1:1 ratio between complex and binder in dry degassed $CHCl_3$ normalised to a ferrocene standard.

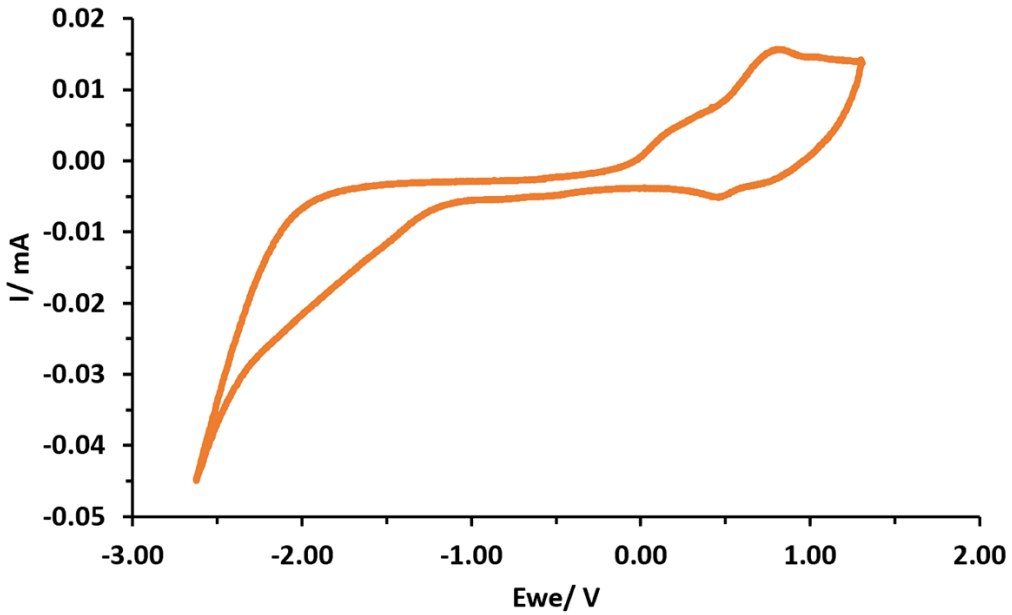

Figure S84. Cyclic voltammetry of complex **3** 2mM in dry degassed $CHCl_3$ normalised to a ferrocene standard.

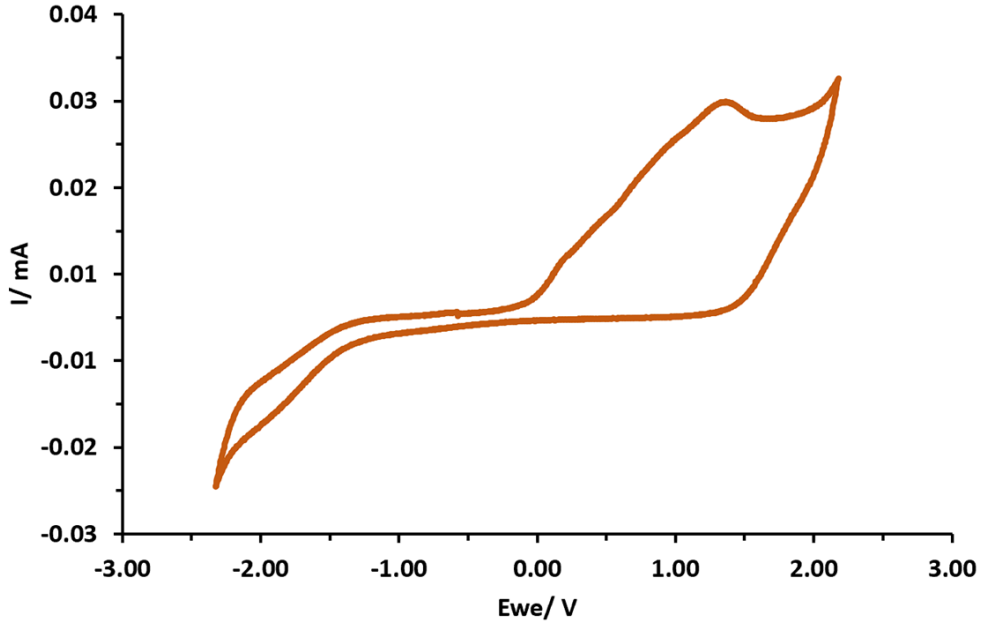

Figure S85. Cyclic voltammetry of co-system **3•5** 2mM 1:1 ratio between complex and binder in dry degassed $CHCl_3$ normalised to a ferrocene standard.

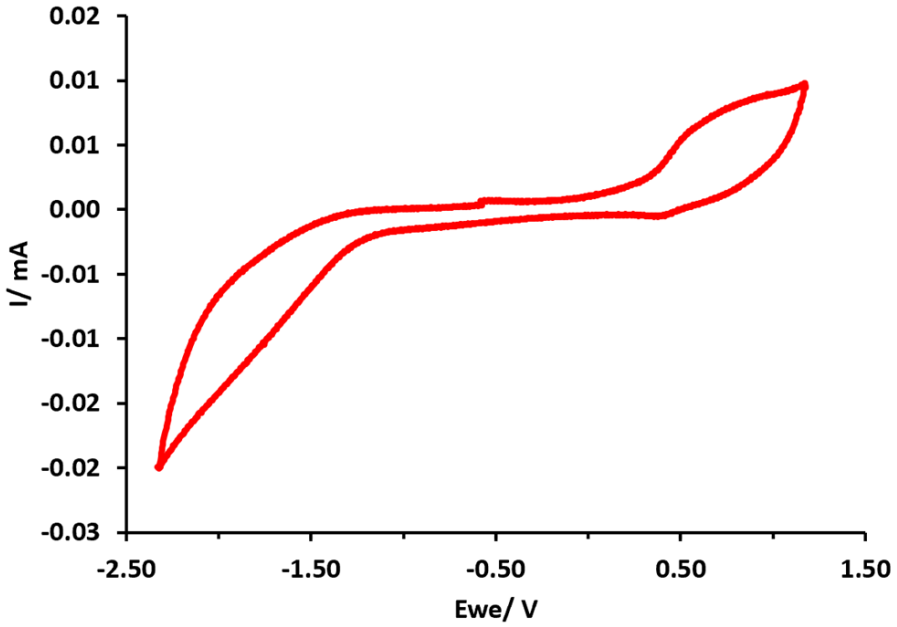

Figure S86. Cyclic voltammetry of complex **4** 2mM in dry degassed $CHCl_3$ normalised to a ferrocene standard.

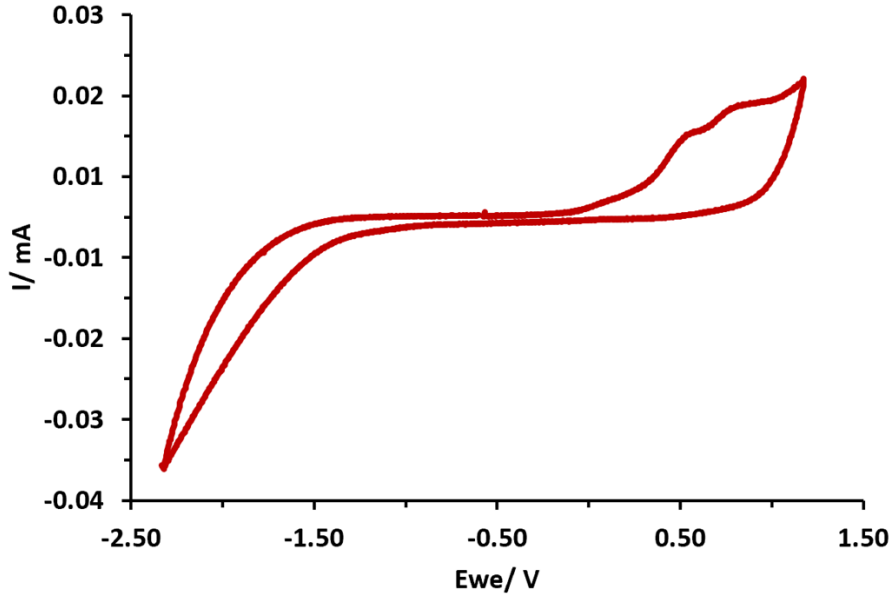

Figure S87. Cyclic voltammetry of co-system **4•5** 2mM 1:1 ratio between complex and binder in dry degassed $CHCl_3$ normalised to a ferrocene standard.

S9. DFT studies

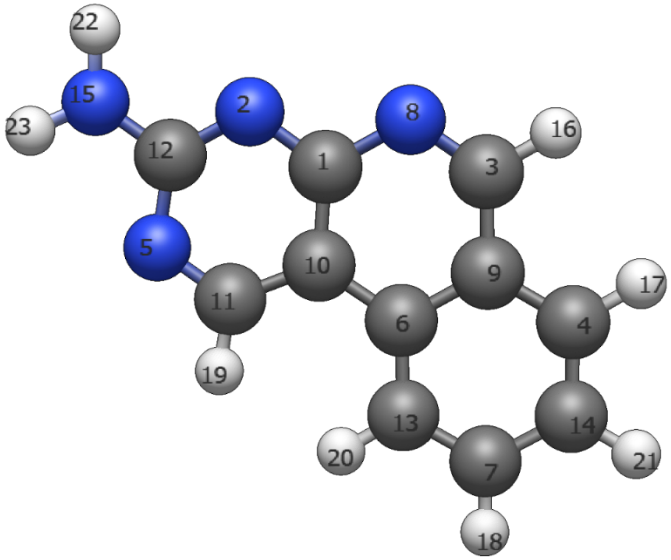

Figure S88. Optimised geometry model used for compound **5**, input file for geometry optimisation was based upon a .cif data file from previous publication. [10] TD-DFT inputs and energy calculations were based upon this optimised input model.

Table S14. Cartesian coordinates for optimised compound **5**.

Center Number	Atomic Number	Atomic Type	Coordinates (Angstroms) X	Y	Z
1	6	0	-1.024676	0.874857	-0.000163
2	7	0	-2.366849	0.958665	-0.002106
3	6	0	0.953505	2.033977	0.004452
4	6	0	3.168106	0.902829	0.000424
5	7	0	-2.509731	-1.450133	0.009269
6	6	0	1.092025	-0.412576	-0.000300
7	6	0	3.259718	-1.507121	-0.004914
8	7	0	-0.347759	2.079376	0.003860
9	6	0	1.758143	0.842654	0.001403
10	6	0	-0.350763	-0.379470	0.000719
11	6	0	-1.192946	-1.512677	0.011330
12	6	0	-3.038340	-0.191497	-0.005056
13	6	0	1.878135	-1.587562	-0.004054
14	6	0	3.915307	-0.259100	-0.002498

15	7	0	-4.397729	-0.127532	-0.043934
16	1	0	1.471961	2.995734	0.007558
17	1	0	3.654125	1.875698	0.001575
18	1	0	3.847904	-2.420956	-0.008074
19	1	0	-0.769336	-2.516231	0.025292
20	1	0	1.402686	-2.563246	-0.007577
21	1	0	5.000540	-0.216179	-0.003319
22	1	0	-4.838659	0.768865	0.092124
23	1	0	-4.924033	-0.972208	0.114733

Energy

E(RB3LYP) = -643.024565950 Hartree

Zero point corrected free energy = -642.848333 Hartree

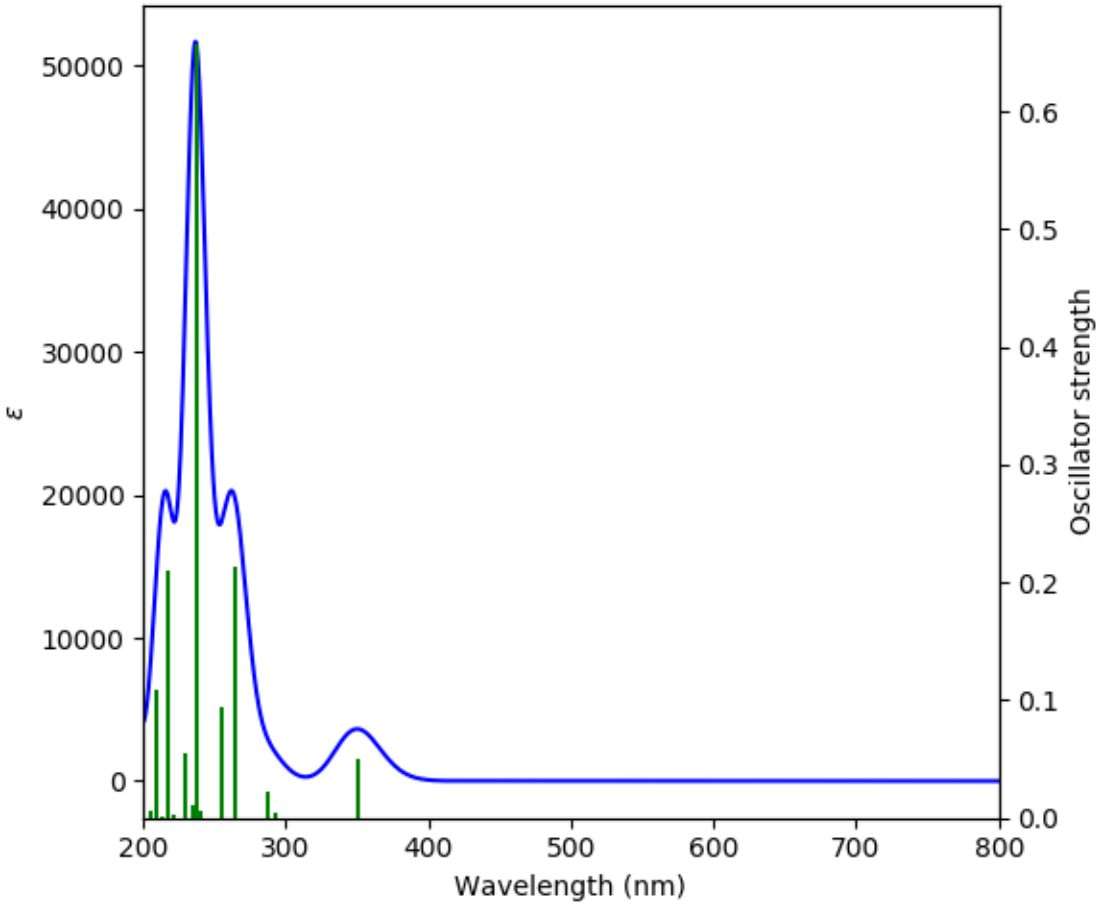

Figure S89. Calculated UV/vis spectrum for compound **5**.

Table S15. Calculated energy levels of the first ten singlet and first five triplet states for compound **5**.

Spin State	Transition configurations	Excitation energy (eV, nm)	Oscillator strength
S_1	HOMO→LUMO (95.5%) HOMO-2→LUMO+1 (2.63%)	3.5413, 350.11	0.0500
S_2	HOMO-1→LUMO (94.9%)	3.6597, 338.78	0.0003
S_3	HOMO-3→LUMO (88.5%) HOMO-1→LUMO+1 (7.3%)	4.2363, 292.67	0.0039
S_4	HOMO→LUMO+1 (55.1%) HOMO-2→LUMO (42.7%)	4.3248, 286.68	0.0230
S_5	HOMO-1→LUMO+1 (87.8%) HOMO-3→LUMO (6.5%)	4.5903, 270.10	0.0002
S_6	HOMO→LUMO+2 (39.6%) HOMO-2→LUMO (31.3%) HOMO→LUMO+1 (25.3%)	4.6841, 264.69	0.2127
S_7	HOMO-4→LUMO (42.1%) HOMO-2→LUMO+1 (20.3%) HOMO-2→LUMO (6.1%) HOMO→LUMO+1 (5.2%) HOMO→LUMO+2 (22.7%)	4.8494, 255.67	0.0941
S_8	HOMO-2→LUMO+2 (84.6%) HOMO-3→LUMO+1 (8.2%) HOMO-2→LUMO (2.2%)	5.1571, 240.41	0.0053
S_9	HOMO→LUMO+2 (31.1%)	5.2321, 236.97	0.6581

	HOMO-4→LUMO (21.1%) HOMO→LUMO+1 (10.6%) HOMO-2→LUMO+1 (10.3%) HOMO-2→LUMO+2 (4.0%) HOMO-5→LUMO (4.6%) HOMO-2→LUMO (12.7%)		
S_{10}	HOMO-3→LUMO+1 (84.2%) HOMO-6→LUMO (2.1%) HOMO-1→LUMO+2 (8.1%)	5.2798, 234.83	0.0112
T_1	HOMO→LUMO (91.1%) HOMO-2→LUMO (3.9%)	2.8435, 436.02	0.0000
T_2	HOMO→LUMO+1 (41.8%) HOMO-2→LUMO (40.3%) HOMO→LUMO (5.2%) HOMO-5→LUMO+2 (2.0%) HOMO-4→LUMO+1 (2.5%)	3.0139, 411.37	0.0000
T_3	HOMO-1→LUMO (88.8%) HOMO-3→LUMO (3.6%) HOMO-1→LUMO+2 (2.1%)	3.3269, 372.67	0.0000
T_4	HOMO→LUMO+1 (49.5%) HOMO-4→LUMO (2.5%) HOMO-2→LUMO (42.9%)	3.5972, 344.67	0.0000
T_5	HOMO-3→LUMO (81.8%) HOMO-1→LUMO+2 (7.0%) HOMO-1→LUMO+1 (4.6%)	3.7499, 330.63	0.0000

Table S16. Calculated MO energies of orbitals involved in transitions for **5**.

Orbital	Energy/ eV		Orbital	Energy/ eV
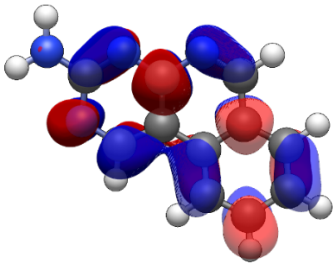 LUMO+2	-0.37		HOMO 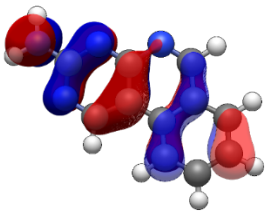	-5.89
LUMO+1 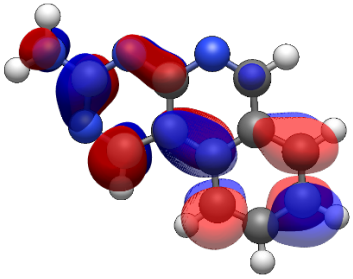	-1.04		HOMO-1 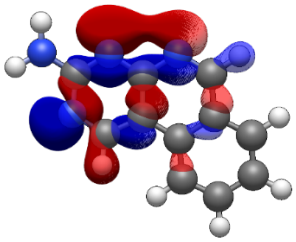	-6.58
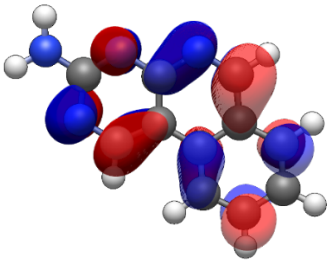 LUMO	-1.82		HOMO-2 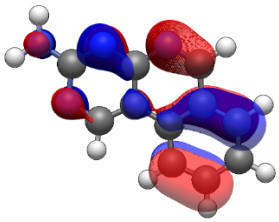	-6.86
			HOMO-3 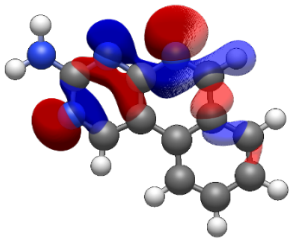	-7.21

			HOMO-4 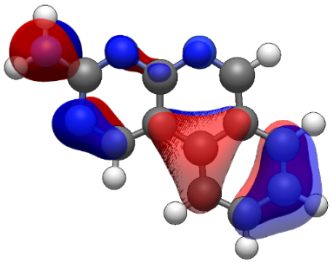	-7.57
			HOMO-5 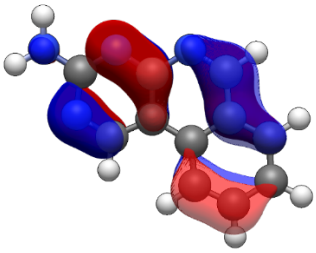	-8.14
			HOMO-6 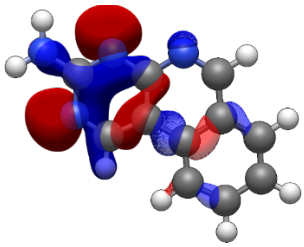	-8.42

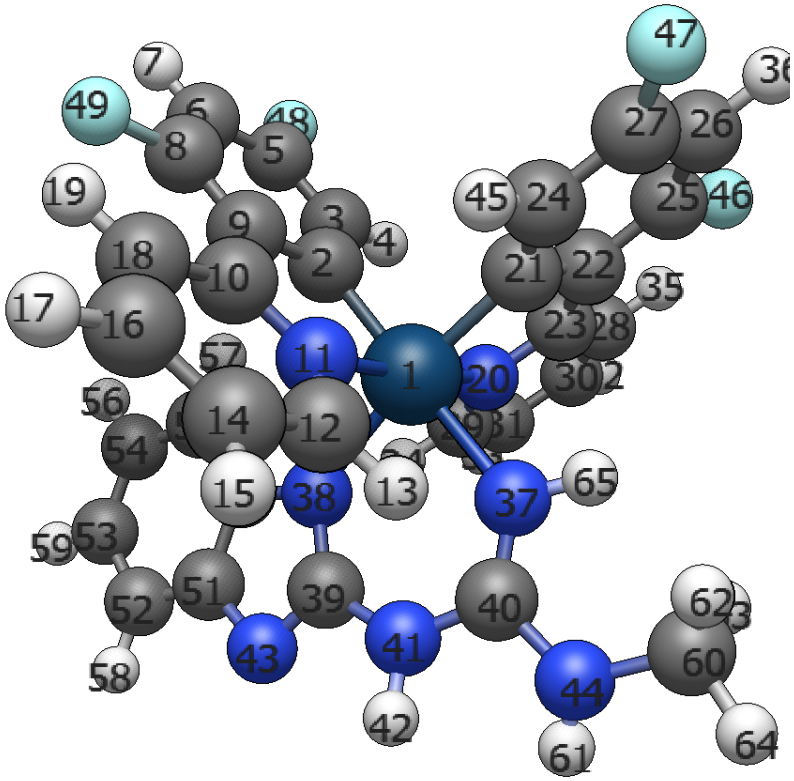

Figure S90. Optimised geometry model used for complex **1**. TD-DFT inputs and energy calculations were based upon this optimised input model.

Table S17. Cartesian coordinates for optimised compound **1**.

Center Number	Atomic Number	Atomic Type	Coordinates (Angstroms) X	Y	Z
1	77	0	0.171949	-0.246891	0.141692
2	6	0	-0.307385	1.624185	-0.442635
3	6	0	-0.097484	2.197913	-1.705711
4	1	0	0.342854	1.633936	-2.520427
5	6	0	-0.468876	3.514422	-1.942193
6	6	0	-1.051542	4.321855	-0.968801
7	1	0	-1.337846	5.346348	-1.170750
8	6	0	-1.239240	3.756796	0.280766
9	6	0	-0.879858	2.434340	0.584113
10	6	0	-1.015211	1.799256	1.891198
11	7	0	-0.523350	0.520837	1.937122
12	6	0	-0.563019	-0.174779	3.088664

13	1	0	-0.147146	-1.172946	3.040921
14	6	0	-1.091843	0.344701	4.260365
15	1	0	-1.101018	-0.257306	5.162548
16	6	0	-1.607225	1.642374	4.234247
17	1	0	-2.037067	2.085644	5.127897
18	6	0	-1.567546	2.368367	3.052052
19	1	0	-1.960489	3.373040	3.009513
20	7	0	0.902439	-0.860656	-1.695019
21	6	0	2.101251	0.335684	0.327763
22	6	0	2.924828	-0.013041	-0.787332
23	6	0	2.240995	-0.661467	-1.908862
24	6	0	2.695520	0.978199	1.422973
25	6	0	4.293081	0.295449	-0.738048
26	6	0	4.885136	0.927030	0.342989
27	6	0	4.055966	1.258946	1.411110
28	6	0	2.811050	-1.061094	-3.128801
29	6	0	0.136980	-1.426035	-2.647445
30	6	0	2.017319	-1.645465	-4.108783
31	6	0	0.654893	-1.831922	-3.870017
32	1	0	2.460099	-1.948083	-5.053517
33	1	0	-0.000984	-2.277310	-4.610096
34	1	0	-0.910653	-1.535778	-2.395270
35	1	0	3.865881	-0.902072	-3.296745
36	1	0	5.944174	1.152988	0.349525
37	7	0	0.748132	-2.211543	0.922331
38	7	0	-1.809435	-1.176935	-0.136796
39	6	0	-2.176588	-2.376267	0.382902
40	6	0	0.021385	-3.251149	1.223718
41	7	0	-1.331262	-3.242937	1.102188
42	1	0	-1.850212	-4.027627	1.473736
43	7	0	-3.426415	-2.779989	0.214585
44	7	0	0.534846	-4.416989	1.769596
45	1	0	2.112953	1.272642	2.289468
46	9	0	5.109298	-0.028086	-1.774095
47	9	0	4.610391	1.875942	2.474659
48	9	0	-0.263620	4.044790	-3.165231
49	9	0	-1.793134	4.553093	1.230022
50	6	0	-2.993047	-0.741109	-0.741037
51	6	0	-3.979948	-1.742440	-0.508340
52	6	0	-5.282592	-1.592740	-1.002212
53	6	0	-5.582097	-0.444739	-1.729228
54	6	0	-4.602433	0.539581	-1.965674
55	6	0	-3.301974	0.407943	-1.480422
56	1	0	-4.864640	1.424970	-2.539672
57	1	0	-2.560282	1.173508	-1.671708
58	1	0	-6.028063	-2.361504	-0.817834

59	1	0	-6.585301	-0.304085	-2.124244
60	6	0	1.967027	-4.600460	1.943935
61	1	0	0.025837	-5.255267	1.519664
62	1	0	2.366794	-3.821774	2.601425
63	1	0	2.529264	-4.587048	0.997825
64	1	0	2.132903	-5.564010	2.430791
65	1	0	1.746625	-2.377806	0.972923

Energy

E(RB3LYP) = -2081.96656471 Hartree

Zero point corrected free energy = -2081.483287 Hartree

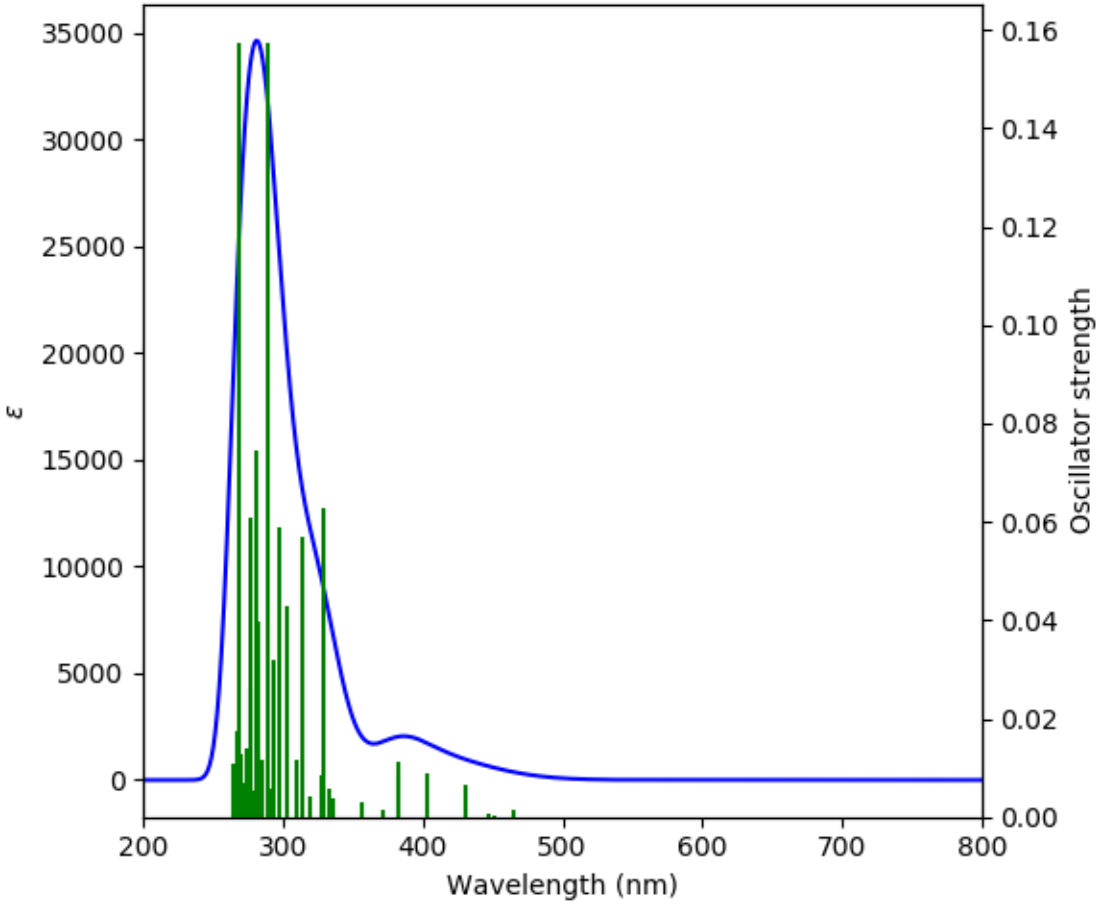

Figure S91. Calculated UV/vis spectrum for complex **1**.

Table S18. Calculated energy levels of the first ten singlet and first five triplet states for complex **1**.

Spin State	Transition configurations	Excitation energy (eV, nm)	Oscillator strength
S_1	HOMO→LUMO (93.4%) HOMO-1→LUMO (4.9%)	2.6677, 464.77	0.0014
S_2	HOMO-1→LUMO (91.8%) HOMO→LUMO (5.0%)	2.7494, 450.95	0.0004
S_3	HOMO→LUMO+1 (96.3%)	2.7755, 446.71	0.0007
S_4	HOMO-1→LUMO+1 (96.7%)	2.8821, 430.18	0.0064
S_5	HOMO-2→LUMO (95.7%)	3.0768, 402.96	0.0089
S_6	HOMO→LUMO+2 (76.2%) HOMO-1→LUMO+2 (3.0%) HOMO-2→LUMO+1 (19.1%)	3.2420, 382.43	0.0085
S_7	HOMO-2→LUMO+1 (74.8%) HOMO→LUMO+2 (20.5%)	3.2441, 382.19	0.0113
S_8	HOMO-1→LUMO+1 (95.2%) HOMO→LUMO+2 (2.1%)	3.3402, 371.19	0.0015
S_9	HOMO→LUMO+3 (96.4%) HOMO-1→LUMO+3 (2.8%)	3.3711, 367.79	0.0000
S_{10}	HOMO-1→LUMO+3 (95.2%) HOMO→LUMO+3 (2.9%)	3.4804, 356.23	0.0032
T_1	HOMO→LUMO (72.5%) HOMO-1→LUMO (13.2%) HOMO-2→LUMO (6.5%)	2.6327, 470.95	0.0000

	HOMO-4→LUMO (3.5%)		
T_2	HOMO-1→LUMO (74.9%) HOMO→LUMO (19.6%)	2.7311, 453.97	0.0000
T_3	HOMO→LUMO+1 (74.4%) HOMO-1→LUMO+1 (15.3%) HOMO-2→LUMO+1 (7.9%)	2.7534, 450.30	0.0000
T_4	HOMO-1→LUMO+1 (70.0%) HOMO-3→LUMO+1 (10.1%) HOMO-2→LUMO+1 (4.4%) HOMO→LUMO+1 (8.1%)	2.7978, 443.15	0.0000
T_5	HOMO-2→LUMO (52.9%) HOMO-4→LUMO (6.2%) HOMO-6→LUMO (4.8%) HOMO-1→LUMO+1 (3.0%) HOMO→LUMO (6.0%) HOMO-1→LUMO (7.9%) HOMO-5→LUMO (8.4%)	2.8350, 437.34	0.0000

Table S19. Calculated MO energies of orbitals involved in transitions for **1**.

Orbital	**Energy/ eV**		**Orbital**	**Energy/ eV**

LUMO+3 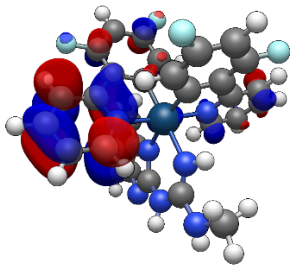	-0.84		HOMO 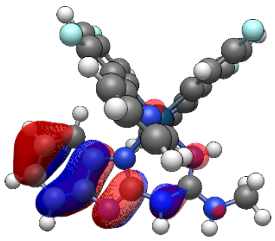	-4.75
LUMO+2 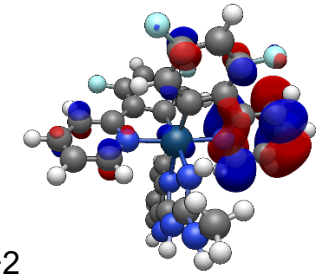	-1.00		HOMO-1 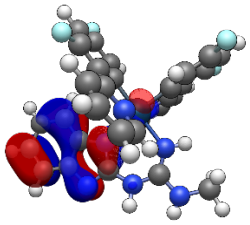	-4.90
LUMO+1 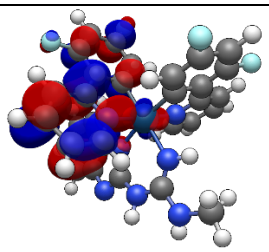	-1.42		HOMO-2 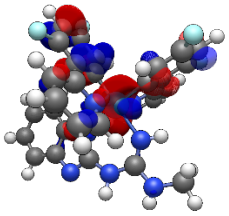	-5.42
LUMO 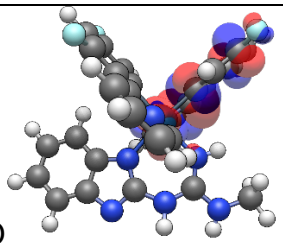	-1.59		HOMO-3 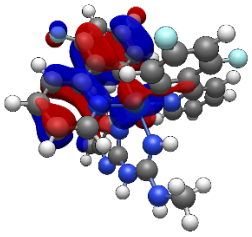	-5.98
			HOMO-4 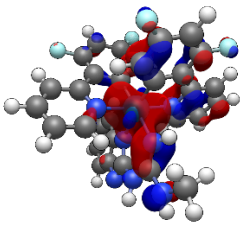	-6.03

			HOMO-5 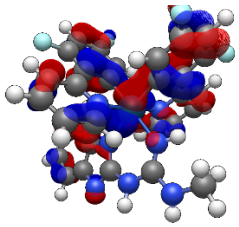	-6.20
			HOMO-6 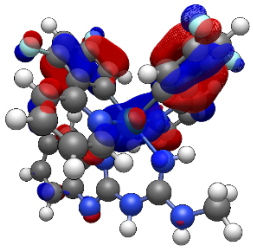	-6.27

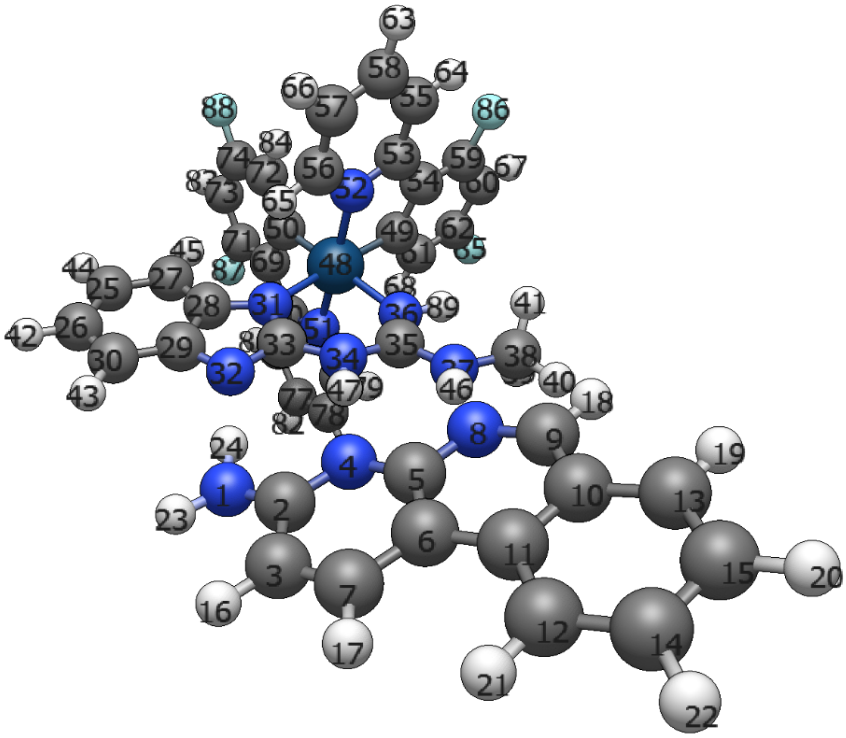

Figure S92. Optimised geometry model used for co-system **1•5**. TD-DFT inputs and energy calculations were based upon this optimised input model.

Table S20. Cartesian coordinates for optimised co-system **1•5**.

Center Number	Atomic Number	Atomic Type	Coordinates (Angstroms) X	Y	Z
1	7	0	4.134791	3.579621	0.149459
2	6	0	5.114531	2.653171	0.130509
3	6	0	6.489861	3.056021	0.059889
4	7	0	4.768641	1.357771	0.202229
5	6	0	5.743671	0.423211	0.190119
6	6	0	7.130441	0.725461	0.098819
7	6	0	7.469011	2.103711	0.040749
8	7	0	5.294461	-0.881689	0.273629
9	6	0	6.169671	-1.851419	0.243229
10	6	0	7.583151	-1.680109	0.137259
11	6	0	8.087041	-0.350109	0.069529
12	6	0	9.490651	-0.178449	-0.026131
13	6	0	8.464431	-2.785869	0.108359
14	6	0	10.334591	-1.272329	-0.052921
15	6	0	9.826191	-2.588609	0.014109
16	1	0	6.735401	4.113231	0.015449
17	1	0	8.508741	2.409391	-0.021961
18	1	0	5.775491	-2.867269	0.306089
19	1	0	8.050781	-3.790299	0.161649
20	1	0	10.506221	-3.434889	-0.008581
21	1	0	9.915021	0.818681	-0.080741
22	1	0	11.407621	-1.117189	-0.127151
23	1	0	4.383251	4.541211	-0.030221
24	1	0	3.143631	3.303031	-0.015711
25	6	0	-2.054319	4.739581	-1.543821
26	6	0	-0.877249	5.510611	-1.553861
27	6	0	-2.046029	3.398691	-1.159521
28	6	0	-0.824249	2.831471	-0.777721
29	6	0	0.365831	3.608321	-0.796451
30	6	0	0.343731	4.953821	-1.183201
31	7	0	-0.476679	1.542171	-0.362651
32	7	0	1.424881	2.818841	-0.398711
33	6	0	0.863321	1.631721	-0.163721
34	7	0	1.713851	0.589401	0.215979
35	6	0	1.404501	-0.644339	0.710959
36	7	0	0.164121	-1.047819	0.856329
37	7	0	2.481291	-1.396919	1.074599
38	6	0	2.346541	-2.765189	1.525419
39	1	0	1.753101	-2.829389	2.447009
40	1	0	3.345271	-3.146219	1.750259

41	1	0	1.887611	-3.424259	0.772189
42	1	0	-0.922959	6.553061	-1.859391
43	1	0	1.259061	5.540511	-1.195731
44	1	0	-2.993759	5.196601	-1.844511
45	1	0	-2.959039	2.818301	-1.167161
46	1	0	3.414151	-1.109099	0.756519
47	1	0	2.705361	0.854631	0.218439
48	77	0	-1.705279	-0.234529	0.096169
49	6	0	-2.566489	-2.031359	0.444549
50	6	0	-3.527079	0.474271	-0.423331
51	7	0	-2.258549	0.660961	1.877929
52	7	0	-1.317119	-1.164279	-1.710381
53	6	0	-1.731709	-2.465329	-1.819801
54	6	0	-2.413259	-2.967279	-0.624951
55	6	0	-1.496089	-3.166349	-3.014021
56	6	0	-0.697249	-0.559769	-2.741241
57	6	0	-0.446059	-1.210199	-3.941531
58	6	0	-0.853479	-2.538539	-4.074231
59	6	0	-2.923799	-4.264089	-0.464361
60	6	0	-3.573859	-4.682419	0.685139
61	6	0	-3.225469	-2.449409	1.609359
62	6	0	-3.710839	-3.747399	1.707109
63	1	0	-0.676839	-3.082199	-4.998051
64	1	0	-1.825339	-4.191299	-3.098721
65	1	0	-0.411389	0.470371	-2.567481
66	1	0	0.054121	-0.681079	-4.745381
67	1	0	-3.957609	-5.690849	0.777029
68	1	0	-3.374499	-1.776689	2.447159
69	6	0	-4.221769	1.136451	0.636169
70	6	0	-3.493159	1.255201	1.896529
71	6	0	-5.512899	1.629841	0.394239
72	6	0	-4.175289	0.336661	-1.659871
73	6	0	-6.151639	1.505451	-0.827901
74	6	0	-5.453289	0.848161	-1.837641
75	6	0	-3.927699	1.904091	3.065359
76	6	0	-1.467099	0.709961	2.965489
77	6	0	-3.108399	1.945491	4.185409
78	6	0	-1.851329	1.338981	4.140249
79	1	0	-0.508169	0.218231	2.856929
80	1	0	-1.178149	1.352221	4.990659
81	1	0	-4.900519	2.372231	3.077019
82	1	0	-3.447479	2.450511	5.085449
83	1	0	-7.149339	1.896650	-0.982651
84	1	0	-3.698419	-0.158929	-2.498341
85	9	0	-4.340589	-4.131749	2.836889
86	9	0	-2.791079	-5.184479	-1.454741

87	9	0	-6.202869	2.263981	1.377169
88	9	0	-6.056479	0.709401	-3.036741
89	1	0	0.092311	-2.001949	1.188959

Energy

E(RB3LYP) = -2708.97695866 Hartree

Zero point corrected free energy = -2708.303831 Hartree

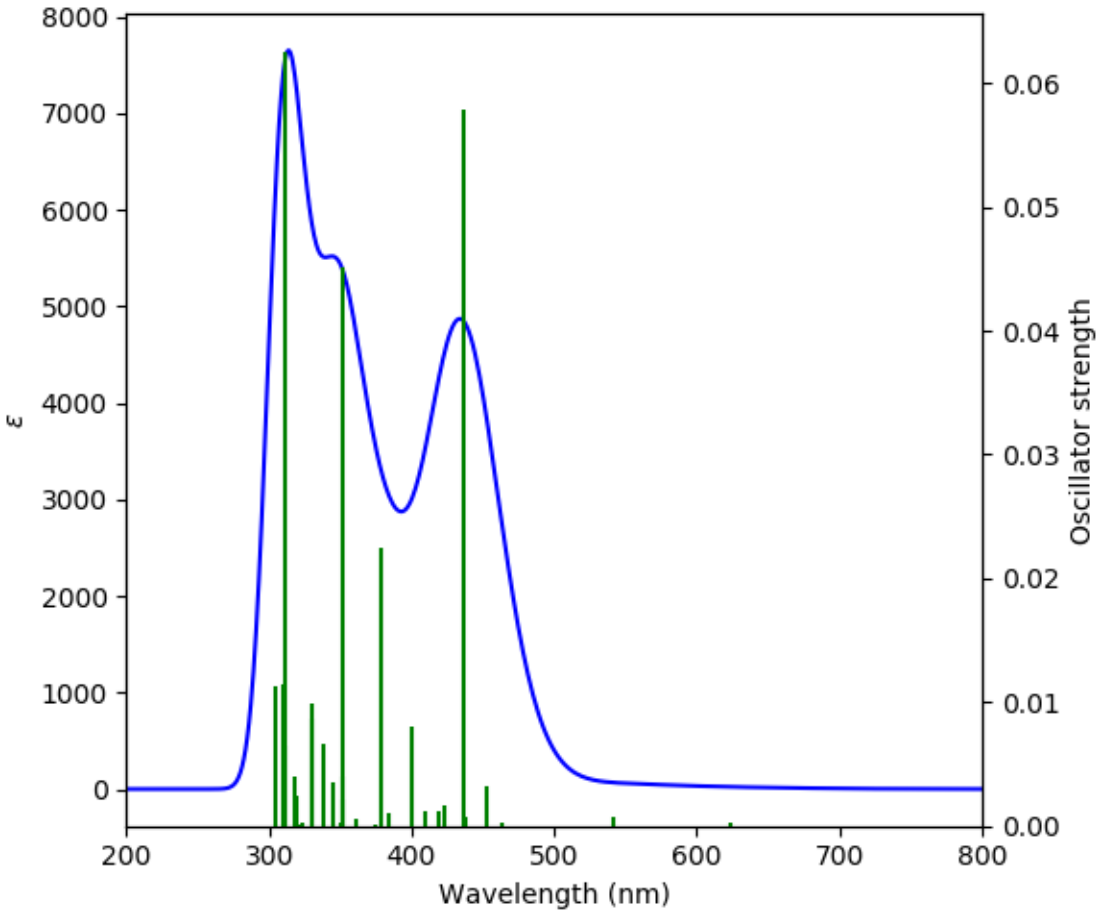

Figure S93. Calculated UV/vis spectrum for co-system **1•5**.

Table S21. Calculated energy levels of the ten highest contributing singlet states and the first five triplet states for co-system **1•5**.

Spin State	Transition configurations	Excitation energy (eV, nm)	Oscillator strength
S_6	HOMO-3→LUMO (97.0%)	2.8418, 436.29	0.0579
S_{10}	HOMO-2→LUMO+1 (89.5%) HOMO-1→LUMO+1 (5.8%)	3.1012, 399.79	0.0081
S_{12}	HOMO-2→LUMO+2 (89.9%) HOMO-1→LUMO+2 (5.8%)	3.2696, 379.21	0.0224
S_{18}	HOMO-4→LUMO+1 (78.4%) HOMO-4→LUMO+2 (13.1%)	3.5288, 351.35	0.0451
S_{23}	HOMO-5→LUMO+1 (41.4%) HOMO-6→LUMO+1 (10.4%) HOMO-2→LUMO+4 (41.2%)	3.7595, 329.58	0.0086
S_{25}	HOMO-2→LUMO+4 (50.0%) HOMO-5→LUMO+1 (36.1%) HOMO-7→LUMO+1 (4.0%) HOMO-4→LUMO+1 (2.6%)	3.7632, 329.46	0.0099
S_{29}	HOMO-2→LUMO+5 (87.2%) HOMO-5→LUMO+2 (5.1%)	3.8962, 318.22	0.0040
S_{32}	HOMO-5→LUMO+2 (66.3%) HOMO-6→LUMO+2 (4.9%) HOMO-7→LUMO+2 (2.9%) HOMO-5→LUMO+1 (3.1%) HOMO-2→LUMO+5 (5.3%) HOMO-3→LUMO+2 (10.4%)	3.9754, 311.88	0.0625
S_{33}	HOMO-3→LUMO+2 (89.3%)	3.9811, 311.43	0.0065

	HOMO-5→LUMO+2 (7.4%)		
S_{34}	HOMO-6→LUMO+1 (54.1%) HOMO-4→LUMO+4 (26.4%) HOMO-2→LUMO+4 (2.0%) HOMO-5→LUMO+1 (7.7%)	3.9988, 310.05	0.0114
T_1	HOMO-3→LUMO (81.6%) HOMO-11→LUMO (2.3%) HOMO→LUMO (8.1%)	1.8836, 658.24	0.0000
T_2	HOMO→LUMO (91.6%) HOMO-3→LUMO (7.0%)	1.9946, 621.60	0.0000
T_3	HOMO-1→LUMO (97.8%)	2.2925, 540.83	0.0000
T_4	HOMO-2→LUMO (99.3%)	2.6756, 463.39	0.0000
T_5	HOMO-1→LUMO+1 (77.8%) HOMO-2→LUMO+1 (5.0%) HOMO-1→LUMO+1 (3.2%) HOMO-4→LUMO+1 (7.5%)	2.6881, 461.23	0.0000

Table S22. Calculated MO energies of orbitals involved in transitions for co-system **1•5**.

Orbital	**Energy/ eV**		**Orbital**	**Energy/ eV**

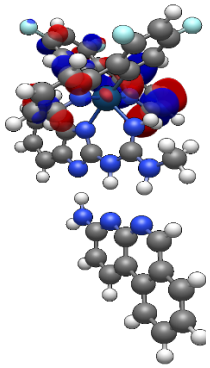 LUMO+5	-0.67		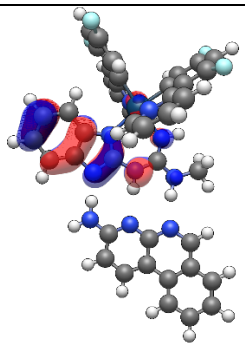 HOMO	-4.65
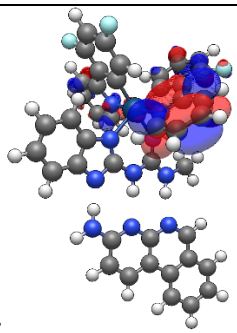 LUMO+4	-0.81		HOMO-1 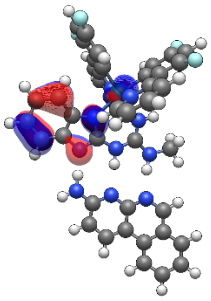	-4.90
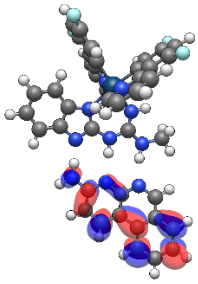 LUMO+3	-1.04		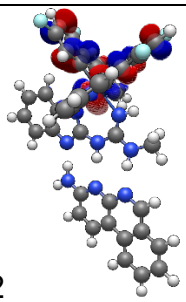 HOMO-2	-5.25
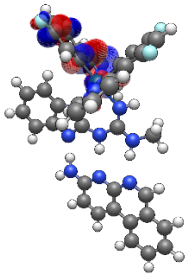 LUMO+2	-1.24		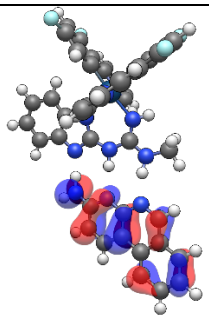 HOMO-3	-5.53

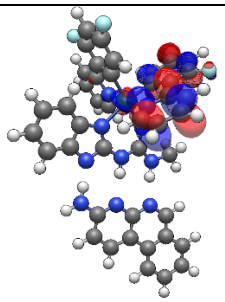 LUMO+1	-1.39		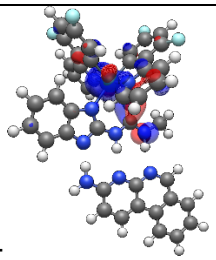 HOMO-4	-5.61
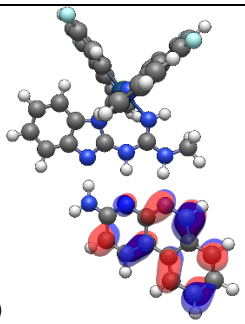 LUMO	-1.88		HOMO-5 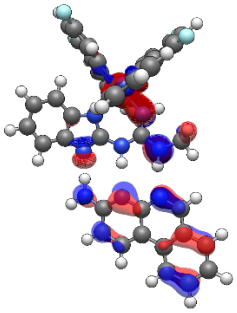	-5.83
			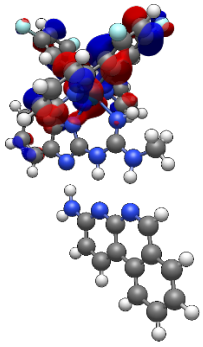 HOMO-6	-6.01
			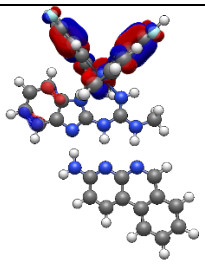 HOMO-7	-6.10

			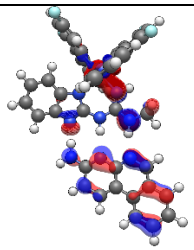 HOMO-11	-6.87

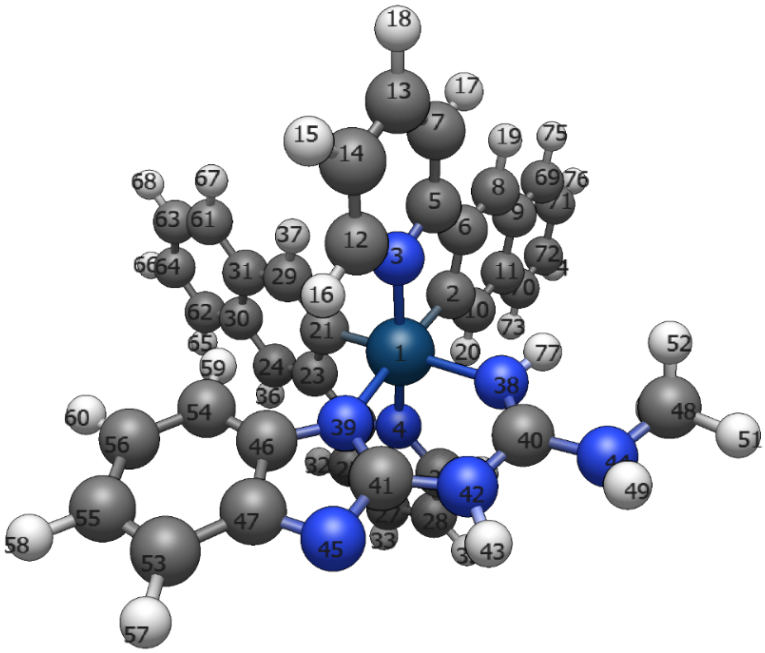

Figure S94. Optimised geometry model used for complex **2**. TD-DFT inputs and energy calculations were based upon this optimised input model.

Table S23. Cartesian coordinates for optimised compound **2**.

Center	Atomic	Atomic	Coordinates (Angstroms)		
Number	Number	Type	X	Y	Z

1	77	0	-0.044860	-0.547501	-0.020530
2	6	0	1.942868	-0.151394	0.049686
3	7	0	0.237371	-0.587249	2.027374
4	7	0	-0.288474	-0.341501	-2.067748
5	6	0	1.518445	-0.382879	2.459556
6	6	0	2.492101	-0.158492	1.385176
7	6	0	1.795240	-0.389494	3.833986
8	6	0	3.844828	0.034014	1.616497
9	6	0	4.743111	0.251003	0.546098
10	6	0	2.827801	0.064523	-0.992367
11	6	0	4.220136	0.267563	-0.789834
12	6	0	-0.754363	-0.786056	2.917262
13	6	0	0.773755	-0.598104	4.752169
14	6	0	-0.528044	-0.798875	4.287325
15	1	0	-1.358550	-0.957908	4.966566
16	1	0	-1.739489	-0.927191	2.489678
17	1	0	2.810529	-0.222406	4.175105
18	1	0	0.988299	-0.598747	5.817114
19	1	0	4.250316	0.023995	2.626152
20	1	0	2.462045	0.088539	-2.017006
21	6	0	-0.407740	1.441517	-0.117933
22	6	0	-0.612065	0.913772	-2.503737
23	6	0	-0.660210	1.928604	-1.451506
24	6	0	-0.913329	3.267800	-1.702370
25	6	0	-0.854948	1.133063	-3.868180
26	6	0	-0.200384	-1.354724	-2.950258
27	6	0	-0.764746	0.086329	-4.774329
28	6	0	-0.426930	-1.187067	-4.308301
29	6	0	-0.399450	2.379389	0.901011
30	6	0	-0.921537	4.216405	-0.655147
31	6	0	-0.651518	3.759353	0.677708
32	1	0	-1.119459	2.127558	-4.207898
33	1	0	-0.956609	0.257985	-5.829583
34	1	0	0.065011	-2.315090	-2.527216
35	1	0	-0.344942	-2.036533	-4.977817
36	1	0	-1.106821	3.623670	-2.711905
37	1	0	-0.205939	2.069462	1.925453
38	7	0	0.451248	-2.687468	-0.067453
39	7	0	-2.143065	-1.258192	0.091349
40	6	0	-0.314275	-3.737854	-0.155876
41	6	0	-2.529648	-2.548036	-0.078474
42	7	0	-1.663472	-3.640456	-0.278507
43	1	0	-2.187840	-4.482025	-0.477711
44	7	0	0.164812	-5.039526	-0.216028
45	7	0	-3.825360	-2.826649	-0.061238
46	6	0	-3.367352	-0.602126	0.251472

47	6	0	-4.393113	-1.586522	0.149755
48	6	0	1.580701	-5.324414	-0.044655
49	1	0	-0.455950	-5.728598	0.189438
50	1	0	2.161324	-4.822037	-0.825042
51	1	0	1.730541	-6.400223	-0.160232
52	1	0	1.974199	-5.020768	0.937476
53	6	0	-5.742444	-1.229783	0.275159
54	6	0	-3.686139	0.740897	0.490892
55	6	0	-6.050037	0.107587	0.506563
56	6	0	-5.033653	1.077286	0.614653
57	1	0	-6.517520	-1.987260	0.194571
58	1	0	-7.089383	0.410899	0.608349
59	1	0	-2.914799	1.496181	0.576773
60	1	0	-5.303952	2.114403	0.798024
61	6	0	-0.651259	4.715116	1.731325
62	6	0	-1.178116	5.597443	-0.879171
63	6	0	-0.903583	6.045789	1.483073
64	6	0	-1.170320	6.494735	0.163965
65	1	0	-1.381977	5.933051	-1.893916
66	1	0	-1.368345	7.547680	-0.017317
67	1	0	-0.447965	4.373593	2.743884
68	1	0	-0.899993	6.761275	2.301518
69	6	0	6.136540	0.451114	0.749913
70	6	0	5.123621	0.487735	-1.865869
71	6	0	6.982697	0.660579	-0.315085
72	6	0	6.468114	0.679137	-1.636746
73	1	0	4.730711	0.505309	-2.880053
74	1	0	7.143218	0.847738	-2.471885
75	1	0	6.523235	0.438258	1.766914
76	1	0	8.045375	0.814405	-0.148332
77	1	0	1.428948	-2.899927	0.095051

Energy

E(RB3LYP) = -1992.30960801 Hartree

Zero point corrected free energy = -1991.700309 Hartree

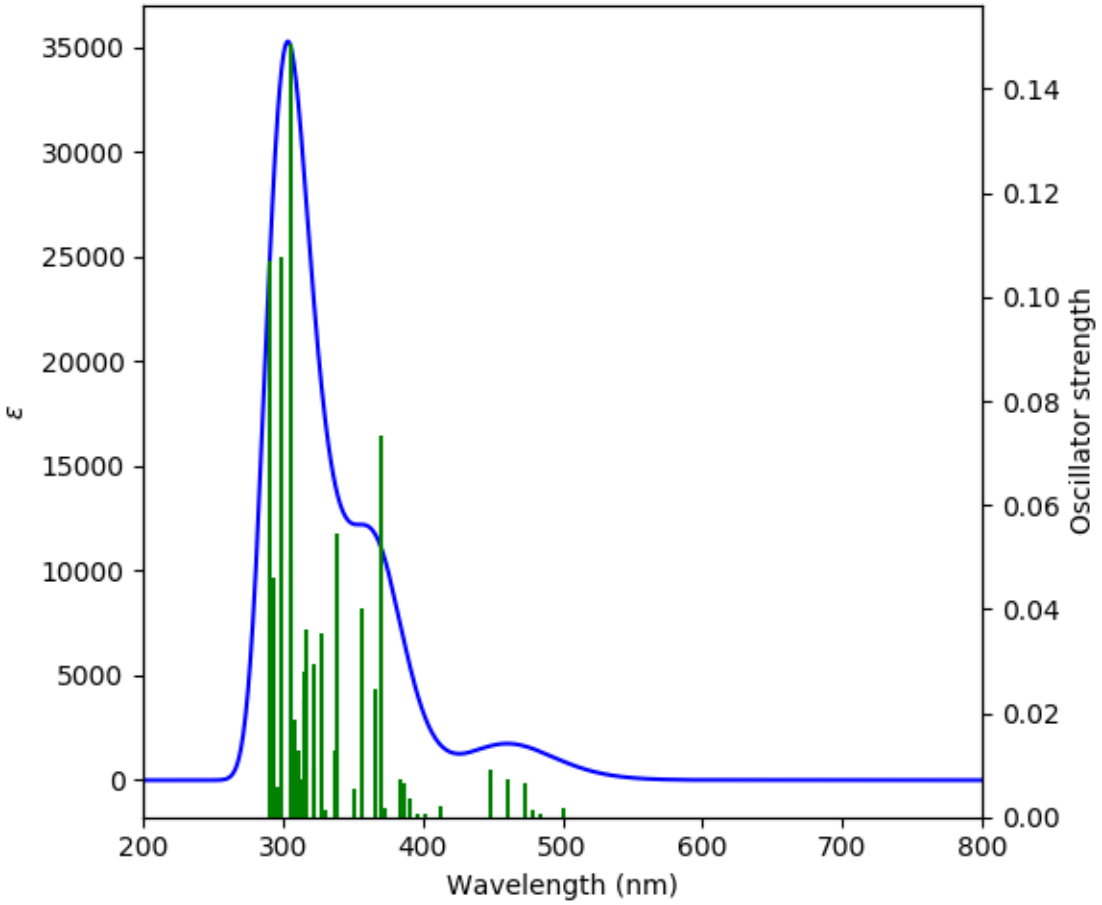

Figure S95. Calculated UV/vis spectrum for complex **2**.

Table S24. Calculated energy levels of the ten highest contributing singlet states and the first five triplet states for complex **2**.

Spin State	Transition configurations	Excitation energy (eV, nm)	Oscillator strength
S_5	HOMO-1→LUMO+1 (95.8%) HOMO-2→LUMO+1 (2.8%)	2.6918, 460.60	0.0073
S_6	HOMO-2→LUMO+1 (94.7%)	2.7698, 447.62	0.0090
S_{14}	HOMO-4→LUMO (73.0%)	3.3556, 369.49	0.0733

	HOMO-6→LUMO (6.6%) HOMO-5→LUMO (5.3%) HOMO-4→LUMO (4.0%) HOMO-2→LUMO+3 (3.5%)		
S_{15}	HOMO-3→LUMO+1 (79.2%) HOMO-4→LUMO+1 (11.8%) HOMO-2→LUMO+3 (3.3%)	3.3929, 365.43	0.0245
S_{16}	HOMO-4→LUMO+1 (56.7%) HOMO-5→LUMO+1 (16.8%) HOMO-6→LUMO+1 (5.2%) HOMO-5→LUMO (2.1%) HOMO-3→LUMO+1 (9.3%)	3.4764, 356.65	0.0403
S_{23}	HOMO→LUMO+4 (78.6%) HOMO-1→LUMO+4 (6.0%) HOMO-3→LUMO+3 (4.7%) HOMO-6→LUMO+1 (2.9%)	3.8565, 321.49	0.0094
S_{24}	HOMO-4→LUMO+2 (30.2%) HOMO-7→LUMO (17.4%) HOMO-3→LUMO+3 (12.7%) HOMO-4→LUMO+3 (9.9%) HOMO-2→LUMO+4 (6.0%) HOMO-7→LUMO+1 (3.7%) HOMO-6→LUMO+2 (2.5%) HOMO-1→LUMO+4 (6.5%)	3.9221, 316.12	0.00359
S_{27}	HOMO→LUMO+5 (65.9%)	3.9741, 311.98	0.0072

	HOMO-7→LUMO+1 (18.1%) HOMO-1→LUMO+5 (4.0%) HOMO-6→LUMO+1 (2.2%) HOMO-2→LUMO+4 (4.0%)		
S_{30}	HOMO-1→LUMO+5 (66.7%) HOMO-2→LUMO+4 (19.0%) HOMO-5→LUMO+2 (2.6%) HOMO-2→LUMO+5 (2.4%) HOMO-7→LUMO (2.7%)	4.0581, 305.52	0.0492
S_{31}	HOMO-2→LUMO+4 (37.8%) HOMO-7→LUMO+1 (19.4%) HOMO-7→LUMO (3.9%) HOMO-5→LUMO+3 (7.1%) HOMO-1→LUMO+5 (15.2%)	4.0660, 304.93	0.1488
T_1	HOMO-2→LUMO+1 (36.6%) HOMO-2→LUMO (9.5%) HOMO-4→LUMO+1 (5.6%) HOMO-3→LUMO+5 (2.6%) HOMO-3→LUMO+3 (2.6%) HOMO-2→LUMO+3 (3.0%) HOMO-1→LUMO+1 (4.8%) HOMO-2→LUMO+5 (5.3%) HOMO+3→LUMO+1 (18.1%)	2.2828, 543.13	0.0000
T_2	HOMO-3→LUMO (28.8%) HOMO-2→LUMO (21.7%)	2.3250, 533.27	0.0000

	HOMO-4→LUMO (16.2%) HOMO-3→LUMO+2 (3.4%) HOMO-7→LUMO (3.8%) HOMO-2→LUMO+1 (4.6%) HOMO-3→LUMO+4 (4.6%)		
T_3	HOMO→LUMO (61.2%) HOMO-1→LUMO (15.0%) HOMO-4→LUMO (4.2%) HOMO-5→ LUMO (2.2%) HOMO-2→LUMO (11.1%)	2.4445, 507.19	0.0000
T_4	HOMO-1→LUMO (53.0%) HOMO→LUMO+1 (3.3%) HOMO-2→LUMO (5.3%) HOMO→LUMO (30.9%)	2.5492, 486.36	0.0000
T_5	HOMO→LUMO+1 (71.4%) HOMO-1→LUMO (7.9%) HOMO-1→LUMO+1 (6.2%) HOMO-4→LUMO+1 (3.9%) HOMO-2→LUMO (2.6%) HOMO-3→LUMO+1 (2.5%)	2.5831, 479.98	0.0000

Table S25. Calculated MO energies of orbitals involved in transitions for **2**.

Orbital	**Energy/ eV**		**Orbital**	**Energy/ eV**

LUMO+5 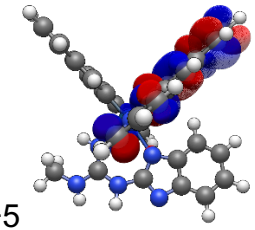	-0.09		HOMO 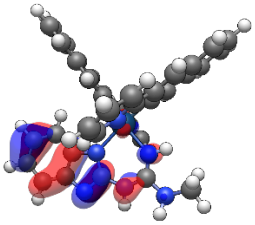	-4.57
LUMO+4 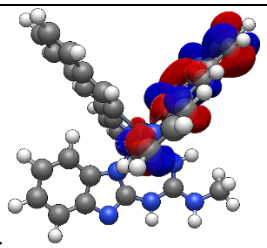	-0.29		HOMO-1 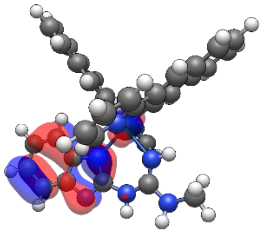	-4.70
LUMO+3 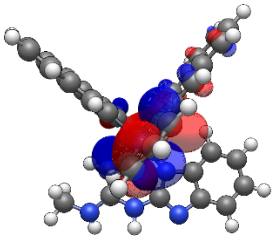	-0.90		HOMO-2 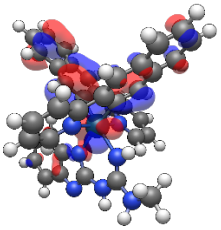	-4.86
LUMO+2 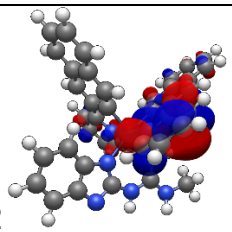	-1.05		HOMO-3 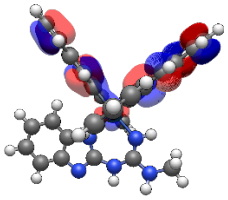	-5.35
LUMO+1 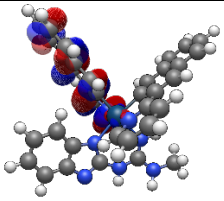	-1.45		HOMO-4 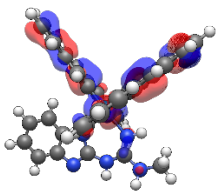	-5.53

LUMO 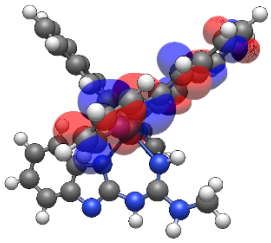	-1.62		HOMO-5 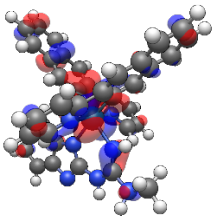	-5.78
			HOMO-6 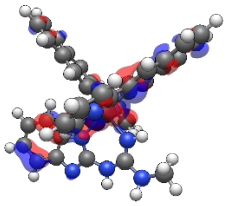	-5.91
			HOMO-7 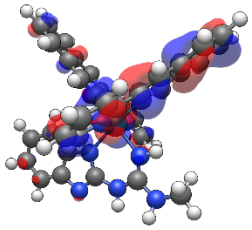	-5.97

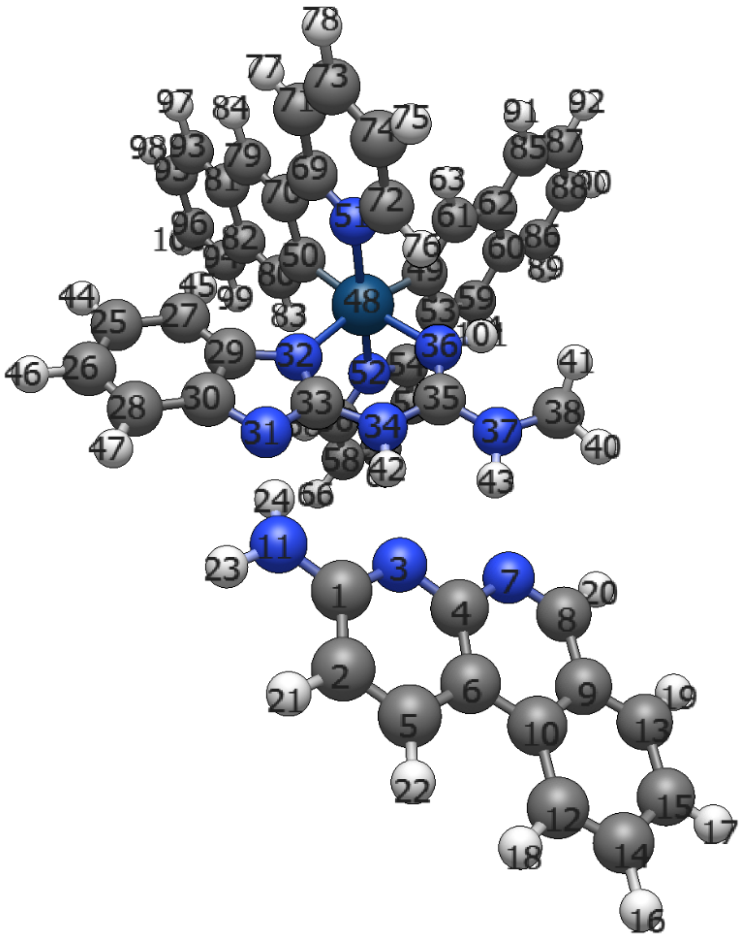

Figure S96. Optimised geometry model used for co-system **2•5**. TD-DFT inputs and energy calculations were based upon this optimised input model.

Table S26. Cartesian coordinates for optimised co-system **2•5**.

Center Number	Atomic Number	Atomic Type	Coordinates (Angstroms) X	Y	Z
1	6	0	5.535550	-2.532351	0.495821
2	6	0	6.922370	-2.896401	0.434311
3	7	0	5.141440	-1.256691	0.352381
4	6	0	6.076890	-0.308071	0.132491
5	6	0	7.861140	-1.931301	0.203471
6	6	0	7.470340	-0.576231	0.033851
7	7	0	5.579120	0.975639	0.005131

8	6	0	6.412970	1.952629	-0.233499
9	6	0	7.827360	1.811679	-0.370319
10	6	0	8.381190	0.507849	-0.226199
11	7	0	4.595410	-3.471211	0.723741
12	6	0	9.786020	0.368229	-0.352559
13	6	0	8.661910	2.923079	-0.631729
14	6	0	10.583840	1.467159	-0.608199
15	6	0	10.025980	2.757159	-0.750439
16	1	0	11.658670	1.336569	-0.701629
17	1	0	10.670140	3.607999	-0.951289
18	1	0	10.247610	-0.608401	-0.250119
19	1	0	8.210540	3.906999	-0.736879
20	1	0	5.981130	2.950199	-0.332209
21	1	0	7.208200	-3.936151	0.565671
22	1	0	8.909090	-2.209301	0.148531
23	1	0	4.874760	-4.440951	0.708091
24	1	0	3.585830	-3.260711	0.565281
25	6	0	-1.598610	-5.140271	-0.417719
26	6	0	-0.394510	-5.860851	-0.309209
27	6	0	-1.628850	-3.749191	-0.318449
28	6	0	0.815500	-5.203411	-0.102849
29	6	0	-0.417920	-3.079751	-0.104629
30	6	0	0.799370	-3.806811	-0.002439
31	7	0	1.837540	-2.919061	0.191721
32	7	0	-0.109790	-1.723101	0.025351
33	6	0	1.235960	-1.727041	0.197561
34	7	0	2.054690	-0.600341	0.327531
35	6	0	1.710510	0.687149	0.628361
36	7	0	0.460400	1.065279	0.745611
37	7	0	2.768940	1.524739	0.828381
38	6	0	2.593090	2.947389	1.026361
39	1	0	2.084430	3.440549	0.183521
40	1	0	3.582110	3.396979	1.140931
41	1	0	2.025600	3.160059	1.941921
42	1	0	3.054850	-0.827251	0.347331
43	1	0	3.700740	1.218039	0.527491
44	1	0	-2.528550	-5.677730	-0.585989
45	1	0	-2.560750	-3.207620	-0.415259
46	1	0	-0.410451	-6.945001	-0.391699
47	1	0	1.750370	-5.753241	-0.024229
r48	77	0	-1.392330	0.082799	0.139141
49	6	0	-2.290690	1.899530	0.145341
50	6	0	-3.200340	-0.752220	-0.246969
51	7	0	-1.934770	-0.461500	2.059251
52	7	0	-1.023450	0.649029	-1.813979
53	6	0	-2.167710	2.614830	-1.102969

54	6	0	-1.478150	1.887289	-2.173639
55	6	0	-1.275080	2.347399	-3.482429
56	6	0	-0.389600	-0.125811	-2.715359
57	6	0	-0.618010	1.550009	-4.410729
58	6	0	-0.166310	0.286609	-4.022119
59	6	0	-2.668600	3.897040	-1.259079
60	6	0	-3.326470	4.557060	-0.195169
61	6	0	-2.936770	2.551370	1.181521
62	6	0	-3.463400	3.865760	1.054331
63	1	0	-3.061460	2.053840	2.141201
64	1	0	-2.568010	4.429570	-2.202609
65	1	0	-1.641270	3.327379	-3.766409
66	1	0	0.347270	-0.373341	-4.712889
67	1	0	-0.463910	1.906129	-5.425419
68	1	0	-0.070550	-1.093661	-2.348589
69	6	0	-3.159750	-1.055320	2.188711
70	6	0	-3.897640	-1.205690	0.933261
71	6	0	-3.597140	-1.470850	3.455261
72	6	0	-1.151340	-0.290691	3.141061
73	6	0	-2.791680	-1.286920	4.570471
74	6	0	-1.540160	-0.685651	4.412891
75	1	0	-0.873450	-0.527431	5.253811
76	1	0	-0.196240	0.181339	2.945311
77	1	0	-4.566940	-1.944350	3.554631
78	1	0	-3.131250	-1.612230	5.549721
79	6	0	-5.165910	-1.759690	0.863761
80	6	0	-3.862470	-0.890390	-1.455379
81	6	0	-5.831730	-1.902420	-0.374789
82	6	0	-5.160970	-1.456070	-1.562019
83	1	0	-3.385960	-0.563800	-2.377119
84	1	0	-5.681420	-2.098580	1.759851
85	6	0	-4.124980	4.529560	2.123991
86	6	0	-3.850540	5.873030	-0.322839
87	6	0	-4.622690	5.804550	1.969871
88	6	0	-4.484870	6.486090	0.733711
89	1	0	-3.742780	6.388350	-1.275169
90	1	0	-4.883260	7.491250	0.624971
91	1	0	-4.233940	4.007710	3.072211
92	1	0	-5.126820	6.295140	2.798691
93	6	0	-7.132700	-2.467590	-0.480669
94	6	0	-5.830770	-1.599830	-2.808819
95	6	0	-7.751360	-2.591030	-1.703649
96	6	0	-7.090430	-2.151510	-2.879539
97	1	0	-7.632090	-2.802470	0.426281
98	1	0	-8.745290	-3.024700	-1.773889
99	1	0	-5.326090	-1.263980	-3.712049

100	1	0	-7.585780	-2.253340	-3.841919
101	1	0	0.356630	2.056629	0.928311

Energy

E(RB3LYP) = -2619.31957086 Hartree

Zero point corrected free energy = -2618.520431 Hartree

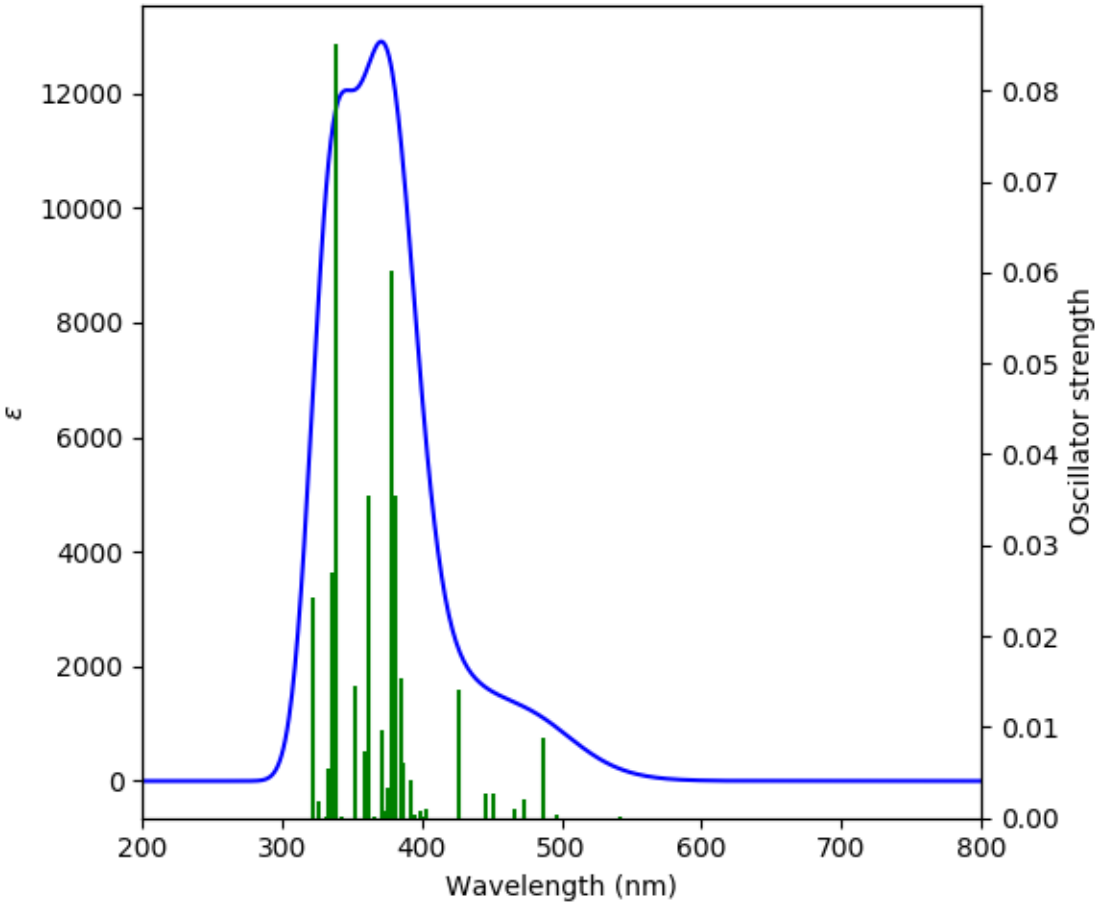

Figure S97. Calculated UV/vis spectrum for co-system **2•5**.

Table S27. Calculated energy levels of the ten highest contributing singlet states and the first four triplet states for co-system **2•5**.

Spin State	Transition configurations	Excitation energy (eV, nm)	Oscillator strength
S_3	HOMO→LUMO+1 (57.3%) HOMO-1→LUMO+1 (38.1%)	2.5489, 486.43	0.0088
S_7	HOMO-1→LUMO+2 (66.1%) HOMO→LUMO+2 (18.7%) HOMO-2→LUMO+1 (6.2%) HOMO-2→LUMO+2 (5.2%)	2.7448, 451.71	0.0026
S_9	HOMO-2→LUMO+2 (91.7%) HOMO-1→LUMO+2 (5.0%)	2.9039, 426.95	0.0141
S_{15}	HOMO→LUMO+5 (58.1%) HOMO-4→LUMO+1 (23.9%) HOMO-5→LUMO+1 (2.6%) HOMO-1→LUMO+4 (2.4%) HOMO-1→LUMO+5 (5.2%)	3.2108, 386.14	0.0060
S_{18}	HOMO-6→LUMO (96.6%)	3.2772, 378.33	0.0602
S_{19}	HOMO-1→LUMO+3 (59.9%) HOMO-2→LUMO+4 (16.6%) HOMO-1→LUMO+5 (9.7%) HOMO-2→LUMO+3 (7.1%)	3.3031, 375.36	0.0034
S_{24}	HOMO-3→LUMO+2 (74.6%) HOMO-1→LUMO+5 (2.5%) HOMO-5→LUMO+2 (5.0%) HOMO-4→LUMO+2 (11.6%)	3.4238, 362.12	0.0355
S_{26}	HOMO-2→LUMO+5 (90.2%)	3.4577, 358.57	0.0074

	HOMO-1→LUMO+5 (4.0%)		
S_{29}	HOMO-5→LUMO+2 (68.0%) HOMO-1→LUMO+8 (2.6%) HOMO-4→LUMO+2 (6.1%) HOMO-8→LUMO+2 (7.5%) HOMO-7→LUMO+2 (7.5%)	3.6637, 338.41	0.0852
S_{32}	HOMO-8→LUMO+1 (44.6%) HOMO-4→LUMO+4 (37.8%) HOMO-5→LUMO+1 (5.0%) HOMO-4→LUMO+1 (2.1%)	3.7277, 332.60	0.0055
T_1	HOMO-5→LUMO+2 (2.1%) HOMO-4→LUMO+1 (2.9%) HOMO-4→LUMO+2 (3.2%) HOMO-3→LUMO+2 (14.5%) HOMO-3→LUMO+5 (2.1%) HOMO-3→LUMO+8 (2.1%) HOMO-2→LUMO+1 (6.0%) HOMO-2→LUMO+2 (14.1%) HOMO-1→LUMO+1 (15.0%) HOMO-1→LUMO+2 (15.6%) HOMO-1→LUMO+8 (2.3%) HOMO→LUMO+1 (3.5%)	2.2824, 543.21	0.0000
T_2	HOMO→LUMO (98.1%)	2.2864, 542.26	0.0000
T_3	HOMO-7→LUMO+1 (3.5%) HOMO-5→LUMO+1 (2.1%)	2.3181, 534.86	0.0000

	HOMO-4→LUMO+1 (5.1%) HOMO-4→LUMO+2 (3.0%) HOMO-3→LUMO+1 (28.6%) HOMO-3→LUMO+4 (3.0%) HOMO-3→LUMO+7 (3.7%) HOMO-2→LUMO+2 (6.1%) HOMO-1→LUMO+1 (11.0%) HOMO-1→LUMO+2 (8.8%) HOMO→LUMO+1 (7.2%)		
T_4	HOMO-1→LUMO (61.9%) HOMO-6→LUMO (25.6%) HOMO-2→LUMO (8.2%)	2.4779, 500.37	0.0000

Table S28. Calculated MO energies of orbitals involved in transitions for co-system **2•5**.

Orbital	**Energy/ eV**		**Orbital**	**Energy/ eV**
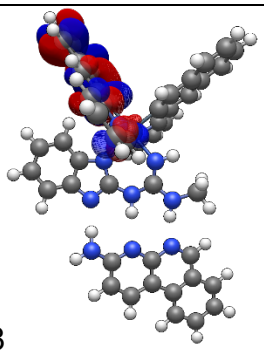 LUMO+8	0.05		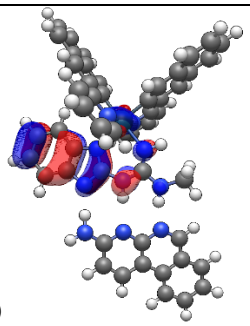 HOMO	-4.52

LUMO+7 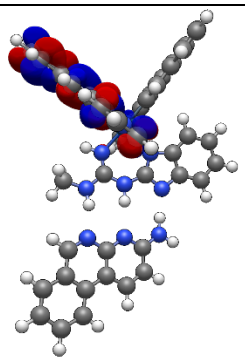	-0.13		HOMO-1 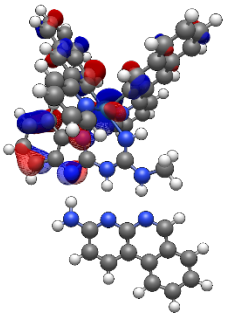	-4.66
LUMO+6 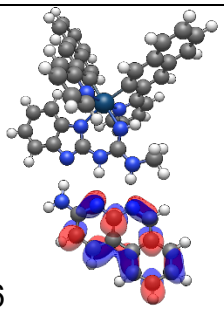	-0.39		HOMO-2 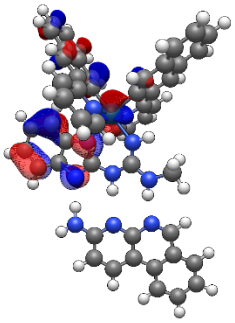	-4.78
LUMO+5 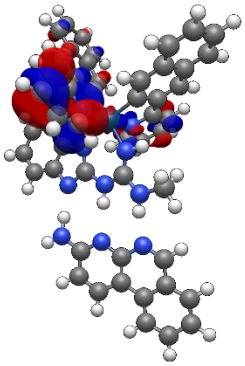	-0.74		HOMO-3 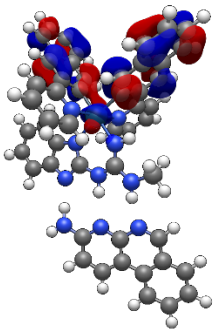	-5.22
LUMO+4 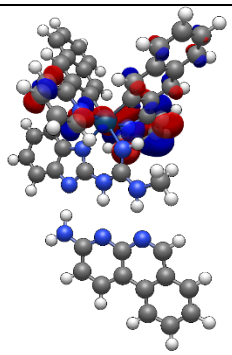	-0.89		HOMO-4 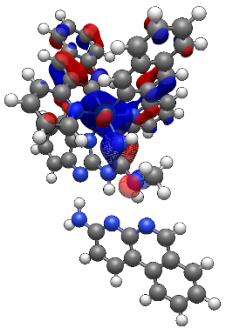	-5.32

LUMO+3 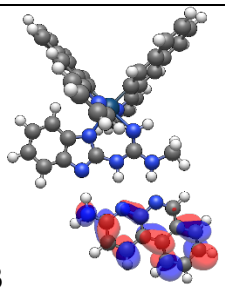	-1.05		HOMO-5 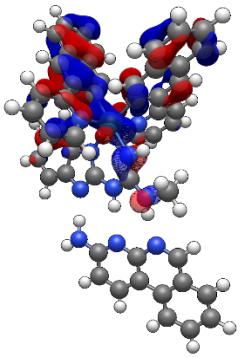	-5.52
LUMO+2 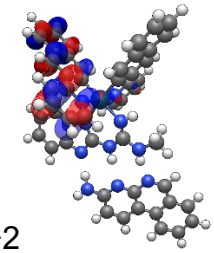	-1.30		HOMO-6 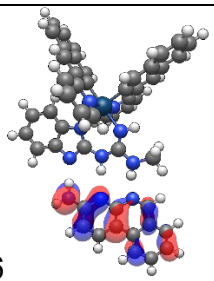	-5.62
LUMO+1 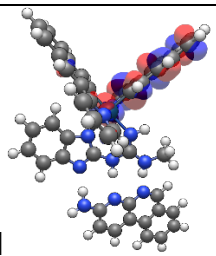	-1.45		HOMO-7 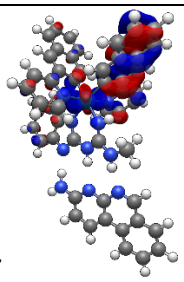	-5.76
LUMO 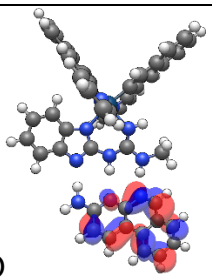	-1.85		HOMO-8 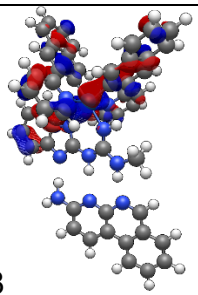	-5.81

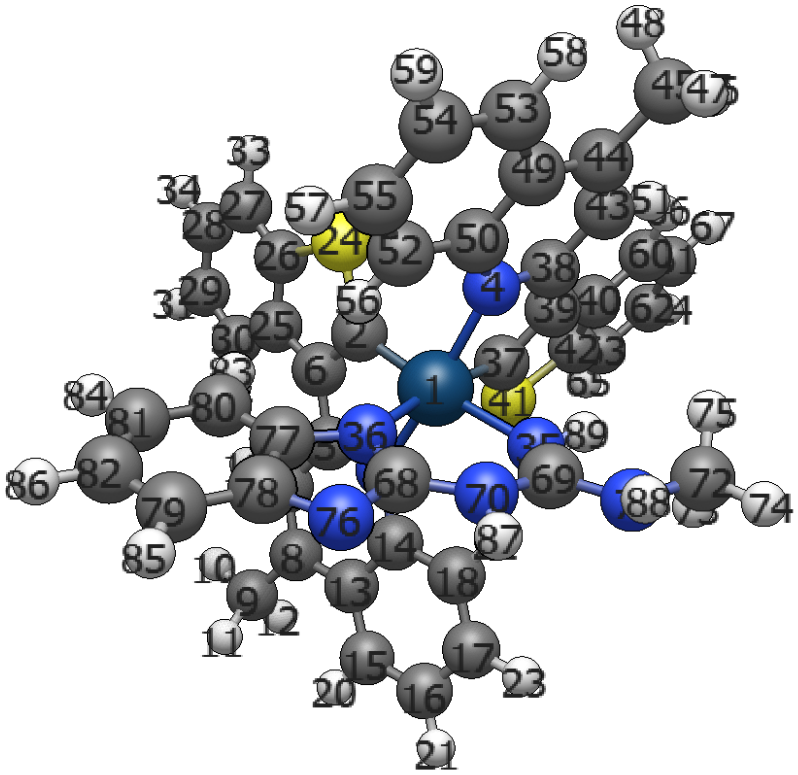

Figure S98. Optimised geometry model used for complex **3**. TD-DFT inputs and energy calculations were based upon this optimised input model.

Table S29. Cartesian coordinates for optimised compound **3**.

Center Number	Atomic Number	Atomic Type	Coordinates (Angstroms) X	Y	Z
1	77	0	0.106354	-0.069980	-0.284289
2	6	0	-0.614337	0.347164	1.510648
3	7	0	-1.744078	0.949992	-0.737256
4	7	0	1.972996	-0.811893	0.450490
5	6	0	-2.434729	1.333792	0.370459
6	6	0	-1.803772	1.049336	1.638284
7	6	0	-3.710004	1.940307	0.250127
8	6	0	-4.310493	2.172185	-0.960603
9	6	0	-5.684093	2.803732	-0.978536
10	1	0	-6.394215	2.180180	-0.423175
11	1	0	-6.088132	2.948312	-1.980882
12	1	0	-5.658209	3.783602	-0.487476

13	6	0	-3.588226	1.800495	-2.137574
14	6	0	-2.293809	1.196904	-1.980135
15	6	0	-4.092584	2.006017	-3.447167
16	6	0	-3.366777	1.657058	-4.564899
17	6	0	-2.087028	1.090358	-4.405821
18	6	0	-1.567307	0.867842	-3.148272
19	1	0	-4.236170	2.207980	1.155195
20	1	0	-5.072792	2.451787	-3.572277
21	1	0	-3.774825	1.824272	-5.557482
22	1	0	-0.581533	0.448882	-3.022554
23	1	0	-1.501514	0.823210	-5.281878
24	16	0	0.103248	0.000784	3.058882
25	6	0	-2.183506	1.325349	3.021239
26	6	0	-1.217336	0.792255	3.917514
27	6	0	-1.327804	0.908601	5.303530
28	6	0	-2.426599	1.576424	5.835967
29	6	0	-3.391871	2.122340	4.979074
30	6	0	-3.276711	2.005180	3.596904
31	1	0	-4.245955	2.649142	5.396401
32	1	0	-4.044285	2.457998	2.981636
33	1	0	-0.566748	0.484865	5.952956
34	1	0	-2.531653	1.677254	6.912570
35	7	0	1.107100	-0.527659	-2.198635
36	7	0	-1.011067	-1.945953	-0.698163
37	6	0	1.183562	1.580856	-0.223993
38	6	0	2.960391	0.120069	0.376008
39	6	0	2.536872	1.472440	0.061127
40	6	0	3.253222	2.743901	0.027143
41	16	0	0.726612	3.221505	-0.585580
42	6	0	2.373419	3.801506	-0.331795
43	6	0	4.313196	-0.259111	0.560436
44	6	0	4.681914	-1.536980	0.905842
45	6	0	6.152977	-1.847655	1.065805
46	1	0	6.705512	-1.533682	0.172635
47	1	0	6.362303	-2.906109	1.223518
48	1	0	6.569649	-1.294219	1.915751
49	6	0	3.641392	-2.494535	1.114844
50	6	0	2.284152	-2.088521	0.871354
51	1	0	5.081016	0.484261	0.393356
52	6	0	1.248822	-3.023749	1.111380
53	6	0	3.888442	-3.821998	1.552561
54	6	0	2.859439	-4.713189	1.763451
55	6	0	1.528262	-4.301482	1.548287
56	1	0	0.227107	-2.714797	0.957723
57	1	0	0.707779	-4.988990	1.732164
58	1	0	4.908297	-4.136427	1.744460

59	1	0	3.071734	-5.721773	2.106274
60	6	0	4.591381	3.090924	0.306998
61	6	0	5.015957	4.412454	0.203935
62	6	0	4.129036	5.430233	-0.173527
63	6	0	2.796707	5.127099	-0.438003
64	1	0	4.476689	6.456731	-0.249210
65	1	0	2.094443	5.909284	-0.713019
66	1	0	5.303573	2.344788	0.636456
67	1	0	6.050181	4.657542	0.430585
68	6	0	-0.834549	-2.735898	-1.787816
69	6	0	1.035205	-1.562708	-2.989656
70	7	0	0.108827	-2.537330	-2.811345
71	7	0	1.871973	-1.741890	-4.064376
72	6	0	2.864912	-0.770345	-4.478298
73	1	0	2.412700	0.203133	-4.710291
74	1	0	3.355376	-1.142698	-5.379622
75	1	0	3.635163	-0.622715	-3.709651
76	7	0	-1.601515	-3.807883	-1.921124
77	6	0	-2.046549	-2.602823	-0.023130
78	6	0	-2.395678	-3.748406	-0.795603
79	6	0	-3.408981	-4.618664	-0.372474
80	6	0	-2.699364	-2.336498	1.187268
81	6	0	-3.705138	-3.212641	1.594073
82	6	0	-4.059780	-4.337501	0.824981
83	1	0	-2.441801	-1.477286	1.792272
84	1	0	-4.226143	-3.019092	2.528455
85	1	0	-3.669390	-5.486152	-0.972762
86	1	0	-4.851138	-4.995946	1.175240
87	1	0	0.041948	-3.283121	-3.490905
88	1	0	1.756981	-2.572367	-4.623661
89	1	0	1.854000	0.119595	-2.424139

Energy

E(RB3LYP) = -3019.73818798 Hartree

Zero point corrected free energy = -3019.053476 Hartree

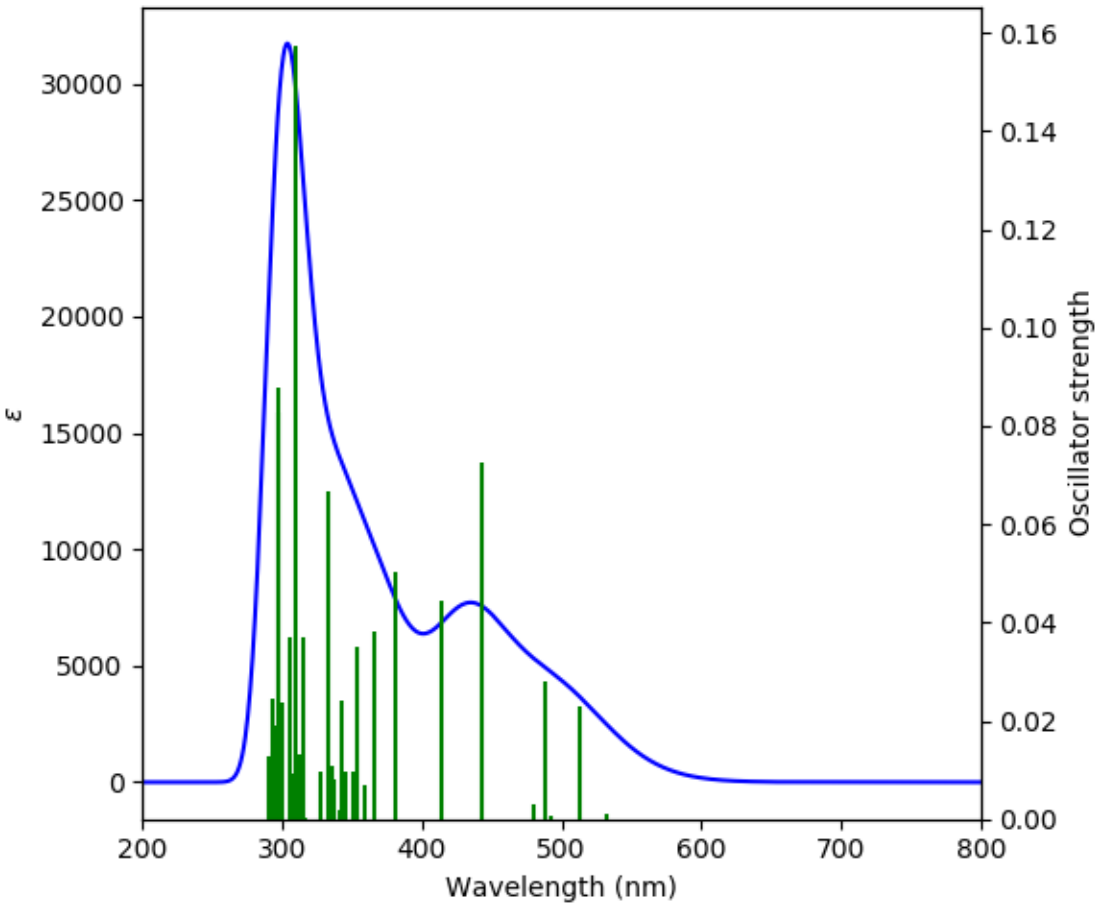

Figure S99. Calculated UV/vis spectrum for complex **3**.

Table S30. Calculated energy levels of the ten highest contributing singlet states and the first five triplet states for **3**.

Spin State	Transition configurations	Excitation energy (eV, nm)	Oscillator strength
S_2	HOMO-1→LUMO (94.5%) HOMO→LUMO (2.1%)	2.4194, 512.46	0.0230
S_4	HOMO-2→LUMO (93.3%) HOMO-2→LUMO+1 (2.2%)	2.5391, 488.30	0.0280

S_6	HOMO-2→LUMO+1 (97.1%)	2.8022, 442.45	0.0727
S_7	HOMO-3→LUMO (96.6%)	2.9922, 414.36	0.0446
S_8	HOMO-3→LUMO+1 (96.7%)	3.2556, 380.83	0.0502
S_9	HOMO-4→LUMO (94.8%)	3.3909, 365.63	0.0382
S_{14}	HOMO-4→LUMO+1 (83.2%) HOMO-2→LUMO+2 (3.4%) HOMO-6→LUMO+1 (3.7%) HOMO→LUMO+3 (5.3%)	3.6200, 342.50	0.0240
S_{19}	HOMO-2→LUMO+2 (56.9%) HOMO-7→LUMO (11.0%) HOMO-5→LUMO (10.9%) HOMO-6→LUMO (6.2%) HOMO-1→LUMO+3 (4.0%)	3.7200, 333.29	0.0668
S_{25}	HOMO-8→LUMO (48.8%) HOMO-3→LUMO+2 (29.7%) HOMO-2→LUMO+2 (2.5%) HOMO-2→LUMO+7 (2.9%) HOMO-9→LUMO (4.6%)	4.0141, 308.87	0.0027
S_{32}	HOMO-1→LUMO+5 (45.7%) HOMO-2→LUMO+4 (10.7%) HOMO-2→LUMO+7 (11.7%) HOMO→LUMO+7 (15.8%)	4.2029, 295.00	0.0189
T_1	HOMO-2→LUMO (49.0%) HOMO-3→LUMO (28.3%) HOMO-1→LUMO (6.4%)	2.1906, 565.99	0.0000

	HOMO-2→LUMO+1 (2.0%) HOMO-3→LUMO+1 (2.01%)		
T_2	HOMO-2→LUMO+1 (47.8%) HOMO-1→LUMO+1 (21.3%) HOMO→LUMO (3.7%) HOMO-1→LUMO (3.0%) HOMO-7→LUMO+1 (2.3%) HOMO-3→LUMO+1 (5.4%) HOMO-3→LUMO (7.8%)	2.2413, 553.18	0.0000
T_3	HOMO→LUMO (58.9%) HOMO-1→LUMO (30.6%) HOMO-1→LUMO+1 (2.3%) HOMO-2→LUMO+1 (4.3%)	2.3041, 538.11	0.0000
T_4	HOMO-1→LUMO (53.6%) HOMO-2→LUMO (2.0%) HOMO-3→LUMO (2.9%) HOMO→LUMO (35.0%)	2.3753, 521.97	0.0000
T_5	HOMO→LUMO+1 (89.8%) HOMO-1→LUMO+1 (3.1%) HOMO-2→LUMO+1 (5.1%)	2.5098, 493.99	0.0000

Table S31. Calculated MO energies of orbitals involved in transitions for **3**.

Orbital	**Energy/ eV**		**Orbital**	**Energy/ eV**

LUMO+7 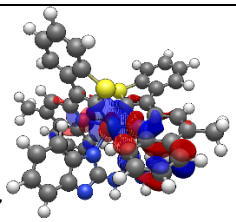	0.16		HOMO 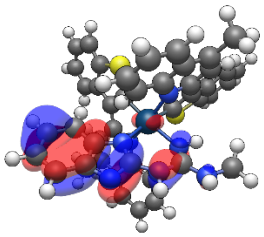	-4.66
LUMO+6 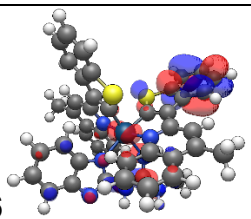	0.14		HOMO-1 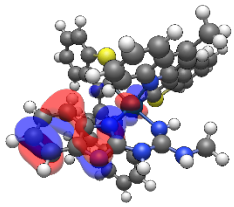	-4.78
LUMO+5 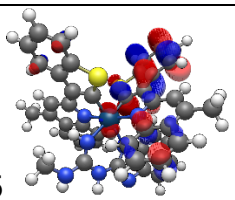	-0.04		HOMO-2 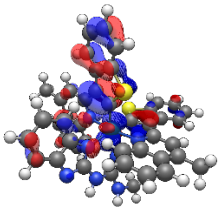	-4.94
LUMO+4 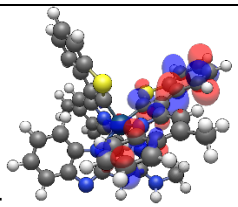	-0.27		HOMO-3 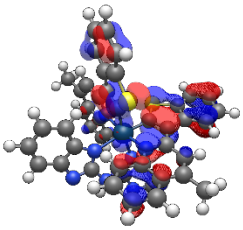	-5.35
LUMO+3 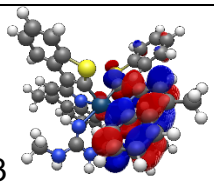	-0.49		HOMO-4 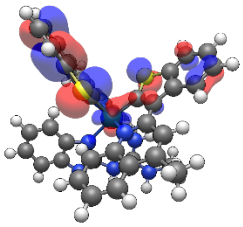	-5.75

LUMO+2 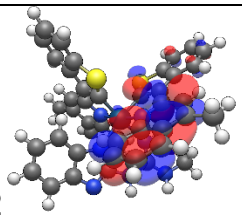	-0.70		HOMO-5 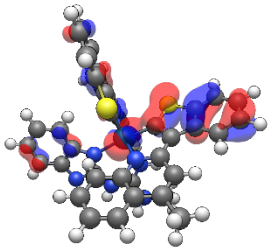	-6.01
LUMO+1 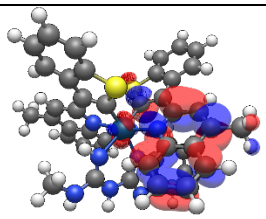	-1.59		HOMO-6 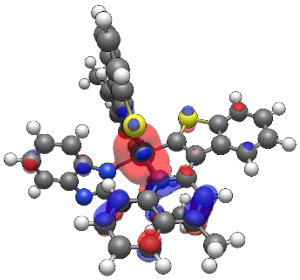	-6.04
LUMO 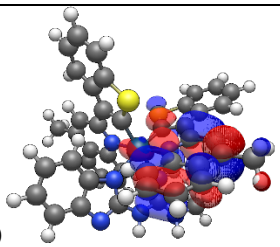	-1.83		HOMO-7 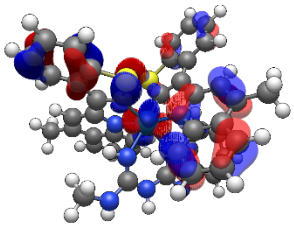	-6.09
			HOMO-8 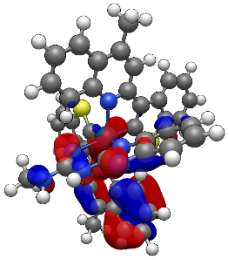	-6.48

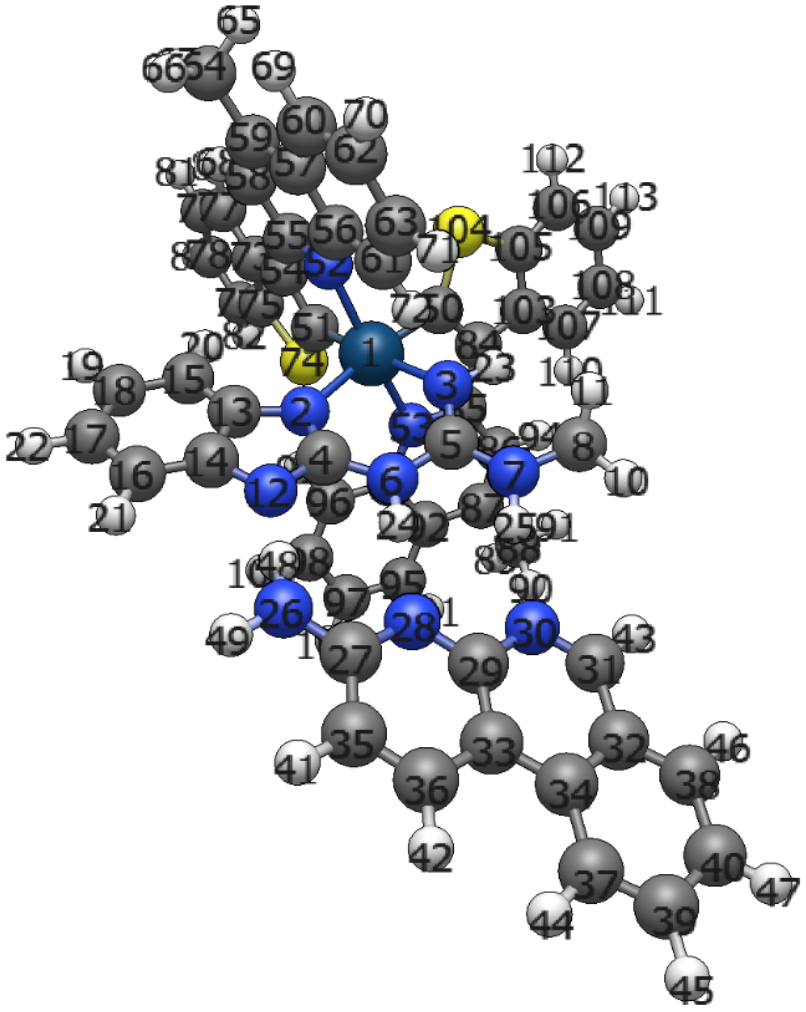

Figure S100. Optimised geometry model used for co-system **3•5**. TD-DFT inputs and energy calculations were based upon this optimised input model.

Table S32. Cartesian coordinates for optimised co-system **3•5**.

Center Number	Atomic Number	Atomic Type	Coordinates (Angstroms) X	Y	Z
1	7	0	4.321331	-3.877999	0.443801
2	6	0	5.320050	-2.992009	0.258211
3	6	0	6.687140	-3.399659	0.414671
4	7	0	5.002390	-1.736199	-0.095349
5	6	0	5.997000	-0.845009	-0.294999
6	7	0	5.575240	0.417971	-0.667849

7	6	0	6.471360	1.349451	-0.858119
8	6	0	7.377610	-1.150799	-0.142419
9	6	0	7.881700	1.174141	-0.719889
10	6	0	8.357270	-0.118049	-0.357149
11	6	0	7.686560	-2.488939	0.220661
12	6	0	8.786959	2.237702	-0.942219
13	6	0	9.757650	-0.295808	-0.229469
14	6	0	10.625260	0.756642	-0.450969
15	6	0	10.144889	2.035672	-0.810019
16	1	0	6.910351	-4.426079	0.691511
17	1	0	8.719870	-2.796428	0.347871
18	1	0	6.098689	2.333811	-1.147159
19	1	0	10.160700	-1.264858	0.045941
20	1	0	11.695270	0.597592	-0.346999
21	1	0	8.394679	3.213711	-1.218639
22	1	0	10.843209	2.849742	-0.979869
23	1	0	4.549611	-4.784419	0.824241
24	1	0	3.333100	-3.557270	0.528851
25	6	0	-1.903929	-4.458271	2.366781
26	6	0	-0.769959	-5.284880	2.471971
27	6	0	-1.840920	-3.207991	1.751341
28	6	0	0.462561	-4.875740	1.968981
29	6	0	-0.608680	-2.793590	1.232301
30	6	0	0.540401	-3.622100	1.350931
31	7	0	1.621320	-2.974340	0.788921
32	7	0	-0.210580	-1.617490	0.594881
33	6	0	1.112460	-1.814610	0.371971
34	7	0	1.987740	-0.891460	-0.205279
35	6	0	1.685330	0.156490	-1.025789
36	7	0	0.443170	0.490110	-1.291979
37	7	0	2.762070	0.787860	-1.568329
38	6	0	2.633519	1.988360	-2.366689
39	1	0	2.061769	1.804320	-3.285859
40	1	0	3.636229	2.306581	-2.660949
41	1	0	2.154309	2.814950	-1.820819
42	1	0	-2.851709	-4.797811	2.776951
43	1	0	-2.719200	-2.578581	1.685521
44	1	0	-0.857669	-6.253740	2.957631
45	1	0	1.344461	-5.505900	2.054621
46	1	0	2.973410	-1.174440	-0.157829
47	1	0	3.695070	0.575001	-1.197279
48	77	0	-1.353690	0.127300	-0.090969
49	6	0	-3.005000	-0.034101	0.994031
50	6	0	-2.093391	1.768109	-0.928219
51	7	0	-0.492431	1.669370	1.121511
52	7	0	-2.545880	-1.235211	-1.268059

53	6	0	-0.665171	2.909730	0.592761
54	6	0	-1.592281	2.997810	-0.517819
55	16	0	-3.225911	1.936939	-2.236569
56	6	0	-2.141751	4.135339	-1.248909
57	6	0	-3.056121	3.692659	-2.244089
58	6	0	0.051019	4.017990	1.120401
59	6	0	0.873109	3.902730	2.211821
60	6	0	0.243199	1.524740	2.282621
61	6	0	0.956839	2.628310	2.855181
62	6	0	1.706329	2.426160	4.041071
63	6	0	0.271390	0.281660	2.961721
64	6	0	1.734350	1.198430	4.667111
65	6	0	0.997080	0.126350	4.124801
66	6	0	1.639419	5.094880	2.724791
67	1	0	1.466379	5.971330	2.093961
68	1	0	2.718209	4.898280	2.746291
69	1	0	1.339329	5.352080	3.748111
70	1	0	-0.037241	4.972990	0.622301
71	1	0	2.253909	3.261190	4.465961
72	1	0	2.308730	1.061450	5.578851
73	1	0	-0.295290	-0.543580	2.559731
74	1	0	0.991670	-0.837590	4.625381
75	6	0	-1.955721	5.527249	-1.127029
76	6	0	-3.728651	4.572599	-3.092739
77	6	0	-2.625101	6.408189	-1.971689
78	6	0	-3.504521	5.939929	-2.957459
79	1	0	-1.310921	5.940640	-0.360959
80	1	0	-4.419831	4.194359	-3.840989
81	1	0	-2.465612	7.477059	-1.856359
82	1	0	-4.018962	6.641269	-3.608369
83	6	0	-3.781850	-1.450251	-0.738689
84	6	0	-4.085990	-0.739291	0.480841
85	16	0	-3.394250	0.717749	2.515001
86	6	0	-5.291260	-0.661501	1.300231
87	6	0	-5.045440	0.098939	2.475811
88	6	0	-6.600360	-1.152181	1.121251
89	6	0	-6.023530	0.327879	3.443411
90	6	0	-7.581110	-0.922462	2.082361
91	6	0	-7.299080	-0.194752	3.246021
92	1	0	-8.075180	-0.027042	3.987531
93	1	0	-5.793180	0.910819	4.331021
94	1	0	-6.878310	-1.689382	0.222531
95	1	0	-8.582980	-1.311152	1.919771
96	6	0	-2.186100	-1.912291	-2.421139
97	6	0	-0.913510	-1.705320	-3.003999
98	6	0	-0.539730	-2.365080	-4.157139

99	6	0	-1.414880	-3.268080	-4.791589
100	6	0	-3.077510	-2.833051	-3.063529
101	6	0	-4.676470	-2.376981	-1.339679
102	6	0	-4.360350	-3.068641	-2.477309
103	6	0	-2.660940	-3.492061	-4.246529
104	6	0	-5.333069	-4.052411	-3.074529
105	1	0	-4.903099	-5.060241	-3.121949
106	1	0	-5.609739	-3.770741	-4.098049
107	1	0	-6.249359	-4.103651	-2.479889
108	1	0	-5.622620	-2.562891	-0.853069
109	1	0	-0.240720	-1.010640	-2.523269
110	1	0	0.446550	-2.183210	-4.576199
111	1	0	-1.111169	-3.783240	-5.698469
112	1	0	-3.341819	-4.187471	-4.726399
113	1	0	0.366780	1.314430	-1.876689

Energy

E(RB3LYP) = -3646.75691618 Hartree

Zero point corrected free energy = -3645.874067 Hartree

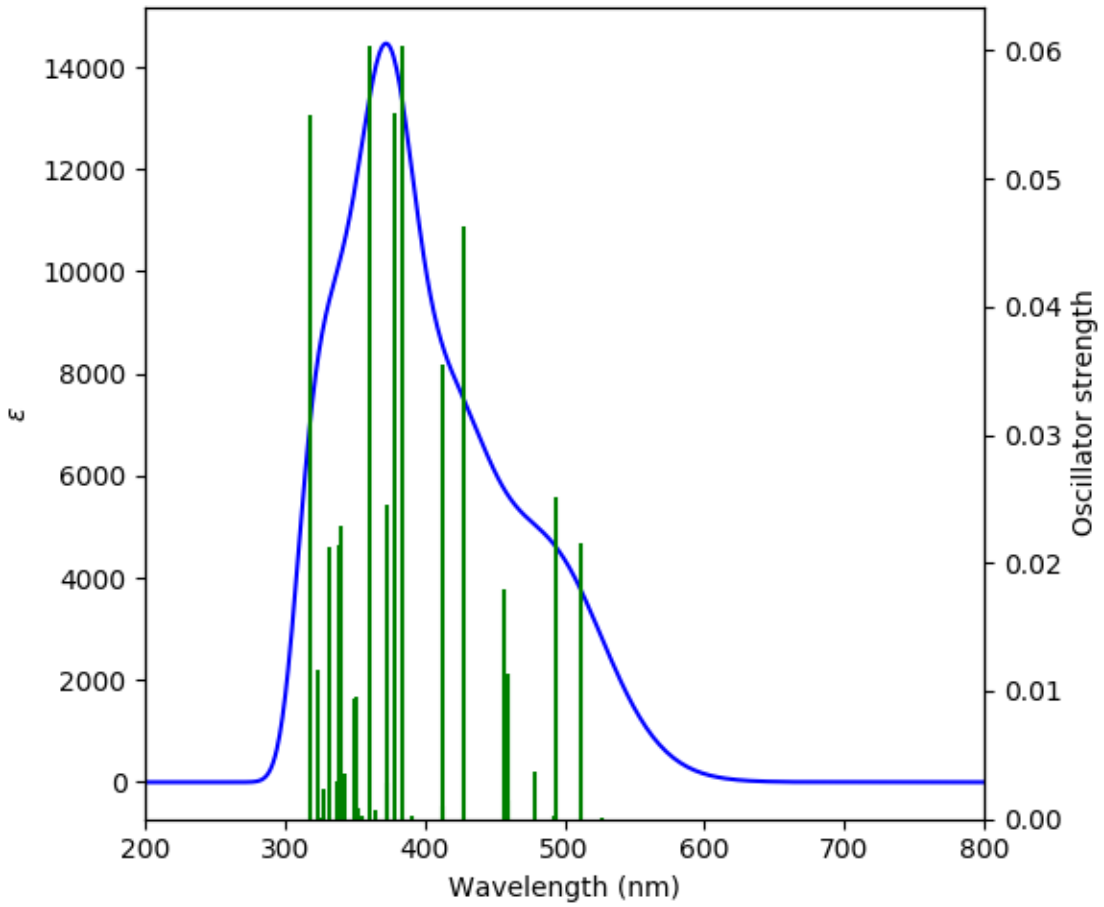

Figure S101. Calculated UV/vis spectrum for co-system **3•5**.

Table S33. Calculated energy levels of the ten highest contributing singlet states and the first five triplet states for **3•5**.

Spin State	Transition configurations	Excitation energy (eV, nm)	Oscillator strength
S_2	HOMO→LUMO+1 (93.4%) HOMO-1→LUMO+1 (4.8%)	2.4212, 512.07	0.0216
S_3	HOMO-1→LUMO+1 (87.0%) HOMO-2→LUMO+1 (4.0%)	2.5312, 493.32	0.0251

	HOMO→LUMO+1 (4.6%)		
S_5	HOMO→LUMO+2 (90.6%) HOMO-1→LUMO+2 (5.4%)	2.5875, 479.17	0.0037
S_9	HOMO-2→LUMO+2 (95.5%)	2.9009, 427.39	0.0463
S_{10}	HOMO-3→LUMO+1 (93.2%) HOMO-3→LUMO (3.2%)	2.9998, 413.31	0.0355
S_{13}	HOMO-3→LUMO+2 (95.0%)	3.2333, 383.46	0.0604
S_{14}	HOMO-5→LUMO (96.3%)	3.2789, 378.13	0.0551
S_{18}	HOMO-4→LUMO+1 (49.9%) HOMO-6→LUMO+1 (41.6%)	3.4396, 360.46	0.0603
S_{29}	HOMO-8→LUMO+1 (67.3%) HOMO-7→LUMO+1 (22.2%) HOMO-10→LUMO+1 (2.7%) HOMO-1→LUMO+4 (3.8%)	3.7361, 331.85	0.0212
S_{35}	HOMO-7→LUMO+2 (60.7%) HOMO-5→LUMO+2 (6.2%) HOMO-2→LUMO+6 (2.7%) HOMO-1→LUMO+6 (23.7%)	3.9040, 317.59	0.0549
T_1	HOMO-9→LUMO+1 (2.3%) HOMO-3→LUMO+1 (21.1%) HOMO-3→LUMO+2 (3.6%) HOMO-2→LUMO+1 (15.8%) HOMO-1→LUMO+1 (37.3%) HOMO-1→LUMO+2 (4.2%) HOMO→LUMO+1 (6.7%)	2.1886, 565.49	0.0000

	HOMO→LUMO+2 (2.5%)		
T_2	HOMO-8→LUMO+2 (2.2%) HOMO-3→LUMO+1 (13.1%) HOMO-3→LUMO+2 (4.9%) HOMO-2→LUMO+1 (2.4%) HOMO-2→LUMO+2 (7.6%) HOMO-1→LUMO+2 (41.2%) HOMO→LUMO+2 (18.9%)	2.2312, 555.67	0.0000
T_3	HOMO→LUMO (91.1%) HOMO→LUMO+1 (3.0%) HOMO-1→LUMO (3.7%)	2.3495, 527.72	0.0000
T_4	HOMO-9→LUMO+1 (3.0%) HOMO-6→LUMO+1 (2.2%) HOMO-3→LUMO+1 (2.5%) HOMO-2→LUMO+1 (6.7%) HOMO-1→LUMO+2 (2.7%) HOMO→LUMO (3.9%) HOMO→LUMO+1 (70.5%) HOMO→LUMO+2 (2.2%)	2.3536, 526.78	0.0000
T_5	HOMO-15→LUMO (2.1%) HOMO-5→LUMO (44.0%) HOMO-2→LUMO (3.6%) HOMO-1→LUMO (43.1%) HOMO→LUMO (3.9%)	2.4916, 497.61	0.0000

Table S34. Calculated MO energies of orbitals involved in transitions for co-system **3•5**.

Orbital	Energy/ eV		Orbital	Energy/ eV
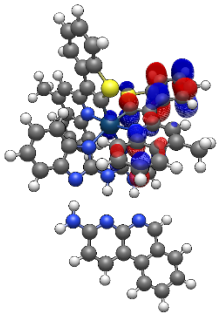 LUMO+7	-0.11		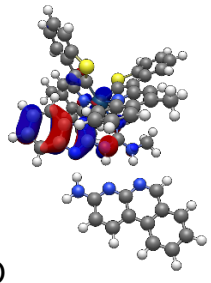 HOMO	-4.60
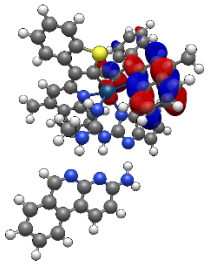 LUMO+6	-0.33		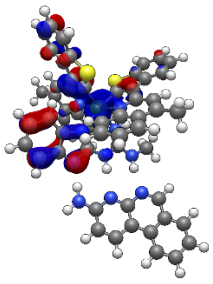 HOMO-1	-4.71
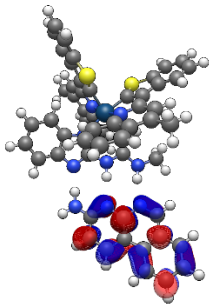 LUMO+5	-0.42		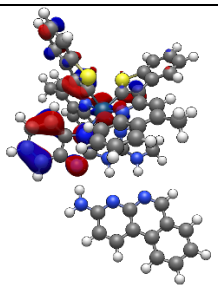 HOMO-2	-4.89
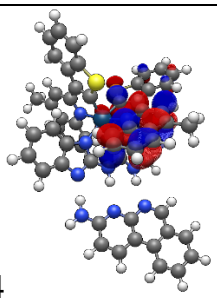 LUMO+4	-0.52		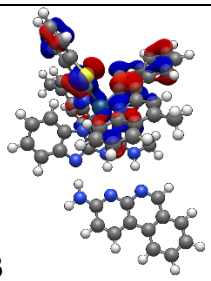 HOMO-3	-5.17

LUMO+3 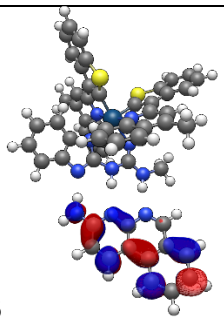	-1.07		HOMO-4 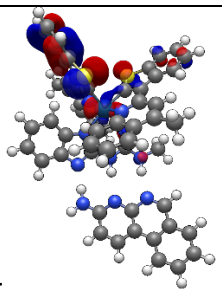	-5.59
LUMO+2 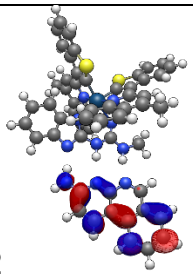	-1.43		HOMO-5 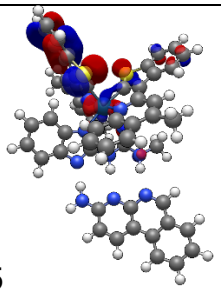	-5.64
LUMO+1 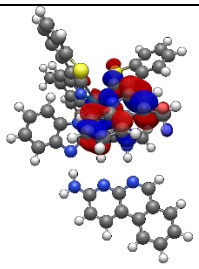	-1.64		HOMO-6 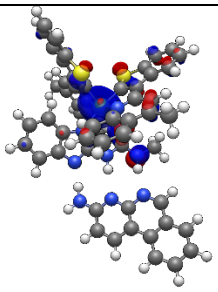	-5.70
LUMO 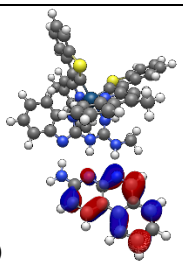	-1.88		HOMO-7 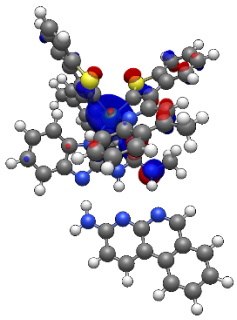	-5.86

			HOMO-8 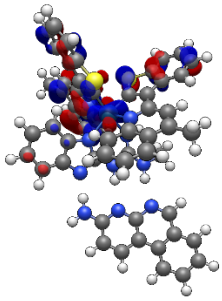	-5.93
			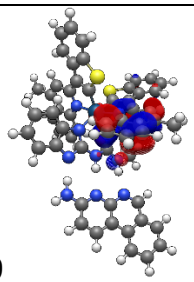 HOMO-9	-6.21
			HOMO-15 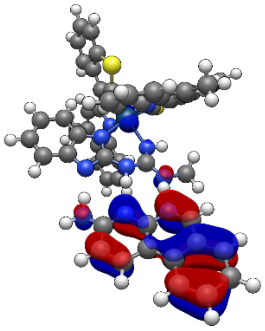	-6.82

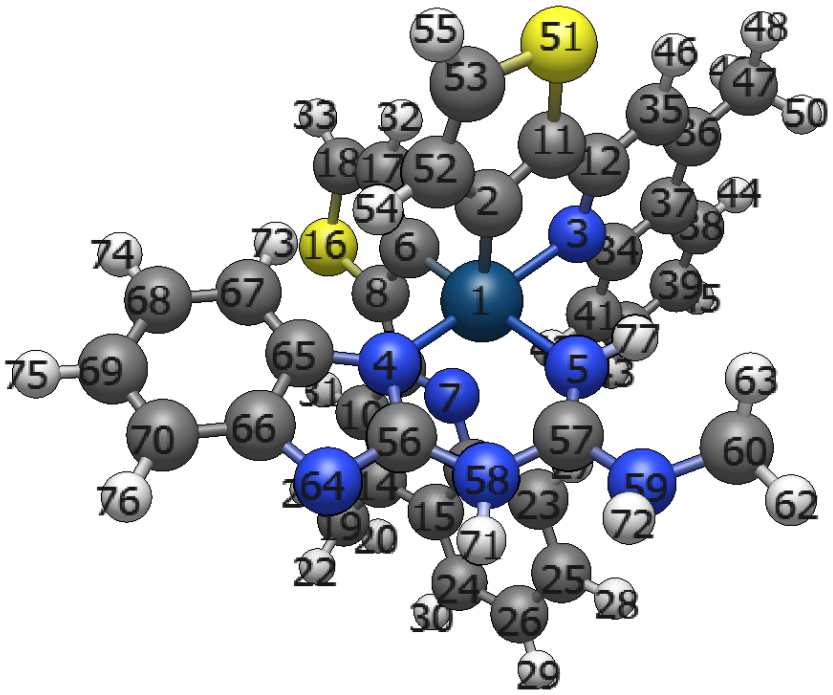

Figure S102. Optimised geometry model used for complex **4**. TD-DFT inputs and energy calculations were based upon this optimised input model.

Table S35. Cartesian coordinates for optimised compound **4**.

Center Number	Atomic Number	Atomic Type	Coordinates (Angstroms) X	Y	Z
1	77	0	-0.245501	-0.439741	0.125478
2	6	0	-1.284637	-2.126215	0.200460
3	7	0	-2.269839	0.313091	-0.178417
4	7	0	1.534971	-1.400319	0.609845
5	7	0	-0.576792	-0.235191	2.269435
6	6	0	0.009893	-0.487851	-1.871326
7	7	0	1.225948	1.393434	-0.287182
8	6	0	0.934125	0.402396	-2.400810
9	6	0	1.652665	1.321550	-1.563646
10	6	0	2.745083	2.106098	-2.034291
11	6	0	-2.658114	-1.984830	0.058192
12	6	0	-3.196321	-0.676863	-0.149507
13	6	0	1.839752	2.287273	0.557990
14	6	0	3.415353	2.967479	-1.206664

15	6	0	2.952311	3.090456	0.145914
16	16	0	1.078155	0.282496	-4.149738
17	6	0	-0.602859	-1.255282	-2.915945
18	6	0	-0.134848	-0.956640	-4.169258
19	6	0	4.593042	3.763101	-1.707616
20	1	0	4.415711	4.842164	-1.619438
21	1	0	4.795965	3.538663	-2.758343
22	1	0	5.499216	3.536697	-1.132548
23	6	0	1.328578	2.460308	1.868410
24	6	0	3.534435	3.985465	1.076667
25	6	0	1.910424	3.353272	2.744810
26	6	0	3.030857	4.116075	2.355163
27	1	0	0.460644	1.879317	2.151282
28	1	0	1.499145	3.470587	3.744199
29	1	0	3.488478	4.810351	3.054219
30	1	0	4.387212	4.583625	0.771519
31	1	0	3.060050	1.986595	-3.066571
32	1	0	-1.354235	-2.017270	-2.739812
33	1	0	-0.429911	-1.396635	-5.113738
34	6	0	-2.699661	1.609816	-0.373002
35	6	0	-4.583240	-0.410004	-0.312960
36	6	0	-5.049710	0.863300	-0.503831
37	6	0	-4.088918	1.927936	-0.534642
38	6	0	-4.465352	3.280813	-0.720424
39	6	0	-3.524362	4.289519	-0.749625
40	6	0	-2.160063	3.970930	-0.596547
41	6	0	-1.756741	2.663662	-0.414029
42	1	0	-0.711484	2.411993	-0.309612
43	1	0	-1.413111	4.759547	-0.625407
44	1	0	-5.516231	3.522462	-0.842801
45	1	0	-3.832564	5.321065	-0.893915
46	1	0	-5.272860	-1.248412	-0.283978
47	6	0	-6.523034	1.128146	-0.677183
48	1	0	-7.094851	0.197554	-0.624927
49	1	0	-6.732186	1.599958	-1.644987
50	1	0	-6.903292	1.803655	0.098970
51	16	0	-3.517602	-3.516003	0.137230
52	6	0	-0.924974	-3.501327	0.377975
53	6	0	-2.004744	-4.345056	0.366894
54	1	0	0.095130	-3.848062	0.494404
55	1	0	-2.006735	-5.422666	0.474211
56	6	0	2.113355	-1.374956	1.842101
57	6	0	0.261358	-0.458442	3.239980
58	7	0	1.557235	-0.779368	2.987126
59	7	0	-0.040533	-0.299422	4.581710
60	6	0	-1.384411	0.054155	5.010733

61	1	0	-1.683771	1.000857	4.550020
62	1	0	-1.374238	0.197242	6.093687
63	1	0	-2.137653	-0.710828	4.767910
64	7	0	3.284166	-1.970229	1.986513
65	6	0	2.445633	-2.151026	-0.143746
66	6	0	3.526281	-2.475507	0.725133
67	6	0	2.435025	-2.612032	-1.466472
68	6	0	3.522902	-3.366876	-1.902400
69	6	0	4.603550	-3.669263	-1.051258
70	6	0	4.614345	-3.230933	0.268541
71	1	0	2.211163	-0.782116	3.758542
72	1	0	0.450326	-0.935528	5.197458
73	1	0	1.611345	-2.399451	-2.134720
74	1	0	3.532852	-3.730920	-2.926827
75	1	0	5.434091	-4.259604	-1.430786
76	1	0	5.432643	-3.467572	0.943136
77	1	0	-1.544055	-0.152996	2.561241

Energy

E(RB3LYP) = -2712.37592708 Hartree

Zero point corrected free energy = -2711.849522 Hartree

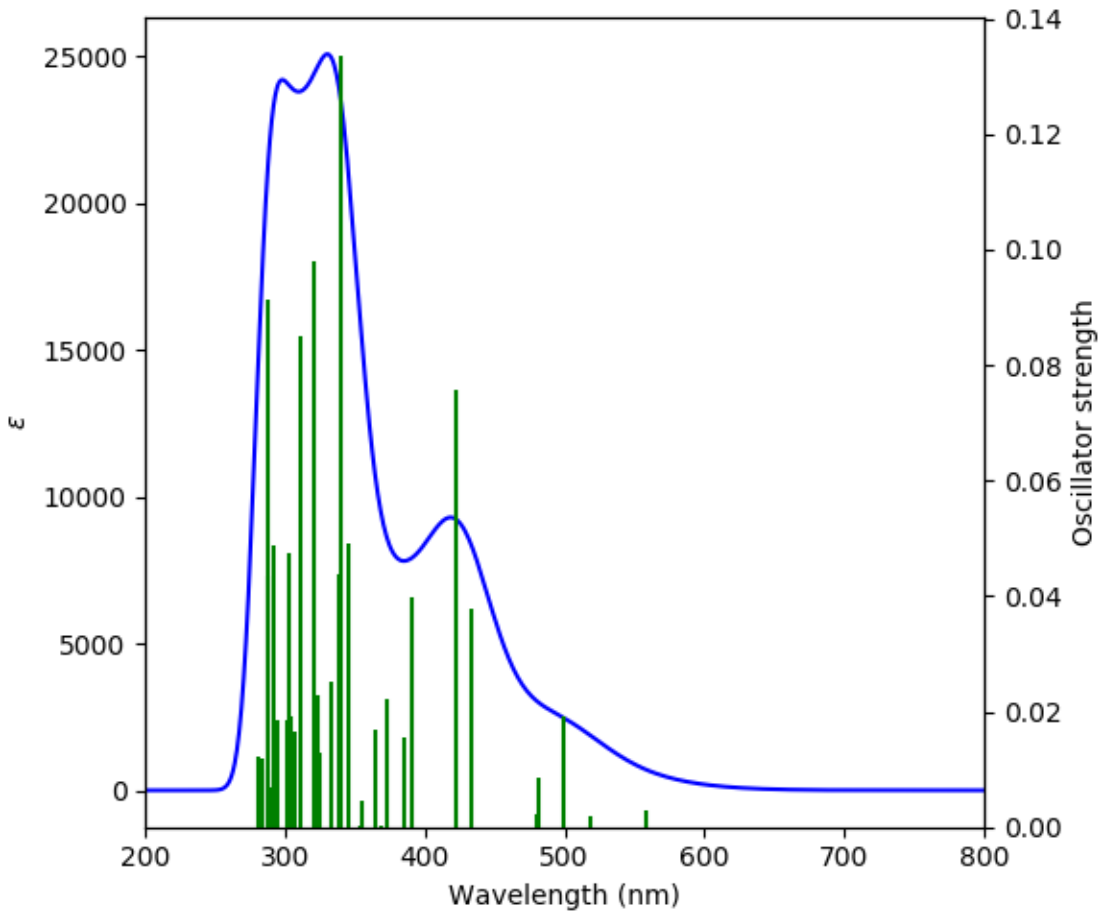

Figure S103. Calculated UV/vis spectrum for complex **4**.

Table S36. Calculated energy levels of the ten highest contributing singlet states and the first five triplet states for **4**.

Spin State	Transition configurations	Excitation energy (eV, nm)	Oscillator strength
S_3	HOMO→LUMO+1 (96.1%)	2.4846, 499.02	0.0193
S_6	HOMO-2→LUMO+1 (89.2%) HOMO-3→LUMO (6.5%)	2.8577, 433.86	0.0379
S_7	HOMO-3→LUMO (87.5%)	2.9402, 421.69	0.0757

	HOMO-2→LUMO+1 (5.9%)		
S_8	HOMO-3→LUMO+1 (85.8%) HOMO→LUMO+2 (5.1%) HOMO-4→LUMO+1 (2.4%)	3.2213, 384.89	0.0397
S_{10}	HOMO-4→LUMO (81.2%) HOMO→LUMO+2 (7.7%) HOMO-6→LUMO (6.4%)	3.3290, 372.43	0.0221
S_{15}	HOMO-2→LUMO+2 (61.2%) HOMO-6→LUMO (12.8%) HOMO-5→LUMO (11.4%) HOMO-4→LUMO (4.2%) HOMO-2→LUMO+2 (3.6%)	3.5856, 345.78	0.0491
S_{16}	HOMO-5→LUMO (60.8%) HOMO-4→LUMO+1 (17.0%) HOMO-2→LUMO+2 (14.9%)	3.6430, 340.33	0.1335
S_{21}	HOMO-6→LUMO+1 (34.5%) HOMO-5→LUMO+1 (32.2%) HOMO-3→LUMO+3 (3.0%) HOMO-2→LUMO+3 (2.7%)	3.8616, 321.07	0.0979
S_{25}	HOMO-3→LUMO+3 (39.0%) HOMO→LUMO+4 (25.9%) HOMO-7→LUMO+1 (2.6%) HOMO-1→LUMO+4 (2.1%) HOMO→LUMO+5 (16.4%)	4.0978, 302.56	0.0474
S_{33}	HOMO-9→LUMO (3.1%)	4.3183, 287.11	0.0913

	HOMO-7→LUMO+1 (2.9%) HOMO-2→LUMO+5 (2.2%) HOMO-2→LUMO+7 (2.3%) HOMO-1→LUMO+4 (44.2%) HOMO-1→LUMO+5 (22.5%) HOMO→LUMO+4 (4.2%)		
T_1	HOMO-5→LUMO (3.6%) HOMO-3→LUMO (17.6%) HOMO-2→LUMO (26.5%) HOMO-1→LUMO (3.8%) HOMO→LUMO (42.2%)	1.9932, 622.03	0.0000
T_2	HOMO-3→LUMO+1 (11.4%) HOMO-2→LUMO+1 (26.0%) HOMO-1→LUMO+1 (8.1%) HOMO→LUMO+1 (43.4%)	2.1195, 584.96	0.0000
T_3	HOMO-3→LUMO (10.4%) HOMO-2→LUMO (16.0%) HOMO-1→LUMO (53.8%) HOMO→LUMO (13.6%)	2.3411, 529.59	0.0000
T_4	HOMO-5→LUMO (3.4%) HOMO-3→LUMO (6.1%) HOMO-2→LUMO (6.4%) HOMO-1→LUMO (38.5%) HOMO→LUMO (42.7%)	2.4081, 529.86	0.0000
T_5	HOMO-4→LUMO+1 (4.1%) HOMO-3→LUMO+1 (4.1%)	2.5521, 485.82	0.0000

	HOMO-2→LUMO+1 (13.9%) HOMO-1→LUMO+1 (69.0%) HOMO→LUMO+1 (2.2%)		

Table S37. Calculated MO energies of orbitals involved in transitions for **4**.

Orbital	**Energy/ eV**		**Orbital**	**Energy/ eV**
LUMO+7 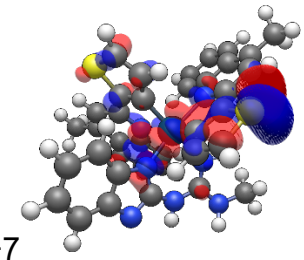	0.63		HOMO 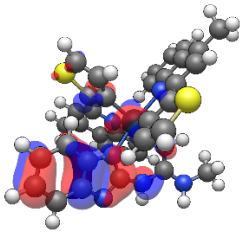	-4.58
LUMO+6 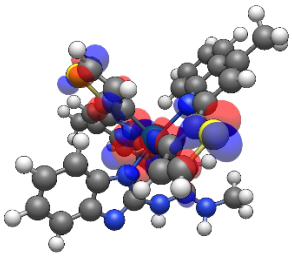	0.41		HOMO-1 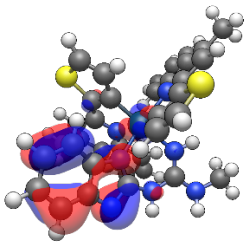	-4.65
LUMO+5 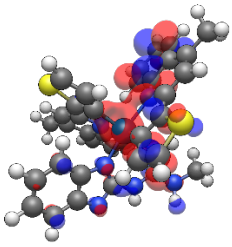	0.23		HOMO-2 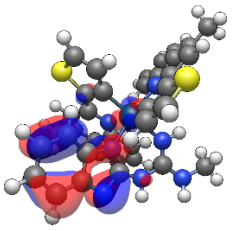	-4.97

LUMO+4 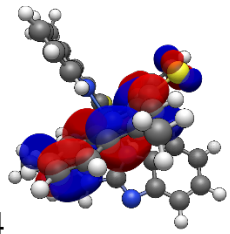	0.19		HOMO-3 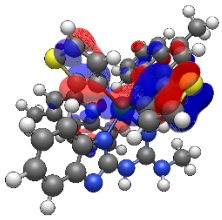	-5.27
LUMO+3 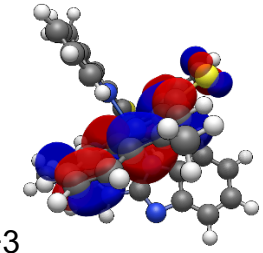	-0.61		HOMO-4 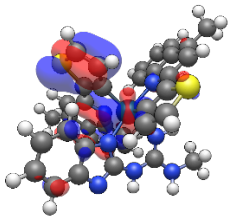	-5.71
LUMO+2 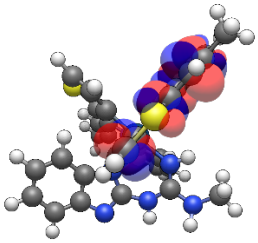	-0.85		HOMO-5 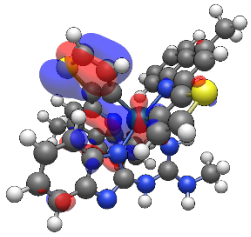	-5.89
LUMO+1 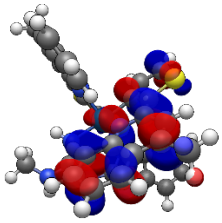	-1.51		HOMO-6 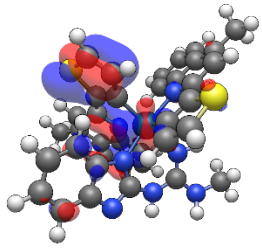	-5.95
LUMO 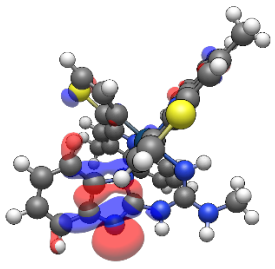	-1.79		HOMO-7 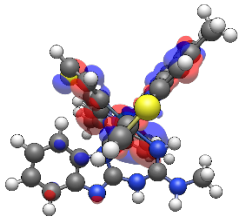	-6.27

			HOMO-8 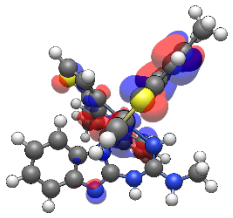	-6.42
			HOMO-9 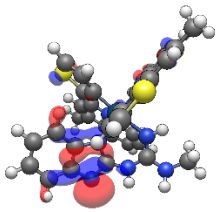	-6.54

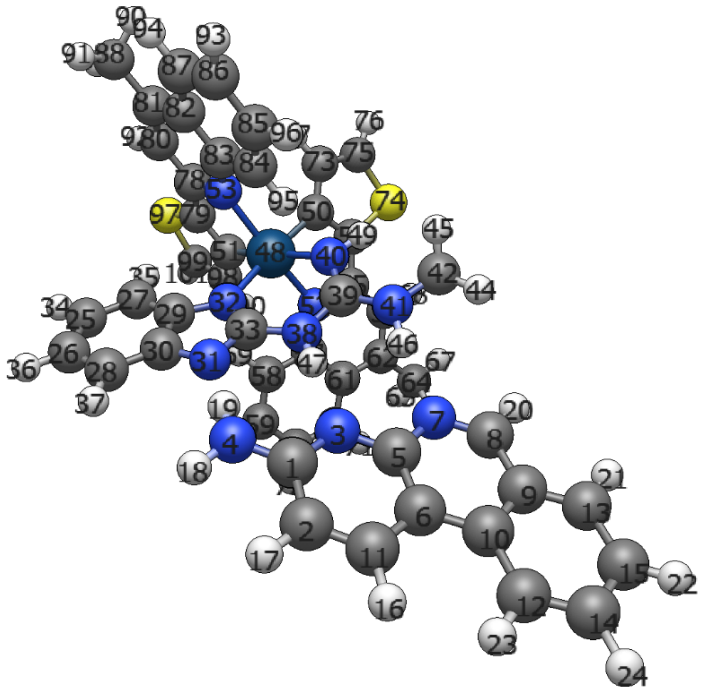

Figure S104. Optimised geometry model used for co-system **4•5**. TD-DFT inputs and energy calculations were based upon this optimised input model.

Table S38. Cartesian coordinates for optimised co-system **4•5**.

Center Number	Atomic Number	Atomic Type	Coordinates (Angstroms) X	Y	Z
1	6	0	-4.616579	-3.016001	0.903179
2	6	0	-5.954089	-3.474611	1.149559
3	7	0	-4.382099	-1.885861	0.217139
4	7	0	-3.561109	-3.730751	1.341159
5	6	0	-5.432679	-1.169651	-0.236661
6	6	0	-6.791169	-1.532811	-0.022561
7	7	0	-5.093429	-0.029851	-0.942411
8	6	0	-6.049330	0.735499	-1.397291
9	6	0	-7.446810	0.491049	-1.233721
10	6	0	-7.837039	-0.683711	-0.530021
11	6	0	-7.011499	-2.738241	0.696019
12	6	0	-9.223929	-0.932222	-0.375431
13	6	0	-8.420590	1.373469	-1.756201
14	6	0	-10.159409	-0.057012	-0.893471
15	6	0	-9.763530	1.106448	-1.590001
16	1	0	-8.022739	-3.081791	0.890709
17	1	0	-6.109519	-4.398681	1.699099
18	1	0	-3.734189	-4.510821	1.957639
19	1	0	-2.602759	-3.318641	1.347129
20	1	0	-5.741390	1.627779	-1.945421
21	1	0	-8.092730	2.262809	-2.289601
22	1	0	-10.514230	1.781708	-1.989671
23	1	0	-9.562869	-1.815982	0.155129
24	1	0	-11.217559	-0.267382	-0.762581
25	6	0	2.598381	-3.217810	3.480589
26	6	0	1.536151	-4.094910	3.768979
27	6	0	2.459411	-2.182970	2.555519
28	6	0	0.300521	-3.952911	3.142059
29	6	0	1.224471	-2.039860	1.911919
30	6	0	0.146481	-2.917371	2.212579
31	7	0	-0.954249	-2.547341	1.467359
32	7	0	0.762251	-1.114921	0.975909
33	6	0	-0.523639	-1.492471	0.772679
34	1	0	3.549651	-3.345980	3.991189
35	1	0	3.280451	-1.507640	2.350029
36	1	0	1.682161	-4.891000	4.495169
37	1	0	-0.526169	-4.622681	3.366499
38	7	0	-1.440649	-0.839051	-0.055111
39	6	0	-1.178289	-0.049021	-1.138811
40	7	0	0.045110	0.303129	-1.456291

41	7	0	-2.274920	0.299449	-1.868711
42	6	0	-2.201640	1.237649	-2.968181
43	1	0	-1.807850	2.220049	-2.666631
44	1	0	-3.211500	1.377329	-3.360821
45	1	0	-1.578450	0.853969	-3.786881
46	1	0	-3.203800	0.125369	-1.469691
47	1	0	-2.401119	-1.186891	0.041959
48	77	0	1.787720	0.492250	-0.130371
49	1	0	0.087710	0.923779	-2.256501
50	6	0	2.450370	1.903570	-1.398841
51	6	0	3.367870	0.828580	1.060229
52	7	0	0.712990	2.202829	0.598479
53	7	0	3.174521	-0.990510	-0.875801
54	6	0	1.741400	3.093400	-1.313301
55	6	0	0.811610	3.266339	-0.236431
56	6	0	0.064610	4.455359	-0.022181
57	6	0	-0.036380	2.336409	1.751869
58	6	0	-0.026180	1.311919	2.729769
59	6	0	-0.767100	1.431889	3.888039
60	6	0	-1.556340	2.574859	4.126269
61	6	0	-0.805690	3.520459	2.009419
62	6	0	-0.758280	4.596999	1.063949
63	6	0	-1.567210	3.598289	3.201699
64	6	0	-1.559060	5.857709	1.265609
65	1	0	-1.281480	6.363479	2.198539
66	1	0	-2.633400	5.644129	1.323289
67	1	0	-1.396600	6.558179	0.441649
68	1	0	0.162310	5.259639	-0.745431
69	1	0	0.577720	0.435059	2.551599
70	1	0	-0.735540	0.630819	4.621019
71	1	0	-2.158030	4.488669	3.391109
72	1	0	-2.142910	2.654479	5.037139
73	6	0	3.407660	1.962160	-2.461971
74	16	0	2.230890	4.279600	-2.515641
75	6	0	3.401110	3.154740	-3.138891
76	1	0	4.019370	3.448120	-3.978221
77	1	0	4.077470	1.149440	-2.720981
78	6	0	4.394531	-0.900380	-0.286861
79	6	0	4.494450	0.086270	0.739909
80	6	0	5.474801	-1.744890	-0.660701
81	6	0	5.335021	-2.704730	-1.625031
82	6	0	4.050021	-2.837600	-2.246921
83	6	0	2.986921	-1.962140	-1.842861
84	6	0	1.722941	-2.116460	-2.459511
85	6	0	1.514681	-3.079470	-3.426311
86	6	0	2.556631	-3.937030	-3.829691

87	6	0	3.799331	-3.810980	-3.244881
88	6	0	6.492011	-3.591850	-2.005891
89	1	0	7.384101	-3.336770	-1.427151
90	1	0	6.739051	-3.494640	-3.070241
91	1	0	6.261341	-4.648570	-1.823521
92	1	0	6.425051	-1.611860	-0.152341
93	1	0	2.382931	-4.692580	-4.590691
94	1	0	4.605591	-4.471170	-3.547671
95	1	0	0.925451	-1.455460	-2.151751
96	1	0	0.529981	-3.176101	-3.876261
97	16	0	5.880320	0.450440	1.758149
98	6	0	3.645690	1.719650	2.147019
99	6	0	4.930290	1.625830	2.615899
100	1	0	2.920590	2.403270	2.574499
101	1	0	5.385710	2.184280	3.424279

Energy

E(RB3LYP) = -3339.45341195 Hartree

Zero point corrected free energy = -3338.665443 Hartree

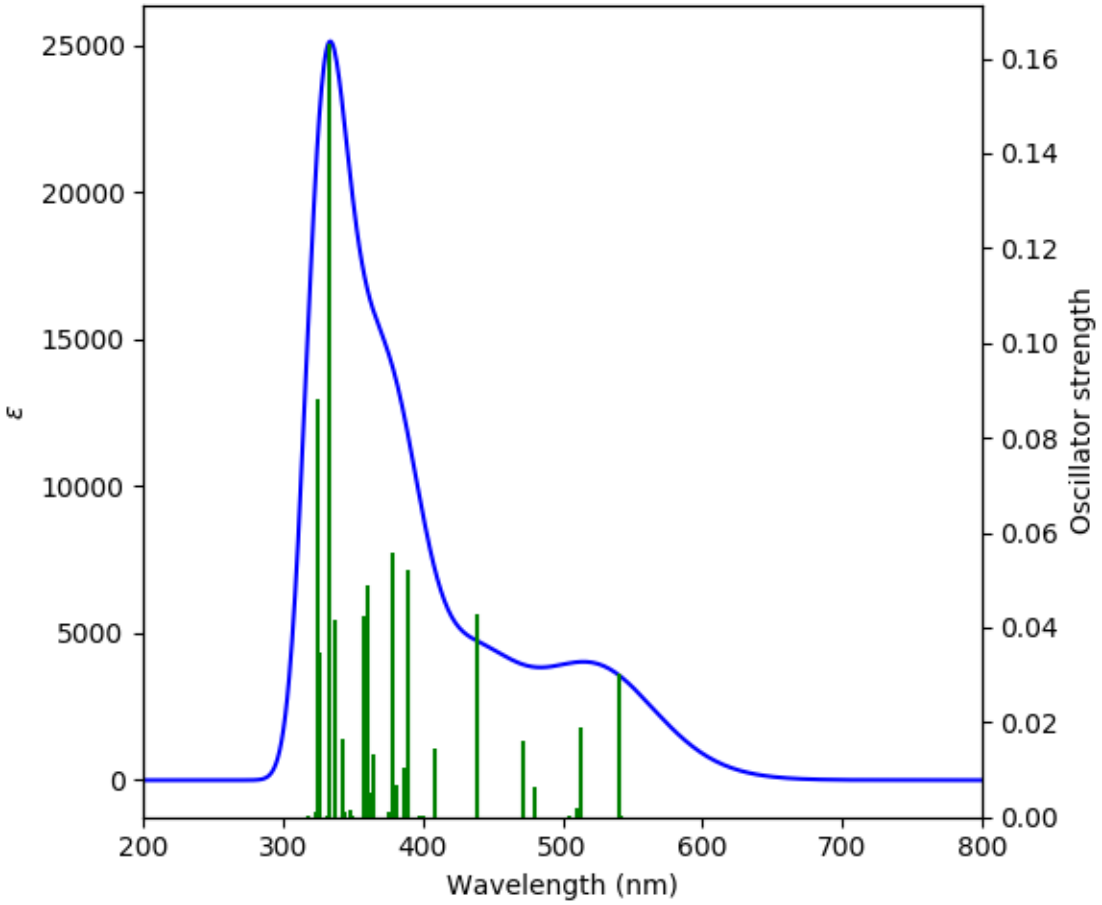

Figure S105. Calculated UV/vis spectrum for co-system **4•5**.

Table S39. Calculated energy levels of the ten highest contributing singlet states and the first four triplet states for **4•5**.

Spin State	Transition configurations	Excitation energy (eV, nm)	Oscillator strength
S_2	HOMO→LUMO+1 (97.2%) HOMO-1→LUMO+1 (2.1%)	2.2952, 540.20	0.0302
S_3	HOMO-2→LUMO+1 (5.9%) HOMO-1→LUMO+1 (52.3%)	2.4140, 513.61	0.0189

	HOMO-1→LUMO+2 (4.2%) HOMO→LUMO+1 (6.0%) HOMO→LUMO+2 (30.0%)		
S_6	HOMO-1→LUMO+2 (88.5%) HOMO→LUMO+2 (8.8%)	2.5853, 479.58	0.0064
S_7	HOMO-2→LUMO+1 (87.3%) HOMO-1→LUMO+1 (9.1%)	2.6257, 472.19	0.0159
S_9	HOMO-3→LUMO+2 (2.7%) HOMO-2→LUMO+2 (92.8%)	2.8261, 438.72	0.0430
S_{13}	HOMO-4→LUMO+1 (39.2%) HOMO-4→LUMO+2 (10.4%) HOMO-3→LUMO+1 (12.2%) HOMO-3→LUMO+2 (30.8%)	3.1799, 389.90	0.0522
S_{21}	HOMO-7→LUMO+1 (4.6%) HOMO-6→LUMO+1 (29.6%) HOMO-4→LUMO+2 (38.5%) HOMO-3→LUMO+2 (14.8%) HOMO-2→LUMO+4 (2.2%)	3.4394, 360.49	0.0488
S_{27}	HOMO-9→LUMO+1 (2.1%) HOMO-7→LUMO+1 (36.3%) HOMO-6→LUMO+2 (2.2%) HOMO-5→LUMO+1 (4.6%) HOMO-4→LUMO+1 (2.2%) HOMO-2→LUMO+4 (43.1%) HOMO-1→LUMO+4 (2.8%)	3.6131, 343.15	0.0164

S_{29}	HOMO-7→LUMO+1 (14.7%) HOMO-7→LUMO+2 (4.4%) HOMO-6→LUMO+1 (2.7%) HOMO-6→LUMO+2 (42.3%) HOMO-2→LUMO+4 (4.7%) HOMO-2→LUMO+5 (9.0%) HOMO-1→LUMO+5 (15.3%)	3.7191, 333.37	0.1632
S_{33}	HOMO-7→LUMO+2 (66.9%) HOMO-6→LUMO+2 (5.9%) HOMO-3→LUMO+5 (2.3%) HOMO-2→LUMO+5 (14.2%)	3.8239, 324.23	0.0883
T_1	HOMO-4→LUMO+2 (2.0%) HOMO-3→LUMO+1 (5.8%) HOMO-3→LUMO+2 (7.1%) HOMO-2→LUMO+1 (18.7%) HOMO-2→LUMO+2 (7.2%) HOMO-1→LUMO+1 (17.3%) HOMO-1→LUMO+2 (14.3%) HOMO→LUMO+1 (6.7%) HOMO→LUMO+2 (12.6%)	2.0528, 603.99	0.0000
T_2	HOMO-3→LUMO+1 (15.3%) HOMO-3→LUMO+2 (3.2%) HOMO-2→LUMO+1 (16.5%) HOMO-2→LUMO+2 (11.0%) HOMO-1→LUMO+1 (10.1%) HOMO-1→LUMO+2 (17.9%) HOMO→LUMO+2 (14.0%)	2.0714, 598.56	0.0000

T_3	HOMO-3→LUMO+1 (8.7%) HOMO-2→LUMO+1 (6.2%) HOMO-1→LUMO+1 (3.2%) HOMO→LUMO+1 (72.8%)	2.1922, 565.57	0.0000
T_4	HOMO-1→LUMO (2.4%) HOMO→LUMO (97.0%)	2.2851, 542.57	0.0000

Table S40. Calculated MO energies of orbitals involved in transitions for co-system **4•5**.

Orbital	**Energy/ eV**		**Orbital**	**Energy/ eV**
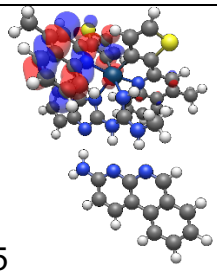 LUMO+5	-0.49		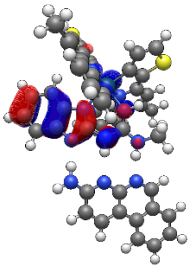 HOMO	-4.48
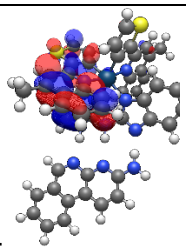 LUMO+4	-0.70		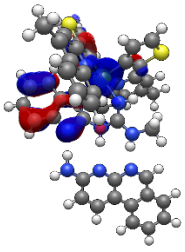 HOMO-1	-4.62
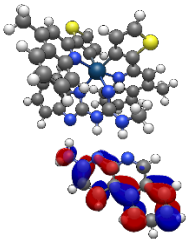 LUMO+3	-1.02		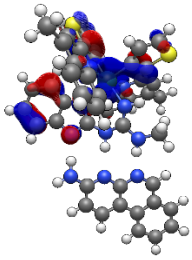 HOMO-2	-4.86

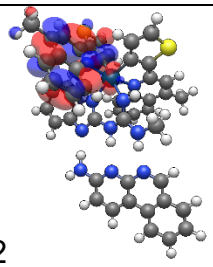 LUMO+2	-1.45		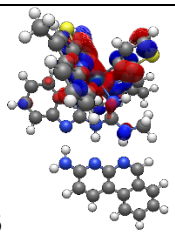 HOMO-3	-5.26
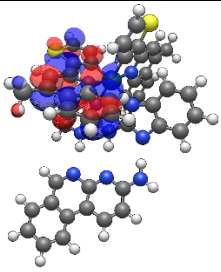 LUMO+1	-1.64		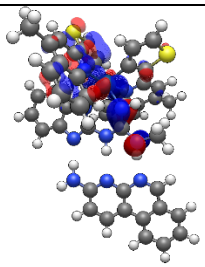 HOMO-4	-5.47
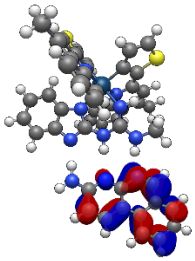 LUMO	-1.82		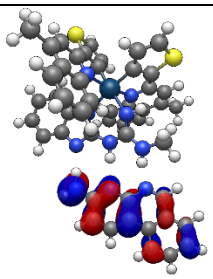 HOMO-5	-5.58
			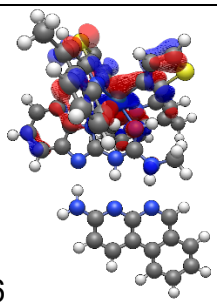 HOMO-6	-5.74
			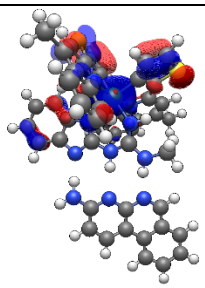 HOMO-7	-5.85

			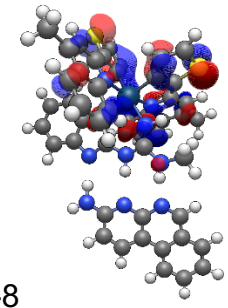 HOMO-8	-6.13
			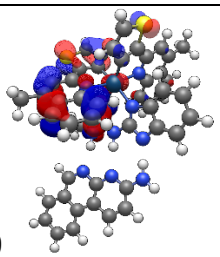 HOMO-9	-6.23

References

[1]- Brouwer, A. M.; Standards for photoluminescence quantum yield measurements in solution (IUPAC technical report). *Pure and Applied Chemistry* 2011, *83* (**12**), 2213–2228.

[2]- Gaussian 16, Revision C.01, M. J. Frisch, G. W. Trucks, H. B. Schlegel, G. E. Scuseria, M. A. Robb, J. R. Cheeseman, G. Scalmani, V. Barone, G. A. Petersson, H. Nakatsuji, X. Li, M. Caricato, A. V. Marenich, J. Bloino, B. G. Janesko, R. Gomperts, B. Mennucci, H. P. Hratchian, J. V. Ortiz, A. F. Izmaylov, J. L. Sonnenberg, D. Williams-Young, F. Ding, F. Lipparini, F. Egidi, J. Goings, B. Peng, A. Petrone, T. Henderson, D. Ranasinghe, V. G. Zakrzewski, J. Gao, N. Rega, G. Zheng, W. Liang, M. Hada, M. Ehara, K. Toyota, R. Fukuda, J. Hasegawa, M. Ishida, T. Nakajima, Y. Honda, O. Kitao, H. Nakai, T. Vreven, K. Throssell, J. A. Montgomery, Jr., J. E. Peralta, F. Ogliaro, M. J. Bearpark, J. J. Heyd, E. N. Brothers, K. N. Kudin, V. N. Staroverov, T. A. Keith, R. Kobayashi, J. Normand, K. Raghavachari, A. P. Rendell, J. C. Burant, S. S. Iyengar, J. Tomasi, M. Cossi, J. M. Millam, M. Klene, C. Adamo, R. Cammi, J. W. Ochterski, R. L. Martin, K. Morokuma, O. Farkas, J. B. Foresman, and D. J. Fox, Gaussian, Inc., Wallingford CT, 2016.

[3]- Y. Yang, M. N. Weaver and K. M. Merz, *The Journal of Physical Chemistry A*, 2009, **113**, 9843–9851.

[4]- J. Tirado-Rives and W. L. Jorgensen, *Journal of Chemical Theory and Computation*, 2008, **4**, 297–306.

[5]- M. D. Hanwell, D. E. Curtis, D. C. Lonie, T. Vandermeersch, E. Zurek and G. R. Hutchison, *Journal of Cheminformatics* **17** (2012)

[6]- N. M. O'boyle, A. L. Tenderholt and K. M. Langner, *Journal of Computational Chemistry*, 2008, **29**, 839–845.

[7]- Tamayo, A. B.; Alleyne, B. D.; Djurovich, P. I.; Lamansky, S.; Tsyba, I.; Ho, N. N.; Bau, R.; Thompson, M. E. *Journal of the American Chemical Society* 2003, *125* (**24**), 7377–7387.

[8]- Balónová, B.; Martir, D. R.; Clark, E. R.; Shepherd, H. J.; Zysman-Colman, E.; Blight, B. A. *Inorganic Chemistry* 2018, *57* (**14**), 8581–8587.

[9]- P. Thordarson. *Chem. Soc. Rev*., 2011, **40(3)**, 1305-1323.

[10]- B. Balónová, H. J. Shepherd, C. J. Serpell and B. A. Blight, *Supramolecular Chemistry*, 2019, **32**, 1–12.